UNIVERSITY of the
WESTERN CAPE

Faculty of Natural Sciences
Department of Earth Science
Environmental and Water Science

Streamflow generating mechanisms in a mountainous Jonkershoek catchment, South Africa

By

Retang Anna Lapalemabu MOKUA

A thesis submitted in fulfilment of the academic requirement for the degree of

Doctor of Philosophy

October, 2022

Supervisors: Professor D. Mazvimavi

Co-supervisors: Dr J.A. Glenday**,** Dr N. Allsopp

ACKNOWLEDGEMENTS

First, I would like to thank Modimo Wa Thaba ya Sione for all the strength, for providing me with this opportunity and for enabling me to complete this study. Ke a leboga Mohwaduba wa Mmaphaka'a boMonare (Psalms 23, *difela tsa Sione* no.111).

I would like to sincerely thank my supervisor Dr Julia Glenday for providing me with the best guidance and support through this study. Thank you for your patience, for always lending an ear and for believing in me even when I was not at my best. A special thanks to Professor Dominic Mazvimavi and Dr Nicky Allsopp for your insightful suggestions, comments and guidance.

This study would not have been possible without the financial support provided by SAEON Fynbos Node, the National Research Foundation (NRF: MND 1901530440376) and the Faculty of Natural Science postgraduate division

As they say, always save the best for last. Thanks to my wonderful family for the love, support, prayers and patience through this journey. To my mother, Julia Mokua and my grandmother whose precious name Anna Lapalemabu Mosehle I carry, thank you Mahlako le Modipadi. I am grateful to my sisters, aunt, uncle and brother for your encouragement. To my late grandfather Ellie Mosodi "Hlabirwa" Mosehle, thanks for being my guardian angel.

Lastly thanks to my friends and colleagues who carried me through this journey and made it less painful and stressful for me. To Sandiso, Luyanda, Oratile, Bongiwe, Kamogelo, Faith, Errol and Siya, thank you. Thanks, Abri your tremendous assistance with field data collection, Evan Swartbooi and Mike Butler for the help with sample analysis.

Special dedication to all the women in STEM, "never shrink yourselves to fit in".

ABSTRACT

The Jonkershoek valley catchment in a mountain region that forms the headwaters of the Eerste River, which contributes water to the Cape Winelands District Municipality and parts of the City of Cape Town in the Western Cape Province, South Africa. These areas include highly urbanized and agriculturally advanced regions, which are vulnerable to occasional water shortages. Understanding the processes and factors accounting for the spatial and temporal variations of streamflow in this area is critical. This information can be used to build appropriate conceptual models of this catchment's functioning to support the management of water resources.

To achieve this goal, multiple techniques were applied to investigate hydrological processes for three gauged sub-catchments (1 to 2.5 km^2) within the Jonkershoek River catchment, namely Bosboukloof, Langrivier and Tierkloof. These sub-catchments were part of a long-term multi-catchment experiment. Bosboukloof and Tierkloof were afforested with *Pinus radiata* since the 1940s, while Langrivier was kept as a control site. The mean annual rainfall for the study period in the selected sites varies from 1100 – 1320 mm/a, and the mean annual runoff ranged from 200 to 900 mm/a. Fractured Table Mountain Group rocks, comprising sandstones, and shales, together with the basement Cape granite and Malmesbury shales, are the dominant lithological types. Streamflow, groundwater levels in boreholes and shallow piezometers, soil moisture, rainfall, hydrochemical and environmental isotopes data were analysed to reveal the spatial and temporal patterns of sources and flow pathways of water, as well as any long-term trends in hydro-climatic variables. Furthermore, the Indicators of Hydrological Alteration (IHA) tool was used to detect changes in streamflow regime and trends over time, particularly related to land use and land cover changes such as the afforestation (i.e., replacement of fynbos by pine plantation) and clear-felling.

The Mann-Kendall trend test and homogeneity tests identified significant decreasing trends and abrupt changes in long-term annual rainfall and streamflow time series (1946-2019). The trend magnitudes and occurrences of abrupt changes varied spatially across the sub-catchments. This spatial variation was attributed to differences in catchment characteristics, particularly topography and land use. The long-term declining trends were driven by the meteorological and hydrological drought near the end of the time series. Evaluation of the potential influence of afforestation (1946-onwards) and clear-felling (1979-1982) indicated a significant decrease in flow post afforestation. Significant increases in flow indices were observed post-clear-felling. These analyses suggest urgent actions such as improved land use planning, and potentially restoring treed areas to indigenous fynbos, are crucial to improving the sustainability of water resources and conservation of eco-systems in the Jonkershoek catchment and the surrounding Cape mountain region.

Stable isotope and hydrogeochemical data (2018-2020) showed marked spatial and temporal variations in water sources and flow paths across the three sub-catchments. High flows were recorded during the wet winter (Apr - Sep), while low flows occurred during the dry summer (Oct - Mar). The hydrochemical analysis, particularly EC concentrations, suggested the occurrence of two different bedrock groundwater aquifers: an aquifer within the Table Mountain Group bedrock in the upper parts of the catchments and another in the granite-shale bedrock. The stable isotope analysis indicated that interflow, including enhanced discharge from both ephemeral and perennial springs, contributed to the wet winter flows, while dry summer flows were due to groundwater discharge from the Table Mountain Group (TMG) aquifer.

Hydrograph separation using recursive digital filtering (RDF) was calibrated with the electrical conductivity data collected during 2018-2020 using the conductivity mass balance method. The results indicated that baseflow contributed 38 to 86 % of the annual average streamflow across the three catchments. The baseflow contributions were higher during the dry summer. In Bosboukloof, baseflow contributes 89% of summer flows and 82 % in winter on average, while average contributions were Tierkloof 73 % and 60 %, and 50% and 34 % for Langrivier. Differences in topography and vegetation were considered to account for these differences. For example, Bosboukloof has the lowest proportion quickflow of the three, while also having the lowest slopes and most scree material, likely to dampen peaks.

Chemistry-based hydrograph separation of the storm event showed that sub-surface flows dominated the storm flow across the study sites, either from rapid flow in rock fractures and/or through scree soils, including push-through. Two-component separation into pre-event vs event (rain) water contributions to streamflow using stable isotopes revealed large fractions of pre-event water, > 90% in all sub-catchments. Further separation of the storm hydrograph into three components, shallow sub-surface flow, direct runoff and bedrock groundwater suggested shallow sub-surface flow made up about 50 % of the storm flow in Bosboukloof. On the other hand, the stormflow in Langrivier was dominated (80%) by the TMG groundwater. The spatial variations in flow components were attributed to the rugged topography and spatial irregularities of fracturing.

The findings of the study suggest a complex hydrological system, not only geologically but also due to the land use/land-cover and rugged topography, providing spatially variable streamflow generating processes and flow pathways. The multi-method approach combining tracer techniques, hydrometric data and statistical methods is novel to this catchment. The study revealed the advantages and challenges of using environmental tracers to conceptualize processes in fractured geology-dominated systems. The findings of this study can be used as a baseline for future research in the catchment and planning of water resources in the Cape region and other areas with similar characteristics. Furthermore, climate

variability and human-induced changes such as afforestation pose a major threat to the future of water resources in the Jonkershoek catchment and the surrounding region.

Keywords: streamflow generation, stable isotopes, hydrograph separation, baseflow, recursive digital filter, conductivity mass balance, Table Mountain Group

DECLARATION

I, Retang Anna Lapalemabu Mokua declare that **"*Streamflow generating mechanisms in a mountainous Jonkershoek catchment, South Africa*"** is my work that has not been submitted for any degree or assessment in any other university. I also declare that it does not contain other persons' data, pictures, graphs, or other information unless specifically acknowledged in the form of references and that all the sources I have used or quoted have been indicated and acknowledged through complete references.

Full name: Retang Anna Lapalemabu Mokua

Signed: 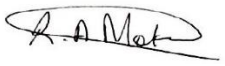 Date:October 2022

TABLE OF CONTENTS

LIST OF FIGURES

LIST OF TABLES

List of Abbreviations and/or Acronyms

^{18}O	Oxygen-18
^{2}H	Deuterium
API	Antecedent Rainfall Index
ASI	Antecedent Soil moisture Index
BFI	Baseflow Index
BFI_{max}	Maximum value of the baseflow index
BRT	Buishand Range Test
CFB	Cape Fold Belt
CMA	Cape Metropolitan Area
CMB	Conductivity Mass Balance
CV	Coefficient of Variance
CD	Coefficient of Dispersion
DWA	Department of Water Affairs
DWS	Department of Water and Sanitation
EFC	Environmental Flow Parameters
EMMA	End Member Mixing Analysis
GIS	Geographic Information Systems
GMWL	Global Meteoric Water Line
IHA	Indicators of Hydrological Alteration
IPCC	Intergovernmental Panel on Climate Change
LMWL	Local Meteoric Water Line
mamsl	Meters above mean sea level
MAP	Mean Annual Rainfall
MAR	Mean Annual Runoff
PBIAS	Percentage Bias
PET	Potential Evapotranspiration
RDF	Recursive Digital Filtering
RMSE	Root Mean Square Error
RVA	Range of Variability Approach
TMG	Table Mountain Group

SAEON	South African Environmental Observation Network
SAFRI	South African Forest Research Institute
SAYB	South African Yearbook
SC	Specific conductivity
SNHT	Standard Normal Homogeneity Test
SPI	Standardized Precipitation Index
SSI	Standardized Streamflow Index
UWC	University of the Western Cape
VSMOW	Vienna Standard Mean Oceanic Water

List of notations

δ^2H	Relative concentration of deuterium isotope
$\delta^{18}O$	Relative concentration of Oxygen 18 isotope
a	Recession constant
‰	Per mil
µS/cm	Micro Siemens per centimetre
H_0	Null hypothesis
H_1	Alternative hypothesis
m^3/s	Cubic meters per second
mg/l	Milligrams per litre
mbgl	Meters below ground level
C_e, C_p, C_t	Concentrations of event, precipitation and pre-event water
Q	Sen's slope
Q_b	Baseflow (m^3/s)
Q_j	Baseflow on a specific day
Q_p	Pre-event water (m^3/s)
Q_r	Direct runoff (m^3/s)
Q_t	Total discharge (m^3/s)
W_{fe}	Uncertainty in the pre-/event water fraction
Z_{MK}	Mann-Kendall statistics

Chapter 1: Introduction

1.1. Background

The Jonkershoek Valley is widely recognized as Africa's oldest experimental catchment site (Slingsby et al., 2021). The site was instrumented in the 1940s to monitor the impacts of non-indigenous pine plantations on hydrology. Despite the considerable research done in this catchment, there are still gaps in knowledge about hydrological processes due to the region's complex fractured rock hydrogeology. This mountainous catchment is dominated by the Table Mountain Group (TMG) geology with a fractured rock aquifer system (Weaver et al., 1999). Processes and factors accounting for spatiotemporal variability in streamflow generation in this area are not adequately understood. Understanding these processes is crucial for sustainable water resources management. This is particularly important in the Cape region of South Africa, which is typified by a Mediterranean climate with long dry summers.

Mountain headwaters serve as important landscape features supplying long-term water storage that supports year-round streamflow and ecosystem services to downstream users (Viviroli et al., 2003). Baseflows of rivers draining areas with Table Mountain sandstones sustain water supplies to humans and ecosystems (Roets et al., 2008). The abundant perennial cold and hot water springs maintain baseflow during the low flow months with sparse rainfall (Hartnady and Jones, 2007). Both the fractured geology and the steep topography contribute to proportionally high runoff generation. The geomorphology, soils, and vegetation of these mountains tend to regulate the flow of both surface water and groundwater (Gilvear et al., 2002; Roets et al., 2008). Therefore, sustainable development and management of surface systems and groundwater resources in terms of quality and quantity region are essential in the TMG geological region.

Hydrological processes in the Jonkershoek have been affected by multiple drivers such as climate change, land-cover change (e.g., commercial afforestation), alterations in wildfire regimes and pollution (air, land, and water, etc.) (Kruger and Wicht, 1976; Scott, 1994; Dye et al, 2001). These changes are putting pressure on water resources and diminishing the options for exploiting new sources of water from mountain headwaters catchments. Changes in climatic variables can have major impacts on regional rainfall patterns and temperatures with a significant impact on headwater catchments (Duah, 2010). Recent prolonged dry periods (2015-2017), with high evaporative demand, manifested in severely reduced runoff from the source catchments in the Western Cape Province (Botai et al., 2018; Wolski et al., 2021). A better quantitative understanding of the processes which control catchment water resources, and their variability in space and time, is important for managing supplies in the long-term across extreme events (Jewitt et al., 2004; Hughes et al., 2014).

The growing demands and pressure on surface water resources, particularly in the context of global change drivers such as climate and land use change have increased interest in understanding the hydrological functioning of headwater catchments and their capacity to deliver water sustainably under

changing conditions. However, detailed catchment process studies have been limited in the TMG geological region, compared to its complexity, heterogeneity, and importance for regional water supply. Such studies are required to improve conceptualisation in numerical hydrological models and our capability to predict the hydrological responses to various changes.

This study will provide knowledge on the spatial and temporal variability of hydrological processes at the sub-catchment scale (< 3 km^2). The study aims to provide an improved understanding of the long-term impacts of change in hydroclimatic variables and land use/land-cover on streamflow generation. This information aids in the planning of the water resources of Cape Town Metropolitan Municipality.

1.1.1. Understanding streamflow generating mechanisms

Mountainous headwater streams in the TMG aquifer system contribute flow to the major rivers and dams in the Cape region. Streamflow dynamics reflect the balance of various hydrological processes, such as infiltration, evapotranspiration, percolation and sub-surface flow which are influenced by multiple catchment physiographic characteristics such as topography, geology, soil and changes in vegetation cover and climate (Carlier et al., 2018). Multiple interacting factors may result in the spatial and temporal variations in streamflow within a catchment making understanding and conceptualisation of these processes a challenge.

Streamflow generating mechanisms have been studied worldwide in many catchments at both large (> 1000 km^2) (e.g., Zhang et al., 2008; Frisbee, 2010; Camacho Suarez et al., 2015; Congjian et al., 2016) and small scales (< 10 km^2) (e.g., Ogunkonya and Jenkins, 1993; Didszun and Uhlenbrook, 2008; Penna et al., 2015; Sun et al., 2017; Zhao et al., 2019). These studies elucidated the large effects of climatic controls such as rainfall, temperature, evaporative demands (Ma et al., 2008; Hu et al., 2011; Tessema et al., 2020) and physiographic controls, such as landscape organization (Soulsby et al., 2003; McGlynn et al., 2004; Muñoz-Villers and McDonnell, 2012; Asano and Uchida, 2018), geology (Uchida et al., 2003; Pfister et al., 2017; Zhao et al., 2019a), surface topography (Rodgers et al., 2005) and vegetation cover (Puigdefábregas, 2005; Zhang et al., 2007) on catchment hydrological processes.

Understanding streamflow generating processes requires high-quality data collection, and high-density monitoring to account for the processes and pathways involved, both on the land surface and through various subsurface media. Long-term monitoring is needed to provide insight into the behavioural features of the catchment system over variable climate conditions (Soulsby et al., 2008). Analysing the long-term trends in hydro-climatic variables is fundamental to understanding climate and land use change impacts on streamflow patterns (e.g., Chapter 3). However, little is known about these trends at a local scale in the TMG region either due to inadequate quality or lacking data. This is common in the sub-Saharan region and hinders resource management (Sivapalan, 2003).

Integration of various data sets such as hydrometric (discharge, groundwater levels), meteorological, soil moisture and tracers data can enhance the characterization of hydrological processes by providing

insight into different physical transport mechanisms of streamflow generation (Birkel et al., 2011a). Collectively these data have the potential to provide different but relevant information about Jonkershoek. For instance, groundwater chemistry and water level data provide information on contributions of different portions of the catchment to streamflow, discharge recessions describe the dynamics of storage and tracers data provides information on the transport/pathways and mixing of new rainfall with stored water already present in the catchment (Fenicia et al., 2008). However, field and laboratory-based methods for the acquisition of data at fine spatial and temporal resolutions are costly, especially for large and mesoscale catchments. However, a lack of data at appropriate spatial and temporal resolutions leads to uncertainty about the nature and effects of various hydrological processes. Such knowledge gaps constrain and lead to inappropriate water resources management decisions.

1.1.2. The importance of knowledge of runoff generation in sustainable water resources management.

Sustainable water resources management require a sound understanding of runoff generation processes, particularly in mountainous catchment characterized by seasonality and highly variable streamflow and rainfall, heterogeneous geology, and vegetation cover. Proper evaluation and optimal protection of surface and groundwater resources concerning quality and quantity depend on a sound understanding of runoff processes (Wenninger et al., 2008; Camacho Suarez et al., 2015).

Runoff generating processes in headwater catchments are complex due to the spatially variable physiographic characteristics which include vegetation cover, soil characteristics, bedrock and surficial geology, and climate features (Uhlenbrook et al., 2002). These characteristics are the key controls of physical mechanisms delivering water to the stream (Brown et al., 1999). Improved knowledge of runoff processes over space and time enables better parameterization of hydrologic models for water resources planning and management strategies such as drought management, flood warning and mitigation, land use planning, and improvement of water quality (i.e., reducing sedimentation and nutrients loads) (Uhlenbrook et al., 2008; Blöschl et al., 2013). This knowledge is of great significance in mountainous catchments as they provide a range of ecosystems and ensure adequate and sustainable supplies for economic and social development.

Most mountain headwater catchments have undergone modification driven by socio-economic developments and population growth, whereby natural vegetation has either been converted to commercial forests or agricultural land (Gebremicael et al., 2019). These alterations increase the complexity of understanding hydrological processes as they impact landscape flow pathways. Land cover has the potential to rearrange surface and sub-surface processes and influence soil properties in a catchment, which combined determines the net impact on water resources (Price et al., 2011). Changes in land use and land cover affect hydrological processes such as rainfall partitioning into different hydrological components, infiltration rate, groundwater recharge, baseflow and surface runoff (Hassaballah et al., 2017; Gebremicael et al., 2019). The disturbances of the surface decrease the rainfall

infiltration rate to the extent that groundwater reserves are insufficiently replenished during the wet season, subsequently reducing dry season flows (baseflows) (Bruijnzeel, 2004).

Land cover modification by commercial afforestation may influence water resource availability in the catchment. For instance, high forest cover is commonly associated with lower baseflows through enhanced evapotranspiration (ET) or results in increased baseflow in catchments with higher vegetation cover due to higher infiltration and recharge of subsurface storage (Bosch and Hewlett, 1982; Bruijnzeel, 2004; Price et al, 2011). Deforestation increases annual runoff due to soil compaction, thereby increasing the risks of floods, erosion, and organic matter losses. Soil water storage capabilities may also decline because of erosion. Increased sedimentation in the stream also compromises water quantity and quality (Castillo Rápalo et al; 2021). On the other hand, forest clearing removes the forest canopy changing the quantity and timing of flows (Scott et al., 2002; Dye et al., 2003; Spencer et al., 2021). Although afforestation can reduce the enhanced peak flows and stormflows associated with soil degradation by deforestation (Bruijnzeel, 2014).

The disturbances by land use and land cover change increase the pathways length and permeability of the respective system flow system delaying infiltrating water (Uhlenbrook et al., 2002). In addition, chemical reactions within the sub-surface (e.g., soil or bedrock) alter infiltrating waters which describe the type of earth material encountered by the water during transit to the stream. Thus, understanding sub-surface processes is an important prerequisite for acquiring information on sources of solutes and contamination in streams, predicting water resources yields, water quality, floods and erosion as well as evaluating catchment vulnerability (Anderson et al., 1997; Hrachowitz et al., 2011). Therefore, to ensure sustainable water sources management of a mountainous catchment, changes in land use and land cover and climate variability should be taken into consideration.

1.2. Problem statement

Parts of the Jonkershoek catchment have undergone drastic land cover changes such as planting with non-indigenous commercial timber species (*Pinus radiata* and *Eucalyptus Grandis)* and periodic extreme loss of vegetation cover due to wildfires. Afforestation coupled with changes in climatic conditions can negatively impact catchment water delivery. Afforestation has a significant impact on the hydrological cycle when replacing shrubland and grassland, reducing streamflow due to the tree's larger consumption of water (Dye, 2001; DWAF, 2004). In the Jonkershoek catchment, extensive research has been conducted which included assessing rainfall characteristics (Wicht et al., 1969; Kruger and Wicht, 1976) and hydrological impacts of afforestation(Scott et al., 2000, Dye, 2001), clear-felling (Lesch and Scott, 1997; Scott, 1997), and wildfire (Britton, 1993; Scott, 1994, 1997; Van Wilgen, 1994). However, little attention has been given to understanding the balance of surface and subsurface hydrological processes which govern streamflow generation.

Various aspects of the TMG aquifer system have been investigated, such as the quantity and quality of groundwater as well as the sustainable level of utilization at the regional scale (e.g., Kotze, 1999; Smart

and Treadoux, 2002; Duah, 2010). However, there are few detailed studies in TMG catchments that focus on the characterisation of surface and sub-surface flow paths, and how these pathways respond to different climatic conditions and land cover changes. Effective management of mountain water resources requires a more detailed investigation into hydrological processes, particularly those describing the spatiotemporal variability of the dominant flow pathways and components within a catchment. This information is often missing for most mountain catchments due to a lack of high-quality datasets which cover the various spatio-temporal scales to deliver an accurate picture of behavioural features of the hydrological system. Owing to the highly heterogeneous topography, high elevation and fractured geology, the quantity, timing, magnitude, and variability of streamflow remain poorly understood in the TMG catchments. This suggests the need for quantitative knowledge of dominant processes and their controls at different spatial and time scales in the Jonkershoek catchment. Accurate quantification of water flow pathways within sub-catchments is essential to aid in improving water management strategies across the catchment and evaluate the vulnerability of the surface and groundwater systems in the context of contamination (i.e., water quality), changes in land use and land cover as well as climate variability. This is critical for mountain catchments that are vulnerable to water scarcity and have been subjected to human-induced environmental changes, particularly modification of natural vegetation by afforestation.

The integration of the existing long-term streamflow and rainfall data with environmental tracer data such as isotopes and hydrochemistry (e.g., Midgley and Scott, 1994; Saayman et al., 2003; Wenninger et al., 2008; Camacho Suarez et al., 2015; Tekleab, 2015; Saraiva Okello et al., 2018) and investigation of existing trends in hydro-climatic variables can provide improved insight into hydrologic processes. This is because such data, particularly tracers integrate small-scale variability in flow pathways to give an effective indication of catchment-scale processes (McDonnell and Kendall, 1992). The integrated information is essential for the conceptualization of hydrological response through the identification of dominant flow pathways and sources of water in the catchment. Inaccurate presentation and quantification of runoff processes increase the uncertainty in hydrologic models, resulting in the improper implementation of water management strategies. Thus, this study aims to provide new insight into runoff generating processes for the better conceptualization of catchment hydrological models and reduced uncertainty in the future development of numerical catchment models.

Additional monitoring data such as soil moisture, and water levels, supported by complementary information such as stable isotopes and hydrochemical measurements can offer a new opportunity to gain insight into the catchment functioning and support the development of conceptual models. The conceptual model can be used in decision support for policymakers and water managers to ensure the sustainable development of water resources in the Cape region.

1.3. Significance of the study

There is a need to gain more in-depth insights into the impacts of the different global change drivers or the long-term management of our water resources in the Cape region. The Jonkershoek River is one of the major tributaries of the Eerste River, which supplies water to surrounding Western Cape municipalities which are highly urbanized and agriculturally advanced (Thomas et al., 2010). In addition, the headwater catchment of the Berg River near Franschoek, which feeds the Berg River Dam, borders the Jonkershoek catchment to the northeast and shares its characteristics. A more quantitative understanding of the hydrological processes in these catchments is required for producing dependable hydrological models, which are used for the following:

- Flood, erosion and drought impact predictions,
- Evaluation of water resources and planning terrestrial and aquatic ecosystem preservation
- Assessment of potential climate and land use change impacts for planning and mitigation.
- Facilitate proper water sharing between different stakeholders for food security, economic needs and improving livelihoods.

1.4. Aim and Objectives

1.4.1. Aim

The study aims to improve the understanding of streamflow generating processes in a mountain catchment with geology dominated by the Table Mountain Group. The study is located within Holland-Hottentots Mountain which is an important source of water for the Western Cape region.

1.4.2. Main objectives

1. To determine the changes of hydro-climatological characteristics within the mountain catchment over time;
2. To determine the spatio-temporal variability of stable isotopes and hydrochemistry, to establish sources and pathways of water contributing to streamflow at a seasonal scale;
3. To determine the seasonal and annual contribution of baseflows to total flows; and
4. To identify and quantify storm runoff generating processes at the sub-catchment scale and develop conceptual models of flow generation at the event scale.

1.5. Hypotheses

The study is based on the following hypotheses.

1) Trends in climate and land use changes have altered the streamflow regimes and yield in the Jonkershoek catchment.
2) Most of the streamflow in the Jonkershoek sub-catchments originates from sub-surface flow during both baseflow conditions and storm events.

3) Sub-catchments with pine plantations will have lower baseflows due to high evapotranspiration rates from the pines and less shallow sub-surface flow because the pines draw down from the shallow scree-soil water storage.
4) During storm events, the storm flow comes from the groundwater or pre-event water.
5) Environmental tracers can reveal the heterogeneities in the surface and sub-surface hydrological processes, and identify and quantify runoff generating processes at the sub-catchment level and both the seasonal and event time scales.

1.6. Dissertation structure

This study is structured into 7 Chapters which will unpack the processes of streamflow generating mechanisms in the Jonkershoek catchment, hydro-climatic variable controls on streamflow, the spatial variability in streamflow sources and flow paths using various hydrograph separations methods. A full description of the chapter contents is given in Table 1.1. Chapters 3 to 5 have each been written as papers for submission in peer-reviewed journals for publication. The relevant literature review for each objective is presented in the respective chapters.

Table.1.1. Summary of the thesis structure

Chapter	Description
1. Introduction	The introductory chapter of the research provides a brief background The problem statement, the significance of the aim of the study and the main objectives
2. Study site description	This chapter gives an overview of the study site, geology, and land cover, as well as hydrological and hydrogeological characteristics.
3. Spatial and temporal characterization of rainfall and streamflow	This chapter analyses the long-term trends in rainfall and streamflow and assesses the effects of past land use changes on hydrologic regimes at a sub-catchment scale using various statistical methods, drought indices and indicators of hydrologic alteration.
4. Spatial and temporal dynamics in stable isotopes and hydrochemical characteristics.	Analyses of stable isotopes and physicochemical parameters characteristics from various water sources within the sub-catchments and main catchment (e.g., springs, stream, groundwater, piezometers, rainfall) to determine seasonal variability in stream water sources and flow pathways. (Mokua *et al.*, 2020)
5. Evaluating the spatial and temporal variations baseflow estimates using numerical digital filters and tracer-based hydrograph separation methods.	This study applied the recursive digital filtering baseflow separation method and calibrated it with the conductivity mass balance method using electrical conductivity to estimate baseflow and evaluate the spatiotemporal variations at the annual, seasonal, and monthly time scales. (In peer review)
6. Storm event runoff generating processes based on hydrograph separation in two headwater sub-catchments.	Identify and quantify key dominant storm runoff generation components through the application of the tracer-based hydrograph separation at the event scale and conceptualize the flow processes at the sub-catchment level.
7. Conclusions and recommendations	Conclude the findings of the study and the suitability of using tracer-based analysis on understanding catchment hydrological functioning and provide recommendations for future studies.

CHAPTER 2: THE STUDY AREA

The study area is nestled within the Cape Fold Belt Mountains (CFB) of the Table Mountain Group (TMG) in the Western Cape (WC) Province. This chapter describes the characteristic features of the study site, including climate, topography, geology, and land cover, and an overview of previous relevant research in the area. In addition, a brief discussion of the physiographic characteristics and hydrogeology of the Table Mountain Group is given.

2.1. Jonkershoek Valley Catchment and sub-catchments

The study site, the Jonkershoek Valley is a headwater catchment situated in the Western Cape Province of South Africa (33° 57′S, 18° 15′ E) and covers an area of approximately 146 km^2. The catchment lies between the Stellenbosch Mountains in the southwest (SW) and the Jonkershoek Mountains in the northeast (NE) approximately, 10 km from the town of Stellenbosch and 60 km from Cape Town (Figure.2.1). The main Jonkershoek River runs SE-NW, and the river flows originate from streams that are oriented perpendicularly to the central valley on both sides. The Jonkershoek River is a major tributary of the Eerste River which is one of the most important rivers in the Cape Region running through the eastern part (NE-SW) of the Cape Metropolitan Area (CMA). The Jonkershoek catchment was established as an experimental catchment in the late 1930s. Gauging weirs and rain gauges were installed on 6 sub-catchments namely, Bosboukloof, Biesievlei, Tierkloof, Lambrechtsbos A, Lambrechtsbos B, and Langrivier by the South African Forest Research Institute (SAFRI) in the 1940s. The Jonkershoek catchment comprises 6 sub-catchments namely, Bosboukloof, Biesievlei, Tierkloof, Lambrechtsbos A, Lambrechtsbos B, and Langrivier on the north-eastern side of the valley and Swarboskloof on the southwestern side. These headwater tributaries have catchment areas of < 1 km^2 to 2.5 km^2. The current study focuses on three of the sub-catchments; Bosboukloof, Tierkloof, and Langrivier. The criteria for the site selection included accessibility to the sites and installation of additional monitoring infrastructure as well as continuous data records of streamflow and rainfall (1946-2019). These sub-catchments also vary in land use and vegetation cover.

The three sampled sub-catchments Bosboukloof, Tierkloof and Langrivier are on the same side of the Jonkershoek Valley, south-facing and essentially parallel, with perennial streams that are tributaries of the main Jonkershoek River (Figure.2. 2 to Figure.2.4).

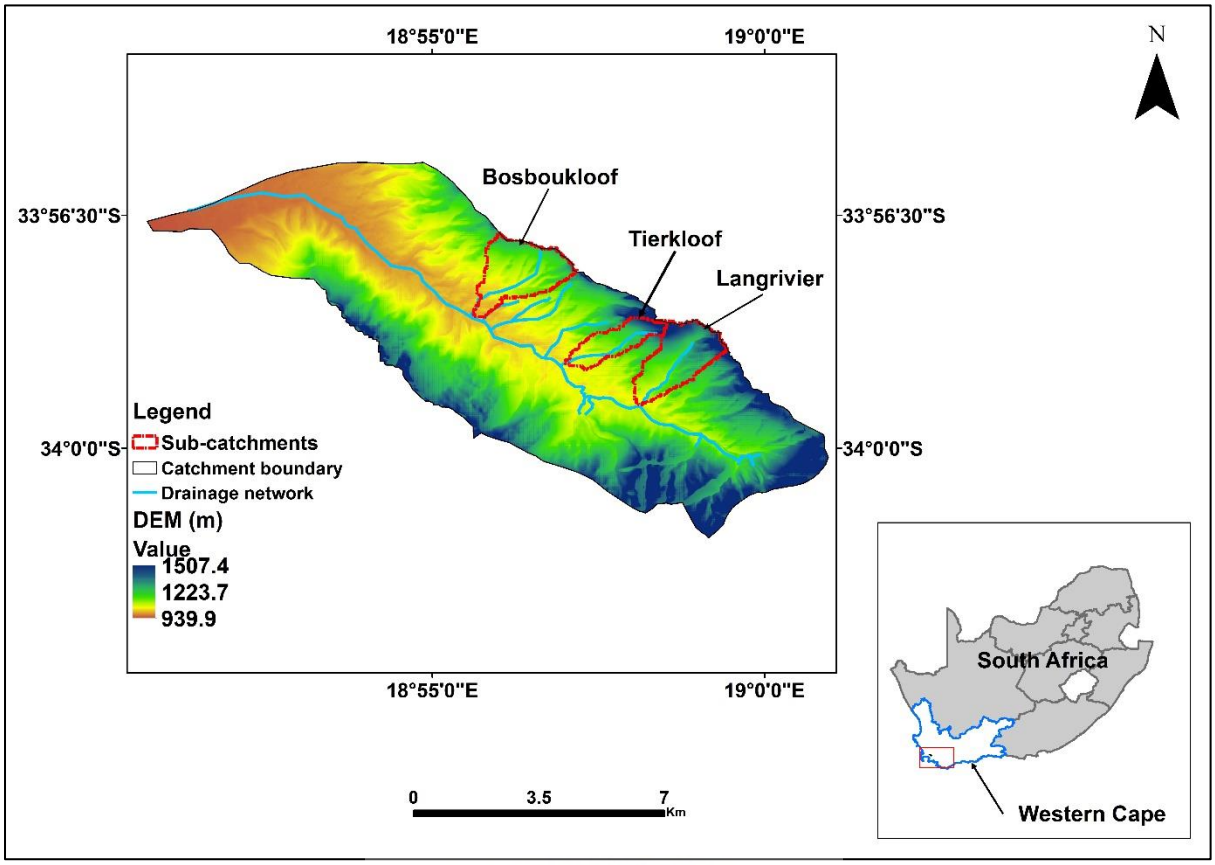

Figure.2.1. Location of Jonkershoek Valley Catchment, indicating study sites and the main monitoring locations.

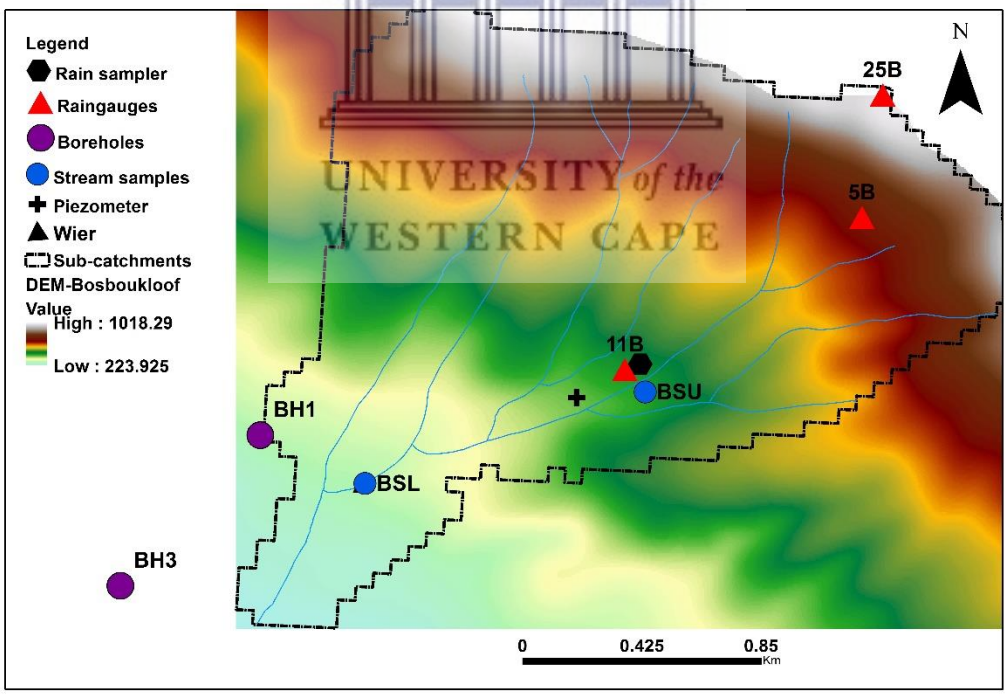

Figure.2. 2. Monitoring sites within the Bosboukloof sub-catchment.

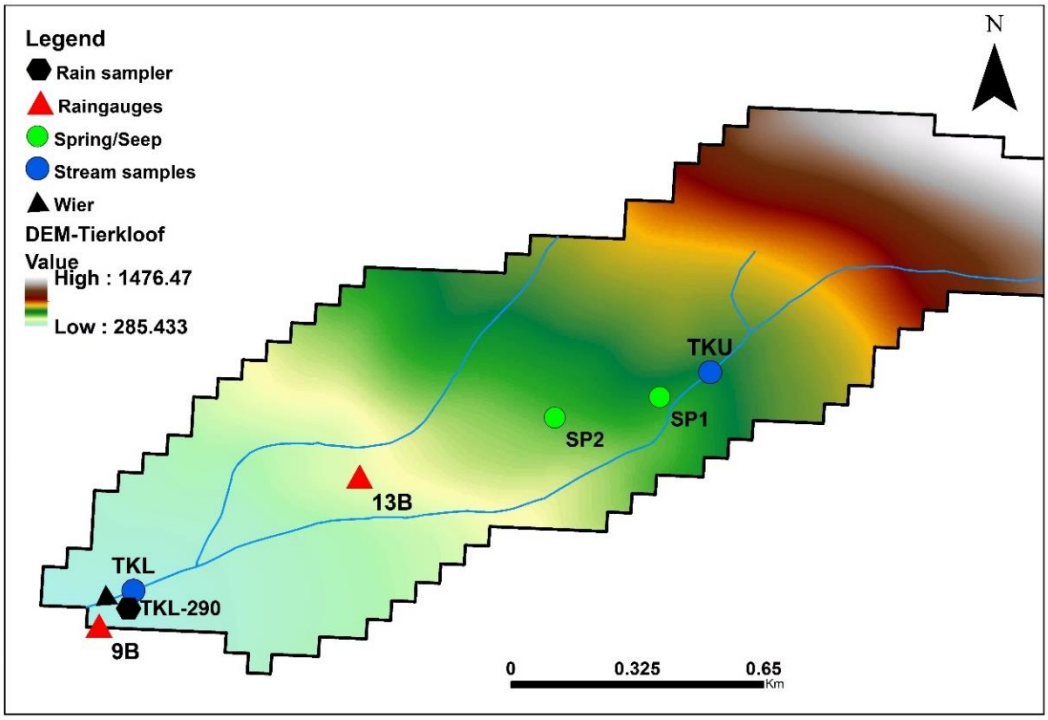

Figure.2.3. Monitoring sites within Tierkloof sub-catchment.

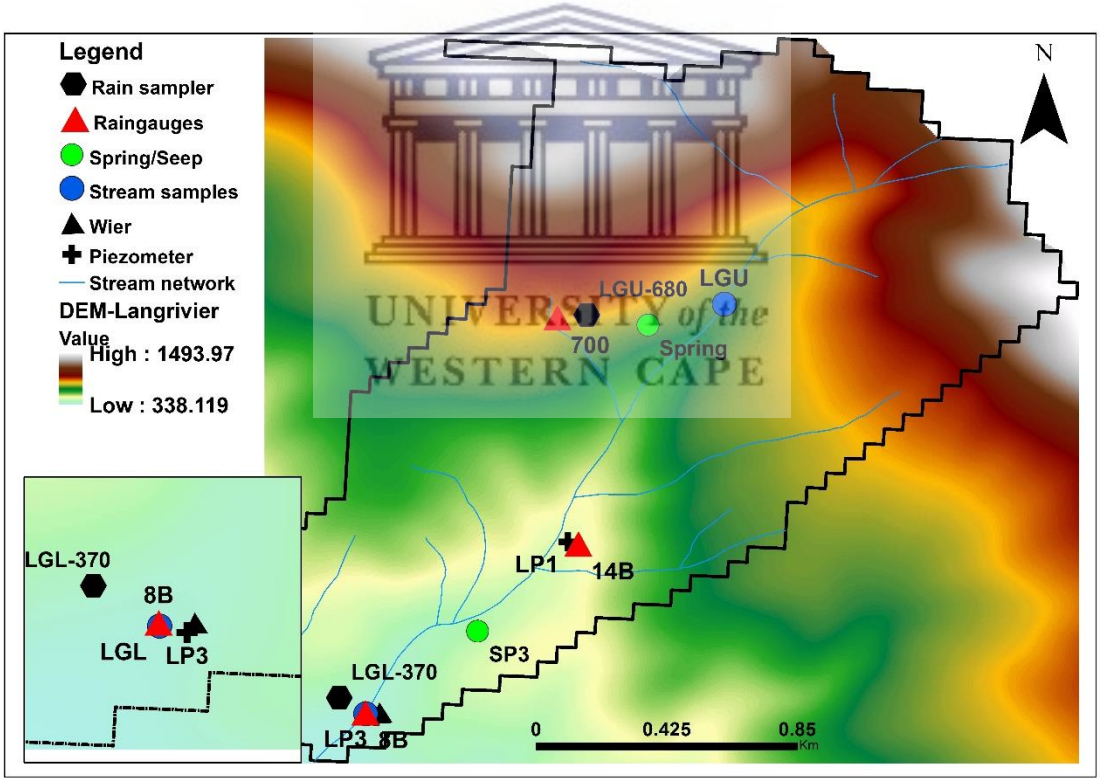

Figure.2.4. Monitoring sites within Langrivier sub-catchment. The insert shows the downstream monitoring stations.

Table.2.1. Summary of the catchment characteristics (Lesch and Scott, 1997).

Name	Area (km^2)	Elevation (mamsl)		Mean slope (degree)	MAP** (mm/a)	MAR* (mm/a)	Vegetation	PET (mm/a)
		Min	Max					
Bosboukloof	2	274	1026	26	1189	276	*Pinus radiata*, fynbos	1335
Langrivier	2.46	366	1460	40	1317	962.4	Fynbos	1461
Tierkloof	1.57	280	1530	46	1137	558.6	Fynbos	1374

*Mean Annual Runoff =MAR (2018-2019), **Mean Annual Precipitation = MAP (2018-2019) catchment average, Potential Evapotranspiration= PET calculated using air temperature from meteorological stations by Hargreaves method (1994).

2.2. Climate and topography

The local topography and drainage system mainly have been influenced by tectonic activities (i.e., Cape Orogeny) (Figure.2.5). The Jonkershoek catchment comprises a long narrow valley, which has been eroded along a line of faulting by the river, elongated northwest to southeast and forming a cul-de-sac "Hoek" which encloses the catchment on the southeastern end (Wicht, 1940). The catchment has a minimum elevation of ± 270 mamsl (meters above mean sea level) with the highest peak reaching an elevation of 1500 mamsl (Scott et al., 2000) (Figure.2.1).

The climate is Mediterranean with hot, dry summers (September to April) and cool wet winters (May-August) (Figure.2.6 and Figure.2.7). The proximity of the WC province to the coast creates a highly variable climate with rainfall influenced by the diverse oceanic and atmospheric circulation systems from both the warm Indian Ocean and the cold Atlantic Ocean. The annual rainfall in the Southwestern Cape province is associated with the teleconnections of the Antarctic Oscillation (AAO) and El Niño Southern Oscillation (ENSO) phenomena.

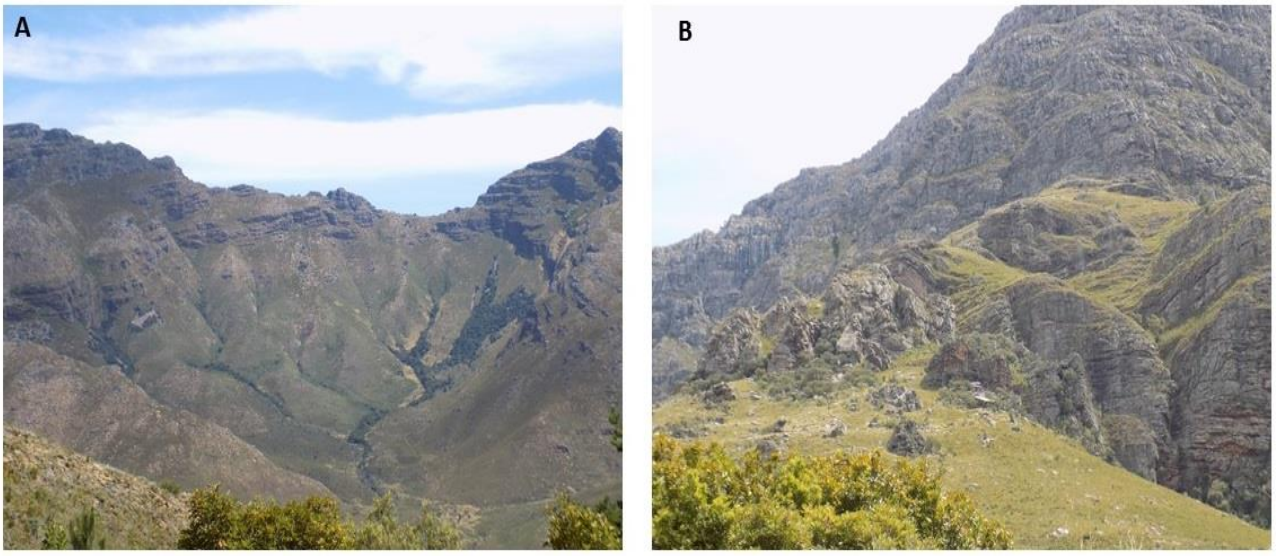

Figure.2.5. Typical topography of the Jonkershoek sub-catchments and exposure of the fractured TMG geology.

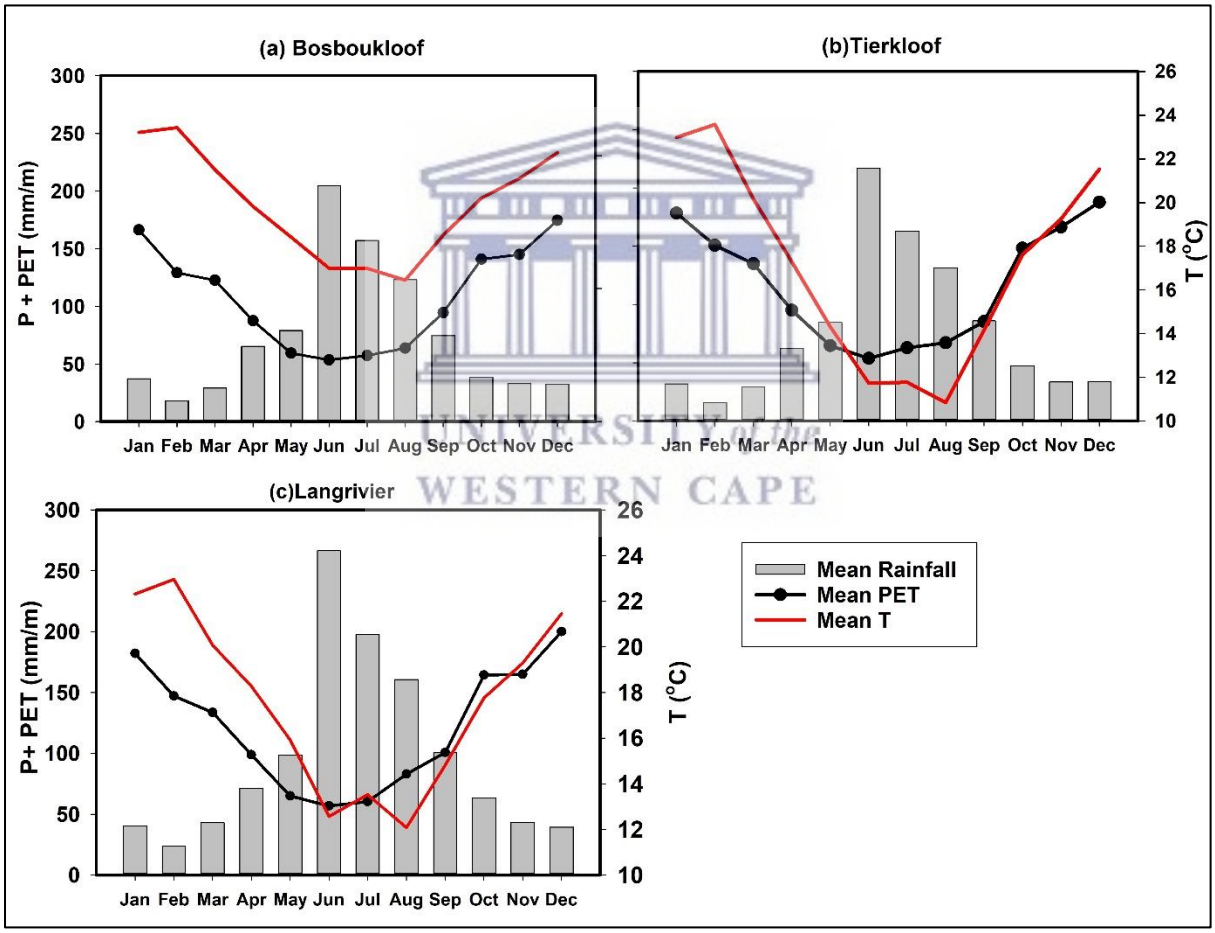

Figure.2.6. Mean monthly rainfall (mm/m), PET (mm/m) and temperature trends of the sub-catchments (a) Bosboukloof, (b) Tierkloof and (c) Langrivier for hydrological years 2018-2019.

Seasonal rainfall patterns are driven by south-easterly dry winds in summer and north-westerly frontal conditions in winter (Wicht, 1934). The highest rainfall occurs on the highest–elevated mountain chains and snowfalls are occasionally experienced on mountain peaks (> 1000 m) during winter (Wicht, 1934; Blake et al., 2010). The area typically receives most of its rainfall during the winter season (May-September), associated with frontal systems, originating over the South Atlantic (Scott, 1997; Du Plessis and Schloms, 2017). Low-pressure cells moving northward from the Atlantic Ocean in the west carries cold fronts and persistent winds inland introducing rain to this region in winter (Chase and Thomas (2007) cited in Du Plessis and Schloms, 2017). These "cut off "of the low-pressure systems cause a disturbance of the airflow (west to east) over the country in the mid-levels of the atmosphere resulting in heavy rains in the western and southern parts. The summer rain is brought in by the strong anticyclonic south-easterly winds originating from high-pressure cells below 25° and 35°S latitudes. According to Wicht et al. (1969), the rainfall is the result of the cooling effect of the south-eastern moisture, the moisture is dry in the valley hence they bring only orographic rain to the higher altitudes during summer.

The regional topography plays a role in determining the climate, hence the rainfall characteristics (intensity and magnitude) in this catchment. Winter rainfall increases from northwest to northeast on the high mountain peaks due to the orographic effect (Wicht, 1934; Fry, 1987). The estimated mean annual precipitation (MAP) exceeds 1000 mm/a (millimetres per annum), with approximately 1,324 mm/a for the monitored sub-catchments (Dye, 2001) and >1500 mm/a in the mountain peaks, with the highest elevation station Dwarsberg, (1234 mamsl) having a MAP of approximately 3300 mm/a (Table.2.1).

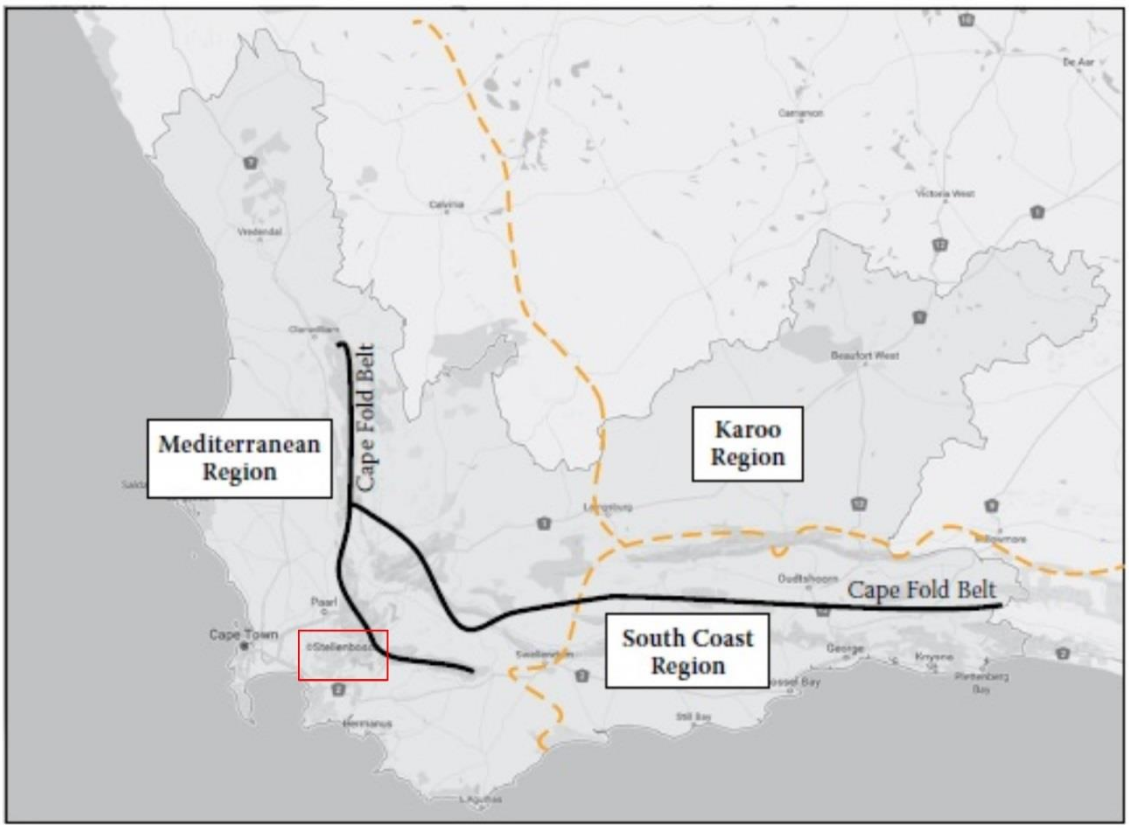

Figure.2.7. Topographic boundary map of the WC province, highlighting the climatic zones (orange dashed line) (after Du Plessis and Schlomb, 2017). The red outline indicates the location of the study site.

2.3. Vegetation, land use and soils

The Jonkershoek catchment like the Cape Fold Belt catchments serves as a home to the indigenous fynbos vegetation, which is mostly restricted to the Cape sandstones (van Wilgen, 1980). The mountain fynbos shrubland dominates the mountain slopes and valleys with little soil cover. The region is dominated by various species of Proteaceae (*Protea repens, Protea neriifolia*), Bruniaceae (*Brunia nodiflora and Widdringtonia nodiflora*), Ericaceae and Restionaceae. The riparian vegetation is dominated by other plant species such as *Ilex mitis*, *Cunonia capensis*, *Pteridium aquilinum*, *Elegia capensis*, *Cannomois virgate*, and *Isochyrolepis gaudichaudiana* (Van Wilgen (1982) cited in Scott et al., 2000, Scott, 1997).

Additionally, the catchment has a history of over 50 years of afforestation with commercial timber plantations of *Pinus radiate* and *Eucalyptus fastigata* mainly in Bosboukloof and Tierkloof, which has resulted in the disturbance and/or removal of the native fynbos vegetation in a large portion of the valley (Figure.2.8). Of the monitored sub-catchments, Langrivier was never planted with timber species and has remained fynbos dominated. The sub-catchments, including Tierkloof, were affected by wildfire in 2015 and the vegetation had not fully recovered at the time of the study. Small remnants of mature plantations (*Pinus* and *Eucalyptus* species) still exist in slope sheltered areas in the sub-catchments, while the remainder is dominated by grass, fynbos species, and recently planted pine saplings.

Bosboukloof, however, was not impacted by this fire and was still dominated by mature pine plantations in 2018-2019.

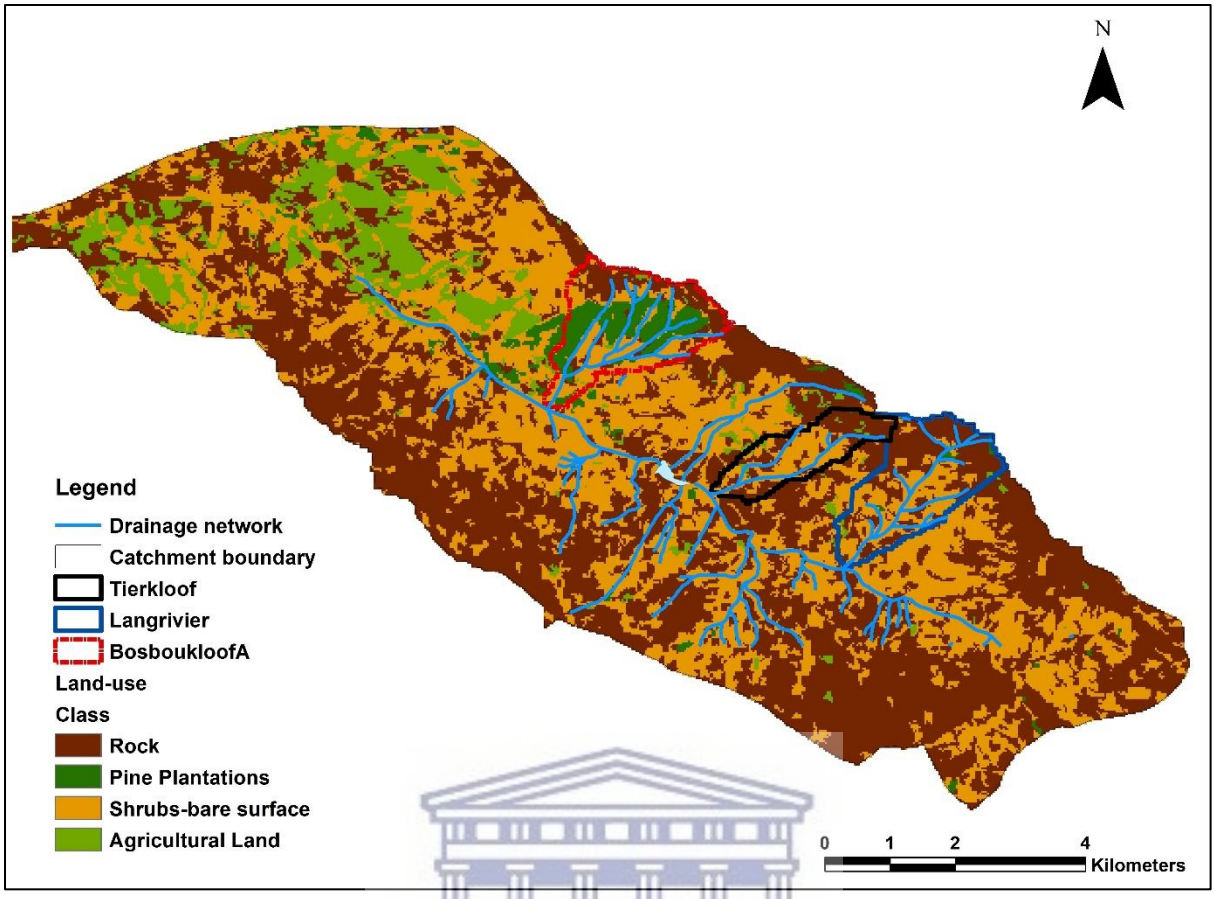

Figure.2.8. Land use/Land cover map of the Jonkershoek catchment indicating the three study sites.

The soils in the catchments are derived from (1) the weathering of shale and porphyritic granite, characterized by white-reddish-brown colour with weakly developed structure and high infiltration capacity and (2) quartzite which are single grained (Fry, 1987). The soils are poorly developed (i.e., friable and structureless) and the soil profile range between 0.8 m and 1.5 m deep (Dye, 2001). However, owing to the heterogeneity of the landscape, depth is a function of the topography and may differ at each sub-catchment due to the nature of the different lithologies. The steeper mid-slope has shallow soil profiles (< 0.5 m to bedrock), and the foot slope is dominated by quartzite-derived soils (> 1 m) with a lower coarse fraction (> 2 mm) (Fry, 1987). The low-lying areas of the catchment are characterized by unconsolidated sandy material which constitutes the area around the main river channel.

Scree and valley-fill alluvial aquifers (i.e., stony sandy soil) are exposed along the main valley and talus material resulting from the weathering of TMG rocks is prominent on the steeper slopes (Rebelo, 2006). The soils of the TMG are nutrient-poor and acidic to support the growth of fynbos vegetation and other plant covers. Organic-rich soils are found near riparian zones and flat or concave areas that

become waterlogged during the wet winter. The production of tannins, fluvic and humic acids from the fynbos vegetation give rise to the reddish-brown colour of the stream water.

2.4. Geology

2.4.1. Local geology

The geology of the Jonkershoek catchment comprises three lithological units, the Malmesbury Group, Cape Granite Suite, and the Peninsula Formation of the TMG on the upper parts of the mountain enclosing the valley on three sides (Van Wilgen, 1981) (Figure.2.10). The tectonic history surrounding the Cape Mountain Belt gives rise to the difference in altitude of the base of sandstones on the NE and SW sides of the catchment which are from 426 to 610 m, respectively (Van Wilgen, 1981). The sedimentary unit was deposited post a period of uplift, which caused the erosion and deformation of the Cape Granite Suite and Malmesbury shale resulting in a flat plain formation. A subsequent period of subsidence led to the sandstones' deposition on this planed surface. Consequently, there is a major unconformity between the basement Cape Granite Suite/Malmesbury Group and the Table Mountain Group (Table.2.2). The Malmesbury Group is the oldest (545-> 750 Ma), comprising of metasedimentary and metavolcanic rocks (greywacke, schist, shale, limestone, conglomerate) (Conrad et al., 2019). There are exposure outcrops of the highly weathered Malmesbury shale in the study area (Söhnge, 1988). In Jonkershoek it is dominated by highly weathered shales exposed along the slopes and roadcuts. The Malmesbury Group was intruded by the Cape Granite Suite, the granite has been dated 552 to 550 Ma (Conrad et al., 2019; Belcher,2003).

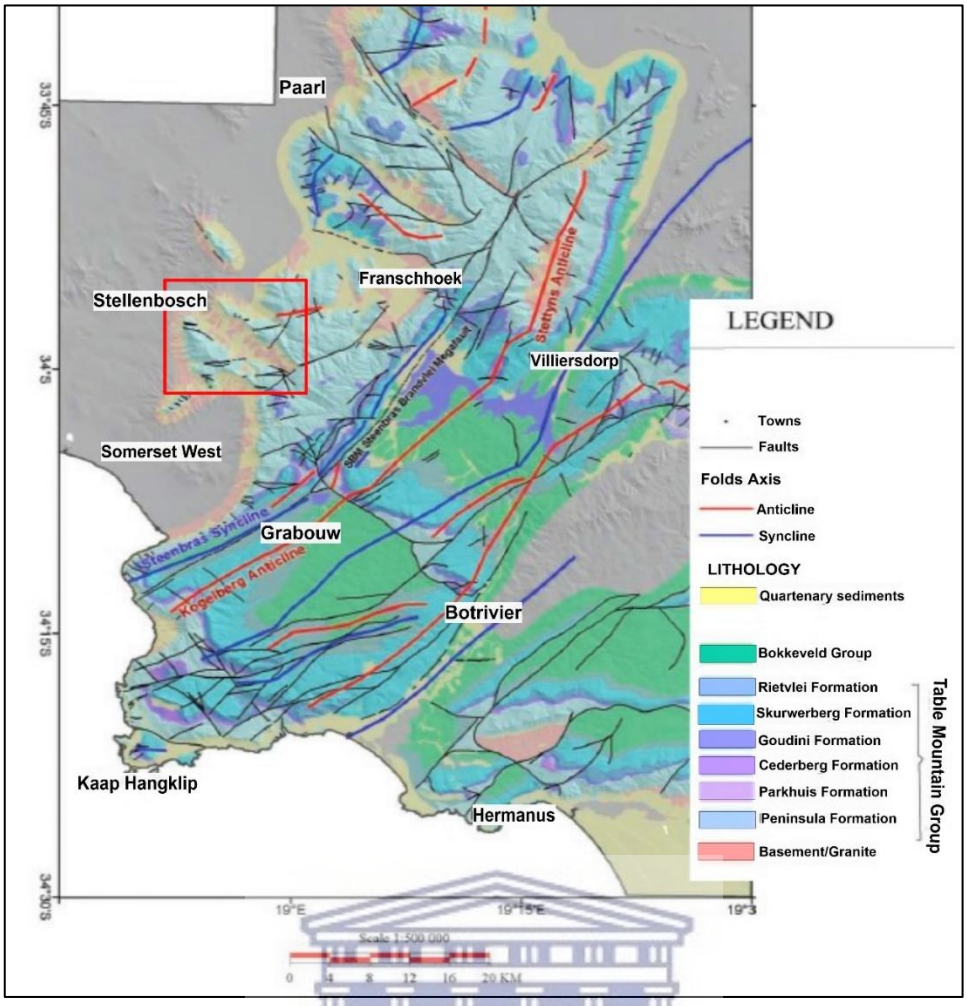

Figure.2.9. Geology of the Table Mountain Group formation and the Jonkershoek study area (red outline) (source: Colvin et al., 2009).

Table.2.2. Stratigraphy of the Table Mountain Group (TMG) (source: Duah, 2010)

Group	Subgroup	Formation	Bed Thickness (m)	Maximum Thickness (m)	Lithology
Bokkeveld			4000		Siltstone, shale, sandstone
Table Mountain (354-417 Ma)	Nardouw	Rietvlei/ Baviaanskloof	0.5 -1	280	Feldsphatic, quartz-arenite
		Skurweberg	1- 2	390	Quartz arenite
		Goudini	0.3 – 0.5	230	Silty sandstone, siltstone
		Cedarberg	0.1 – 0.3	120	Shale, siltstone
		Pakhuis	variable	40	Diamictite, shale
		Peninsula	1-3	1800	Quartz arenite
		Graafwater	0.1 – 0.5	420	Impure sandstone, shale
		Pikenierskloof	0.3 – 1.5	900	Quartz arenite, conglomerate, shale
~~Major unconformity~~~~~~					
Basement (495-545 Ma)		Gamtoos and Kaaimans argillite comprising moderately to light metamorphic sedimentary rocks and Cape Granite Suite			
Malmesbury (545->750 Ma)		Meta sediments Comprise, shales			

The Cape Granite Suite forms the floor in the Jonkershoek valley. The weathered granites in the catchment are exposed along the slopes outcropping as large boulders, and evident at road cuts, at elevations greater than 500 mamsl on both the northern and southern flanks. The weathered granite has produced clayey soils (whitish) with angular coarse grains which cover most of the surface. The granite in this catchment is porphyritic and constitutes of alkali feldspar phenocrysts, alkali feldspar, albite-

oligoclase, quartz and biotite with accessory magnetite (Söhnge, 1988). Exposure of massive coarsely porphyritic outcrops occurs along with the road cuts and slopes (e.g., Langrivier and Tierkloof).

The sedimentary sequence of the Peninsula Formation unconformably overlies the Malmesbury Group shale and the Cape Granite Suite, with a thickness of ~ 550 m in Table Mountain and surrounding areas. The thickness may be difficult to measure due to extensive thrusting and folding (Diamond, 2014). The Peninsula Formation comprises early to late Ordovician white sandstone and quartz arenite with intermittent thin shale bands (Rust, 1967). It forms the largest part of the geology at the mountain peaks in the Jonkershoek. Peninsula Fm consists of thickly bedded highly folded and faulted, jointed, siliceous and less erodible quartzitic sandstone outcrops as cliffs (~30 %) and creates steep slopes in the upper parts of the catchment while the highly weathered shales and feldspathic granites are exposed on the foot-slopes, with gradients of 15° to 29° (Thamm, 2000). The sandstones consist of quartz grains, minor feldspar, chert grains with occasional shale bands, and clay mineral matrix (Söhnge, 1988). The sandstones present a tainted whitish-reddish brown colour in some places owing to the atmospheric exposure which led to oxidation. Minor faults are also present (Figure.2.10). The sedimentary package of the Peninsula Fm is characterized by multiple small folds dipping 10° to 20° NNE near Swartboskloof sub-catchment on the southern flank (Söhnge, 1988) and 40° NNE which occurs on the northern flank of the catchment in the Langrivier sub-catchment (CGS MAP, 1: 125 000). The sandstone beds are slightly gentle where they are in contact with the granite floor at 50°– 80° westerly.

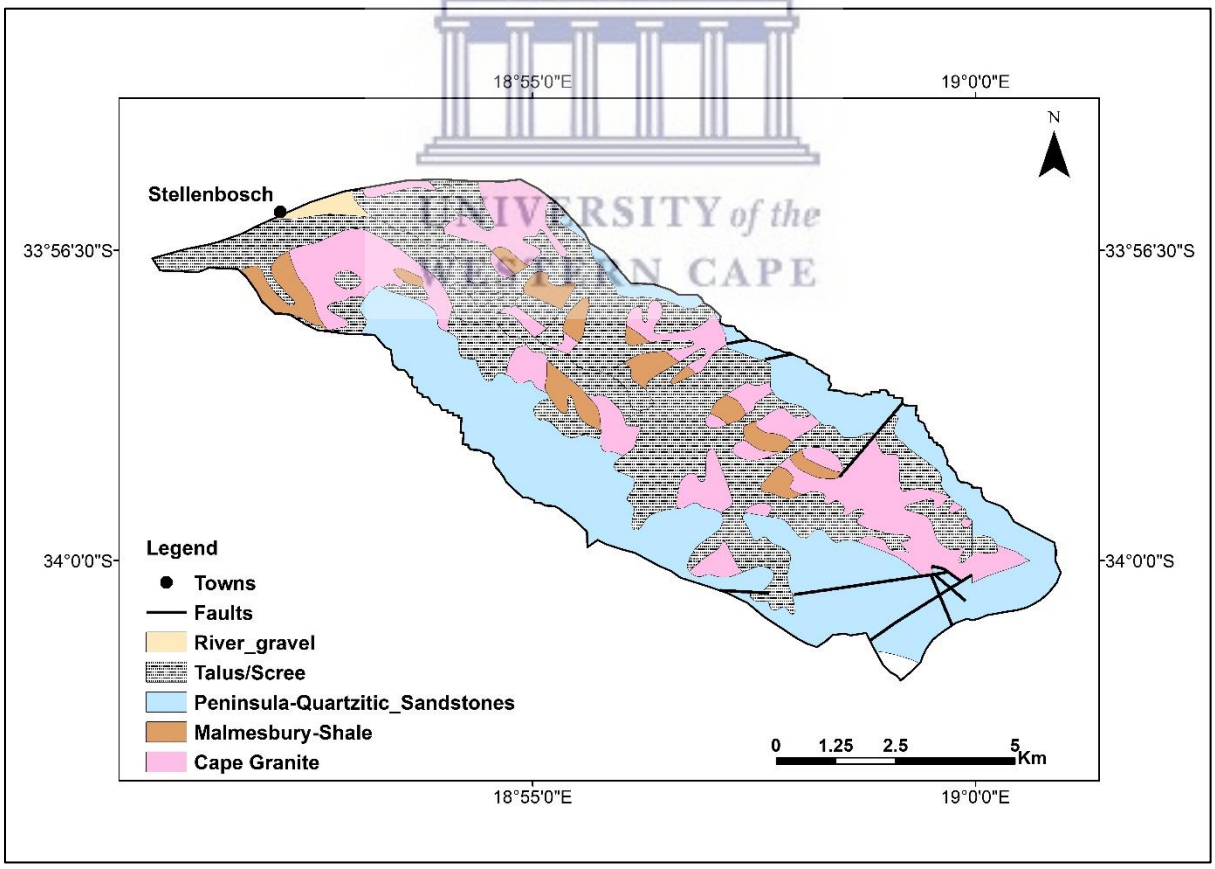

Figure.2.10. Geology map of the Jonkershoek catchment (source: Council for Geoscience, 1:125 000).

The talus and scree deposits which cover most of the slopes are derived from eroded granite and sandstones (Söhnge, 1988) (Figure.2.10 and Figure.2.11). The surface geology is dominated by a variety of deposits such as talus scree with sandstone clasts, scree containing granite boulders and sandstones, granite- and -sandstone-derived colluvium, avalanche scree devoid of sandy matrix and river–borne alluvium (Söhnge, 1988). The erosion in this catchment resulted in an "amphitheatre" feature in some sub-catchments (e.g., Bosboukloof and Swartboskloof).

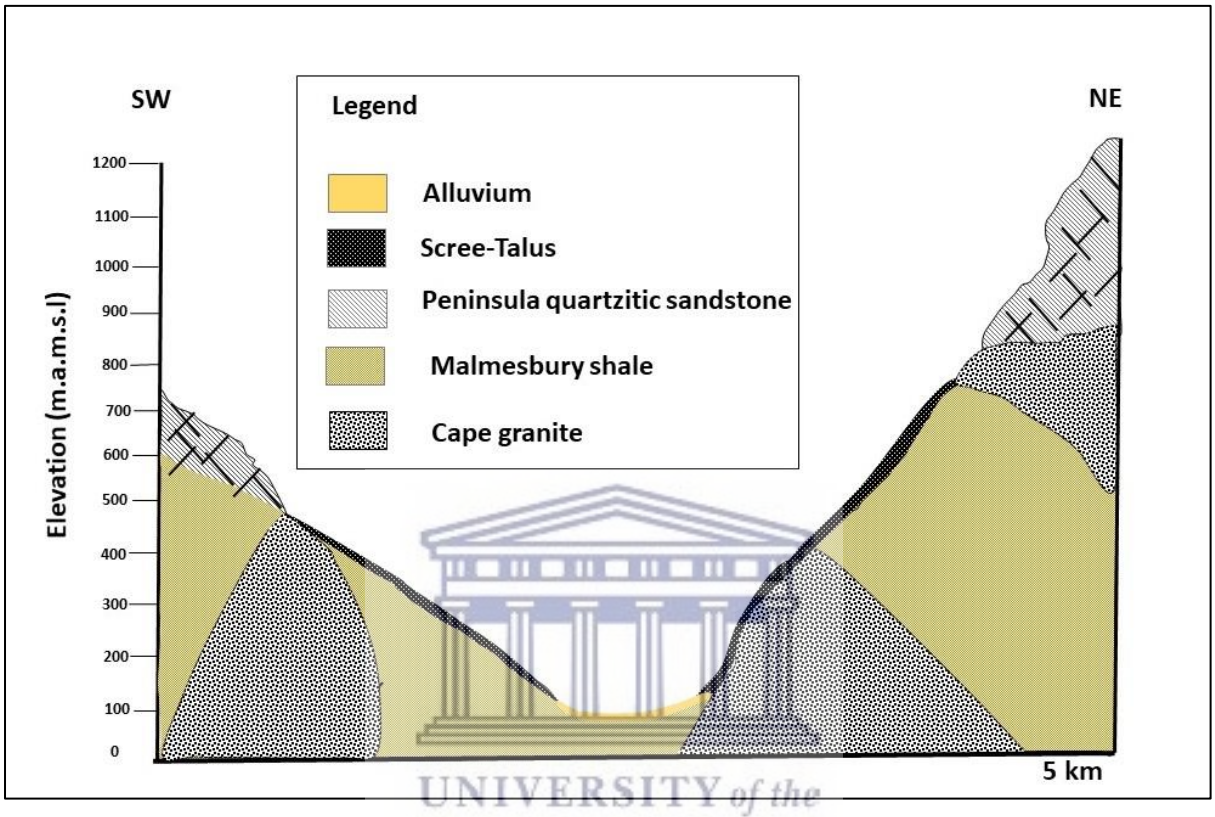

Figure.2.11. Cross-sections (SW-NE) of the Jonkershoek catchment including the main lithologies (the dashed line indicates the interpolated contacts).

2.5. Hydrogeology and hydrology

2.5.1. Hydrostratigraphy

The hydrological characteristics of the Table Mountain Group aquifer have been covered extensively in the literature. The TMG aquifer system is one of the three main aquifers in South Africa in terms of yield and aerial distribution (Weaver et al., 1999). The greater sub-surface volume, greater depth, maximum recharge potential and wide-aerial extent (248, 000 km^2) of the thickly bedded clean quartzites (900 to 4000 m) with relatively low mineralization (TDS < 300 mg/l) and low pH (<6) (Kotze, 2002), make it hydrologically important and ideal for groundwater exploitation (Xu et al., 2009, Thamm and Johnson, 2006). According to Rosewarne (2002), the physiographic settings of the regional TMG aquifer resulted in two hydrogeological domains the intermontane and coastal domain. The Jonkershoek

valley forms part of the intermontane domain characterized by direct recharge from the rainfall and occasional snowmelt, deep groundwater circulation, high elevation cold springs and low conductivity of groundwater. The water quality and the springs will be discussed further in the subsequent sections.

Table.2.3. Stratigraphy and hydrostratigraphy of the Table Mountain Group (Blake et al., 2010), (Duah, 2010). The red box represents the hydrostratigraphic units in the Jonkershoek valley.

Hydrostratigraphy		
Superunit	**Unit**	**Sub-unit**
	Quaternary Aquifer	
Major unconformity		
	Gydo Mega-aquitard	
Table Mountain Superaquifer	Nardouw Aquifer	Rietvlei Subaquifer
		Verlorenvalley Mini aquitard
		Skurweberg Subaquifer
	Winterhoek Mega-aquitard	Goudini Meso-aquitard
		Cederberg Meso-aquitard
		Pakhuis Mini aquitard
	Peninsula Aquifer	Platteklip Subaquifer
		Leeukop Subaquifer
	~~Major unconformity~~~~~~~~	
Basement rock	Basement Aquicludes	

According to the hydrostratigraphy of the TMG (Blake et al., 2010), the Jonkershoek catchment forms part of the Peninsula aquifer unit of the main TMG aquifer system which covers areas such as Franschoek, Stellenbosch and Kogelberg (Table.2.3). The model illustrates that the Peninsula Formation aquifer in the Jonkershoek and surrounding areas (i.e., Franschoek, Stellenbosch and Kogelberg) is, shallow and outcrops at the surface only on the upper cliffs and mountain peaks or has been eroded by the basement. The top aquifer elevation range from 500 to 2500 mamsl and the bottom range from 0 to -1313 mamsl (Blake et al., 2010).

2.5.2. Hydraulic properties

The past tectonic activities caused lower greenschist-facies metamorphism resulting in cementation and recrystallization of sedimentary grains in the TMG. These processes altered the primary porosity of the TMG of most sandstones, hence the TMG aquifer is dominated by secondary porosity enhanced by the joints, fissures, faults and micro folds (Kotze, 2002). Therefore the flow of water through the rocks in the Cape Supergroup is primarily via fractures and the porosity of aquifer rocks is highly dependent on the interconnectivity of the different fractured systems(Harris et al, 1999).

The TMG sandstones in the Swartboskloof sub-catchment of the Jonkershoek were reported to show low groundwater storage due to their steep topographic gradients and the non-horizontal bedding planes (Stone, 1985). In areas where the granites are fractured and deeply weathered associated with clays, Stone (1985) found that the weathered granites are likely to provide highly porous conditions capable of storing considerable quantities of groundwater and the low permeability of clay would result in slow release of stored water, which was indicated by the long recession of discharge during dry periods.

2.5.3. Groundwater and springs characteristics

2.5.3.1. Groundwater recharge and discharge

The groundwater recharge in the TMG aquifer is driven by single or multiple rainfall events and occurs at high elevated areas > 1000 m (Diamond and Harris, 2000). The highest recharge rate of 137.17 mm/a was reported in hydrological unit 5 which covers the Jonkershoek catchment related to a MAP of 1842 mm/a meaning that about 7.5% of rainfall becomes recharge. Kotze (2002) estimated the recharge in Jonkershoek to be 18% of the average monthly rainfall (66 mm). Brendenkamp et al. (1995) estimated the recharge rate in the order of 35% of 1063 mm/a MAP in the neighbouring Zachariashoek catchment. Based on the high altitude of the TMG sandstones and the orographic rainfall, it could be assumed that significant groundwater recharge occurs directly from the winter rainfall, which has been reported to exceed 1500 mm/a at the tops of the Jonkershoek Mountains (SAEON, 2020).

Owing to the nature of the geology in this catchment, recharge in the TMG aquifer potentially occurs primarily through the main geological structures (i.e., contact zones, fault zones, inter-fractures, and joints). The fractures extend to a depth > 200 m in some places promoting rapid recharge and infiltration to deeper groundwater (Diamond, 2014). Rainfall infiltration and groundwater recharge near the surface in the TMG aquifers are promoted by the weathered nature of the shallow rock layers and fissures (Wu, 2005).

Recharge processes at the elevated TMG area of the catchment may differ from those on the lower slopes covered by scree-talus consisting of boulders of sandstones and fragments of weathered granite. However, there maybe be an interconnection between the TMG aquifer and the granite aquifer owing to the weathering, fracturing and localised faulting processes enhancing the water-bearing properties of the granite aquifer (Harris et al., 2010). The highly permeable scree covers the slopes and can vary in

depth becoming deeper at the foothill slope. Recharging water in deep scree material moves rapidly down the profile, whereas in shallower soils where the scree overlies the less permeable granitic material, the contacts limit the vertical movement of water (Fry, 1987).

Sõhnge (1988) and Stone (1985) found that the talus scree on the slope of Swartboskloof receives water from the hidden fractures in the basement granite and shale which has the potential to enhance infiltration during rain events. The typically high gravel and rock content, bulk density and high pore volume of the TMG derived soil cover support high infiltration capacity and percolation (Versfeld,1981 cited in (Scott, 1997). According to Stone (1985), the streams in Swartboskloof sub-catchment display influent and effluent characteristics acting as an area of discharge and recharge. The study suggested that the stream loses water in the centre of the catchment, linked to the channel size and high composition of debris and scree. This could be an important recharge mechanism for the granite aquifer and/or the scree-talus aquifer in addition to rainfall.

The interaction of physiographic characteristics such as climate (rainfall and temperature characteristics), vegetation cover, soil conditions (thickness/texture), lithology, antecedent moisture conditions and morphology of the catchment determine recharge (Parsons, 2002; Wu, 2005). This might be the case in Jonkershoek, where slopes are covered by fynbos shrubs, pine plantations, deeply weathered bedrock, scree-talus and the soils are poorly developed. Vegetation cover controls the rate of infiltration of rainfall, unlike in non-vegetated or forested catchments, the stable vegetation cover slows down runoff and promotes infiltration through the porous soil horizons. However, in semi-arid regions with spatially variable intra-annual rainfall, interception and evapotranspiration may result in reduced recharge. Therefore, only a small fraction of the intercepted water may reach the soil through stem flow and recharge the groundwater table which sustains the streamflow during the dry summer as delayed seepage. The interception loss amounts to approximately 12% of the rainfall in the pine-forested catchments (Wicht et al., 1976).

2.5.3.2. Discharge: Springs and seep zones

According to Lin (2008), in an anisotropic fractured system such as the TMG, the preferential flow paths are likely to be interrupted, emerging at the surface rather than proceeding vertically in the form of interflow before it can recharge the bedrock water table. The groundwater discharge occurs as interflow at the soil-rock interfaces and preferential fracture zone above the local stream water table and gives rise to springs and seepages. The springs may also occur where water-bearing fractures (i.e., faults, fissures) in the TMG sandstones intersect the surface or at the contact between the Peninsula sandstones and the impermeable shale indicating that groundwater flow is limited to the upper levels where the fracture network is best developed (Wu, 2008). The springs and seep zones are found to be significant streamflow contributors in mountainous catchments of the TMG geology region sustaining the streamflow, especially during the dry summer (Roets et al., 2008; Xu et al., 2003).

The TMG springs are controlled by lithological contacts or changes in permeability associated with the fault (Colvin et al., 2009). The seepages are exposed by the construction of roads or paths. Meyer (2002) identified distinct types of TMG springs: shallow circulating, lithology-controlled, and fault-controlled springs. Shallow circulating springs are low yielding, seeps from networks of joints, irregular fractures and bedding place draining reservoirs during and after rain events. These types of springs display ephemeral characteristics, drying up as the dry summer commences. Lastly, the lithology-controlled springs are characterised by discharge due to the presence of impervious layers (i.e., interbedded shale layers) (Figure.2.12). This type accounts for the perennial cold springs within the TMG.

The absence of deep-seated faults limits the occurrence of thermal springs within the Jonkershoek catchment. The TMG cold springs may occur in two ways, either as lateral flow in the unsaturated zone, promoted by fractures re-emerging as springs, or where the confining layer hinders further percolation by forming a shallow perched aquifer/water table (Hughes, 2010) (Figure.2.12). The lateral flow is induced by gravity as the main source of movement or alignment of fractures and contributes to streamflow in the catchment with steep topography (Hughes, 2010; Issar and Kotze, 2003). The decrease in vertical percolation may decrease as the fracture density decrease with depth (Hughes, 2010). Furthermore, springs may issue where infiltrating recharge water intersects the regional groundwater table with the surface. The springs and seepages in the Jonkershoek catchment appear at the base of the Peninsula Fm, immediately above the granite (Söhnge, 1988). These springs and seeps are seasonal and not connected to the greater groundwater flow system (Kotze, 2002), indicating interflow, or rejected recharge which is characteristic of the Peninsula aquifer. As observed in the Table Mountain springs, it is reasonable to suggest that the TMG springs in the Jonkershoek occur at the unconformity between the TMG and low permeability Cape granite or the Malmesbury Group. In Jonkershoek the springs are occurring as waterfalls or drips along the roadcuts hence the geological discharge points of these TMG springs are also uncertain as in most TMG areas (Diamond, 2014)

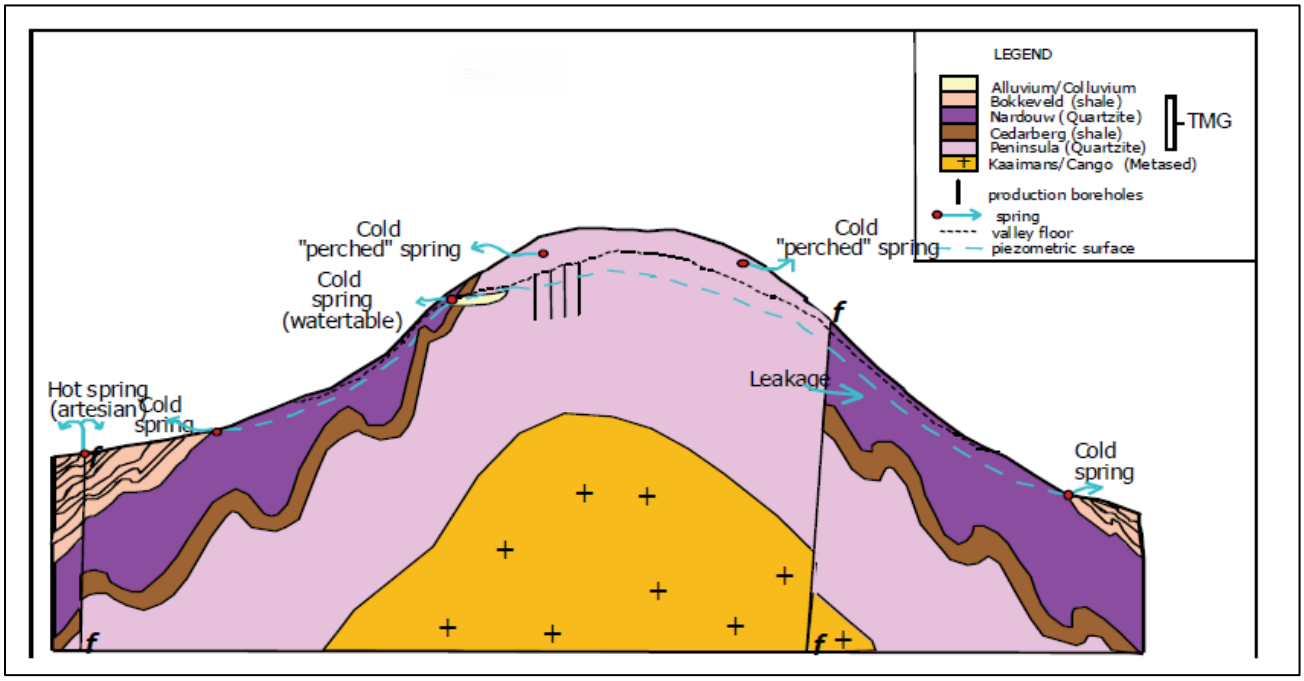

Figure.2.12. Illustration of common spring type in the TMG area example from Kammanassie (Cleaver et al., 2003)

2.5.4. Surface water hydrology

South Africa is classified as a semi-arid region characterised by low annual rainfall of 490 mm/a, however, the country depends highly on surface water resources as the main source of water supply. However, due to the current water scarcity, large groundwater systems such as the TMG aquifer are being considered as additional future sources of bulk water supply. The groundwater discharge from the TMG sustains the river systems in the Western Cape Province which contribute to various ecosystem services. Most of the tributaries are perennially deriving their source waters from the Cape fold Mountains (Clark and Ractliffe, 2007).

Streamflow sources in the TMG

Streamflow at most mountainous headwater catchments is derived from groundwater storage. The rate and mechanism of the discharge depend highly on the rainfall, storage and catchment physiographic characteristics (Smakhtin, 2001). The surface water network in the Cape Fold Belt is dominated by perennial rivers and streams which are linked to the groundwater discharge from the TMG aquifers (e.g., Peninsula Fm aquifer) through various lithological structures (Colvin et al., 2009). According to Colvin et al. (2009), the TMG aquifer discharge directly contributes to flow in headwater tributaries maintaining their perennial character throughout the year.

Streamflow can be generated by various mechanisms, namely: direct channel precipitation, overland flow (on either saturated soils or surfaces with low infiltration capacity), and subsurface flow pathways i.e., interflow (which may include translatory flow), and groundwater outflow (Freeze, 1974; Renshaw et al., 2003). Researchers (e.g., Midgley and Scott, 1994; Xu and Beekman, 2003; Saayman et al., 2003,

Roets et al., 2008) have put forth conceptual models regarding the roles and relative contributions of these components to streamflow in TMG catchments. Saayman et al. (2003) developed a conceptual model for the Zachariashoek catchment, located east of the Jonkershoek, suggesting multiple dominant flow pathways, with a surface runoff on the steep slopes as well as recharge in the mountains contributing to spring flow or seep groundwater discharge in the foothills. Midgley and Scott (1994), showed that 90 % of the streamflow is due to the large displacement of groundwater from storage rather than surface runoff in the Jonkershoek. This suggests that the streamflow in these regions is dominated by subsurface flow which follows multiple geologically controlled paths occurring as springs and seeps (Colvin, 2008). These springs are the function of annual and seasonal rainfall usually reflecting the isotopic composition of the high-altitude rainfall during the winter/recharge season (Diamond and Harris,1997).

Roets et al. (2008) developed a conceptual model describing groundwater discharge mechanisms and contributions to surface resources using GIS (Geographic Information System) techniques based on geomorphological, geological and ecological characteristics of the TMG aquifer. The main processes were: (1) groundwater flow and (2) interflow/translatory flow (rapid or delayed) (Figure.2.13). Groundwater flow refers to discharge from the saturated zone through seepage faces and spring discharge associated with geological structures (fault zone or contact areas) at various locations on hillslopes (Buttle, 1998; Kotze, 2002). For this process to occur one geological unit an aquitard, and the aquifer boundary conditions will give rise to a semi-confined or confined aquifer that will discharge water at geological contacts or faults provided the water table is high enough (Roets et al., 2008). This process provides continuity of flows to the stream during extended periods of dryness or between rainfall events.

Interflow is a lateral subsurface flow that does not contribute to the water table of a persistent aquifer, contributes in two ways, either as rapid or delayed flow. Delayed interflow may result from partially saturated flow via a transient perched water table, or where there is the interconnection of fracture networks, both mechanisms dependent on the antecedent soil moisture conditions in a catchment (Roets et al., 2008). Rapid interflow results from preferential flow paths, or where a soil or rock horizon acts as a flow barrier, hindering direct downward percolation of water.

Translatory flow occurs in the unsaturated zone and can play a significant role as a source of runoff headwater catchment. Like interflow, translatory flow occurs either as delayed or rapid flow. The dominance of this process has been reported in many headwater catchments with a contribution of >80% to total flow (Midgley and Scott, 1994; Blume et al., 2008). Blume et al. (2008) reported large pre-event water fractions with lag times of hours between surface and groundwater in the Malalcahuello catchment, Chile. They concluded that the large pre-event water contributions were due to the replacement and rapid down-slope transport of old water. According to Kirchner (2003), streamflow in small headwater catchments responds quickly to rainfall input but the fluctuations in tracers such as water isotopes or chloride are strongly damped. These processes result from the displacement or push

out of previously stored recharge by the next recharge event infiltration. The discharge is driven by the gravitational force downslope replacing or flushing out old water. The rapid and delayed flow mechanisms depend on the antecedent soil moisture conditions and the intensity and duration of the rainfall.

In addition to these three processes, other mechanisms such as overland flow and direct channel rainfall may contribute to runoff in the TMG (Roets et al., 2008) (Figure.2.13). However, these processes are only significant during flood events, whereby steep slopes and exposed rock common in TMG headwater catchments promote overland flow or in low-lying areas with less vegetation cover (Hewlett and Bosch, 1984). Wildfires which are frequent in the Cape Floristic Regions also reduce vegetation cover and change soil properties (Freeze, 1980). Wildfires influence the soil hydraulic conductivity resulting in more hydrophobic soils (Scott, 1997), hence instigating infiltration excess overland flow.

Roets et al. (2008) linked the relative contributions of these different mechanisms in adding water to the channel to the topographical position of a river reach. The catchment topography was divided into four zones namely, the headwater, mountain, foothill and lowland reach. The dominant processes at mountain reach during both dry and wet winter baseflow conditions were interflow as discharge from the TMG springs and seeps and rejected recharge to the TMG aquifer. At foothill reaches, the dominant additional contributors to streamflow were limited to the bank storage discharge, depending on antecedent conditions. In the wet winter, increased baseflow at both mountain and foothill reaches is sourced from increased TMG groundwater discharge. The mountain reaches are also likely to receive increased interflow, delayed translatory flow and limited bank-storage discharge in the wet winter. At the headwater reach, increased spring flow and increased interflow were assumed to be the dominant processes.

Dry summer or low flow period streamflow is derived from groundwater storage. However, various factors such as infiltration characteristics of the soil, the hydraulic characteristics and extent of the aquifer, the rate, frequency and amount of recharge, evapotranspiration, distribution of vegetation type, topography and climate influence the flow regime (Smakhtin, 2001). In fractured geology systems such as the TMG, the dry summer baseflow is generated by groundwater discharge from perched springs (headwater reach), TMG springs and seeps and interflow (re-emerging rejected recharge) is more dominant in maintaining the perennial streams at mountain reach (Roets et al., 2008). According to Smakthin (2001), in steeply sloping terrains the groundwater re-emerges as drainage in fracture zones (springs) above the main water table and has a significant lateral component that intersects the groundwater surface. The rate and duration of release will depend on the fracture size and density, as well as storage. At foothill reach, groundwater from mountain reach TMG springs, primary groundwater discharge zone from TMG (confined to semi-confined aquifers) as well as bank storage are the dominant processes during the low flow period (Roets et al.,2008).

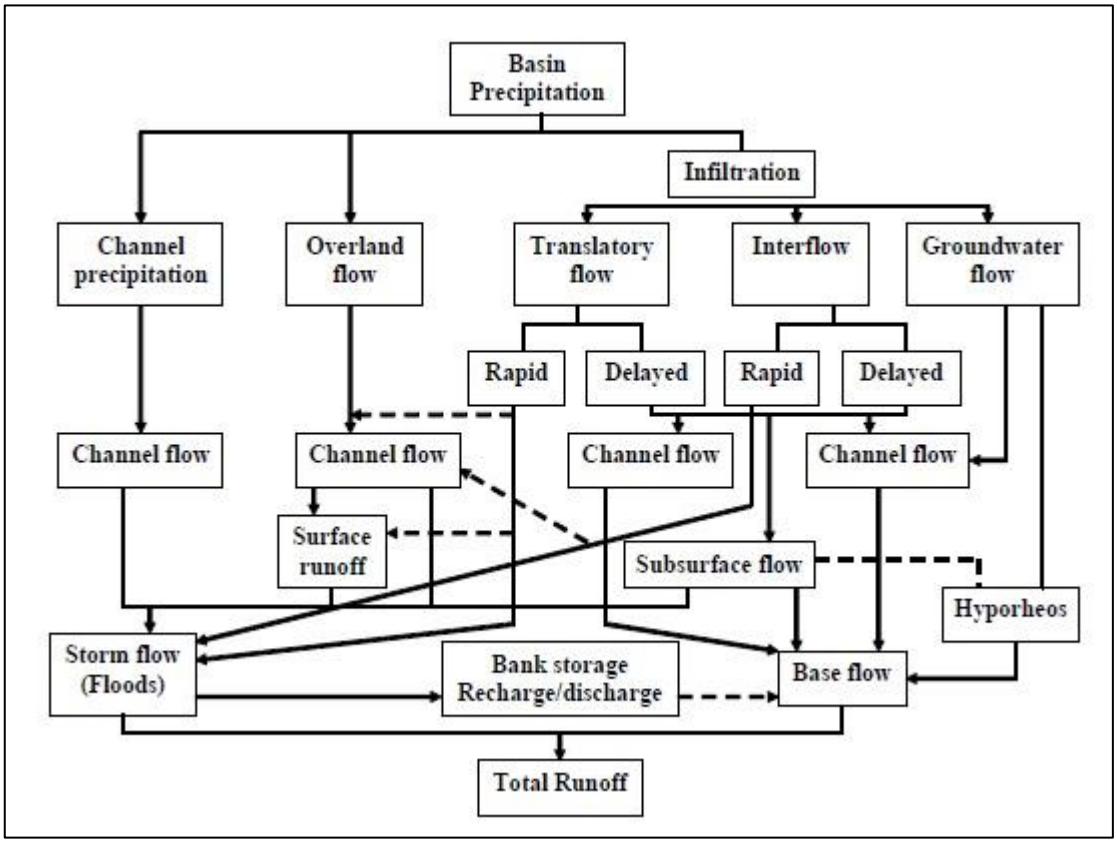

Figure.2.13. Schematic presentation of runoff generation processes in the TMG (Roets et al., 2008).

2.5.5. Water quality

Water chemistry measurements can reveal essential information such as the flow pathways and effects and scale of chemical processes such as water-rock interactions (Hugenschmidt et al., 2015). They can further provide valuable information on the quality of water which is critical for regional water resources management. Knowledge of the number of dissolved solutes such as major ions, salinity, and total dissolved solids (TDS) is crucial for the sustainable development of an aquifer as these parameters could compromise the quality of water.

The stream chemistry results from an interplay between a range of factors such as atmospheric deposition, groundwater recharge, weathering of rock and riparian vegetation (Smit, 2002). The TMG headwater streams are characterised as pristine. The surface water is relatively "pure" due to the chemically inert geology giving rise to low ionic concentrations and TDS (<100 mg/l) (Clark and Ractliffe, 2007). The hydrochemical concentrations in the TMG dominated streams and rivers are extremely low due to high rainfall in the mountain areas and weathering of rocks which have resulted in the past leaching of minerals from the sandstones and the intrusive granites. Moreover, the Peninsula Formation rocks are generally poor in feldspar and mica minerals (containing K, Na and Ca) except for quartz and small quantities of iron (Fe) (Day and King, 1995). The major ions in these catchments have low resolution mostly less than 3 ppm. Duah (2010) reported EC values of 10.9 mS/m (109 µS/cm) in Gevonde, while Gale (1992) showed values of < 80 µS/cm in the Palmiet River. The Palmiet River

makes a great comparison with the Jonkershoek as they are both headwater streams and similar geology (i.e., the Peninsula Formation sandstones) and terrain dominated by mountain fynbos.

The hydrochemical characteristics of streamflow in the TMG intermontane region are affected by talus-soil water and riparian vegetation. The stream water has a pronounced reddish-brown colour and can be foamy, which is attributed to the presence of the indigenous fynbos vegetation that covers the steep mountain slopes (Midgley and Schafer, 1992). The leaching of dissolved organic carbon (DOC, > 10 mg/l) such as tannins, phenols, humic/fluvic acids and saponins from the fynbos vegetation litter and roots acidify the soil, resulting in highly acidic, low pH and deep brown colour of stream water (Drever, 1997). The carbonate buffering from the arenaceous bedrock compositions can reduce the pH of surface water to 4 (Day et al., 1998)

The general pH of the TMG stream water is low (4 to 6) relative to that of groundwater (between 5 and 8). Most of the stream water pH values reflect that of rainwater (Britton et al., 1993). Britton et al. (1993) reported stream water pH values within the range of 4.95 to 5.47 and rainwater values of 3.74 to 5.11 in the Swartboskloof catchment. Midgley and Schafer (1992) reported a higher average value of 6.16 and values between 5.15 and 6.72 for pine-dominated catchments (i.e., with red colour soils like those of the Jonkershoek) within the Southern Cape.

Groundwater in the TMG aquifer is generally considered to be of high quality due to the low chemical concentrations and inert quartzitic nature of the host rock (Smart and Tredoux, 2002; Clark and Ratcliffe, 2007; Diamond, 2014). The TMG springs are generally of high quality, with electrical conductivity (EC) values ranging between 10 and 35 mS/m (millisiemens per meter) and TDS < 30 mg/l (Miller et al., 2017). The Peninsula Fm groundwater has slightly lower EC values compared to other geological units of the TMG, particularly those that are dominated by shales (e.g., Pieknierskloof and Graafwater) and those in the coastal areas. The medians are in the ranges between 20 and 50 mS/m and rarely exceed 100 mS/m which is well within the acceptable maximum limit for the town supply (Smart and Tredoux, 2002). Rosewarne, (2002) reported remarkably consistent water chemistry in the TMG aquifer with low dissolved solids < 100 mg/l. Duah, (2010), are also reported EC values between 37.5 and 90 mS/m from groundwater boreholes in Gevonden which were in the same range as those reported by Meyer (2002). The chemistry of the springs reflected its origin from the quartz-dominated Peninsula formation (Miller et al., 2017), while the general absences of calcium and magnesium and low salinity are indicative of the flushing of salts by high elevation rainfall during recharge (Smart and Tredoux, 2002).

According to a study by Madlala et al. (2018), the dominant groundwater type in the Upper Berg River (i.e., neighbouring catchment to Jonkershoek) are Na-Cl (37.93%), Na-Ca-Cl-HCO_3 (20.69%), and Na-Ca-HCO_3-Cl (13.79 %) whereby the dominance of Na, Ca and Cl reflects surface water influenced by the relatively short residence time of water, limited rock-water interactions, and minor atmospheric deposition of NaCl during rainfall. This suggests that the TMG groundwater chemistry is Na-Cl type

water rather than of (Ca, Mg)) or (Cl, SO4)) which constitutes more than 60% of the analysed area (Smart and Tredoux, 2002) and Ca-Mg-CO_3 constitutes less than 20 % (Simone, 2001). Furthermore, it may be concluded that water-rock interactions are among the dominant processes controlling the groundwater chemistry in this area. Currently, there are no available groundwater data for the Jonkershoek, nonetheless, the information can be extrapolated from that of the neighbouring catchment with similar geology.

2.6. Past hydrological research in the Jonkershoek catchment

Hydrological research in the Jonkershoek has been ongoing since the late 1930s, providing useful information on the hydrological and ecohydrological processes in the catchment. The growing concern about the effects of the expanding plantation forestry on the catchment water availability led to long-term monitoring in the Jonkershoek. This made way for numerous other hydrological and ecohydrological investigations relating to afforestation and streamflow yields as part of the South African hydrology research programme. Mountainous headwater catchments of this calibre play a crucial role in regional water supply and for environmental purposes. Therefore, they should be managed sustainably.

Early studies have highlighted the changes in hydrological processes such as streamflow yields related to recurring wildfires and land use changes (Scott, 1993; Dye, 2001; Scott and Prinsloo, 2008). The drastic changes in land use have resulted in great losses in the native vegetation whereby the indigenous fynbos vegetation has been replaced by alien trees such as *Pinus* (more dominant) and *Eucalyptus* (less dominant) species, leading to large reductions in streamflow (Kruger, and Wicht, 1976; Scott et al., 2000). According to Scott et al (1998), commercial plantations in South Africa (SA) cover an area of 1.5 million hectares comprising 57% pine, 35% eucalyptus and 8% wattle (i.e., 1.2% of the land in SA). These forested areas are concentrated in high rainfall (MAP >750 mm/a) mountainous catchments with perennial streamflow and constitute 53-60% of the mean annual streamflow (Scott et al., 1998, Jacobson, 2003). The estimated reduction in the mean annual runoff is 3.2 % (1417 x 10^6 m^3/yr.) which equates to a mean incremental water use of ~100 mm/a for the planted area (Scott et al., 1998). This led to the formulation of the Streamflow reduction Activity (SFRA) under the *National Water Act* to regulate water consumption by timber plantation forest owners (Kruger and Bennett, 2013).

Large evidence exists on the negative effects of the plantations in the Jonkershoek and other afforested regions in South Africa on streamflow yield (Kruger and Wicht, 1976; Scott, 1994; Scott and Prinsloo, 2008). The past studies in Jonkershoek have demonstrated how the changes related to the establishment of commercial timber plantations have altered streamflow. For instance, Kruger and Wicht (1976) and Van Wyk (1987) reported a streamflow reduction trend of 340-360 mm per annum over 16 years due to afforestation. According to Dye et al. (2002), the invasive species in these catchments showed increased evapotranspiration (ET) rates compared to native fynbos vegetation. Their study indicated that invasive trees which mostly occupy the riparian zones along the stream channel potentially decrease

streamflow yields, for instance, the wattle thicket (*Acacia mearnsii*) showed annual ET rates of 1503 mm compared to the 1332 mm for fynbos. They concluded that the removal of invasive trees is likely to bring significant hydrological changes by decreasing ET and enhancing streamflow.

Lesch and Scott, (1997) showed that thinning (trimming of the stems) of the pines can increase annual streamflow up to 74 % (19-99), however, there was still a concern that the effects may be short-lived as the remaining plantation trees may soon occupy the site (Scott and Gush, 2017). A comparative study between wildfire and pine plantation effects on streamflow yield (Scott, 1997), indicated that the frequent wildfires had more minor hydrological impacts in the fynbos compared to afforestation with pines in terms of the total flow compared, storm response ratios and peak flows their study indicated a total flow increase of 96% after clear-felling and 12% after a wildfire. Whereby minor increase in total flow after the wildfire treatment compared to clear-felling was attributed to the increase in water repellence in the soil induced by fire.

Research on hydrological processes particularly runoff generating processes is still lacking in mountainous headwater catchments of Southern Africa. These kinds of studies are fundamental to providing an understanding of the hydrologic response and of how the catchment physiographic characteristics (e.g., Land use/land cover change) affects catchment water delivery. For example, the spatiotemporal variations can be driven by geological settings and climatological similarities which could enhance the complexities in understanding streamflow generation from hydrologically important mountainous areas in response to global change impacts such as climate changes (Cowie et al., 2017). Therefore, such knowledge is crucial to improve our understanding of controls of catchment hydrological response in the TMG region with spatially variable processes possibly driven by heterogeneity in geology and topography. Less than a handful of studies exist on runoff generating processes in the Jonkershoek or (Britton et al., 1993; Midgley and Scott et al., 1997) and TMG geological region (Saayman et al., 2003, Bugan et al., 2012).

Saayman et al. (2003) investigated streamflow generating mechanisms in Zachariashoek, a neighbouring catchment to the current study site Jonkershoek. Their study suggested large contributions from delayed flows, assumed to be a combination of both interflow and groundwater flow during the dry summer. The proportion of delayed flow contributions was found to be larger at the lower elevations of the catchment due to increased valley bottom area and potential large subsurface storage as compared to the upper portions.

Midgley and Scott's (1994) used stable isotopes to determine runoff generation during 8 rain events in the Jonkershoek Valley and indicated that a substantial proportion (>90%) of streamflow generated during the rain events comes from water previously stored in the catchment's subsurface (old water) displaced by the new rainwater recharging the soil. This was supported by Bugan et al. (2012) in the Sandspruit catchment, a tributary of the Berg River north of Jonkershoek who also applied stable isotopes to and water balance model approach. They indicated that the streamflow was driven by

interflow from the soil horizon constituting 94.68% of the total runoff with 4.92 % overland flow and minimal groundwater contribution.

A hydrochemical study by Britton et al. (1993) in Swartboskloof, one of the sub-catchments of Jonkershoek indicated that streamflow was dominated by delayed sub-surface flows during the summer period, while the winter stormflow was dominated by direct runoff. Similar trends have been reported elsewhere in the world under different climatic conditions, geology, topography and land use (Muñoz-Villers and McDonnell, 2012; Camacho Suarez et al., 2015; Penna et al., 2015). A multi-tracer study by Camacho Suarez et al. (2015) in the semi-arid Kaap catchment, South Africa, indicated a strong correlation between antecedent rainfall index (API) and runoff response. High APIs enhanced saturated excess overland flow and low soil moisture conditions activated preferential vertical flow.

The findings of most studies in the TMG geological region did not fully address the possible effects of the spatial variation in physiographic characteristics between the sub-catchments such as topography, climate, catchment scale, bedrock geology and soils could influence runoff generation processes (Hewlett and Hibbert, 1967). Thus, the knowledge gap exists about the mechanisms of runoff generation, these processes have not been fully explored in the TMG catchments

Therefore, the Jonkershoek Valley provides a suitable study site to investigate hydrologic processes in the Table Mountain Group (TMG) geological region and aquifer system. In addition, the Jonkershoek contributes to the local water supply system and other critical supply catchments in the region have similar catchment properties, meaning that the findings of this study may be of assistance to water resources management in this part of the TMG area. The catchment is dominated by TMG geology, mostly composed of highly fractured quartzitic sandstone, with spatially variable complex surface and sub-surface flow pathways due to the nature of the fractures (Saayman et al., 2003; Lin and Xu, 2007). The TMG geology overlies Malmesbury Group shales and granite intrusions, which are less water-bearing and form the bedrock of the lower slopes and main valley floor. The geology in the catchment area plays a significant role in its water retention. In addition, both native mountain fynbos vegetation and managed timber plantations of alien species (*Pinus sp.*) are present, and the distribution of these vegetation types varies across sub-catchments feeding different tributary streams (Scott et al., 2000).

The catchment was initially established as an experimental site, the Jonkershoek Forest Research Station, in the late 1930s to monitor the effects of afforestation on stream water yields. The custodianship for hydrological monitoring in the catchment has changed over the years and was inherited by SAEON (South African Environmental Observation Network) Fynbos Node in 2010 (Slingsby et al., 2021). The catchment has been instrumented since 1940 and the long streamflow and rainfall record provides a unique opportunity to explore the responses to the changing environment. This can assist in process understanding and inform hydrological modelling. The established network of rain gauges and weirs across multiple neighbouring sub-catchments offers the opportunity to assess spatial patterns and their links to catchment characteristics, including vegetation cover. Three

instrumented sub-catchments with a contrasting land cover were used in this study: Bosboukloof, dominated by pine plantations; Tierkloof, previously dominated by pines, but having a mix of fynbos and pine saplings at the time of the study; and Langrivier, dominated by fynbos vegetation.

CHAPTER 3: SPATIAL AND TEMPORAL VARIATIONS OF HYDROCLIMATIC CHARACTERISTICS

3.1. Introduction

Understanding the mechanisms of streamflow generation in headwater catchments requires a sound knowledge of the main drivers of the catchment hydrologic cycle. This chapter evaluates the long-term variations of hydro-climatic variables in the Jonkershoek catchment. Analysis of historic hydro-climatic datasets provides essential information on the impacts of climate variability and land use on hydrological responses. The Mann-Kendall trend test and the homogeneity tests for abrupt changes were applied to investigate changes in hydro-climatic variables over time at the sub-catchment level. Drought indices, the Standardized Precipitation Index (SPI) and Standardized Streamflow Index (SSI), were used to establish the relationship between meteorological and hydrological droughts, and what this implies about streamflow generating mechanisms. The alteration of flow regimes related to the changes in land use and climatic variables were determined using Indicators of Hydrological Alteration (IHA). The findings of this study are important to inform policymakers on the impacts of global change drivers (i.e., climate change and land use), allowing pro-active mitigation and adaptation.

The headwater streams generate runoff to rivers and surrounding ecosystems downstream. Most of the streams originate where groundwater emerges as springs and sustains streamflow during low flow periods (Roets et al., 2008). However, most mountainous catchments and Mediterranean climate regions are sensitive to changes in precipitation or the projected warming and are expected to experience significant drying due to shifting climate patterns (Viviroli et al., 2011; Gutierrez-Jurado et al., 2020). This together with modifications in land use or land-cover will impact streamflow (Milly et al., 2005). The knowledge of the impacts of these changes on streamflow regimes in the TMG headwater catchments remains limited. Thus, understanding the long-term trends in hydro-climatic variables such as rainfall and discharge is of high significance as they can help in better planning and decision-making for local water resource management.

The Intergovernmental Panel on Climate Change (IPCC) has projected an average global warming up of about 0.1°C per decade and precipitation changes (IPCC AR4, 2007; IPCC, 2014). The alteration of local precipitation patterns may significantly affect the severity of meteorological droughts, causing deficits in surface and groundwater resources (i.e., hydrological drought), therefore influencing social and economic development as well as the environment (Viviroli et al., 2011). Furthermore, this is likely to affect future water availability. According to Viviroli et al. (2007), this is a concern, particularly in semi-arid and arid regions which depend highly on mountain water resources.

The effects of climate change on rainfall, temperature and hydrological response have already been detected in most Southern African regions (Love et al., 2010). Love et al. (2010), reported declining trends in annual rainfall and discharge as well as an increase in dry spells in the south-eastern part of

Africa. Climate change models in South Africa have indicated a decrease in high rainfall events in the southwest region and a possibility of minor increases in annual variability, which may affect surface water storage systems (Mason et al., 1999; Hewitson and Crane, 2006; Lumsden et al., 2009; Ziervogel et al., 2010b).

Recent studies on the regional climatic patterns in the Western Cape Province (WC) (e.g., Du Plessis and Schloms, 2017; Burls et al., 2019; Mahlalela et al., 2019; Wolski et al., 2021) have reported multi-decadal declines in winter rainfall events and seasonal shifts to a shorter rainy period which were linked to El Nino events. Acosta et al. (1997), predicted up to 25% loss in winter rainfall in the Western Cape. Studies by Burls et al. (2019) and Wolski et al. (2020) linked the changing trends in rainfall patterns to climate change, pointing out diverse climatic drivers on sub-regional scales such as changing frontal behaviour interacting with topography and hemispheric drivers. These factors are likely to influence water delivery. This suggests the need for an in-depth understanding of rainfall characteristics (e.g., patterns, variability and intensity) as well as spatial and temporal variability of hydrological processes to evaluate the vulnerability of surface and groundwater systems at a catchment scale (Uhlenbrook et al., 2002; Ngcobo et al., 2013).

The impacts of climate change on freshwater resources are already detectable in many semi-arid and arid regions. For example, the prominent impacts of the Cape Town meteorological-hydrological drought (2015-2017) were reported to have manifested through low runoff from source catchments (Otto et al., 2018). The higher than normal temperatures, low relative humidity and increased evaporation also amplified the hydrological drought. Furthermore, the increase in potential evaporation and temperature are likely to affect hydrological responses across regions (Warburton et al., 2005). This can affect flows and increase variability. The study also indicated an increase in daily maximum temperature which is more likely to influence summer season rainfall. Other studies in the semi-arid regions and eastern parts of Africa (e.g., Feyissa and Gemede, 2015) showed that higher temperatures will lead to increased evaporation, alterations in rainfall patterns, reduced streamflow and increased frequency of drought, increasing the vulnerability of water resources. According to Schulze (2011), similar changes are projected for South Africa and pose a threat to the already vulnerable water resources.

Duah (2010) analysed rainfall trends at a regional scale in the TMG and reported that 6 of the 21 stations showed significant negative trends but concluded that the rainfall in the study area has not changed significantly. He further calculated the Standardised Precipitation Index (SPI) during the 1950-2007 period for 25 stations across the TMG aquifer in the WC. This study found that the long-term 12-month (SPI) for the stations (e.g., Lambertsbaai, Graafwater, Redelinghuy) showed a shift from a drier period occurring in the late 1960s to early 1970s, to a wetter period from the mid-eighties to early 2000s which was significant for regional groundwater recharge. A study by Rouault and Richard (2003), reported an increased duration of the wet period between the 1980s to late 1990s in the South-Western Cape and

showed that the total number of wet and dry events has increased. Warburton and Schulze (2005) also observed a similar trend in the Quaternary catchments of South Africa.

In addition, the ongoing changes in land use and land cover for commercial afforestation and the invasion of alien species in mountainous headwater catchments pose a threat to freshwater resources due to the resulting increase in evapotranspiration rates. According to previous studies (e.g., Van Wyk, 1987; Scott et al, 2000); Dye et al., 2002), the afforestation in Jonkershoek has resulted in large streamflow reductions. For instance, Kruger and Wicht (1987) reported > 300 mm in streamflow reductions per annum over 16 years, while Scott et al. (2000) showed that the streamflow reductions were more pronounced in wet winters and years, and during the first 15 years after planting compared to the drier times and later years. Dye et al. (2002) reported an annual ET of 1503 mm/a which was 171 mm greater than the indigenous fynbos.

Although these studies provided valuable insight into the effect of land use change on streamflow production at a larger temporal resolution, this is often not sufficient to be used directly in hydrological modelling. For this reason, statistics that describe streamflow such as the indicators of hydrological alteration (IHA) (Richter, 1988) are often used to examine the alterations in flow regimes at multiple temporal scales and can provide useful information to improve hydrological models. Thus, this approach will be applied in this study to investigate the effects of long-term climate-driven (i.e.,, changes in rainfall) and anthropogenic effects (i.e., land use change) on flow regimes. Both factors are key controls on streamflow production and should be taken into consideration when investigating hydrological processes in mountainous catchments.

However, few studies have examined trends in hydro-climatic variables in the TMG region (e.g., Duah, 2010). A review of the existing literature showed that despite the available long-term hydro-meteorological data, few studies have examined the existence of temporal trends in both rainfall and streamflow in the Jonkershoek catchment. Understanding trends of hydro-climatic variables at a variety of spatial scales is needed to develop appropriate water management strategies. This topic has been under-researched in small-scale headwater catchments of the TMG geological region as many of these studies were conducted at regional scales. The multi-method approach including, drought indices and statistical methods can provide a better insight into the long-term effects of hydro-climatic variability on streamflow generation. The results of such a study will inform proper decision-making, providing water managers not only with knowledge of how but also why the hydrological change is happening (Harringan et al., 2014).

This study focuses on the detection of changes in annual and seasonal rainfall (1946-2019) and streamflow (1946 to 2019) over time and potential driving factors in the context of climate and land use/cover change across the Jonkershoek sub-catchments. Based on the review of previous local and regional studies, it can be hypothesised that.

i. the ongoing climate and land use change cause a notable change in annual rainfall and streamflow
ii. which may affect the seasonal distribution of rainfall and high and low flows in the catchment and that,
iii. the difference in land use/cover will result in varying hydrological responses across the sub-catchment.

This study adds to the existing literature on hydroclimatic data analysis in the TMG outcrop areas at a local scale and contributes toward a better understanding of mechanisms of streamflow generation in this setting. Also, this will offer a beneficial reference for understanding local climatic variability and the impact on catchment water delivery as well as aid in predicting responses to projected future climate changes not only for Jonkershoek but also for other catchments with similar hydro-climatic and topographical characteristics. The study has four objectives:

a) to examine the spatial and temporal variability in rainfall and streamflow trends at annual, seasonal and monthly levels to detect possible changes over time ;
b) to identify past drought events at different time scales (1-,3-,6- and 12 months) across the sub-catchments;
c) to establish the linkage between meteorological to hydrological drought by cross-correlations at different timescales; and
d) determine hydrologic alterations associated with rainfall or land use changes in flow indices (e.g., multi-day minimums and maximums, fall and rise rates, low and high pulses counts and baseflow index) over time, using Indicators of Hydrological Alteration (IHA) (Mathews and Richter, 2007).

3.2. Study area

The study was conducted in three sub-catchments of the Jonkershoek catchment namely, Bosboukloof, Langrivier and Tierkloof see Section 2.1**.** The three study sites were chosen based on their topographic gradients to reveal spatial variations in rainfall and streamflow as well as the availability of long-term rainfall, temperature, and streamflow data. Additionally, these sub-catchments were part of a long-term multi-catchment land cover experiment and so have different land cover histories Bosboukloof and Tierkloof were afforested with pines, starting in 1940 and 1956, respectively. These catchments are now managed for commercial timber production with rotational block harvesting. Langrivier was kept as a control site with indigenous fynbos vegetation throughout this period (Scott et al., 2000). Altitude increases gradually from west to east.

The mean annual flow for the three sub-catchments for 2012-2019 along with the long-term mean (1946-2019) is presented in Figure.3.1. This time interval (2012-2019) includes the study monitoring period (2018-2019), the period of the recent Cape Town drought and will add context for the subsequent

chapters. Figure.3.1 shows the mean monthly values of rainfall, potential evapotranspiration (PET) and temperature for the three sub-catchments. The PET was computed using the Hargreaves method (Hargreaves and Samani,1982) due to the limited climatic data. Other meteorological data such as solar radiation was missing for the analysed period and only temperature data were available from the sub-catchments.

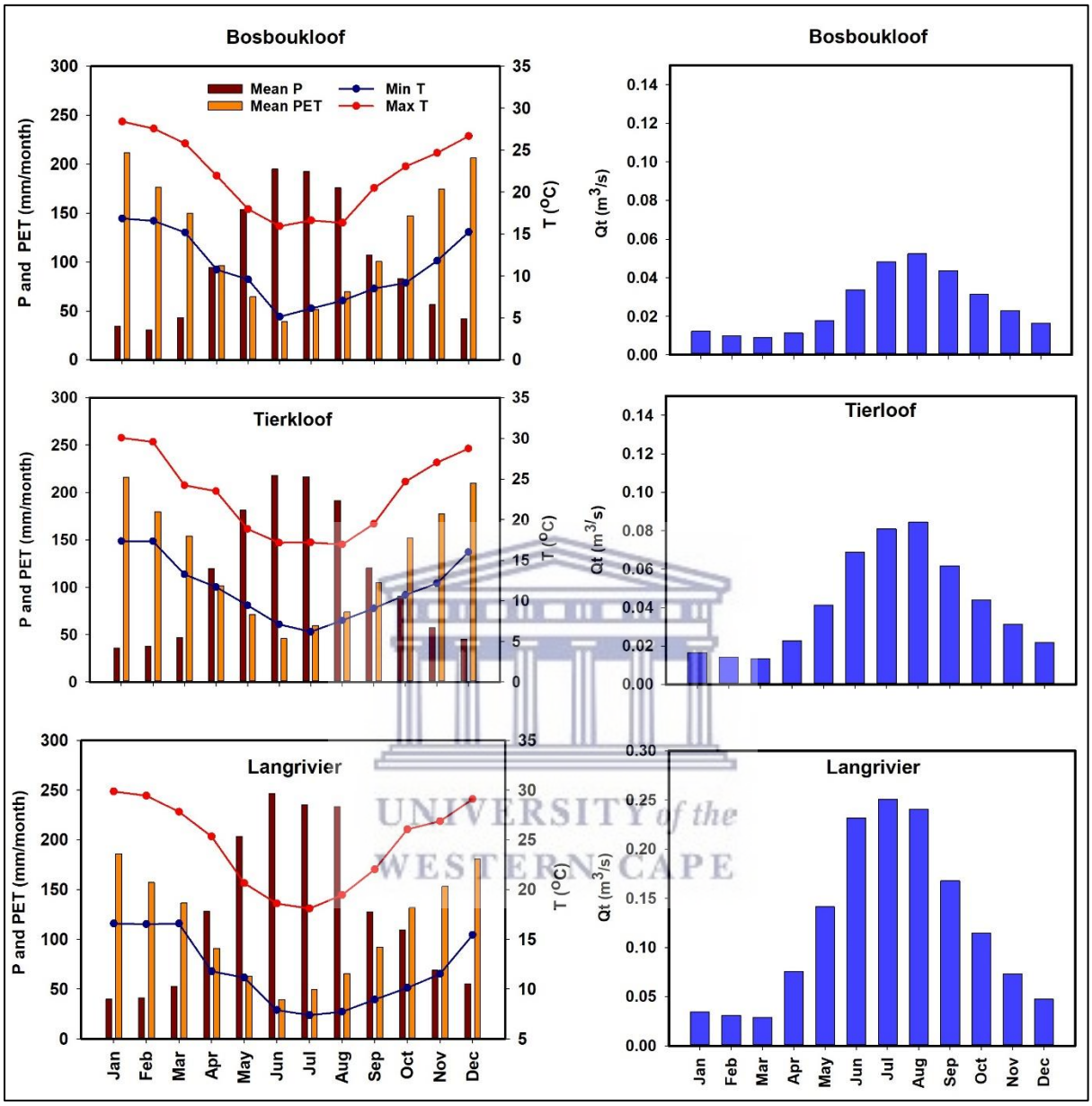

Figure.3.1. Mean monthly precipitation (P), potential evapotranspiration (PET) discharge (Qt), including minimum and maximum temperature (T) and of the three study sites *(*2012-2019*)*. (Precipitation and PET data from stations 11B, 9B and 8B). Note the difference in the scales of discharge.

3.3. Methodology

3.3.1. Data collection and source

Data used in this study include streamflow for the hydrological years 1946-2019 and rainfall from 1946-2019 obtained from the South African Environmental Observation Network (SAEON) (http://www. http://www.saeon.ac.za/). In this study, a "hydrological year" was defined as the 12 months from 01 October to 30 September. For example, the water year 1946 utilized monthly rainfall data from 1 October 1945 through 30 September 1946. The emphasis for this study was on the drought indices for water years 2012 to 2019 which is the period of record for the recent instrumentation set managed by SAEON, covering the recent drought period 2015-2017 and the sampling period 01/2018-03/2020 (Chapter 4,5, and 6). Winter is the main rainy season in the study area which refer from April to September and summer is the dry season from October to March.

Rainfall data used was measured hourly from 6 stations across the catchment, each sub-catchment had a minimum of two rain gauge stations details are listed in (Table.3.1). More details on the monitoring instruments in the catchment area are provided by Slingsby et al. (2021). The rain gauges had a resolution of 0.25 mm. Only rainfall stations with data between the periods 1945 to 2019 were selected. Two stations were used from each sub-catchment which were distributed spatially along an altitude gradient, one downstream and another upstream at higher altitudes. The upstream station in Bosboukloof was at a higher elevation (close to the mountain peaks) than those in Tierkloof and Langrivier. Streamflow records were available for the period between 1946 and 2019, measured at gauging weirs in each of the three sub-catchments. The streamflow was also measured continuously at hourly intervals which were aggregated to monthly and annual flow rates for each station (Table.3.2). Values for short periods of missing data, on the order of days, for both rainfall and streamflow were patched using relationships to nearby stations. For comparison of streamflow and rainfall trends, the records from 1946 to 2019 were used.

Table.3.1. Rainfall stations, location and data records

Site	Id	Latitude	Longitude	Altitude mamsl	Duration (Hydro years)	No. years	Missing data*
Bosboukloof	11B	33°57'31.72"S	18°56'20.48"E	370	1946-2019	68[a]	7%
	5B	33°56'51.52"S	18°56'51.64"E	827	1946-2019	70	5%
Tierkloof	9B	33°58'45.51"S	18°57'03.43"E	297	1946-2019	70	5%
	13B	33°58'31.63"S	18°57'26.21"E	452	1946-2019	68[a]	7%
Langrivier	8B	33°59'15.51"S	18°58'10.60"E	370	1946-2019	70	5%
	14B	33°58'56.84"S	18°58'34.11"E	498	1946-2019	68[a]	7%

*All data have a 4-year gap between 2008 and 2011, [a]missing data 1990-1991 which contributes to the percentage of the missing data.

Table.3.2. Streamflow gauging stations and data records

Site	Latitude	Longitude	Altitude mamsl	Data period (Hydrological years)	Length of period (years)	Missing data*
Bosboukloof	33°57'44.98"S	18°55'50.45"E	273	1946-2019	71	4%
Tierkloof	33°58'45.51"S	18°57'03.43"E	370	1946-2019	71	4%
Langrivier	33°59'15.51"S	18°58'10.60"E	297	1946-2019	71	4%

* Includes the 3 years of missing data (2009-2011)

3.3.2. Data quality control and distribution tests

Quality control and data distribution analyses were done on the long-term streamflow and rainfall records using descriptive statistics testing for outliers (Grubbs' test), distribution fitting (Kolmogorov-Smirnov test) and normality testing (Shapiro-Wilk test), applying a significance level of 5%. Both the daily, monthly and annual rainfall and streamflow passed the normality test. Although the annual rainfall and streamflow were normally distributed, the rainfall time series from all stations and all streamflow time series were moderately skewed.

Grubbs' test (Grubbs, 1950; Grubbs and Beck,1972) was used to asses for outliers, the test identifies outliers in a univariate data set using the mean value and the standard deviation considering only the value of data points but not the real order of data (Adikaram et al., 2014). Flagged potential outliers were assessed and all were attributed to extreme rainfall events confirmed across multiple stations, hence they were not removed.

Homogeneity tests

Homogeneity tests are required to assess the reliability and accuracy of the hydroclimatic dataset before analysis. The homogeneity tests of hydroclimatic data allow detection of changes within the time series which may be caused by factors such as a change in instruments or relocation of observation stations, which could influence the hydro-meteorological data interpretations (Yue and Hashino, 2003; Hafi and Ali, 2019). The time series data inhomogeneity can affect the assessment of hydroclimatic extremes and trends (Daba et al., 2020). Changes in central tendency, as detected by homogeneity tests, can also occur due to changing climate conditions, and in the case of streamflow, changes in land cover and management. The rain gauges and streamflow recording instruments in the Jonkershoek have been upgraded over time, however, to our knowledge no major relocation of observation stations used in this study has been done. Thus, it could be assumed that these factors would have minimal impacts as rainfall amounts of long durations are less likely to be sensitive to the changes.

A homogeneity test was applied to detect abrupt change points and shifts in mean annual and seasonal streamflow and rainfall data. The time series (1946-2019) of streamflow and rainfall (1946-2019) from Bosboukloof, Tierkloof and Langrivier sub-catchments were analysed using Pettitt's test (Pettitt, 1979) and Standard Normal Homogeneity Test (SNHT) (Alexandersson, 1986). The homogeneity test is more suitable to evaluate daily data with at most 10% missing values (Kang and Yusof, 2012). The two methods were selected for this analysis as they provide different information on the changes in the time series data. Pettitt's test is a distribution-free rank-based Mann-Whitney test, used to detect if an abrupt shift occurs in the mean annual streamflow and rainfall time series, however, has low sensitivity to changes near the beginning and end of the time series (Huo et al., 2013). The SNHT is a likelihood ratio test that is more likely to detect changes near the beginning and end of the time series and less sensitive to abrupt changes in the middle (Alexandersson and Moberg, 1997). More details on these tests have been widely documented in the literature (Kang and Yusof, 2012; Kazemzadeh and Malekian, 2018). It is assumed that the potential abrupt change could be at any date of the time series. The significance of the identified change points between the sub-series is evaluated by a statistical two-tailed T-test at a 5% significance level (*p*-value) and a 95% confidence interval. The time series was considered homogenous if no or one of the two tests rejects the null hypothesis (H_0) at the confidence level of 95%.

3.3.3. Data analysis

3.3.3.1. Trend analysis

Mann Kendall trend test

The Mann Kendall (MK) non-parametric trend test (Mann, 1945; Kendall, 1975) was applied to detect monotonic trends in precipitation and streamflow. The application of this method has been documented in many works of literature (e.g., Zhang et al., 2012; Ahmad et al., 2015; da Silva et al., 2015; Fiaz Hussain, Ghulam Nabi, 2015). Recommended by the World Meteorological Organization (WMO),

some of the many advantages of the MK are its robustness against non-normal distributions and that it is not strongly affected by outliers and missing values (Nkiaka, Nawaz and Lovett, 2017). The Mann-Kendall trend test has proven to be more effective on longer time series but may also be used for datasets as short as 10 values (da Silva et al., 2015b; Kocsis, Kovács-Székely and Anda, 2020). Data availability allowed for the analysis to be conducted for hydrologic years 1946 to 2019 for rainfall and 1946-2019 for streamflow, which was considered long enough for the decadal-scale climate variability.

The magnitude of the trend in the times series was estimated by Sen's slope (Sen, 1968). Sen's method (Gilbert, 1988) uses a linear model to estimate the slope of the trend, and the variance of the residuals should be constant in time (da Silva et al., 2015). To eliminate the influence of positive autocorrelation/ or serial correlation components in the time series and improve the testing ability of the MK test, the Modified Mann-Kendall (MMK) non-parametric trend test was applied (Hamed and Rao, 1998). The MMK method ensures that the null hypothesis (H_0) is correctly rejected and eliminates the effect of dependence on the yearly data. According to (Hamed and Rao, 1998; Yue et al., 2002), the presence of positive autocorrelation in the data increases the chances of detecting trends and overestimating the significance of trends when there is none, while negative autocorrelation results in underestimating the significance of trends. For detailed information on the MMK methods the reader is referred to (Hamed and Rao, 1998; Yue et al., 2002; Wang et al., 2019).

The MMK test was applied to the long-term rainfall and streamflow time series to detect statistically significant trends and compute Sen's slope. The trends were computed at 95% ($p \leq 0.05$) confidence intervals in a two-tailed test. The presence of a statistically significant trend is evaluated using the Z_{MK} value. The null hypothesis (H_0) states that there is no significant trend, and the data are independent and randomly ordered. The null hypothesis is rejected if the *p*-value is less than the applied significance level i.e., $p \leq 0.05$ at a 95% confidence interval suggesting there is a monotonic trend in the time series, therefore accepting the alternative hypothesis (H_1). At the significance level of 5%, the null hypothesis of no trend is rejected if $|Z_{MK}|>1.96$. A positive Z_{MK} value indicates an increasing (upward) trend, and a negative Z_{MK} value signifies a decreasing (downward) trend.

The change in mean annual rainfall over time was expressed as a percentage mean. The percentage change over the length of the period (1946-2019) was estimated following the assumption of the linear trend (Hafi and Ali, 2019). The methods estimate the magnitude by Theil-Sen's median slope and assess the mean over the period, as follows.

$$change = \left\{\frac{median\ slope * period\ length}{Mean}\right\} x\ 100 \qquad (3.1)$$

3.3.3.2. Standardised Precipitation Index (SPI)

To characterize meteorological drought and severity in the Jonkershoek catchment, the Standardised Precipitation Index (SPI) (Mckee et al., 1993) was applied. The SPI is based on the probability of a precipitation amount occurring in a set time step or interval. Index values represent the number of

standard deviations by which the observed precipitation deviates from the long-term average for the given time step. Time steps from 3 to 24 months are deemed suitable for SPI drought assessments given the time needed for the deficit of precipitation to reflect in soil moisture, streamflow and groundwater levels (Rouault and Richard, 2003). Long-term monthly precipitation data of more than 30 years is recommended for SPI analysis to establish meaningful probabilities. For our study, 71 years of record length were used (1946-2019).

To calculate SPI, the probability distribution of rainfall amounts for the given time step must first be found using the long-term rainfall data. Precipitation data, particularly for shorter time steps, is rarely normally distributed. In this study, a gamma distribution was fitted to estimate the probability distribution. The cumulative probability of each observed value in the time series was found using this distribution and then converted to a standard normal distribution to produce SPI values (Abramowitz and Stegun, 1965; Thom,1996). For a detailed description of the method, the reader is referred to Zhang et al. (2012) and Tigkas et al. (2013). The wet and dry periods were defined using the SPI values categories (Table.3.3).

Table.3.3. Classification of SPI/SSI values shows the distinct categories of drought severity and the probabilities (Nalbantis and Tsakiris, 2008; WMO, 2012; Zhang et al., 2012).

Scale	SPI classes	classification/category	Probability of events (%)	Cumulative probability
1	≥2	Extremely wet/no drought	2.30	0.977-1.00
2	1.5 to 1.99	Very wet/no drought	4.40	0.933-0.977
3	1 to 1.49	Moderately wet / no drought	9.20	0.841-0.933
4	-1 to 0.99	Near normal/Mild drought	68.20	0.159-0.841
5	-1.5 to -0.99	Moderately dry	9.20	0.067-0.159
6	-2 to -1.49	Severely dry	4.40	0.023-0.067
7	<-2	Extremely dry	2.30	0.000-0.023

For this study, an SPI analysis was performed on the long-term monthly precipitation data for the hydrological years 1946-2019 from six stations in three sub-catchments namely, Bosboukloof, Tierkloof, and Langrivier within the Jonkershoek. The SPI value for a particular sub-catchment was assumed to be the average of the two stations in that sub-catchment (e.g., the SPI value of Bosboukloof is the average of 11B and 5B). According to Barker et al. (2016), once the rainfall data from various stations have been converted to SPI values, the influence of "areal average rainfall" no longer applies

because the transformation of SPI to a standard normal distribution with a mean zero and standard deviation of 1, makes it comparable over space and time.

The analysis of drought was computed with the time series of monthly, yearly and seasonal rainfall amounts for hydrological years 1946 to 2019 at 3-, 6- month and 12- month time scales. The 3-month SPI values were calculated for the October-December, January–March, April-June and July-September intervals which equate to the first and second halves of the dry summer and the first and second halves of the wet winter, respectively. The 6-month index, calculated for October-March and April-September, describes the full dry summer and wet winters, respectively. The 12-month timescale (e.g., October 1945- September 1946) was used to assess the longer-term drought, suitable for water resources analyses (Labedzki et al., 2007).

3.3.3.3. Standardized Streamflow Index (SSI)

The Standardised Streamflow Index (SSI) was applied to assess streamflow patterns and identify hydrological droughts and severity in this study. Annual and monthly streamflow data from 1946 to 2019 (71 years) with the 2009-2011 gap, were used. The SSI calculation follows the same approach and principles as the SPI. However, due to the heterogeneity in catchment characteristics, a wider variety of probability distribution types are often assessed (lognormal, Pearson Type III, gamma, general extreme value, Weibull, generalized Pareto) to find a suitable fit for streamflow data (Vincente-Serrano et al., 2011). In the Jonkershoek catchment, fits for the lognormal and gamma distributions were tested using distribution fitting analysis. The lognormal distribution was found to be the best fit for the monthly and annual streamflow time series as it produced moderately skewed data compared to the other tests see Table.3.6. The SSI values were computed at similar time scales as the SPI except with a different probability distribution. The same classification of wet periods and hydrological droughts based on SSI value ranges were applied as the meteorological classification defined using SPI values (Table.3.3).

The streamflow may integrate the response of catchment rainfall from various parts of the catchment. To understand the relationship between the SPI and SSI, cross-correlation was conducted using the Pearson correlation coefficient. The SSI-1 was correlated with the SPI for 1-, 3-, 6- and 12 months to detect the streamflow response and lag with the SPI. This comparison can provide an indication of the time taken for the rainfall deficit to propagate to the hydrological cycle to the streamflow deficit (Barker et al., 2016; Nkiaka et al., 2017).

3.3.3.5. Analysis of flow indices

The hydrological alterations over time likely due to changes in land cover or climatic variability were analysed using the Indicators of Hydrologic Alteration (IHA) approach (Richter et al., 1997) This method requires a minimum of 20 years of streamflow data (Richter et al., 1997; Taylor et al., 2003). In this study, the IHA was used to characterize the intra- and inter-annual variability in flow magnitudes, duration of annual extreme flows and frequency (Table.3.4). Mean daily streamflow records (1946-

2019) from the three gauges were analysed using, (1) the single-period analysis and (2) the two-period analysis. The single-period analysis identifies significant trends in the time series using linear regression for each parameter with a year as an independent variable for 71 years and calculates a *p*-value for the regression line at 95% confidence of interval and a statistical significance level of 5% ($\alpha = 0.05$) (Table.3.4). Not all the parameters were used for this analysis, for instance, the "number of zero-flow days" was excluded because there were no days without flows from all the gauging stations. More detailed information on the worldwide application of the IHA is provided in several publications (e.g., Kannan et al., 2018; Yang et al., 2018; Gebremicael et al., 2019).

The two-period analysis was used to assess the changes in flow regimes caused by human disturbance such as afforestation and clear-felling in Bosboukloof and Tierkloof. For the two periods analysis, the IHA uses a Range of Variability Approach (RVA) to assess the extent of alteration before afforestation/clear-felling (pre-impact) and after afforestation/clear-felling (post-impact) on flow indices (Table.3.4). The RVA describes the percentage of the frequency in which the IHA parameters fell within the specific boundary. The target boundaries are defined in the range of 25% and 75 % per centile, which are referred to as the low and high categories of RVA (Matthew and Richter, 1997). The boundaries between the categories are based on the per centile values (i.e., low = 0 % - 33 %, middle = 33 % - 66 % and high = 66% -100%) of the flow parameters using non-parametric analysis. Non-parametric statistics are recommended because of the skewed nature of most hydrological datasets. The following equation is used to calculate the degree of hydrologic alteration (HA):

$$HA\ \% = \frac{Observed\ frequency - Expected\ frequency}{Expected\ frequency} * 100 \qquad (3.2)$$

where, the observed frequency and expected frequency represent the number of years with values in the category (25^{th} and 75^{th} per centile value) during the pre-and post-impact periods, respectively. A value close to zero indicates minimal hydrological alteration, whereas a positive value indicates that the frequency of the value in that category increased and negative values indicate that the frequency decreased.

Bosboukloof and Tierkloof sub-catchments were selected as case studies for this analysis as they had data for planting and clear-felling. Langrivier was not included in this analysis as it was never afforested (Scott et al., 2002). The afforestation in Bosboukloof started in 1940, however, the streamflow monitoring data was available from 1946 onwards. Therefore, the analysis was done to evaluate the effect of afforestation vs deforestation/clear-felling on flow indices. Clear-felling occurred between 1979 and 1982, therefore the defined periods of analysis were afforestation (1946-1978) and clear-felling (1979-1989). The clear-felling period was limited to 10 years assuming minor hydrologic alterations due to the new planting cycle or the absence of pines during this period as a result of the 1986 fire which burned > 80 % of the sub-catchment (Scott et al., 2002; du Plessis and van Zyl, 2020). In Tierkloof the planting started in 1956, therefore, the selected periods of analysis were pre-

afforestation (1946-1956) vs afforestation (1957-1978). No information was available regarding plantation rotations for recent years (i.e., post-1994) and clear-felling in Tierkloof.

Table.3.4. List of Indicators of Hydrologic Alteration (IHA) parameters applied in this study (Richter et al., 1998; Kannan et al., 2018).

Group	Parameter details	Regime characteristics	Parameter
1	Magnitude of monthly flow	Magnitude, timing	Median value of 12 calendar months
2	Magnitude and duration of annual extreme flow conditions	Magnitude, duration	Annual min and max, 1-, 7-, 30- and day flow
3	Rate and frequency of water condition change	Magnitude, frequency duration	Rise and fall rate, the median of all positive differences between the consecutive daily values

3.4. Results

3.4.1. General descriptions of the rainfall and streamflow time series

The results of the statistical analysis for rainfall revealed spatial variations between the stations and sub-catchments (Table.3.5). The mean annual rainfall ranged from 1208 – 1692 mm/a across the stations, winter rainfall of 919-1292 mm/a and summer ranged from 289-399.6 mm/a. The rainfall exhibited an increasing pattern from the west (outer part) to the east (interior) of the Jonkershoek catchment. The lowest average rainfall was recorded in Bosboukloof 11B. The high-altitude stations are 5B in Bosboukloof and 14 B in Langrivier. Interestingly, the stations in Tierkloof showed uniform distributions of rainfall between the stations. The CVs were also computed to determine the inter-annual and seasonal variability as a percentage of the mean rainfall. The annual rainfall exhibited high inter-annual variability with CV ranging from 20.8 -29.1 % (Table.3.5).

Seasonal rainfall showed higher variability than total annual rainfall values, the summer season (Oct-Mar) had the highest variation with CV 32.1-43.3% than the lowest variation observed for the winter season (Apr- Sept) rainfall (CV 22.1-31%) (not presented). The result of the Kolmogorov-Smirnov normality and distribution test (i.e., Gamma, Lognormal) indicated that the time series was symmetrical for 50% of the stations and moderately skewed for the other half. Though all the time series data were normally distributed for most of the rainfall stations.

Table.3.5. Descriptive statistics of annual rainfall (1946-2019) at the three study sub-catchments. Including the Kolmogorov-Smirnov test p-value at a 95% confidence interval.

	Bosboukloof		**Tierkloof**		**Langrivier**	
	11B	5B	9B	13B	8B	14B
Period of analysis (Years)	69	71	71	69	71	69
Annual P (mm/a)	1208	1559	1376	1350	1553	1692
Annual Min P (mm/a)	550.5	639.5	571	529.3	708	859.0
Annual max P (mm/a)	2065.6	3638	2436.3	2404	2730.4	3072.3
CV (%)	20.8	29.1	22.4	22.0	21.0	21.1
Skewness	0.26	1.51	0.58	0.15	0.24	0.69
p-value	0.832	0.443	0.865	0.564	0.446	0.381

Min= minimum, max= maximum, P= precipitation, CV= coefficient of variation.

The descriptive statistics of the annual streamflow series are shown in (Table.3.6). Like rainfall, the annual, minimum and maximum streamflow exhibit large spatial. The highest average annual flows were recorded in Langrivier (0.120 m^3/s) and the lowest in Bosboukloof (0.026 m^3/s) which were a few magnitudes less. Tierkloof showed moderate average annual streamflow (0.042 m^3/s) nearly half of that of Langrivier. Moreover, the annual average flow also showed higher inter-annual variation for all sub-catchments with CV ranging from 31.8 to 37.5 %. Tierkloof exhibited lower intra-annual variability. The results of the distribution statistical analysis indicated the streamflow time series from the three gauging stations were moderately skewed (0.7-1.0), though, normally distributed with $p > 0.05$ at a 5 % significance level.

Table.3.6. Descriptive statistics of annual streamflow series (1946-2019) at the hydrometric stations in Bosboukloof, Tierkloof and Langrivier. Including the Kolmogorov-Smirnov test p-value at a 95% confidence interval.

	Bosboukloof	**Tierkloof**	**Langrivier**
Period of analysis (Years)	71	71	71
Annual Mean (m^3/s)	0.026	0.042	0.120
Annual min flow (m^3/s)	0.008	0.017	0.048
Annual max flow (m^3/s)	0.060	0.092	0.267
CV (%)	37.4	31.8	37.5
Skewness	0.77	0.98	1.00
p- value	0.603	0.047	0.278

Note: Min= minimum, max= maximum

3.4.2. Evaluation of trends and abrupt changes in rainfall and streamflow.

3.4.2.1. Homogeneity tests abrupt changes

Rainfall

The Pettitt's and Standard Normal Homogeneity Test (SNHT) statistics for homogeneity were used in a two-tailed test to detect the change points/ abrupt changes in the time series of seasonal and annual

rainfall records at a significance level of 5 %. The results of the test statistics for rainfall are presented in Figure.3.2 and Table.3.7.

Considering the history of the catchment conditions and instrumentation (Du Plessis and Van Zyl, 2021; Slingsby et al., 2021), it is apparent that the abrupt changes in the rainfall time series couldn't be due to equipment changes, relocation or other changes to the station. The equipment was changed around the same time for all stations and to our knowledge no major relocation of stations took place. The equipment change in this catchment occurred at the same site in 2011, 2017-2018 (Slingsby et al., 2021). Furthermore, change points could not be linked to the clear-felling period (1979-1982) and/or natural fires which occurred in 1986 and 2014. If they had similar patterns, it could be considered that the change points were due to artificial disturbances. Therefore, the detected abrupt changes should be accepted. These data were further applied for Mann Kendall-trend analyses and climate-based studies (e.g., Standardized Precipitation Index) in the subsequent section.

Rainfall time series from stations 5B in Bosboukloof, 9B in Tierkloof and 8B in Langrivier mean annual rainfall were presented graphically as these stations had longer records compared to the others (Figure.3.2). The statistically significant downward change points were detected across the sub-catchments; however, the change points were gradual Table.3.7. The change points showed a decrease from high mean annual rainfall to a low mean annual rainfall after the change points.

Pettitt's tests identified significant downward change points in annual rainfall for Bosboukloof in the early 1990s (5B) and late 1990s (11B) (Figure.3.2). Similar downwards change points were detected for Langrivier stations. However, the significant downward change points in Tierkloof occurred a few years later in 2002 at both stations. Inconsistencies of the change points for rainfall time series between the sub-catchment were also observed during the wet winter (Apr-Sep) and dry summer (Oct- Mar) seasons.

Table.3.7. Results of the Pettitt and SNHT homogeneity test for rainfall stations, also showing the p-values and change points at a confidence interval of 95 %. Winter (April-September), Summer (October- March)

Station	**Period**	**Pettit's**			**SNHT**		
Bosboukloof		*p*- Value	Change point	*T test*	*p*-Value	Change point	*T test*
5B	Annual	***<0.0001***	**1993**	*	***0.037***	**2003**	*
	Summer	***<0.0001***	**1985**	*	***0.017***	**1985**	*
	Winter	***0.000***	**1995**	*	*0.048*	2003	
11B	Annual	***0.006***	**1999**	*	***0.002***	**2007**	*
	Summer	*0.140*	1985		*0.090*	1998	
	Winter	*0.057*	2001		***0.006***	**2002**	*
Tierkloof							
9B	Annual	***0.039***	**2002**	*	***0.006***	**2013**	*
	Summer	*0.144*	1986		*0.426*	2014	
	Winter	***0.046***	**2002**	*	***0.047***	**2013**	*
13B	Annual	***0.006***	**2002**	*	***0.000***	**2007**	*
	Summer	*0.083*	1998		*0.153*	2007	
	Winter	*0.012*	2002	*	*0.001*	**2007**	*
Langrivier	Annual	***0.009***	**1993**	*	***0.000***	**2013**	*
8B	Summer	***0.030***	**1990**	*	***0.037***	**2005**	*
	Winter	***0.013***	**1993**	*	*<0.0001*	**2013**	*
14B	Annual	***0.005***	**1998**	*	*0.035*	**2007**	*
	Summer	*0.066*	1985		*0.437*	2005	
	Winter	***0.005***	**1993**	*	*0.007*	**2007**	*

Note:* Indicates a downward shift, Significance level at $\alpha = 0.05$

As shown in Table.3.7, the majority of the change points in the wet winter occurred between 1993 and 2002 for all stations. However, most of the rainfall stations did not show significant change points during the dry summer except 5B in Bosboukloof and 8B in Langrivier for the Pettitt's test. Like Pettitt's test, the SNHT test showed significant downwards change points in the time series of the mean annual rainfall. Though these change points occurred later between 2003 and 2013. The changes point at station 5B in Bosboukloof occurred earlier in 2003 than at the other stations. Overall, it was observed that the change points were different for the individual stations though they were all inhomogeneous.

Streamflow

The results for the homogeneity tests statistics for streamflow time-series for the Bosboukloof, Tierkloof and Langrivier gauging stations are presented in Table.3.8. The graphical representation of the significant change points has been presented in Figure.3.2. The result of Pettitt's and SNHT tests identified significant downward change points at annual and seasonal scales for the three gauging

stations. The detected change points in the streamflow time series were gradual across the investigated sub-catchments (Figure.3.2.(d-f)).

After the evaluation of the historical background of the catchment and measurements, no explanation could be found to link the change points to equipment change or changes in weir infrastructure. The change points coincided with other human-induced alterations in the catchment and climate-related changes. Therefore, these abrupt changes should be accepted. The time series were applied for trend analyses for hydrological and climate-based investigations in the subsequent section.

Pettit's test identified consistent significant downward change points for Bosboukloof (1996-1997) (Table.3.8). A similar observation was made in Tierkloof (1962-1965) annual streamflow time series. In Langrivier, change points were different at both annual and seasonal scales and occurred much earlier in the year 1965 compared to other sub-catchments. The change points for the dry summer occurred much later in 1985, whereas the annual scale and the wet winter change points were consistent in 1959 and 1962, respectively. Conversely, the results of the SNHT test in Langrivier identified significant downward change points for the winter time series occurring in 1957, whereas the other sub-catchment did not show significant change points. In general, all stations showed a decrease in mean annual streamflow after the change point with highly variable mean annual flows in Tierkloof and Langrivier (Figure.3.2. (e and f)). The flow indicated a drying trend towards the end of the time series. This was confirmed by the Mann-Kendall tests, the Standardized Precipitation Index and Standardized Streamflow Index (Figure.3.4).

Table.3.8. Results of the Pettitt's and SNHT homogeneity tests for streamflow, also showing the *p*-values and change points (1946-2019) at a confidence interval of 95%.

Station	**Period**	**Pettit's**			**SNHT**		
Bosboukloof		*p*- value	Change point	T-test	*p*-value	Change point	T-test
	Annual	***0.006***	**1997**	*****	***0.047***	**1998**	*****
	Summer	***0.007***	**1997**	*****	*0.109*	1998	
	Winter	***0.026***	**1996**	*	*0.114*	1996	
Tierkloof							
	Annual	***0.003***	**1963**	*****	***0.043***	**1959**	*****
	Summer	***0.003***	**1965**	*****	***0.015***	**1958**	*****
	Winter	***0.015***	**1962**	*****	*0.067*	1962	
Langrivier	Annual	***0.010***	**1959**	*****	***0.040***	**1958**	*****
	Summer	***0.023***	**1985**	*****	*0.293*	2014	
	Winter	***0.020***	**1962**	*****	***0.011***	**1957**	*****

Note:* Indicates a downward shift, Significance level at α=0.05

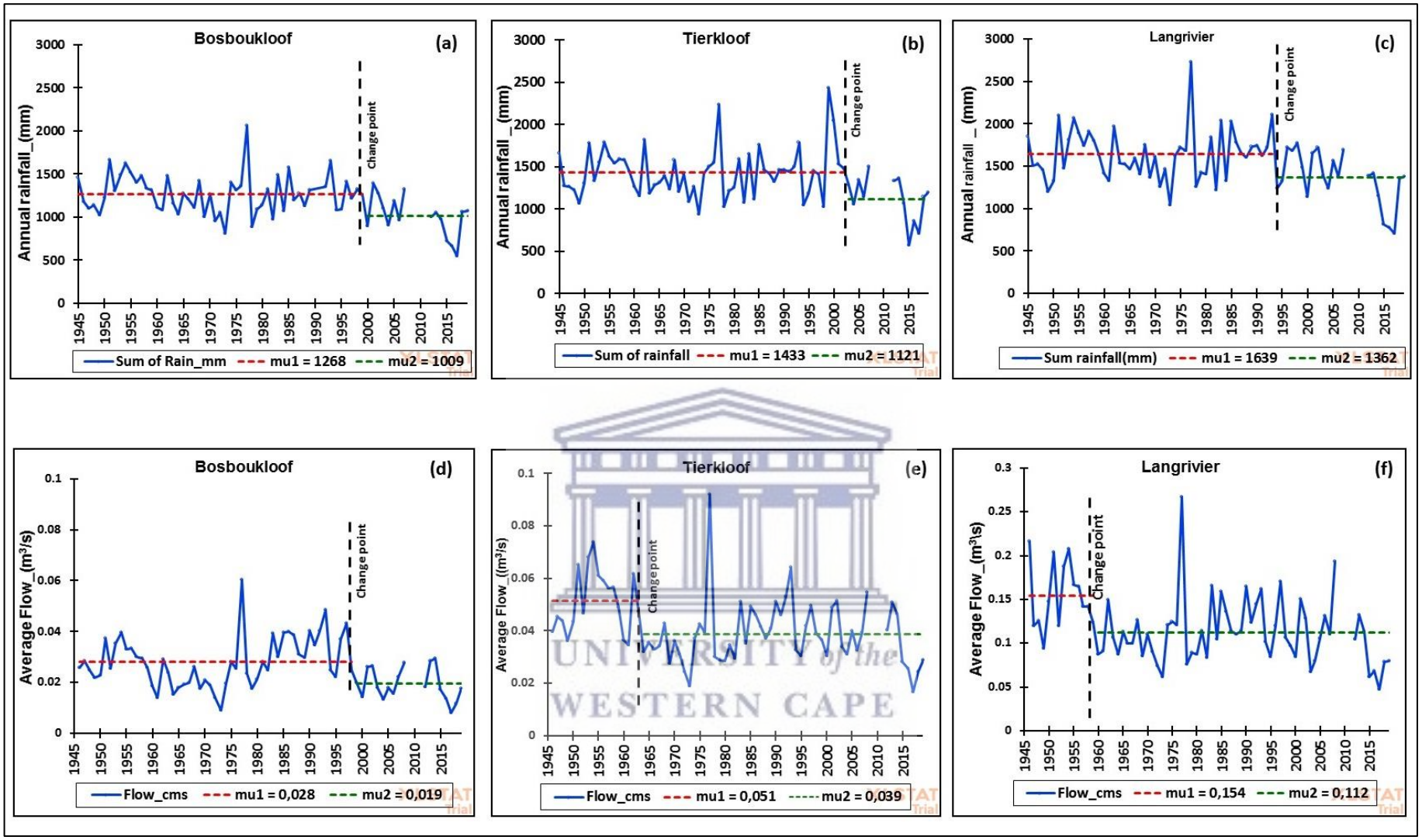

Figure.3.2. Significant change points and downward shifts for the Pettitt's test in the mean annual rainfall (Top, a-c) and mean annual streamflow (bottom, d-f) with means for each sub-series (Mu1 and Mu2). Rainfall presented are from stations 5B (Bosboukloof), 9B (Tierkloof) and 8B (Langrivier).

3.4.1.2. Mann-Kendall trend test

Rainfall

The Modified Mann-Kendall (MMK) trend test was performed to detect monotonic trends in monthly, annual and seasonal rainfall and streamflow for the three sub-catchments from 1946 to 2019. The results of the trend test (Z_{MK}) and Sen's slope (Q) for all the stations are presented in Table.3.9. The spatial distribution of the significant trends is presented in Figure.3.3.

The long-term average annual rainfall showed statistically significant decreasing trends for all stations (Z_{MK}= -4.74 to -1.92) at a significance level of 5% (Table.3.9). The values of the Sen's slopes reached -8.77 and were mostly steeper for stations 5B (Q = -8.77) in Bosboukloof and 14B (Q =-6.33) in Langrivier. Most of the statistically significant decreases occurred during winter for most of the stations Table.3.9. The wet winter (Apr-Sep) rainfall was decreasing at most of the stations with a change percentage over time ranging from -39.4 % to -26.1 % for Bosboukloof stations, from -19.19 % to -15.67 % for the stations in Tierkloof and -28.6 % to -21.1% at the Langrivier stations. The steepest Sen's slopes were recorded for Bosboukloof (Q = -4.09 to -2.81). The trend analysis statistics for average dry summer rainfall (Oct-Mar) indicated significant decreasing trends for the higher altitude rain gauges with a negative change percentage Bosboukloof 5B (-33.5%, Z_{MK}=-2.52) and Langrivier 14B (-25.8 %, Z_{MK}=-1.84) (Figure.3.3.). Analysis of trends in monthly rainfall identified significant decreasing trends for April and May and the summer month of October (Appendix A, Table.A.2). Statistically significant trends could not be detected for most of the winter months (June, July, Aug and Sep).

Table.3.9. Summary Mann-Kendall test results (1946-2019) for annual rainfall (mm/a), trend detections (values in bold means significant decreasing trends) including the p values for the MK test.

Site	Period	Z_{MK}	Sen's slope	*p*- value	Trend
				0.05	
Bosboukloof					
11B	Annual	**-3.12**	**-4.284**	***0.002***	***, Decr**
	Summer	-1.49	-0.802	*0.216*	
	Winter	**-2.81**	**-3.470**	***0.005***	***, Decr**
5B	Annual	**-4.74**	**-8.77**	***0.000***	***, Decr**
	Summer	**-2.52**	**-1.651**	***0.009***	***, Decr**
	Winter	**-4.09**	**-6.731**	***<0.0001***	****, Decr**
Tierkloof					
9B	Annual	**-1.92**	**-3.043**	***0.015***	***, Decr**
	Summer	-1.07	-0.572	*0.023*	
	Winter	-1.89	-2.334	*0.094*	
13B	Annual	**-2.15**	**-3.268**	***0.012***	*, Decr
	Summer	-1.70	-0.941	*0.088*	
	Winter	**-1.98**	**-2.789**	***0.033***	***, Decr**
Langrivier					
8B	Annual	**-2.66**	**-4.555**	***0.008***	***, Decr**
	Summer	-1.50	-1.276	*0.134*	
	Winter	**-2.21**	**-3.507**	***0.009***	***, Decr**
14B	Annual	**-3.38**	**-6.333**	***<0.0001***	***, Decr**
	Summer	**-1.84**	-1.422	***0.020***	*, Decr
	Winter	**-3.37**	**-5.221**	***<0.0001***	***, Decr**

Note:[a]Observations missing (1990-1991), [b](2009-2011), Level of significance: * If trend at $\alpha = 0.05$; no symbol = not statistically significant,

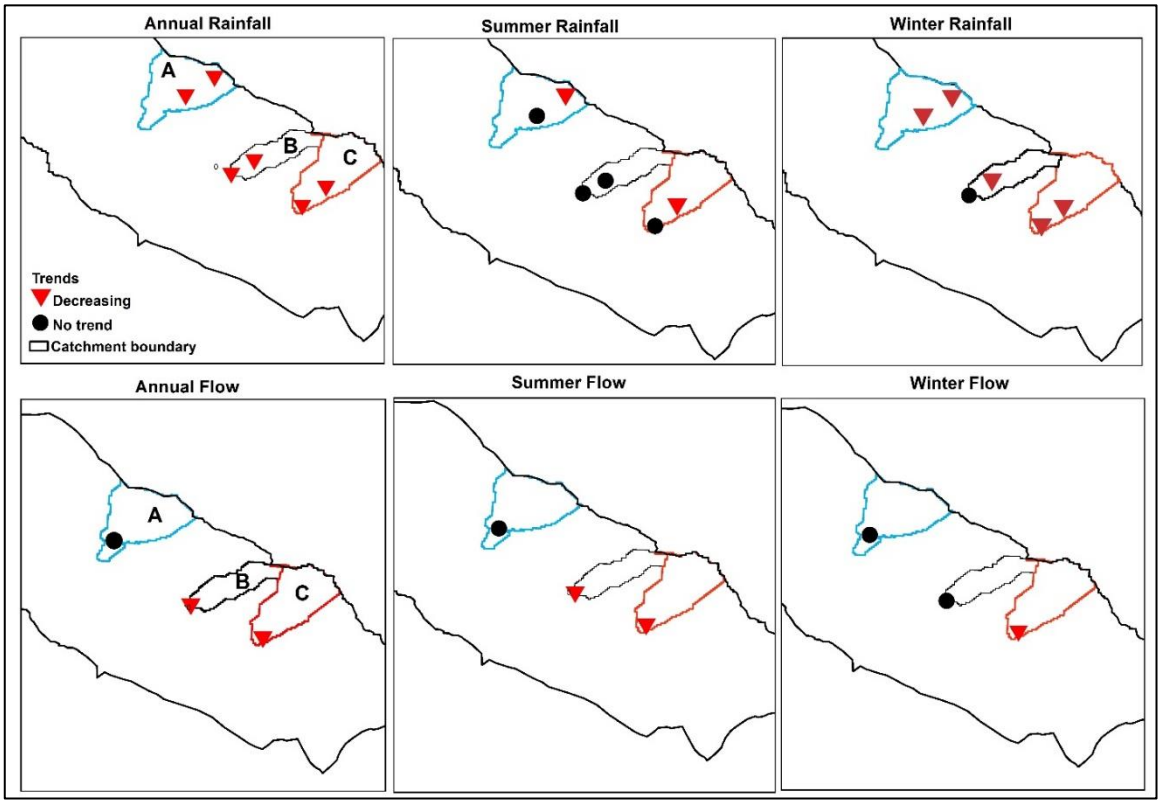

Figure.3.3. Trend maps of rainfall and streamflow based on Mann Kendall test analysis for. (A) Bosboukloof, (B) Tierkloof) and (C) Langrivier.

Streamflow

The summary of streamflow Modified Mann Kendall (MMK) test and Sen's slope estimator (Q) results of all gauging stations are presented in Table.3.10. Significant trends for the annual and seasonal streamflow at the individual sub-catchments are presented in Figure.3.3. Like the rainfall trend test, the significance level of 0.05 (95 % confidence level) was used to detect significant trends in the monthly, seasonal and annual streamflow time series. Interestingly, the results showed that not all the gauging stations had statistically significant trends, particularly in Bosboukloof. Statistically significant trends were not detected at Bosboukloof at both the annual and seasonal scales. The corresponding change percentages were negative with values of -20.8 % at the annual scale, -27.2 % for summer streamflow and -21.6 % for winter streamflow. The Mann-Kendall test identified significant decreasing trends at Tierkloof and Langrivier for both the annual and seasonal scales at a 0.05 significance level. The decreasing trends in the annual time series showed Z_{MK} values of -2.41 for Tierkloof with a negative change percentage of -28.7. Langrivier had a Z_{MK} value of -2.76 with a negative change percentage of -32.7 % (Table.3.10). The decrease in mean annual flow was more pronounced towards the end of the time series

The time series indicated that a significant decrease in mean annual flow occurred from 1976. The statistically significant decreasing trends were notable for the dry summer time series in Tierkloof (Z_{MK} =-3.06, change percentage = -42.38 %). In Langrivier the decreasing trends were identified

for both the dry summer (Z_{MK}=-2.74, -33.44 %) and wet winter time series (ZMK= -2.34, -31.67 %) (Figure.3.4). Most of the significant decreasing trends were observed during the dry summer months of January, February, March and October (Z_{MK}= -3.48 to -1.85) at all gauging stations see Appendix A (Table.A. 1). For the winter period, statistically significant trends were found in April, May and September across the gauging stations.

Table.3.10. Summary of Mann-Kendall trend test results (1946-2019) for discharge (m3/s), standard deviation, Sen's slope and trend detections for all gauging stations (values in bold means significant trends).

Site		**Period of analysis (Years)[a]**	**Z_{MK}**	**Sen's slope**	***p*-Value**		**Trend**
					0.05	0.01	
Bosboukloof	Annual	71	-1.53	0.000	*0.258*	0.277	
	Summer	71	-1.60	0.000	*0.094*	0.171	
	Winter	71	-1.35	0.000	*0.407*	0.310	
Tierkloof	Annual	71	**-2.41**	**-0.000**	***0.115***	**0.080**	***, Decr**
	Summer	71	**-3.06**	**-0.0001**	*0.003*	**0.002**	****, Decr**
	Winter	71	-1.81	-0.0002	*0.159*	0.159	
Langrivier	Annual	71	**-2.76**	**-0.001**	*0.028*	**0.006**	****, Decr**
	Summer	71	**-2.74**	**-0.000**	*0.006*	**0.006**	****, Decr**
	Winter	71	**-2.34**	**-0.002**	*0.054*	**0.020**	***, Decr**

Note: [a]Observations missing 3 years (2009-2011). Level of significance: * If trend at α = 0.05; no symbol= the significance

3.4.3. Evaluation of meteorological and hydrological drought

3.4.3.1. Meteorological drought characteristics

The meteorological drought events at seasonal (SPI-6) and annual (SPI-12) timescales were identified using the categories described in Table.3.3. The time series of the SPI values showed fluctuation between dry and wet years, with extended (> 5 years) durations of relative wetness from the late 1940s to late-1950s and again in the mid-to-late 1980s (Figure.3.4 (a-c)). An extended (> 5 years) drought period occurred between 2012 and 2017. The drought moved from moderate (-1.14 to -0.78) in 2012 to the extreme (-3.22 to -1.47) in 2017, and then became more moderate from 2018 to 2019 (-0.85 to -0.64) across the sub-catchments (Figure.3.4.(a-c)). However, the extreme drought (2015-2017) was more pronounced in Langrivier and Tierkloof compared to Bosboukloof with the SPI values reaching -3.2. The time series for all three sub-catchments showed that 1977 was the wettest year recorded, with SPI values ranging from 2.5 to 3.4. The seasonal and monthly SPI values were not presented, though they showed almost similar patterns of fluctuations between moderate to extreme droughts for all the study sites. However, they were used for the cross-correlation between the SPI and SSI in the subsequent section 3.4.3.3.

3.4.3.2. Spatio-temporal variation in Standardized Streamflow Index (SSI)

The Standardized Streamflow Index (SSI) was applied to investigate the streamflow-based drought across the sub-catchments. Figure.3.4 illustrates spatial and temporal patterns of SSI values for the three sub-catchments from 1946 to 2019 for annual (12-month) time scales also see Appendix A (Table.A.3). Though, there were minor spatiotemporal variations in the SSI values between the sub-catchments.

The 12-month SSI values exhibit variable trends of high and low flow years across the sub-catchments (Figure.3.4. (a-c)). Multiple years of high flows occurred from the mid-1940s to the mid- 1960s (SSI= -0.68 to 1.99) which was followed by a period of moderate to extremely low flows from the late 1960s to early 1970s (SSI= -2.1 to -1.3) across the sub-catchments. Another period of moderately low flows occurred between 1978 and 1982 in Tierkloof and Langrivier, however, it was not observed in Bosboukloof. In Bosboukloof and Tierkloof, moderate to severe low flows occurred from 1964 to 1974 (SSI= -1.55 to 0.44) with a few years of severe hydrological droughts, whereas Langrivier showed fluctuations between moderate and severe droughts during this period. Furthermore, Tierkloof and Langrivier showed multiple years (the early 1980s to mid-2000s) of fluctuations between extreme and moderate hydrological droughts, compared to lower intensity variability in Bosboukloof.

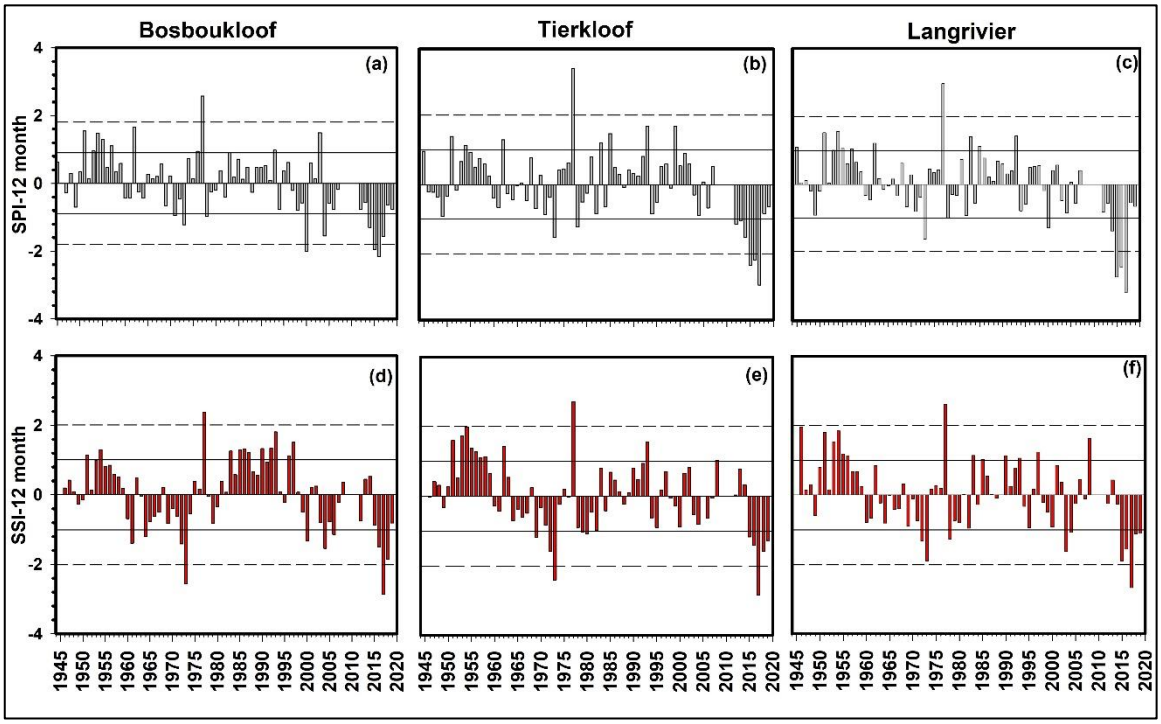

Figure.3.4. The Standardized Precipitation Index (SPI) and Standardized Streamflow Index (SSI) values for 12- month's time scale. The solid line represents the threshold between the normal and the dry/wet categories, while the dashed line represents the threshold between moderate and extreme drought/wetness.

The SSI results also indicated multiple years of low flows towards the end of the time series from 2015 to 2019. The hydrological drought intensified from 2015 towards 2019 which was a few years later than the meteorological drought which started in 2012, though the SSI outputs indicated that the hydrological drought lasted a year longer (i.e., till 2019) than the meteorological drought. The drought severity increased from moderate (-1.81 to -0.82) in 2015 to extreme (-2.83 to -2.55) in 2017 and decreased in 2018 (-0.85 to -0.54). In general, occurrences of dry years (i.e., moderate to extreme) were similar across the sub-catchments. Moreover, the time series indicated that 1977 (SSI = 2.38-2.71) was the wettest year, while 1973 (-2.55 to -1.9) and 2017 (SSI=-2.86 to -2.67) were the driest years and had the lowest flows (Figure.3.4).

3.4.3.3. Relationship between meteorological and hydrological drought

The cross-correlation between SSI-1 and the SPI-*n* (1-,3-,6- and 12 months) was applied to determine the relationship between meteorological and hydrological drought using Pearson correlation (Pearson's r) (Table.3.11). The graphical presentation of the correlation between the SSI-1 and SPI-*n* at the three sub-catchments is illustrated in Figure.3.5. The results of the cross-correlation reflect spatial variability and a significant relationship between the variables with $p < 0.05$. The most pronounced differences were found for the short-term (1- and 3 months) and long-term 12-month scale between Bosboukloof and Langrivier (Figure.3.5). For Bosboukloof, the correlation coefficient increased considerably with the SPI time scales, and the strongest correlation ($r^2 = 0.64$) occurred at the 12-month timescale (Table.3.11). The 1-month time scale

showed a weaker correlation of r^2 = 0.40 relative to r^2 = 0.57 and 0.64 for 6- and 12- months, respectively. Conversely, Langrivier the SSI-1 was strongly correlated with the short SPI accumulation periods of 1- and 3- months (r^2 = 0.70) relative to the 12- months (r^2 = 0.46) SPI accumulation periods. The correlation coefficient at 12- months was smaller relative to Bosboukloof and Tierkloof. The results showed less variation in SSI-1 and SPI-*n* relationship in Tierkloof, the correlation was strong and the same (r^2 = 0.60) at all time scales (Figure.3.5).

Table.3.11. The results of Pearson correlation analysis between one-month SS1 and SPI-n (1-,3-,6-and 12-months), including minimum and maximum SPI values.

Variable timescale	**Bosboukloof**			**Tierkloof**			**Langrivier**		
	SPI			**SPI**			**SPI**		
	r	**Min**	**Max**	***r***	**Min**	**Max**	***r***	**Min**	**Max**
SSI-1/SPI-1	0.385	-2.76	3.14	0.612	-2.83	3.18	0.700	-2.38	3.08
SSI-1/SPI-3	0.496	-3.65	2.8	0.608	-3.11	2.92	0.671	-3.53	2.72
SSI-1/SPI-6	0.568	-3.24	2.56	0.596	-3.17	2.61	0.569	-4.44	2.58
SSI-1/SPI-12	0.638	-3.16	2.76	0.574	-3.46	2.88	0.469	-3.98	2.76

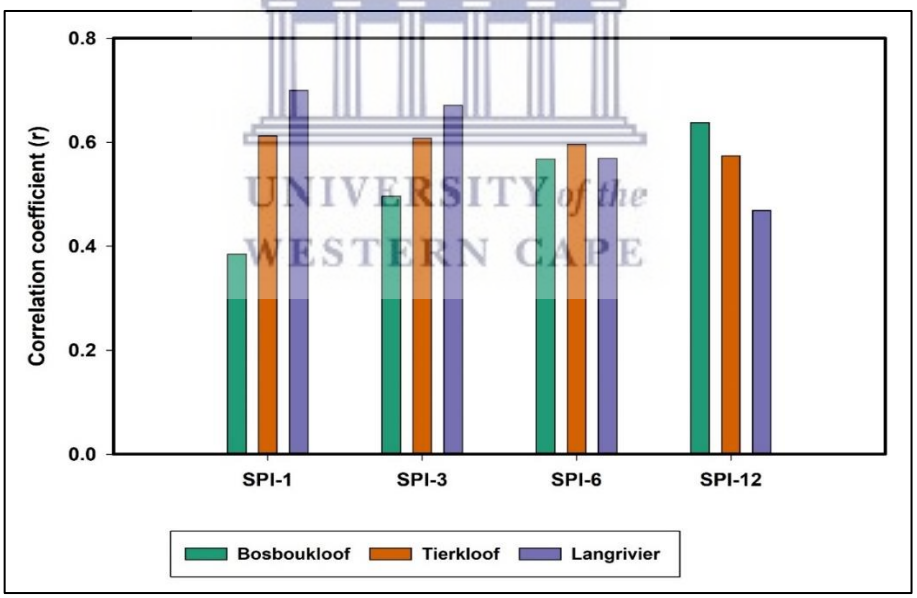

Figure.3.5. Cross-correlation and correlation coefficients (r) between SSI-I and SPI-*n* at different time scales for the three sub-catchments.

3.5. Spatiotemporal variations in trends of flow indices

3.5.1. Magnitudes and durations of annual extremes

Table.3.12 presents the statistics of flow parameters for Bosboukloof, Tierkloof and Langrivier. The results reflected spatial variations in median flow extremes for the 1-,7- and 30-day minimum and maximum. As expected, the highest median flows were recorded in Langrivier which also showed the lowest coefficient of dispersion (CD), followed by Tierkloof with Bosboukloof showing the lowest medians for most of the flow extremes (Table.3.12). Moreover, Bosboukloof and Tierkloof showed a higher baseflow index compared to Langrivier which was expected considering the low flows, especially in Bosboukloof.

Table.3.12. Descriptive statistics of selected flow parameters for the three sub-catchments indicating the medians (m^3/s) and coefficient of dispersion (CD).

Streamflow	**Bosboukloof**		**Tierkloof**		**Langrivier**	
Parameters	Median	CD	Median	CD	Median	CD
1-day min (m^3/s)	0.0032	0.73	0.0091	0.35	0.0070	0.29
7-day min (m^3/s)	0.0036	0.66	0.0094	0.37	0.0073	0.27
30-day min (m^3/s)	0.0038	0.70	0.0105	0.40	0.0081	0.31
1-day min (m^3/s)	0.0657	0.68	0.4450	0.50	0.6917	0.93
7-day max (m^3/s)	0.0467	0.69	0.2060	0.56	0.2791	0.91
30-day max (m^3/s)	0.0318	0.69	0.1154	0.52	0.1425	0.84
Baseflow index	0.29	0.43	0.24	0.31	0.16	0.38
Rise rate (m^3/day)	0.00037	0.56	0.0012	0.95	0.0001	2.04
Fall rate (m^3/day)	-0.00035	-0.60	-0.0009	-0.74	-0.0011	-0.62
Number of reversals	135	0.16	130	0.14	124	0.14

Note: Min= Minimum, Max= Maximum

Trends in high and low flow magnitudes

The single period analysis of the IHA was used to detect statistically significant trends or changes in flow magnitudes, duration of annual extremes and rate and frequency over time for the period 1946-2019. The results of the trend analysis for the selected IHA parameters are shown in Table.3.13. The results showed that the detected trends were not consistent for all three sub-catchments over the analysis period. The annual minimum flows showed no significant trends for all three sub-catchments (Table.3.13). However, significant trends were observed for the annual maximum flows in Tierkloof and Langrivier. Both sub-catchments experienced a decrease in the 1-,7-, and 30- day maximum flows (Figure.3.6). No significant trends were detected in most of the parameters in Bosboukloof, except for the fall rate and the number of reversals. Figure.3.6 shows that the observed decrease in the median of the annual 7-day maximum flow in Tierkloof occurred towards the end of the times series (2013-2017) which was consistent with the periods of severe to extreme meteorological and hydrological droughts.

Trends in frequency, rate, and duration of indices

The summary of relative changes in frequency and rate of the extremes is presented in (Table.3.13). The rise and fall rate parameters provide information on how slow/rapid the flow hydrograph responds or on abrupt changes in the interannual flow. The results showed non-significant trends for frequencies of rise rates within the sample years. Conversely, statistically significant trends for the fall rate were detected for Bosboukloof and Tierkloof, the increase was notable toward the end of the time series, whereas it was found to decrease in Langrivier (not presented). Also notable was the significant decrease in the number of reversals at all the sub-catchments, particularly in Langrivier (slope= -0.4014). The number of reversals indicates the change in the direction (rise vs fall rate) of the daily flow (i.e., the number of times flows switched from rising or falling period).

Table.3.13. The results of trend analysis of the selected flow attributes. Trends that were significant at the 5% level are shown in bold.

Parameter	**Bosboukloof**			**Tierkloof**			**Langrivier**		
	Slope	*p-Value*	*CD*	*Slope*	*p-Value*	*CD*	*Slope*	*p-Value*	*CD*
Flow extremes (m^3/s)									
1-day min	-0.00002	*0.1*	0.74	-0.00002	*0.1*	0.36	-0.00001	*0.5*	0.30
7-day min	-0.00002	***0.05***	0.67	-0.00002	*0.1*	0.38	-0.00001	*0.5*	0.28
30-day min	-0.00002	*0.1*	0.68	-0.00002	*0.25*	0.40	0.00000	*0.5*	0.32
1-day max	-0.00030	*0.25*	0.69	-0.00137	***0.025***	0.50	-0.00973	***0.05***	0.94
7-day max	-0.00015	*0.25*	0.70	-0.00061	***0.05***	0.56	-0.00133	*0.5*	0.91
30-day max	-0.00010	*0.25*	0.70	-0.00035	***0.05***	0.52	-0.00099	***0.025***	0.85
Baseflow index	-0.00081	*0.25*	0.39	0.00042	*0.5*	0.31	0.00073	*0.25*	0.38
Rise rate (m^3/day)	0.00037	*0.5*	0.56	0.00001	*0.5*	0.96	-0.00132	*0.25*	2.04
Fall rate (m^3/day)	-0.00035	***0.005***	-0.60	0.00001	***0.005***	-0.75	-0.00115	***0.05***	-0.61
Number of reversals	-0.25890	***0.025***	0.16	-0.23480	***0.05***	0.14	-0.4014	***0.001***	0.14

Note: Min= Minimum, Max= Maximum, CD = Coefficient of Dispersion

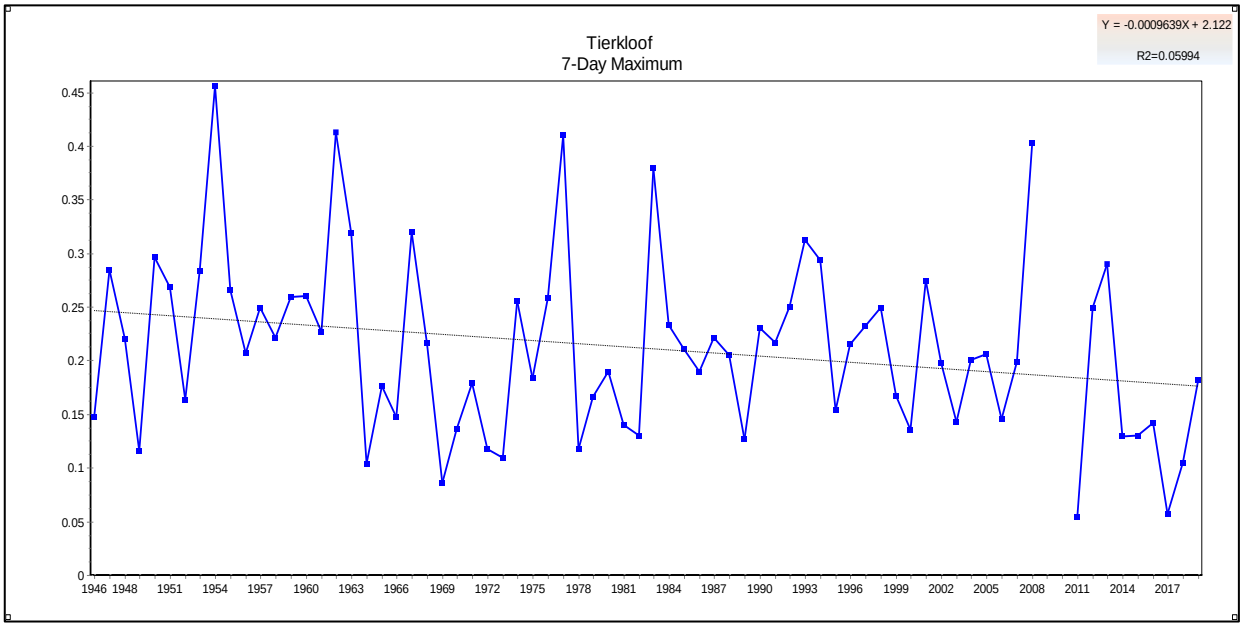

Figure.3.6. Results of the IHA analysis for 7 days maximum in Tierkloof.

3.5.2. Changes in flow indices related to land use (Afforestation and clear-felling)

Table.3.14 presents the results of the hydrologic alterations related to afforestation and clear-felling planting schemes in Bosboukloof and Tierkloof sub-catchments. The analysis indicated significant differences between the mean annual runoff during the afforested and clear-felled period for Bosboukloof, with an increase of 88.7 mm in mean annual runoff (MAR) during the clear-felled period. However, the difference in mean annual rainfall between the two periods was relatively small (31.3 mm/a). Moreover, the results showed a significant (p-value = 0.006) difference in runoff ratio between the two periods (Table.3.14). Conversely, the results indicated a large decrease in MAR during the afforestation period for Tierkloof compared to the pre-afforestation period. The mean annual runoff decreased by nearly 70 % with a significant decrease in runoff ratio from 0.77 to 0.61 (p-value < 0.05). Overall, the results showed that the clear-felling period in Bosboukloof was followed by increased runoff, whereas the planted period was associated with a decrease in the annual runoff.

Table.3.14. Summary statistics for the evaluated periods showing the mean annual precipitation (MAP) and mean annual runoff (MAR), runoff ratios and runoff ratio p-value at a 5% level of significance.

	Bosboukloof		**Tierkloof**	
	Afforested 1946-1978	Clear-felled 1979-1989	Pre-afforestation 1946-1956	Afforested 1957-1978
No.of years	32	10	10	21
MAR (mm/a)	399.61	487.99	1114.28	859.31
MAP (mm/a)	1266.2	1234.9	1433.3	1387.6
Runoff ratio	0.31	0.39	0.77	0.61
p-value	0.006		0.001	

Changes in monthly flow magnitudes

The range of variability approach (RVA) was used to assess the alteration of flow regimes associated with afforestation and clear-felling. Figure.3.8 show the degree of hydrologic alteration (HA) for the flow magnitudes and duration of annual extremes, rates, and frequency of flows. The positive HA values indicate a higher frequency of values in the given RVA category (low, middle, or high), and vice-versa for the negative HA values.

As shown in Figure.3.7 (a-b), the monthly median flow increased substantially following the clear-felling, particularly for July, September and October with a significant increase between 30 % and 50% ($p < 0.05$). The monthly flows from July to September were almost similar during the clear-felled period at 0.052 m^3/s. On the other hand, the flow magnitude decreased substantially during the afforested period in Tierkloof (Figure.3.7.b). A notable significant decrease occurred between July and October; the highest decrease occurred in July estimated at -54% ($p = 0.027$).

Bosboukloof showed an increase (positive HA) in the frequency of high RVA (i.e., 66-100 per centile) category values for almost all the months during the clear-felled period (Figure.3.8.a). The most increase occurred in October and from December to May, including the winter months of July and September. Conversely, during the afforested period in Tierkloof, the frequency of values in the high category decreased substantially, except for June which showed an increase in the frequency of high RVA category value and mean monthly flow estimated at 15% (Figure.3.8.c). Furthermore, the afforestation period was followed by an increase in the frequency of low RVA category values (< 33 per centile) up to 2.2. Overall, during the afforested period, most hydrological alteration occurred in the monthly median flows during the high flow winter months and was less during the summer months (November-March).

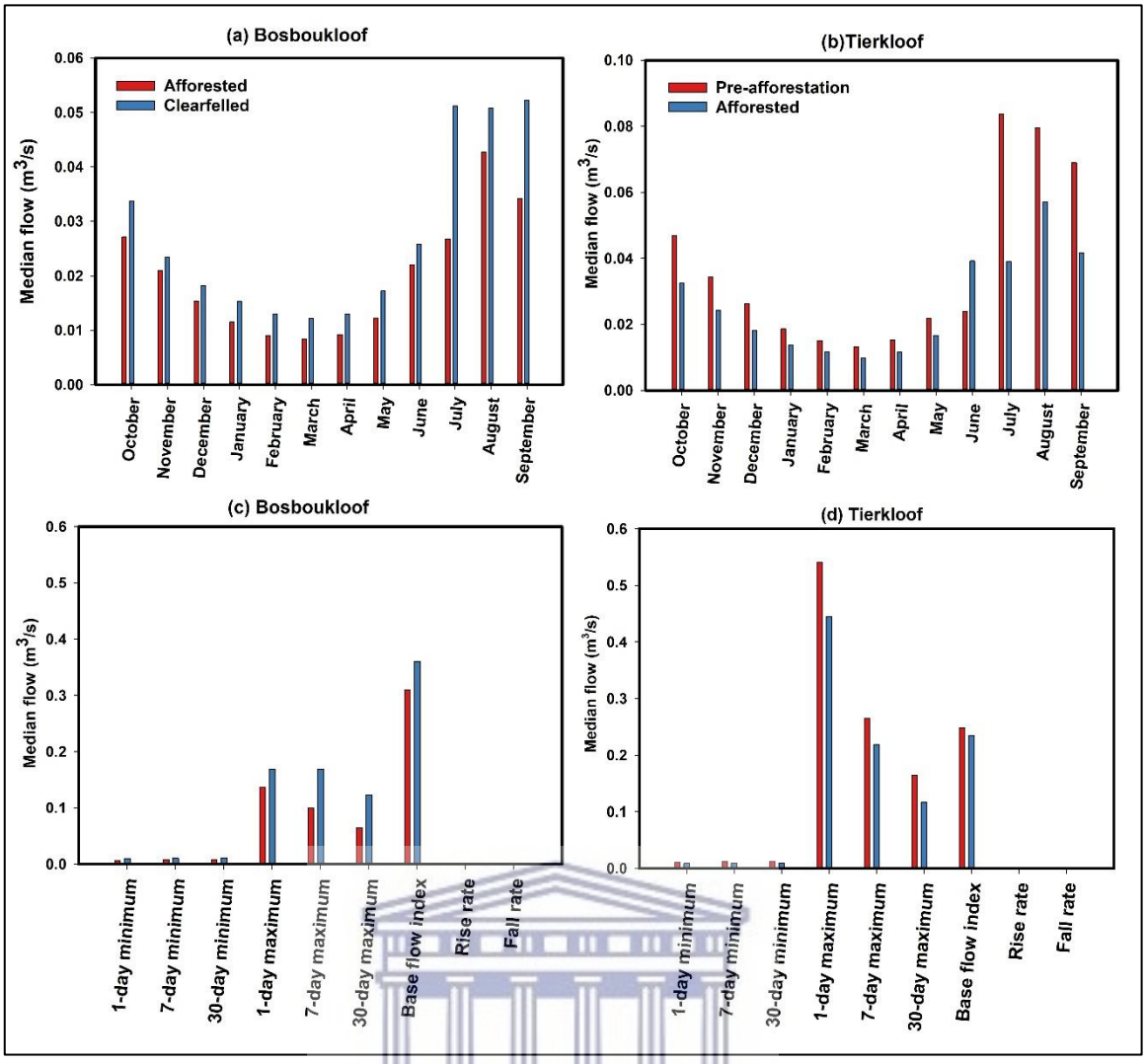

Figure.3.7. Comparison of the hydrologic alterations (RVA analysis) for (a,c) Bosboukloof: afforested vs clear-felled and (b,d) Tierkloof: pre-afforestation vs afforested.

Hydrologic alterations of extreme low and high flow

Like the monthly median flows, the minimum and maximum annual extremes increased for the clear-felled period in Bosboukloof, but a large decrease occurred during the afforested period in Tierkloof. The results showed the highest increase occurred for the 7-day and 30-day maximum estimated at 8 % to 10 % and the baseflow index ranged from 3.1 to 3.5.

Conversely, afforestation in Tierkloof resulted in a decrease in the 1-, 7- and 30-day maximum flows estimated at -18 %, -10% and -27%, respectively. The RVA analysis further showed an increase in the frequency of the high RVA category values for the minimum and maximum flow during the clear-felled period, especially for the 1-,7- and 30- day minimum (Figure.3.8.c). The high category RVA for the multiday minimum values increased significantly (p = 0.004) during the clear-felled period compared to the annual maximum flows. On the other hand, the number of reversals showed a decrease in the frequency of values in the high RVA category.

In Tierkloof, the annual minimum and maximum extremes, baseflow index and number reversals showed a decrease in the frequency of the high RVA category values and an increase in the frequency of low category RVA values during the afforested period (Figure.3.8.d). However, the fall rate showed an increase in the high category values. A minor decrease was also found in the baseflow during afforestation estimate at - 8%, with an increase in the frequency of low category RVA values.

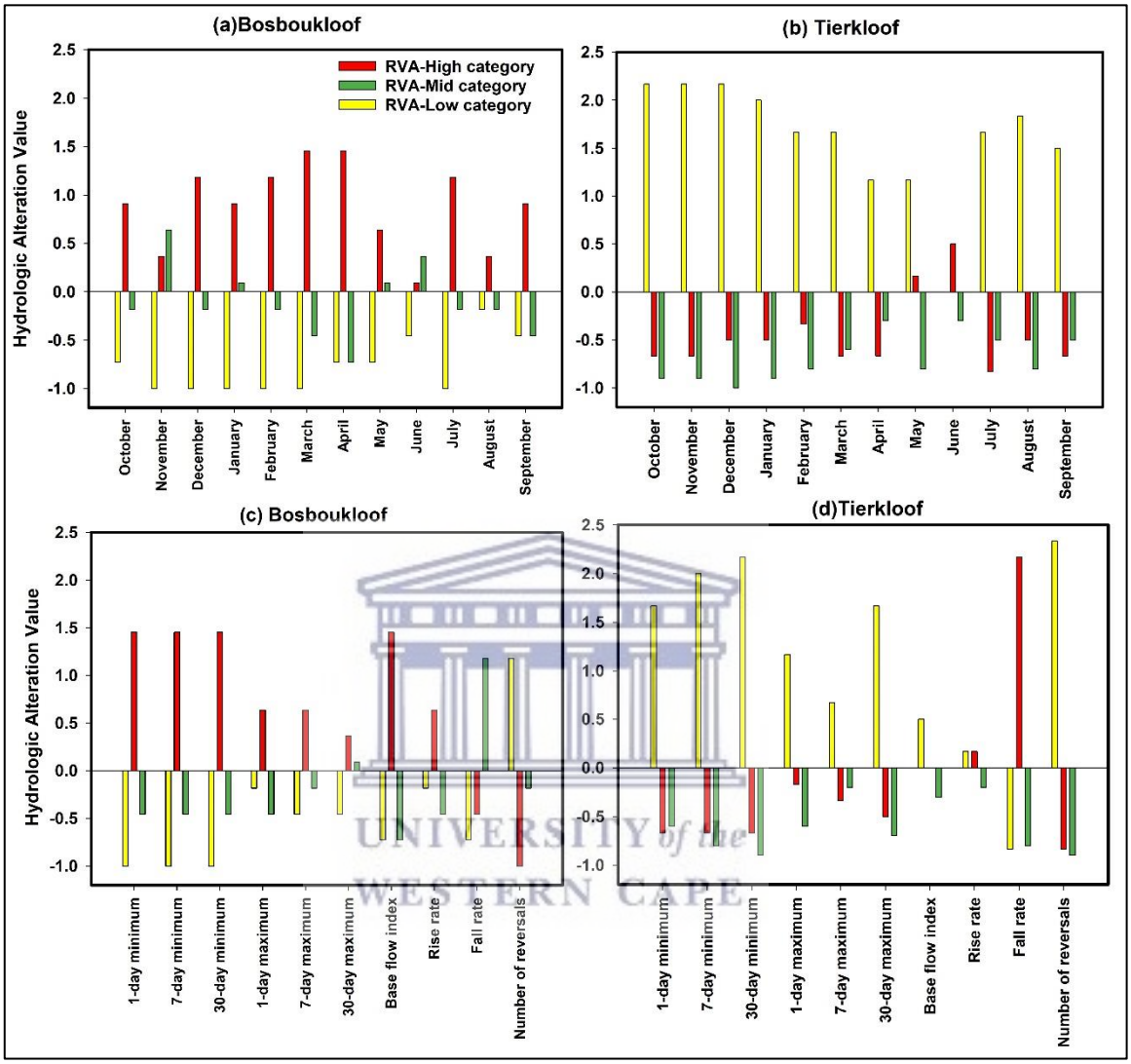

Figure.3.8. Hydrologic alteration values for the monthly flow and annual extremes at (a,c) Bosboukloof and (b,d) Tierkloof. RVA=Range of Variability.

3.6. Discussions

3.6.1. Trends in hydroclimatic variables in the Jonkershoek sub-catchments

Significant trends and change points were identified by the Mann-Kendall trend test, Sen's slope estimator and homogeneity tests for the long-term precipitation and streamflow data from 1946 to 2019 at the three sub-catchments. The rainfall and streamflow in the catchment exhibit spatial and temporal variation which was attributed to the difference in altitude of the sub-catchments and rain gauges. For instance, the contribution of clouds (35%) to precipitation through cloud interception was reported for high elevation stations in Langrivier and an estimated contribution of >200 mm to the total summer rainfall (Mbali, 2016). Moreover, differences in streamflow due to the catchment characteristics (e.g., Landscape, land cover, climate) have been identified as the main control of streamflow response in headwater catchments (Didzun and Uhlenbrook, 2008; Price et al, 2011).

Interestingly, the homogeneity tests (Pettit's and SNHT) identified inconsistent years of change points in rainfall and streamflow time series at both annual and seasonal timescales for all three study sub-catchments (Figure.3.2). The change points in rainfall were gradual, therefore, the change points could not have been due to changes in equipment or the relocation of the stations. Therefore, the detected change points were attributed to an increase in climatic and interannual variability in rainfall.

Similar to rainfall, the change points for streamflow time series were different for the different sub-catchments. The change point in Bosboukloof coincided with that for rainfall, whereas the identified change point in Langrivier coincided with a period of drought as indicated in (Figure.3.5). Thus, the abrupt changes in these sub-catchments were considered climate-related, indicating a quick reaction to climate shifts probably due to the low storage (Hewlett and Bosch, 1984) and small scale. Hence, the rainfall deficits manifest rapidly into streamflow deficits. Conversely, the change point in Tierkloof was consistent with the establishment of the pine plantation. Thus, it can be concluded that the downward shift/ decrease in mean annual flow was mostly due to the plantations as already reported by previous studies (Kruger and Wicht, 1976; Scott et al., 2000; Dye, 2001). Also, this could partially be the result of climate trends, supported by the declines in rainfall. The streamflow in Bosboukloof was less responsive to plantation compared to Tierkloof. Catchments that are less responsive to changes or disturbances such as Bosboukloof are commonly associated with large storage capacity and more complex flow pathways (Spencer et al., 2021). The impacts of plantations on streamflow magnitude and annual extreme will be discussed in the subsequent section 3.6.3.

The Modified Mann-Kendall test indicated significant decreasing trends in annual and seasonal rainfall time series for most of the stations across the sub-catchments. These findings are consistent with Duah (2010) for the nearby stations in Franschoek suggesting shifts in climatic patterns in this

region. He also reported gradual increases in temperature trends across Western Cape which may have contributed to the decreasing trends in rainfall. Most of the significant decreasing trends in the rainfall were observed in the wet winter season for almost all the stations which are similar to the results of Acosta et al. (1999), Burls et al. (2019) and Du Plessis and Schlom (2017).

For the monthly scale, rainfall and streamflow showed decreasing trends in April, May and October (Appendix A, Table.A. 1 and Table.A.2). The decreasing rainfall trends in May and October were consistent with the findings of Du Plessis and Schloms, (2017) for most stations of the Mediterranean region. April and May are the transition month from dry summer to wet winter and while October marks the transition from wet winter to dry summer in the region. Therefore, the former may suggest an early onset and the latter indicates early termination of the rainfall season. Similar results were reported for the rainfall in the Western Cape Province (WC) by Mahlalela et al. (2019). This was linked to changes in the duration of rainfall events associated with cold fronts as described by (Burls et al., 2019). Furthermore, the decrease in winter rainfall was attributed to the displacement of the poleward South Atlantic storm track and the jet stream, steering rainfall away from Cape Town (Mahlalela et al., 2019). Overall, climate variability could be considered the main reason for the decrease in rainfall which resulted in a significant decrease in streamflow from the source catchment (Figure.3.5).

3.6.2. The relationship between meteorological and hydrological drought

The drought indexes analysis showed that the sub-catchments have been subjected to droughts with varying severity and duration over time, and high frequencies of droughts in the near-normal category (Table.3.3). The drought severity and duration did not reflect the spatial variation. The meteorological droughts were consistent with the findings of previous studies in the WC (e.g., Rouault and Richard, 2003; Duah, 2010). These droughts have been partially linked to the El Ninõ Southern Oscillation systems (Philippon et al., 2012). In the case of the 2015-2017 drought, Soussa et al. (2018) concluded that the poleward shift of the Southern Hemisphere moisture corridor resulted in changes in local rainfall patterns.

The cross-correlation revealed spatial variations when looking at the relationship between the hydrological and meteorological drought, particularly between Bosboukloof and Langrivier which was not expected considering the small catchment scale (Table.3.11). The hydrological drought accumulation periods were found to be more site-specific. This may also reflect some spatial variability observed in the SPI and SSI values. Spatial variations in drought response are commonly found to be the results of catchment properties among others vegetation cover, geology, storage, climate and soil characteristics (Barker et al., 2016). This may be the case for the Jonkershoek sub-catchments which exhibit variations in rainfall, streamflow, and land cover. The spatial variation between the transition period from meteorological to hydrological drought, suggests the influence of catchment properties especially those related to catchment storage (i.e., baseflows index, soil

conditions and geology of the aquifer). For example, the short accumulation period (1-3 months) in Langrivier is common in responsive catchments with little storage associated with fractured geology and steep slopes (Vincente-Serrano and Lopez-Moreno, 2005).

Conversely, the propagation of meteorological to hydrological drought in Bosboukloof has been estimated to be longer at 12 months which is the result of strong seasonality, especially in catchments with higher evapotranspiration. High ET rates in Bosboukloof have been reported by Lesch and Scott (1997) and Dye (2001). However, a detailed investigation of the relationship between the catchment and drought characteristics is required to understand the spatiotemporal variations. Further analysis using other indices such as the Standardized Precipitation and Evapotranspiration Index (SPEI) can provide a better insight into the influence of climate. This information is crucial for drought monitoring and sustainable management of water resources in forested headwater catchments.

3.6.3. Hydrologic alteration of flow attributes

Flow indices trends

Analysis of the hydrologic alterations in flow attributes over time identified significant decreasing trends in magnitude and duration of flow extremes (Table.3.13). The trend results varied for the individual sub-catchments. Significant trends were mostly found in 1, 7- and 30-day maximum flows, especially in Tierkloof and Langrivier. These suggest strong variation in the magnitude and duration of annual extremes and can be attributed to the uneven distribution of rainfall and differences in streamflow response within the catchment, which increase the importance of heterogeneities in physiographic characteristics (Barker et al., 2016).

The decrease in annual maximum extremes across the investigated sites coincided with the trends in annual rainfall and streamflow. Thus, these trends were attributed to interannual variability in rainfall and streamflow. It can be speculated that the decrease in winter rainfall influences groundwater recharge resulting in decreased streamflow production in the sub-catchments as they rely largely on baseflows from the Table Mountain Group (TMG) aquifer (Saayman et al., 2003; Roets et al., 2008a, 2008b). The precipitation in most TMG catchments contributes to groundwater recharge instead of direct surface water due to the fractured nature of geology. Moreover, Tierkloof showed the most decreasing trends in flow attributes, it is also important to note that these trends were consistent with the afforestation period, thus it can be difficult to pinpoint these patterns only to climate variability.

Hydrologic alteration in response to afforestation and clear-felling

Previous studies in the Jonkershoek catchment have demonstrated that in the past decade the streamflow regimes have been altered due to afforestation (Lesch and Scott, 1997; Scott et al., 2000; Scott and Prinsloo, 2008). This study applied statistics including IHA to evaluate the potential hydrologic alteration of flow magnitude and duration of annual extremes by the pine plantation schemes. The results indicated significant declines in median monthly flow magnitudes and annual extremes following afforestation and a significant increase in the flow indices after clear-felling (nearly 33 years later). These results are mostly consistent with the findings of previous studies on the impacts of afforestation on streamflow in Jonkershoek (Scott et al., 2002). Though the largest changes in monthly median flow occurred during the wettest winter months for both the clear-felled and afforested periods, Scott et al (2002) also reported the largest reductions during the autumn months (February to April).

A significant reduction occurred in minimum and maximum flows as well as the baseflow index. The observed reductions in the 1-, 7- and 30-day maximum flows and the wet winter (July-Sep) monthly flows during the afforested period in Tierkloof indicate the decrease in peak flows, which were consistent with the decrease in the frequency of high category RVA values (Figure.3.7.d).

A study by Dye et al. (2001), found that the invasive species had high ET estimates compared to the indigenous vegetation with a difference of 177 mm/a. Moreover, the increment of the vegetation cover during this period may have potentially influenced the partitioning of incoming rainfall to contribute more evapotranspiration and enhance infiltration capacity via preferential flow pathways and reduced surface runoff. The latter may also explain the decrease in the runoff ratio, implying the reduction may have not only been due to high ET but also the increase in vegetation cover upslope. Comparable results have been reported in other forested or disturbed catchments in various parts of the world (Saraiva Okello et al., 2015; Albaugh et al., 2015; Gebremicael et al., 2019).

Conversely, large increases in monthly flows and annual extremes were recorded during the clear-felled period in Bosboukloof. It can be said that the decrease in vegetation cover and canopy interception, contributed to allowing incoming rainfall to be converted to surface runoff. This was confirmed by the increased frequency of values in the high RVA category (i.e., high flows), the median monthly flow particularly during the wettest months (July-September), baseflow index and annual low and high flow extremes. Scott et al. (2002) reported similar findings which indicated a 38 to 53 mm/10% flow increase per area clear-felled. Overall, these results demonstrate that land use changes contributed significantly to the hydrologic alterations in the Jonkershoek sub-catchments.

3.7. Limitations

Evaluation of the long-term variability in hydroclimatic variables and the impacts on streamflow regimes requires the comparison of numerous records of meteorological and hydrometric data such as rainfall, temperature and streamflow. This can provide good insight into the potential vulnerability of headwater catchments to the changing climate. However, this analysis was limited by the availability of long-term temperature data to correlate with the rainfall and streamflow data to fully investigate the influences of climate-driven changes on streamflow regimes. Furthermore, the lack of data recorded for the plantation rotations post-1994 limited the evaluation of the impact of afforestation on flow regimes in the recent year including the study period. These data could improve our understanding of the impacts of the ongoing afforestation and climate variability on streamflow regimes in this catchment.

3.8. Conclusions

The investigation of changes in long-term rainfall and streamflow and the effects of climate-driven and land use/cover changes on streamflow regimes was conducted in Jonkershoek at a sub-catchment level. The application of statistics showed that the hydroclimatic variables have been altered with significant decreasing trends in annual and seasonal rainfall at all the stations. Significant decreases in streamflow were identified at annual and seasonal scales. The detected change points for annual rainfall were gradual across the sub-catchments and were mostly not consistent with those of streamflow. The identified change points in Tierkloof and Langrivier were consistent with the past land use/cover changes (the mid-1950s) and earlier meteorological drought cycles (early 1950s), respectively. Moreover, the change points in Bosboukloof coincided with that observed in rainfall. Therefore, it can be concluded that both the climate variability and changes in land use by afforestation are the reason for these changes which contributed to a decrease in flow across the catchment.

Results of the SPI and SSI analysis indicated large fluctuations between dry and wet years as well as patterns of low and high flow years with the longest drought periods of 5 years. The propagation of meteorological drought to hydrological drought varied spatially. In Bosboukloof the SSI-*n* was strongly correlated with long-duration SPI, whereas in Langrivier it was strongly correlated with the SPI at a shorter time scale. Based on these results it is evident that physiographic characteristics such as vegetation cover, topography, drainage pattern and storage can affect catchment response influenced drought propagations. Moreover, this shows that the drought indices can be a great addition to an improved understanding of the catchment hydrologic behaviour.

Evaluation of hydrologic alteration of flow indices also indicated significant decreasing trends in Tierkloof and Langrivier, in median monthly flows, annual extremes, and rate and frequency which

were consistent with the observed land use change and meteorological droughts, respectively. The comparison of the impacts of different planting practices showed that afforestation in Tierkloof has altered the flow parameters, with a significant decrease in the magnitude of monthly median flow, especially in winter months. The RVA indicated a reduction in high flows and low flows increased. Though the clear-felling in Bosboukloof was found to have improved the flow attributes, particularly the monthly median flows, annual maximum extremes and baseflow index. The increase in the baseflow index is of significant importance in these catchments as it sustains the flow during the dry season. Based on these findings, it can be speculated that land use change is the main driver of the observed hydrologic alterations.

Studies of hydro-climatic trends at catchment scales could be beneficial for drought forecasting and the proper development of regional water management strategies. Further investigations analysis of hydrologic alteration in recent years, on the onset and magnitudes of meteorological and hydrological droughts and continued monitoring of impacts of the land use change, are required. Such studies should focus on the small scale in the TMG mountainous headwater catchment. The results of this type of study should be made more available to multiple stakeholders to inform the development of effective mitigation, improve catchment water resources management and implement adaptation measures in the Cape Town Metropolitan Area.

CHAPTER 4: SPATIAL AND TEMPORAL VARIATIONS IN STABLE ISOTOPES AND HYDROCHEMICAL CHARACTERISTICS.

This chapter is an edited version of Mokua, R. A., Glenday J., Nel, J & Butler, M.(2020). Combined use of stable isotopes and hydrochemical characteristics to determine streamflow sources in the Jonkershoek catchment, South Africa, *Isotopes in Environmental and Health Studies*. 56(3), pp. 1–22. doi: 10.1080/10256016.2020.1760861.

This chapter focuses on the application of the stable isotopes of water ($\delta^{18}O$ and $\delta^{2}H$) and hydrochemical data to assess seasonal changes between sources of stream water and flow pathways in baseflow conditions for three headwater sub-catchments (~1.5 to 3 km^2) of the Jonkershoek. The findings will be applied to develop a conceptual model highlighting the main water sources and flow pathways during the dry summer and the wet winter.

4.1. Introduction

Headwater catchments in the Table Mountain Group (TMG) geological formation, such as the Jonkershoek Valley, are primary water sources for the Cape region of South Africa. These catchments are of great importance as they supply water to domestic, industrial, and agricultural sectors, as well as support unique ecosystems. Owing to the current state of water scarcity in the region, investigation of the TMG aquifer system as an additional source of bulk water supply for the City of Cape town has been ongoing (Wu, 2005; Duah, 2010; Harris et al, 2010).

Understanding how rainwater is partitioned in these catchments, and particularly the role of the TMG groundwater in contributing to streamflow is fundamental for water resources management. This study aims to add to the understanding of hydrological processes in this region by investigating streamflow generating mechanisms that support baseflow in headwater streams at the end of a major drought.

Streamflow generating processes in mountain catchments can vary in space and time, controlled by the physiographic characteristics and hydro-climatic factors of the catchment, which influence stream response, residence time, flow pathways and travel times (Hewlett and Hibbert, 1967; Kendall and Coplen, 2001; Uhlenbrook et al., 2002; Didszun and Uhlenbrook, 2008). This variability poses a challenge in modelling runoff generation and incorrect representation of processes in modelling results in improper water management strategies. Other studies across the world have attempted to differentiate the roles of various streamflow generating mechanisms in headwater catchments, including overland flow (infiltration excess and saturation excess), interflow, channel precipitation, and groundwater outflow (Hewlett and Hibbert, 1967; Sklash and Farvolden, 1979; Beven, 1991, 2012; Uhlenbrook et al., 2002; Soulsby et al., 2003). Several studies (Soulsby et al., 2003; McGlynn et al., 2004; Guastini et al., 2019) have shown that considerable

spatial and temporal variations in dominant runoff generation mechanisms can exist at a small scale (< 10 km^2) due to the heterogeneity in physiographic and hydro-climatic factors such as soil moisture and rainfall.

Studying hydrological processes in areas with fractured geology and high rainfall variability, such as the TMG region, is a challenge due to the high variability both spatially and inter- and intra-annually of streamflow, groundwater levels and low ionic concentrations (Clark and Ractliffe, 2007; Diamond, 2014). The extremely high rainfall > 3300 mm/a (recorded at the highest point Dwarsberg station, 1214 m) can result in the leaching of minerals and flushing of salts (calcium and magnesium) (Smart and Tedroux, 2002). Environmental tracers, such as the stable isotopes of water oxygen ($\delta^{18}O$) and hydrogen ($\delta^{2}H$/ deuterium) in conjunction with other hydrochemical properties such as concentrations of major ions, dissolved silica, and electrical conductivity (EC), can offer more insights into catchment runoff processes than the use of hydrometric data alone (Buttle et al., 1998). These techniques have the potential to improve water management practices in this hydrologically complex and water-stressed region.

Stable isotopes of water are the most conservative tracers as their concentrations do not change due to contact with soil or rock, however, as the water moves through the hydrological cycle it undergoes a phase change which may influence the isotopic composition through a process of fractionation (Ingraham, 1998). This fractionation due to evaporation results in the different isotopic fingerprints across water sources that contributes to streamflow. Differences have been observed in isotopic compositions of rainfall across space and time due to continentality, amount of precipitation, altitude and climate/temperature (Ingraham,1998). Craig (1961) showed that the fractionation between the oxygen and hydrogen isotopes is similarly leading to the development of a covariance regression line, the Global Meteoric Water Line (GMWL). This is used to determine the effects/degree of fractionation due to evaporation. These differences have been recorded at different scales, during a single storm and between storms with large differences observed on a seasonal scale (Harris et al., 2010).

Few studies have investigated runoff generation processes in the TMG mountain region, using hydrochemical and isotope tracers for hydrograph separation and exploring conceptual models of flow paths (Midgley and Scott, 1994; Saayman et al.,2003). Midgley and Scott, (1994), sampled 8 winter storm events in headwater tributaries of the Jonkershoek and found evidence that runoff generation during sampled events was mainly due to the displacement of old water, with new water from the storms making up less than 10% of the event streamflow. A conceptual model by Saayman et al. (2003) for the nearby Zachariashoek catchment, suggested multiple dominant flow pathways with a surface runoff on the steep slopes as well as recharge in the mountains feeding springs or groundwater discharge in the foothills. These studies did not address spatial and temporal variations in water sources in baseflow conditions both across seasons and with differing catchment

conditions. Nevertheless, they do provide potential conceptual models for testing and further development in Jonkershoek.

Studies elsewhere in the region have highlighted spatiotemporal variability in isotopic composition in rainfall, linked to altitude effects, continental effects, and the varying frontal and convective weather systems across seasons with related amount effects (Harris et al., 2010; Diamond, 2014). Comparing stable isotope signatures of mountain springs to those of rainfall, these studies found that springs had relatively depleted values, indicating recharge from colder storms and/or higher elevations. Some had little inter-annual and seasonal variation indicating deep well-mixed groundwater sources, while others had temporal patterns correlated to interannual rainfall signatures, indicating shorter flow pathways (Harris et al., 2010; Diamond, 2014). Given the levels of local variability, it is evident that isotopic and hydrochemical approaches are still under-utilized in the TMG aquifer areas particularly for understanding the diversity of, and potential patterns in streamflow generation and surface water-groundwater interactions.

In this study, stable isotope and hydrochemical tracer techniques were applied to examine potential water sources and flow pathways feeding baseflow, as opposed to storm event peaks in three headwater catchments (~3 km^2). The sub-catchments are characterised by different vegetation cover (*Pinus radiata* vs fynbos) and to a lesser degree topography and drainage pattern. Based on the review of local and regional literature as well as the findings of the previous chapter (Chapter 3) it can be hypothesised that (i) these small headwater catchments will show differences in streamflow response, owing to the high variable topography (slope, size), climate, land use and soil characteristics, (ii) which may result in different flow pathways and (iii) the afforested sub-catchment would have more contribution from deep groundwater due to high evapotranspiration rates (ET) from the pine plantations which is more likely to utilize use up shallow soil water. The aim is to develop a conceptual model of processes contributing to baseflow during both the dry and wet winters in these catchments.

This study forms part of a larger and longer-term research effort at the site which will include the investigation of storm events in a future study (Chapter 6). The objectives of the present study are to assess whether the spatial variations in stable isotopes and hydrochemical parameters can be used to, (1) characterise the isotopic compositions of precipitation to inform the interpretation of seasonal streamflow isotope response, (2) characterise the spatio-temporal variations in the stable isotope composition in streamflow, groundwater and spring to identify seasonal variability in sources of stream water and flow pathways (3) to demonstrate the value of stable isotope and hydrochemical parameters in constraining stream water sources and flow pathways in a fractured geology system.

4.2. Materials and Methods

4.2.1. Study site

The study was conducted in Bosboukloof, Tierkloof and Langrivier (Figure.4.1). More details of the study site location, physiographic and land use are presented in Chapter 2. A summary of the sub-catchment characteristics is presented in Figure.4.2 and Table.4.1. (Table.4.1).

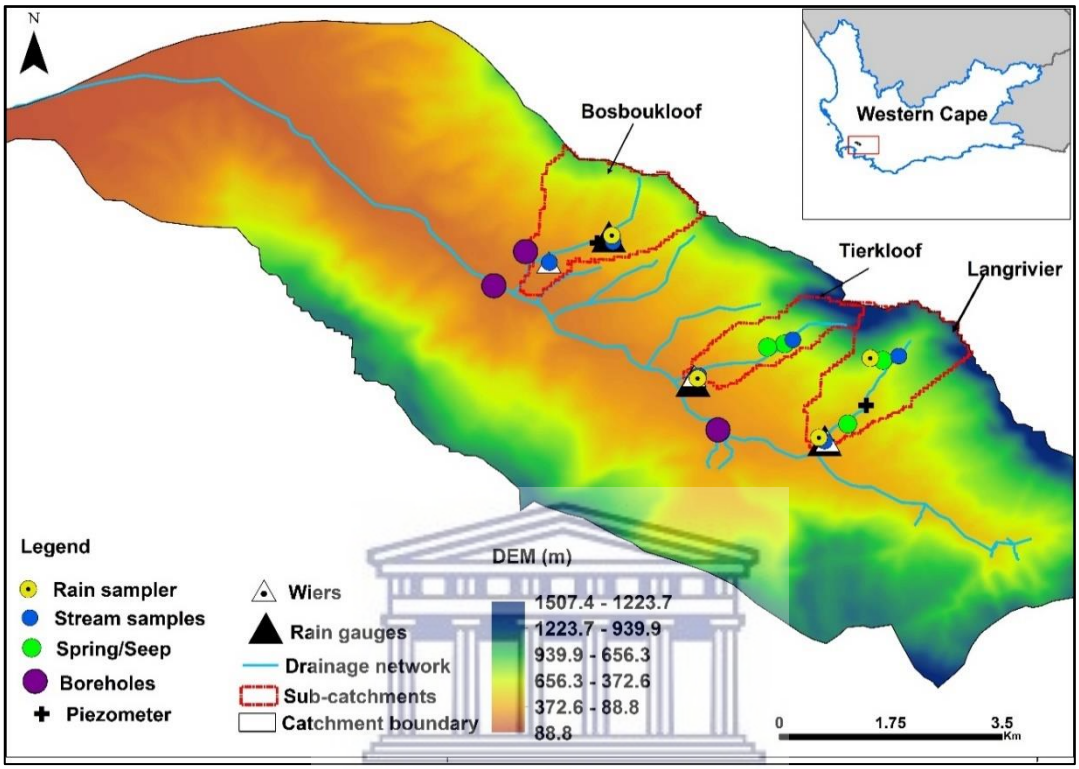

Figure.4.1. Sampling sites, elevation, and stream network in Bosboukloof, Tierkloof and Langrivier. Please note some monitoring stations are closely located (e.g., weirs, lower rain gauges and rainfall samplers) see Figure.2. 2Figure.2.4 for a more detailed map of the sampling site.

Table.4.1. Summary of the study site characteristics, including Mean Annual Precipitation (MAR) and Mean Annual Runoff (MAR) for the hydrological years 2018-2019 (SAEON, 2019).

	Bosboukloof (BS)	**Tierkloof (TK)**	**Langrivier (LG)**
Area (km^2)	2.09	1.45	2.46
Altitude range (mamsl)	274- 1026	280-1530	366-1460
Stream length (km)	1.66	1.88	2.31
Slope (degrees)	26	49	40
Average daily flow (m^3/s)	0.011* ,0.026 [a]	0.011* ,0.041 [a]	0.036* ,0.144 [a]
MAR (mm/a)	232	558.6	962.4
MAP (mm/a)[b]	1200	1137	1317

Note: * summer average daily flow, [a] winter average daily flow, [b]averaged rainfall

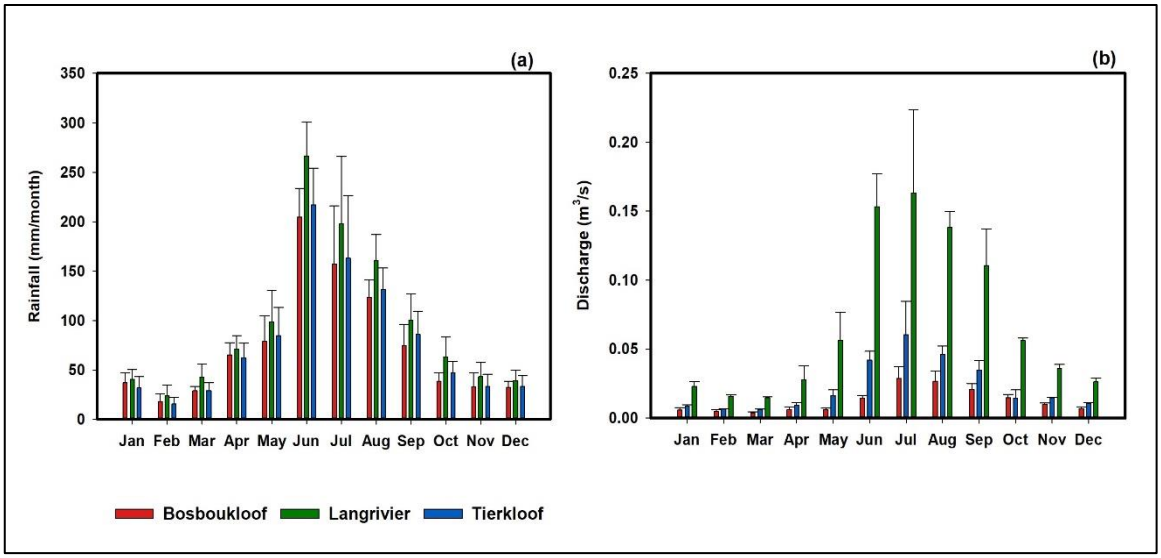

Figure.4.2. Mean monthly(a) rainfall and (b) discharge for the three sub-catchment during the study period (2018-2019).

The geology is composed of highly fractured and thickly bedded Peninsula Formation quartzitic sandstones of the Table Mountain Group (TMG) within the Paleozoic Cape Supergroup, which unconformably overlies the basement of Malmesbury shales with significant granite intrusions (Thamm, 2000). The less erodible TMG rock outcrops create steep slopes in the upper parts of the catchments while the highly weathered shales and granites are exposed on the foot-slopes, with gradients of 15° to 29° (Britton et al., 1993). The soils in the catchments are generally poorly sorted and comprise colluvial sandstone mixture accumulations over weathered shale and granite mantles, characterized by reddish-brown colour and high infiltration capacity (Scott and Prinsloo, 2008). Of the bedrock types present, the TMG quartzites, being highly fractured, have generally been found to have higher-yielding aquifers than the basement shales and granites (Xu, et al., 2009). The fractures strongly control the hydraulic properties regarding groundwater flow paths and create a connection between the surface and groundwater (Lin, 2007). The scree and valley-fill alluvial aquifers have also been noted in the TMG-dominated catchments (Britton, 1993).

4.2.2. Sample collection and analytical methods

Field campaigns were conducted to collect water samples for analysis of stable isotopes (^{18}O and ^{2}H) and hydrochemistry (EC and major ions) from the monitoring sites during the hydrological years 02/2018 to 03/2020 (Figure.4.1). No sampling was done between March and July 2019 due to logistical issues. Monthly water samples were collected from rain-water collectors, streams, springs, boreholes, and piezometers across the two sub-catchments during both the dry summer (October-March) and wet winter (April-September) seasons (Table.4.2). The sampling sites were selected depending on accessibility and availability of monitoring instruments. Samples were not

collected on rainfall days and can therefore be considered baseflow samples given the fast flow recession of these steep, small catchments.

The Jonkershoek catchment is equipped with a network of tipping bucket automatic rain gauges, Model TR-5251 (Texas electronics Inc, USA). managed by the South African Environmental Observation Network (SAEON). For this study, cumulative rainwater samplers were installed alongside four of these gauges to evaluate spatial and altitude effects on rainfall amount and stable isotopes. Two in Langrivier, at upstream (LGU- 680 mamsl) and downstream (LGL- 370 mamsl) sites, one in Bosboukloof (BS- 400 mamsl), and one in Tierkloof (TK- 290 mamsl). The rain samplers were designed and modified according to the International Atomic Energy Agency rainfall sampling standards and improved to reduce evaporation (IAEA, 2002;2009; Gröning et al., 2012).

The stage over 90^{o} V-notch gauging weirs was recorded on an hourly basis. Stream samples were collected as grab samples from upstream (channel head) and downstream near the channel outlet in each sub-catchment, 1 to 2 km apart, to gain insight into any changes in contributing flow pathways as the water travels downstream. TMG spring samples were collected near the stream headwaters (> 500 mamsl), close to the geologic transition between the TMG quarzitic sandstones and the Malmesbury shales and granites below. These springs discharge from the network of fractures and may be a mix of primary groundwater discharge, and interflow from saturated or unsaturated zones (Roets et al., 2008, Hughes, 2010).

The samples were collected from perennial (SP1) and ephemeral (SP3) seeps in Tierkloof, a minor perennial seep (SP2) on the mid-slopes and ephemeral spring flowing during the wet winter (May to September) in Langrivier. Since the high elevation TMG geology in all three sub-catchments is similar, this spring was representative of the upper altitude springs in these catchments. The exact location or points of the seeps and spring were uncertain, these samples were collected from waterfalls and rock drips. Two shallow piezometers were sampled in Langrivier (LP1, 1.5 m deep) mid-slope and (LP3, 2.8 m deep) downstream. Piezometers installed to similar depths at mid-slope and downstream locations in Bosboukloof were consistently dry during the study period.

Groundwater samples were collected from three boreholes drilled into weathered granite-shale zones (1) one mid-slope, at an elevation of 277 mamsl near Bosboukloof (BH1) with an average depth to water of 30.6 m.b.g.l (meters below ground level) during the dry summer and 27.3 m.b.g.l during the wet winter. (2) An artesian borehole (BH2) on the valley floor in the central Jonkershoek Valley 312 mamsl which did not have a water level logger, and (3) BH3 located down the valley along the main river within the alluvium and basement granite.

Table.4.2. Summary of water samples collection data during the investigation period (2018-2020), all water samples were collected once a month.

	Water type	Sampling site	Elevation (m)	Sample No.	
				Dry	Wet
Bosboukloof (BS)	Rainfall	BSU-400	400	10	7
	Stream	Upstream (BSU)	410	12	13
	Stream	Downstream (BSL)	280	14	12
	Groundwater	Borehole (BH1)	280	12	12
Tierkloof (TK)	Rainfall	TKL-297	297	13	9
	Stream	Upstream (TKU)	621	13	12
	Stream	Downstream (TKL)	297	13	12
	Seep	SP1 (Perennial)	611	13	12
	Seep	SP2 (ephemeral)	597	7	3
Langrivier (LG)	Rainfall	LGU-680	680	13	9
	Rainfall	LGL-370	370	12	9
	Stream	Upstream (LGU)	715	12	13
	Stream	Downstream (LGL)	370	13	13
	Shallow GW	Piezometer (LP1)	490	12	13
	Shallow GW	Piezometer (LP3)	375	13	13
	Spring	TMG spring (Ephemeral)	690	2	11
	Seep	SP3 (Perennial)	474	7	5
Jonkershoek	Groundwater	Borehole (BH2)	312	10	11
	Groundwater	Borehole (BH3)	224	9	8

Note: SP = Seep, U= upstream, L= downstream, BH =Borehole, LP =Langrivier piezometer

The average seasonal water depths at BH1 were 3.5 m.b.g.l during the summer season and 2.97 during the winter season. Borehole BH1 was pumped daily for water supply during the study period, hence it was only used for isotopes and hydrochemistry analysis, while BH3 was monitored for both sample analysis and water levels. No additional information was available on the characteristics of the boreholes (i.e., total depth, screen depth and borehole lithological log).

Samples for isotopic analysis were collected in 50 ml High-Density Polyethylene (HDPE) plastic bottles with inserts and a cap, while those for chemical analysis were collected in 200 ml HDPE plastic bottles. The samples were stored in a refrigerator immediately after collection. The water samples were analysed for stable isotopes ($\delta^{18}O$ and $\delta^{2}H$) at the Environmental Isotope Laboratory (EIL) of iThemba LABS (Johannesburg) and the Department of Environment and Water Science laboratory (EWS) at the University of the Western Cape (UWC) using a Los Gatos Research (LGR-DLT 100 model 908-0008) Liquid Water Isotope Analyser. The analytical precisions were ±1.5‰ $\delta^{2}H$, ± 0.5‰ $\delta^{18}O$ for iThemba LABS and ± 0.6‰ $\delta^{2}H$, ± 0.2‰ $\delta^{18}O$ for EWS.

The relative abundance of stable isotopes was expressed in parts per thousand (‰ or per mil) and reported in delta (δ) notation relative to the VSMOW (Vienna Standard Mean Ocean Water) where:

$$\delta = ((R_{sample}/R_{SMOW})-1) * 1000 \quad (4.1)$$

R_{sample} represents the isotope ratio of $^{2}H/^{1}H$ or $^{18}O/^{16}O$ of the water sample and R_{SMOW} represents the isotope ratio of $^{2}H/^{1}H$ or $^{18}O/^{16}O$ of the standard (VMSOW). For data normalization, the two in-house standards (W-31, W-32) were calibrated directly against VSMOW2 and SLAP2 international standard waters. The data were normalized to the VSMOW/SLAP scale.

The amount-weighted average annual and seasonal isotopic ratios for rainfall were calculated using the standard weighting mean value for the monthly samples (McDonnell et al., 1990).

The weighted mean values of $\delta^{18}O$ or $\delta^{2}H$ were calculated by the equation:

$$\delta^{18}O\ (‰) = \frac{\sum_{i=1}^{n} P_i \delta_i}{\sum_{i=1}^{n} P_i} \quad (4.2)$$

where, P_i is the recorded rainfall amount (mm) for the *i*th period, *n* is the number of cumulative rainfall samples and δ_i represents the value for ^{18}O or ^{2}H. The relationship between the isotopic values of different water samples with the Local Meteoric Water Line (LMWL) and the Global Meteoric Water Line (GMWL) was presented by the dual-isotope plots see section 4.3.2. The GMWL is used as defined by (Craig, 1961) as $\delta^{2}H = 8*^{\delta}O + 10$.

The deuterium excess "*d*-excess" was proposed by Dansgaard (1964) to quantify the extent to which the LWML deviates from the GMWL and sources of water vapour where:

$$d = \delta^{2}H - 8*\delta^{18}O \quad (4.3)$$

A handheld multi-parameter probe (YSI, USA) was used for in-situ measurement of electrical conductivity (EC) measured as specific conductance (temperature compensation to 25°C), dissolved oxygen (DO), temperature (T) and pH. Due to the low total dissolved solids (TDS) of the water in this catchment, the EC meter was calibrated with a low standard of 84 µS/cm. Major ion concentrations in dry summer samples were analysed at Elsenburg laboratories using ICP-iCAP 7000i (Thermo-Scientific Inc,no additional analytical precision data provided in Table B. 1 (Appendix B), and were generally below the instrumental detection limits (Ca^{2+}= 3 mg/l, K^{+} = 1 mg/l, Mg^{2+} = 2 mg/l, Na^{+} = 1 mg/l). For this reason, major ion concentrations were not used for this study.

Streamflow time-series analysis was performed using SAEON weir records between January 2018 and January 2019 which corresponded with the collected environmental tracer data. Statistical analyses were performed using the student's t-test (paired and unpaired) applying a significance level of 0.05. Measurements taken on the same dates at separate locations were considered paired samples. The Pearson correlation was applied to evaluate the relationship between the stable isotope and hydrochemical tracers between the three sub-catchments.

4.3. Results

4.3.1. Hydrological responses

Rainfall and discharge characteristics of the three sub-catchments for the period between 2018 and 2019 are presented in Figure.4.3 and Table.4.3. Roughly 22 % of rainfall fell in dry summer and 78% during the wet winter for all the investigated sub-catchments. The three study sites differed in rainfall and streamflow response. Bosboukloof had the lower rainfall with monthly averages of 37 mm/m for the dry summer (Oct-Mar) and 140 mm/m for the wet winter (Apr-Sep) season. The monthly averages for Tierkloof were 39 mm/m and 150 mm/m, for the dry and wet winters, respectively. Langrivier recorded higher rainfall in both seasons with monthly averages of 51 mm/m in the dry summer and 194.3 mm/m for the wet winter.

Most of the streamflow was generated during the wet winter between May and September. The wet winter runoff accounted for about 70%, 78% and 80% of the annual runoff (2018 and 2019) in Bosboukloof, and Langrivier, respectively. Bosboukloof had the lowest flows with dry and wet winter average daily flows of 0.009 m^3/s (0.39 mm/day) and 0.022 m^3/s (1 mm/day), respectively also see Figure.4.3. Tierkloof recorded average daily flow for the dry summer was 0.012 m^3/s (0.73 mm/day) and 0.037 m^3/s (2.2 mm/day) for the wet winter. Langrivier daily average flows during the dry and wet winter were 0.035 m^3/s (1.2 mm/day) and 0.14 m^3/s (3.8 mm/day), respectively. The recorded largest daily peak flows for Bosboukloof were an order of magnitude lower than those for Tierkloof and Langrivier (0.03 to 0.1 m^3/s). In Tierkloof, the highest peak flows during 2018 and 2019 ranged from 0.15 to 0.53 m^3/s, and Langrivier were in the ranges of 0.1 to 0.8 m^3/s during the wet winter.

Table.4.3. Summary of the seasonal hydrometric characteristics for the three sub-catchments, for analysis period 2018-2019. (Wet Winter season= April to September, Dry summer = October- March).

		Bosboukloof		**Tierkloof**		**Langrivier**	
Season/period	Year	Summer	Winter	Summer	Winter	Wet	Dry
Rainfall (mm/a)	2018	211	848	194.7	915	1090	266
	2019	235	832.2	270	987	1024	354
Runoff (mm/a)	2018	42	144.8	110.6	398.8	782	173
	2019	83	196.2	130	478.6	771	198

The groundwater levels from the BH3 responded to the rainfall inputs, particularly during the wet winter (Figure.4.4.b). The groundwater levels from the floodplain borehole (BH3) indicated varying responses to the rainfall during the wet winter. The water depth in BH3 showed a

significant rise in the water table during the winter season with levels of 2.97 m compared to the water table depth of 3.4 m during dry summer with an annual average of 3.2 m. The water table rose significantly from August to September which is the peak of the rainy season. To our knowledge, little is known about the total depth of this borehole and the volume of groundwater pumped daily, especially during the dry season. The greatest decline in the water table was observed during the dry summer (November to February) when the rainfall is scarce or sporadic.

The average annual water table depth was 0.79 m and 2.62 m at piezometer LP1 and LP3, respectively (Figure.4.4.b). The shallow upstream piezometer (LP1) showed seasonal variability in water table depth. The dry summer had an average of 1.08 m, while the average for the wet winter was 0.82 m. The water table depth showed a significant response to large rainfall events (> 20 mm/day) during the winter which was consistent with the high flows (Figure.4.4). The water table at the LP3 near the weir showed a response to rainfall but had minimal seasonal variation than LP1 which showed an average increase of 26 cm during the wet winter. The water table during dry summer had an average of 2.67 m and 2.57 m during the wet winter.

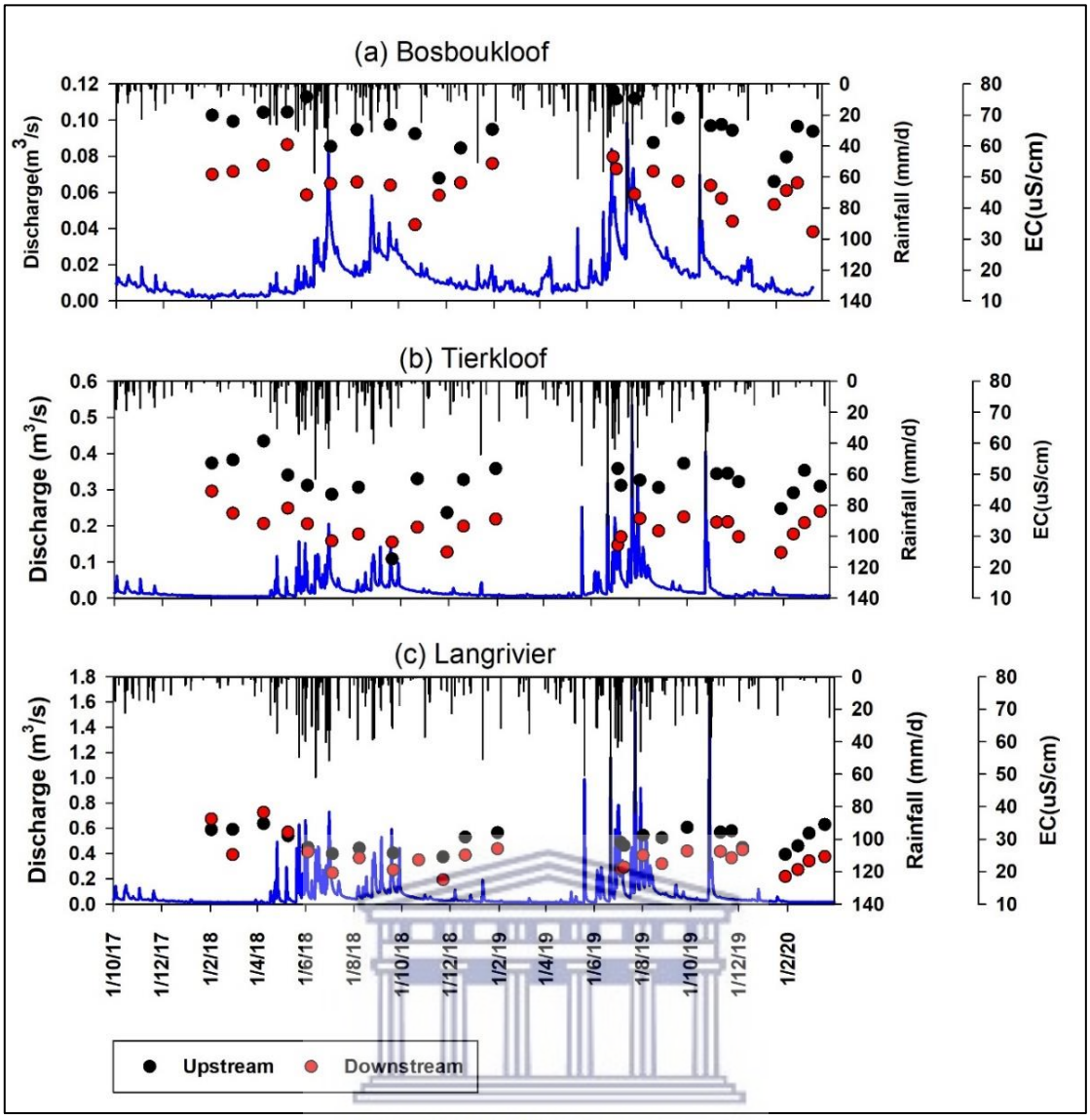

Figure.4.3. Temporal variability of mean daily discharge, rainfall and the EC values during the sampling period in (a) Bosboukloof, (b) Tierkloof and (c) Langrivier.

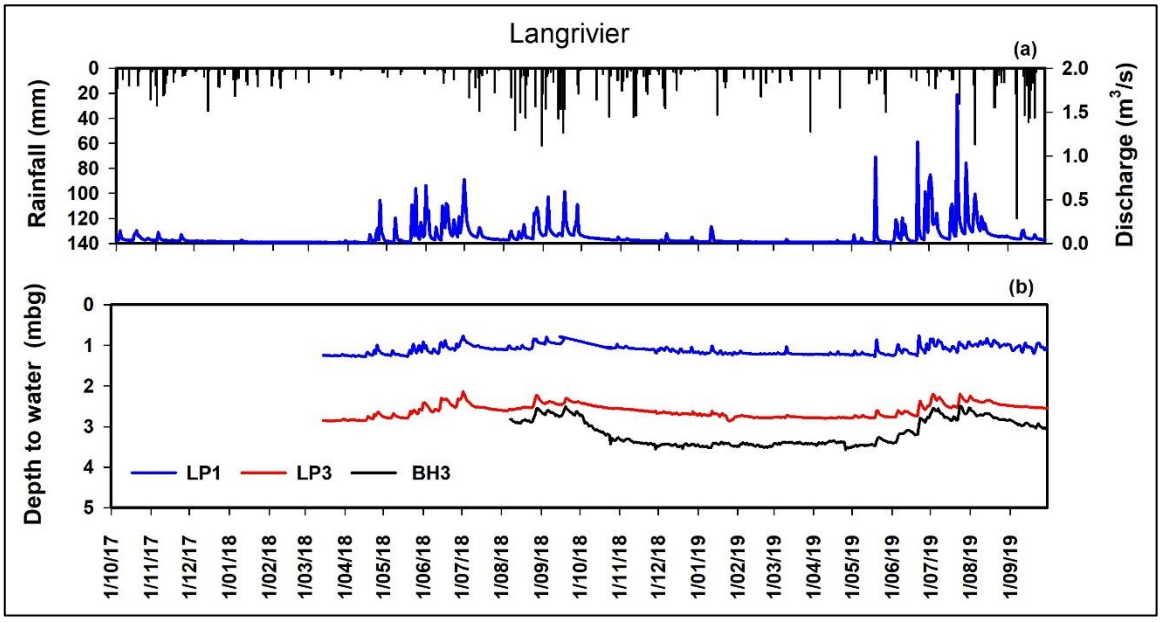

Figure.4.4. Temporal variations in daily water levels from groundwater borehole (BH3) and piezometers (LP1 and LP3), including daily rainfall, discharge, in Langrivier 2018 and 2019.

4.3.2. Spatial and temporal variations in physico-chemical parameters

4.3.2.1. Characteristics of EC measurements in surface and sub-surface water sources

The streamflow and groundwater in most of the TMG geological region are characterised by very low ionic concentrations. The stream water is mostly pristine in this geological region. This was evident in the streamflow samples in the Jonkershoek. The graphical presentation of the spatial and temporal characteristics of electrical conductivity (EC) across sub-catchments are shown in Figure.4.3. The seasonal variations in the EC and major ions (Na and Cl) concentrations from different water sources are presented in Figure.4.5.

In all catchments, spatial variations in EC were large between the upstream and downstream samples (Figure.4.5 and Figure.4.6). The values were higher at the downstream compared to the upstream stream sites, reflecting a shift from a less mineralized source to flow through a highly mineralized zone and a mix of water from different pathways. For example, in Bosboukloof the mean value increased from 44.5 µS/cm upstream to 62.3µS/cm downstream, while in Tierkloof it increased from 34.5 µS/cm upstream to 47.8 µS/cm on downstream see Appendix B (Table B. 3). However, the spatial difference in means EC were larger and statistically significant in Bosboukloof (18.72 µS/cm, $p < 0.001$, n=26), Tierkloof (14.42 µS/cm, $p < 0.001$, n=26) and smaller in Langrivier (4.7 µS/cm, $p < 0.001$, n = 26). As shown in Figure.4.5 and Figure.4.6, spatial variations between the stream water EC in the three tributaries with values were large ranging from 32.3 to 77.8 µS/cm, 22.7-60.7 µS/cm and 17.5 to 39.1 µS/cm in Bosboukloof, Tierkloof and Langrivier respectively.

The streamflow samples exhibited lower EC than the groundwater and piezometer samples. Though the streamflow samples in Bosboukloof had similar a concentration range as the piezometer soil water (i.e., LP1 and LP3) sampled in the Langrivier catchment, particularly during the dry summer (Figure.4.5). This demonstrated the influence of surficial flow pathways and temporary storage in the scree-soils which dominates the catchment slopes. The samples also showed more overlap with the seeps (SP3) during both the dry and wet winters were high (Figure.4.5.a and b).

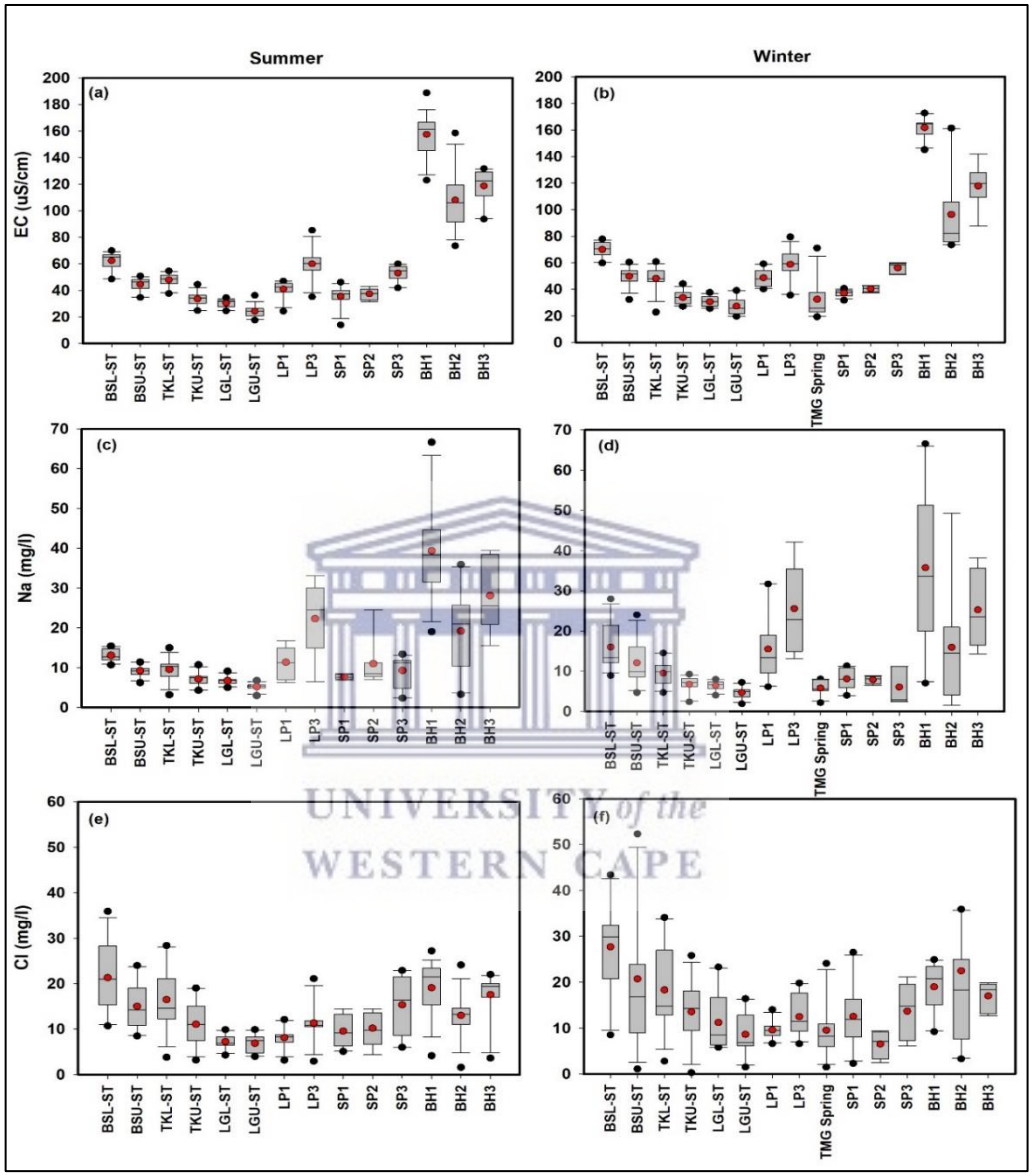

Figure.4.5. Boxplots of spatial and seasonal variation of EC (A, B), Sodium (C, D) and chloride (E, F) concentrations of the stream (ST), spring, seep (SP-3), piezometer (LP1 and LP3) and groundwater samples (BH1, BH2, BH3) at Bosboukloof (BS), Tierkloof (TK) and Langrivier (LGL).

4.3.2.2. Characteristics of major ions concentrations in surface and sub-surface water sources

The differences in Na and Cl observed at the different monitoring sites i.e., streamflow, piezometers, borehole groundwater, seeps and upper catchment springs across the two seasons were presented in Figure.4.5 and Appendix B.(Table. 3). Figure.4.6 presents a time series of the hydrochemical parameters from sampled water sources between 2018 and early 2020. All samples exhibited low concentrations of < 25 mg/l for Na and < 100 mg/l for Cl. The Na and Cl concentrations of streamflow samples showed similar trends as EC with high values in Bosboukloof, followed by Tierkloof and low values in Langrivier (Figure.4.5.c-f).

In terms of sodium (Na), there was no marked seasonality in concentrations across the three sub-catchments. The concentration of the streamflow samples showed little fluctuation between low and high concentrations during summer and winter 2018, respectively (Figure.4.6.c-f). Though the trend was less pronounced in 2019, whereby the concentrations remained constant for most of the streamflow samples. On the other hand, those piezometers and borehole groundwater samples showed large fluctuations with a gradual decrease during winter to early summer. However, it must be noted that the fluctuation in borehole groundwater samples is also observed in the water levels, especially at BH1.

Minor spatial variations in Na concentrations were observed for the streamflow samples across the sub-catchments (Figure.4.5.c and d). The dry summer concentrations had strong correlations with R^2 values between 0.74 and 0.88 and showed significant relationships in sodium concentrations between the sub-catchments (p <0.05). The wet winter Na concentration in Langrivier and Tierkloof streamflow water samples showed no correlation, while a strong correlation was observed for concentrations between Bosboukloof and Tierkloof (R^2=0.78, p = 0.006, n= 10). Moreover, as observed in the EC values, the concentrations increased from upstream to downstream. Nonetheless, statistically significant (p < 0.05) spatial variations were observed between the upstream and downstream samples across the sub-catchment.

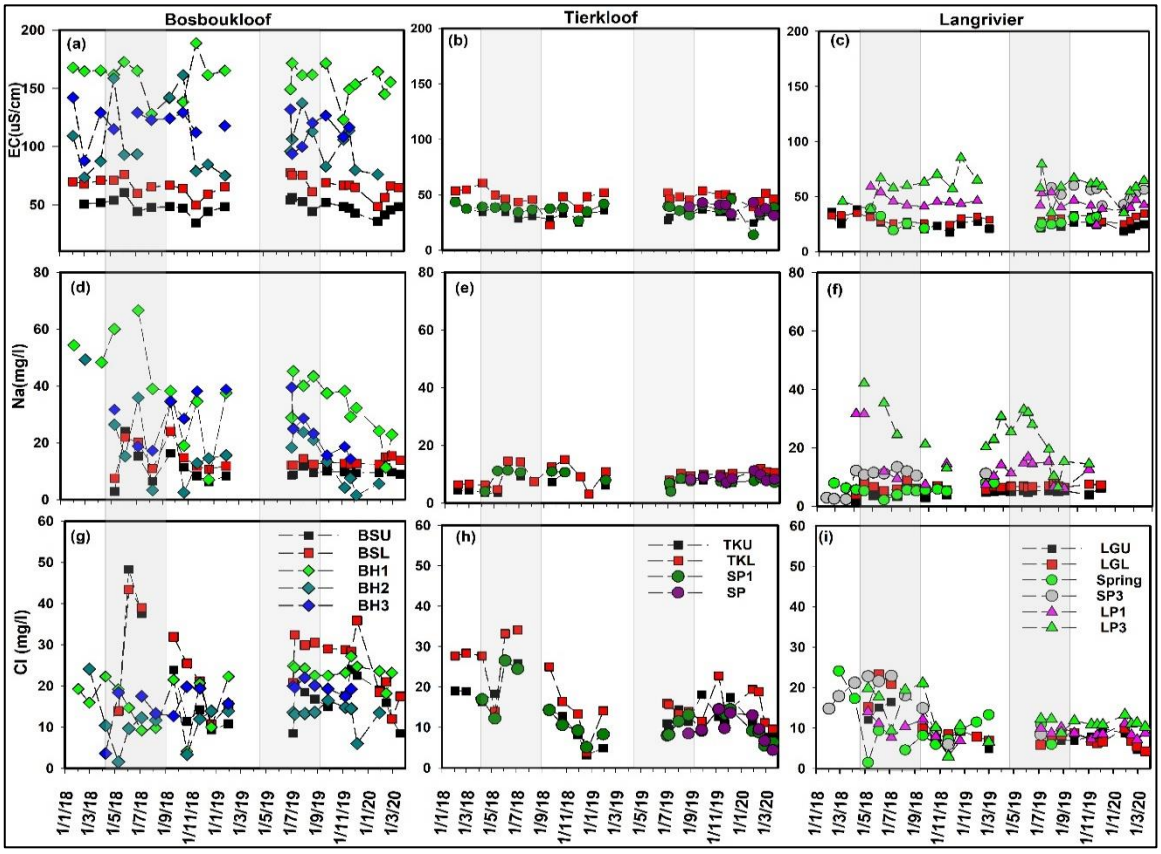

Figure.4.6. Temporal variation of EC, sodium and chloride concentrations of stream, TMG spring, seep (SP), piezometer (LP) and groundwater boreholes. The shaded area indicates the wet winter.

The streamflows and groundwater sampled from boreholes, piezometers and springs had chloride (Cl) concentrations that exhibited seasonality and varied spatially. The lowest concentrations were recorded in samples collected during the dry summer (October to March), whereas the highest values were measured during the wet winter coinciding with high flows. The concentrations showed a gradual increase at the beginning of the wet winter (May) followed by a decline indicating dilution during the peak of the wet winter (June to September) (Figure.4.6.g - i). A gradual increase in concentration during summer is evident in Bosboukloof and Tierkloof streamflow samples as well as in the groundwater samples during the 2019 dry summer. However, unexpected decreasing trends were observed during mid-summer (i.e., early 2020), the opposite of what was observed for EC. Similar to EC and Na, the downstream chloride concentrations were significantly higher than those of upstream samples for all sampled streamflow (Figure.4.6).

Conversely, the borehole groundwater samples showed a decreasing trend indicating dilution or flushing during the wet winter (Figure.4.6.g). The concentrations during the wet winter were a few magnitudes less than those for streamflow samples, seeps and piezometers samples across the sub-catchments. An opposite increasing trend was observed during the dry summer.

Large spatial variations were observed between Bosboukloof chloride concentration which had a wider range (15.0-35.9 mg/l) and Langrivier (5.8-7.2 mg/l) streamflow samples during the dry

summer. During the wet winter, the Cl concentrations at both Bosboukloof and Langrivier were 43.4 - 63.2 mg/l and 4.6 -11.2 mg/l, respectively. Moreover, the Cl concentrations between Bosboukloof and Langrivier sub-catchments were strongly correlated (R^2= 0.79, $p < 0.05$, n=10), as well as between Bosboukloof and Tierkloof with R^2= 0.78 (p <0.05, n =10). during the wet winter. No significant relationships in chloride concentrations were observed during the dry summer ($p > 0.05$, n =11) between the three sites.

4.3.3. Stable isotope characteristics and seasonal variations of rainfall

The relationship between the $\delta^{18}O$ and $\delta^{2}H$ isotopic composition of rainfall across the stations, the LMWL and GMWL are shown in Figure.4.7. The isotopic values were plotted against the LMWL of the Cape Town region (Harris et al., 2010) with the equation $\delta^{2}H = 6.41*\delta^{18}O + 8.66$ ($R^2 = 0.88$). The LMWL was chosen as a reference for this study as it was developed from a long-term dataset (1996-2008), and the data represent similar climatic conditions to the current study site.

The isotopic compositions of rainfall across the four stations varied spatially and exhibited seasonality (Figure.4.7). The annual amount-weighted $\delta^{18}O$ and $\delta^{2}H$ values were more depleted during the wet winter in comparison to the dry summer values (Table.4.4). The amount-weighted mean or averaged seasonal isotopic values showed seasonality and distinct variability between the stations (Figure.4.7). The amount-weighted mean of the higher elevation stations LGU 680 was more depleted compared to other stations plotting on the LMWL, followed by station by BSU-400 and TKL-290 across the seasons. The lowest station LGU-270 had a more isotopically enriched amount-weighted mean which fell below the LMWL and GMWL. The seasonal amount-weighted mean values for the stations are presented in Table B. 2 (Appendix B).

The slopes and intercepts (deuterium excess) of the regression lines for the rainfall samples reflected less spatial variation across the stations especially during the dry summer as shown in Table B. 2 (Appendix B). The $\delta^{18}O$ vs $\delta^{2}H$ regression line for dry summer rainfall samples gave slopes of < 6, while those for the wet winter ranged from 6.0 to 8.45 across the stations.

The dry summer precipitation showed mean *d*-excess values between 8 ‰ and 12 ‰, which were within the range of the GMWL value of 10 ‰. The mean d-excess wet winter values were between 13.8 and 14.7 ‰, which was much higher than that of GMWL. Though it was close to the mean *d*-excess of the typical value of 16 ‰ for the TMG geological region.

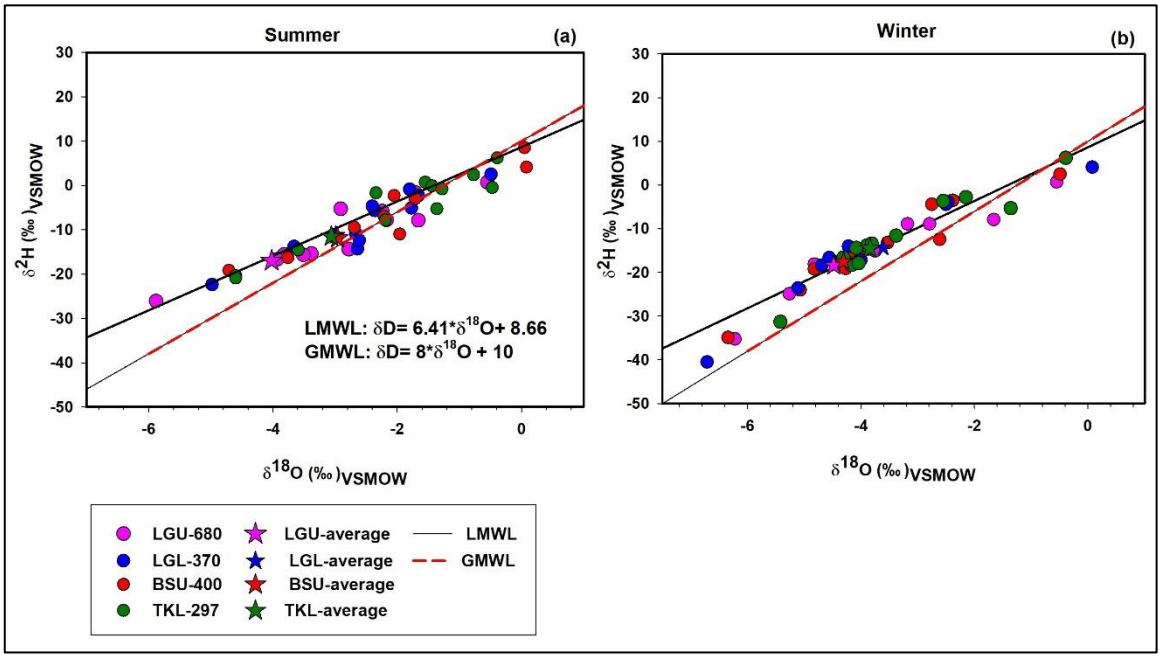

Figure.4.7. δ^2H vs $\delta^{18}O$ plots of rainfall in Jonkershoek (A) summer season versus (B) winter season at the four stations including the LMWL adopted from Harris et al. (2010) and GMWL (Craig, 1960)

Table.4.4. Summary of mean seasonal rainfall, mean isotope values and standard deviation (SD) for both dry summer and wet winters from the four rain samplers (2018-2019). Also shows the amount-weighted average for the annual rainfall. (Please note the rainfall is the total for the sampled days).

Location	**Elevation (mamsl)**	**Rainfall (mm/a)**		**Isotope values (‰), mean (& SD)**				**Amount- weighted mean (‰) (Annual)**		**D excess (‰)**	
		Dry (Oct-Mar)	Wet (Apr – Sep)	Dry (Oct-Mar)		Wet (Apr-Sep)				Dry (Oct-Apr)	Wet (Apr-Sep)
				$\delta^{2}H$	$\delta^{18}O$	$\delta^{2}H$	$\delta^{18}O$	$\delta^{18}O$	$\delta^{2}H$		
				n =13	n=13	n= 9	n= 9	n=22	n=22	n=13	n=9
LGU_rain	680	584[a]	1304[a]	-12.8(9.9)	-3.13(1.6)	-16.4(5.0)	-4.12(0.79)	-6.86	-28.4	12.1	14.7
BSU-rain	400	507	1148	-9.6(13.7)*	-2.56(2.1)*	-14.5(6.7)	-3.93(0.91)	-3.69	-15.2	8.7	13.8
LGL-rain	370	670	1464	-10.4(10.3)[b]	-2.78 (1.5[b]	-14.0(7.3)	-3.93(1.05)	-4.03	-17.0	10.2	14.2
TKL-rain	290	491	1263	-7.2(11.2)	-2.30(1.6)	-12.5(5.6)	-3.60(0.76)	-3.77	-14.7	11.2	14.5

[a] rainfall data missing 8 %, *n=10, [b]n= 12

4.3.3.1. Isotope effects due to altitude

The relationship between the rainfall and elevation at the respective stations was evaluated to explore the influence of altitude on $\delta^{18}O$ and $\delta^{2}H$ compositions of rainfall. The $\delta^{18}O/^{2}H$ values versus altitude were plotted for the annual and seasonal scales (Figure.4.8). The isotope/altitude gradient in this catchment was described by a regression line $\delta^{18}O$ = a +b*altitude (*h*), where *h* is the elevation in meters.

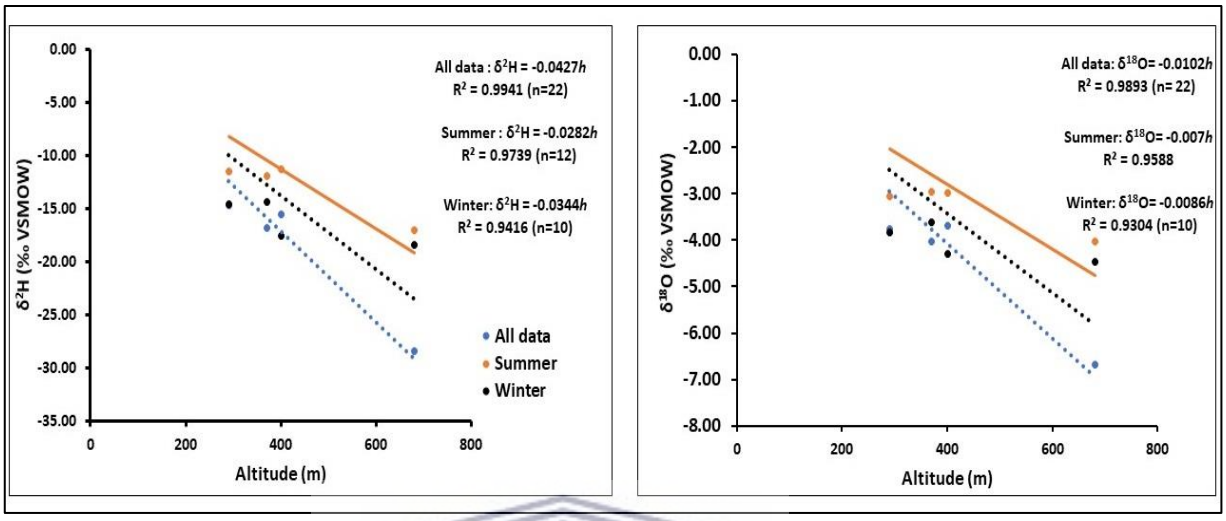

Figure.4.8. Relationship between amount-weighted average isotopic compositions ($\delta^{2}H$ and $\delta^{18}O$) in rainfall and altitude at seasonal and annual time scales. *h* =altitude.

The rainfall isotopic compositions at the lower elevation stations showed less negative values (i.e., isotopically enriched) compared to the more negative (depleted) values at LGU-680 m. The rainfall $\delta^{18}O$ and $\delta^{2}H$ values were strongly correlated with elevation (Figure.4.8). Moreover, they showed a decrease in increasing altitude. For the annual values, the altitude effect accounted for -0.10‰ per 100 m increase in altitude (R^2= 0.98, n=22) and -0.42 ‰ /100 m (R^2=0.99, n=22) for $\delta^{18}O$ and $\delta^{2}H$, respectively. The gradient of altitude effects also showed temporal variations, particularly for $\delta^{2}H$. The seasonal isotopic compositions showed an altitude effect of -0.07 ‰ /100 m for $\delta^{18}O$ and $\delta^{2}H$ with -0.28 ‰/ 100 m (R^2= 0.97, n=12) during the dry summer. During the wet winter, the altitude effect for $\delta^{18}O$ was close to that for the dry summer at -0.08 ‰ /100 m. The altitude produced an effect of -0.34 ‰ /100 m (R^2= 0.95, n=12) for $\delta^{2}H$.

4.3.3.2. Amount effect

Figure.4.9 presents the relationship between monthly rainfall amount and isotopic compositions of rainfall during the dry summer and wet winters. The magnitude of the amount effect is defined by a similar linear relationship as the altitude effect.

The $\delta^{18}O$ and $\delta^{2}H$ of rainfall showed a linear correlation with the rainfall amount, especially during the wet winter. Moderate correlations were observed during the dry summer with R^2 values between 0.36 and 0.50 ($p < 0.05$) for $\delta^{2}H$ and R^2 = 0.49 to 0.65 (p-value = 0.011 -0.015, n =12) during winter. The strongest correlation was observed for $\delta^{18}O$, the gradient of the amount effect ranged from -5.8 to -0.10 ‰ per 100 mm increase in rainfall (Figure.4.9.b). The magnitude of the amount effect for $\delta^{2}H$ during the dry summer was -1.5 to -0.27 ‰/100 mm. The wet winter $\delta^{18}O$ and $\delta^{2}H$ values were strongly correlated with rainfall amount, the regression coefficients ranged from (R^2= 0.46-0.81, p <0.05) for $\delta^{2}H$ and (R^2=0.61- 0.77, p <0.05) for $\delta^{18}O$, the strongest correlations were recorded for Tierkloof station followed by the Langrivier station (Figure.4.9.c).

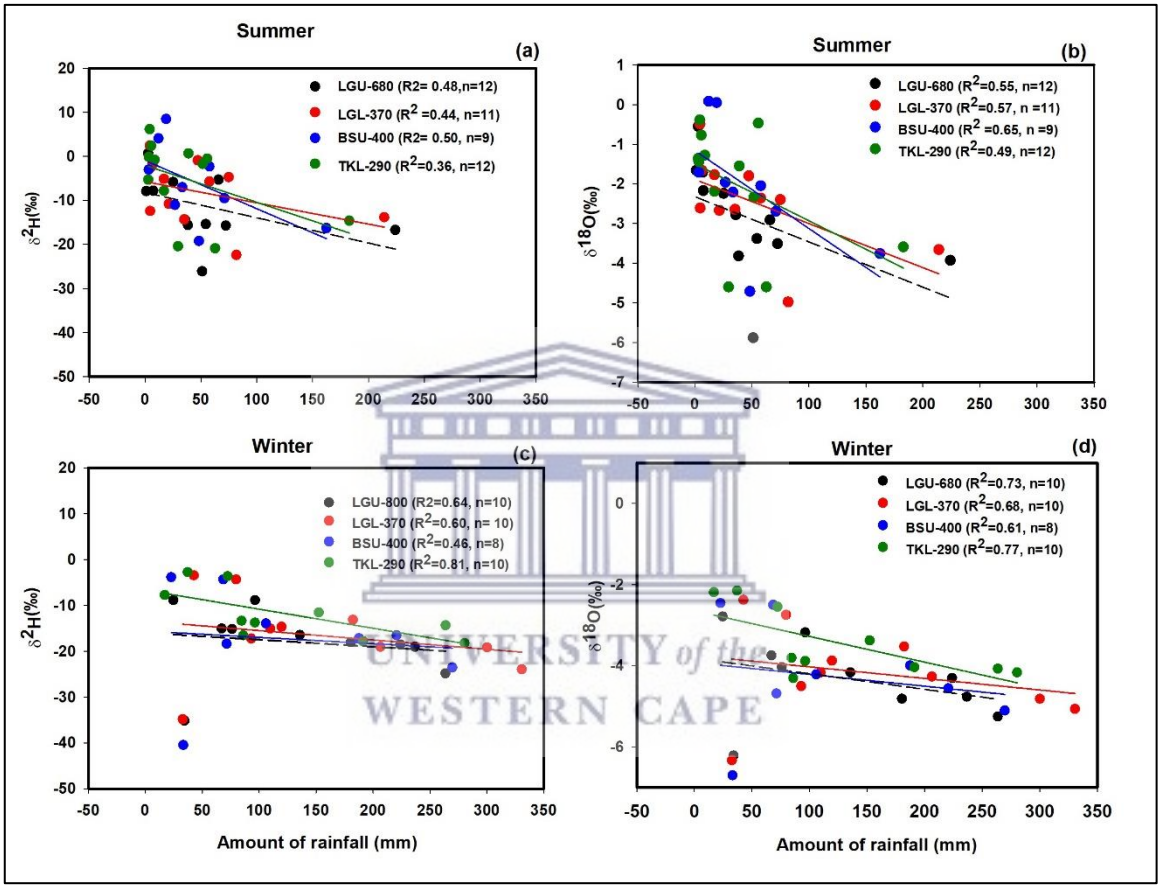

Figure.4.9. Plots of the relationship between monthly rainfall isotopic values and monthly rainfall during summer and winter seasons.

In terms of spatial variations, the magnitude of the amount effect of $\delta^{18}O$ was -2.4%/100 mm which was the same for all stations, while $\delta^{2}H$ was in the range of -3.8 to -10.2 %/100 mm. Stations LGU (680 m), BSU (400 m) and TKL (270m) showed the highest dependency on rainfall relative to LGL (370m) with depletion rates of -10.2‰/100 mm, -4.2 ‰/100 mm and -3.8 ‰/100mm for $\delta^{2}H$, respectively.

Contrary to the amount and elevation effect, the evaluation of the relationship between temperature and stable isotopes the $\delta^{18}O$ and $\delta^{2}H$ were negatively correlated with $R^2 < 1$, (p-value varies from 0.1 to 0.38) during both the dry summer and wet winter (results not shown). It is important to note that to obtain meaningful results for this kind of analysis, long-term data, and a wide range of temperatures over a large scale are prerequisites. Considering the small scale of the catchment it was difficult to conduct this kind of analysis successfully.

4.3.4. Variations in surface and subsurface water isotopes

The time-series analysis showed that the baseflow stream water isotopes, $\delta^{18}O$ and $\delta^{2}H$ did not exhibit consistent seasonal variation during the observation period (Figure.4.10). However, small variations were observed during the beginning of the 2018 wet winter. An increasing trend to more depleted isotope ratios in baseflow samples was notable following significant winter rainfall events in May 2018 and an increase in flow, which was visible across all sub-catchments. This was evident following the major events between July and September 2018 whereby the rainwater, spring, and groundwater were gradually more enrichment during this period. Tierkloof and Langrivier showed an increasing trend in streamflow isotopic compositions following the 2019 rainy season which was followed by a gradual decrease to more negative values towards the dry summer. Overall, the streamflow samples collected in June and July 2018 and 2019 appeared to become more isotopically depleted reflecting dilution following major events.

Strong correlations were observed in the monthly streamflow $\delta^{2}H$ and $\delta^{18}O$ values between Bosboukloof, Tierkloof and Langrivier with (R^2= 0.69 to 0.86, p <0.05, n=13) for in the dry summer. During the wet winter, the $\delta^{18}O$ values Langrivier were moderately correlated with those in Bosboukloof and Tierkloof (R^2 = 0.55 to 0.60, p = 0.04 -0.05), whereas a weak correlation was observed between $\delta^{18}O$ values in Bosboukloof and Tierkloof (R^2= 0.29, p = 0.33, n=10). In the case of $\delta^{2}H$, strong correlations were occurred between Bosboukloof and Tierkloof with R^2= 0.71 (p <0.05, n= 10) and between Tierkloof and Langrivier (R^2= 0.87, p = <0.05, n=13).

The isotopic compositions did not vary significantly from upstream to downstream in Langrivier and Tierkloof ($p > 0.05$). However, in Bosboukloof, $\delta^{18}O$ composition showed a minor increase becoming more enriched moving downstream with larger differences observed during the wet winter, in May and July (Figure.4.10.a). Nonetheless, the differences between the isotopic values for Bosboukloof upstream (BSU) and Bosboukloof downstream (BSL) samples were statistically significant ($p \geq 0.05$). As a result, the mean isotopic values for a sampling day from the upper and lower stream site were considered for the $\delta^{18}O$ and $\delta^{2}H$ graphs for each sub-catchment ((Figure.4.10 and Figure.4.11).

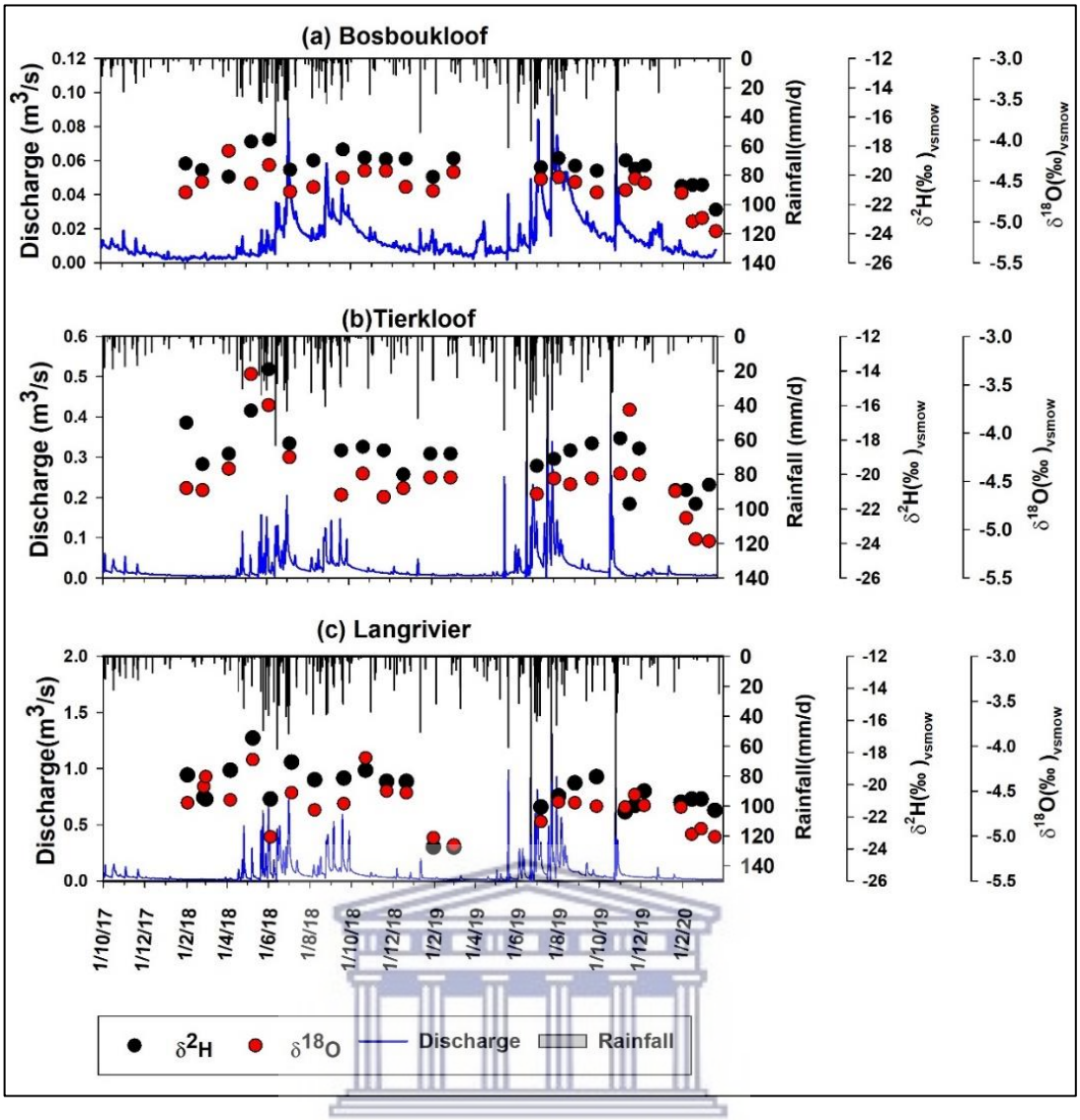

Figure.4.10. Time series of daily rainfall and discharge and $\delta^{18}O$ and $\delta^{2}H$ compositions of streamflow for (a) Bosboukloof, (b) Tierkloof and (c) Langrivier.

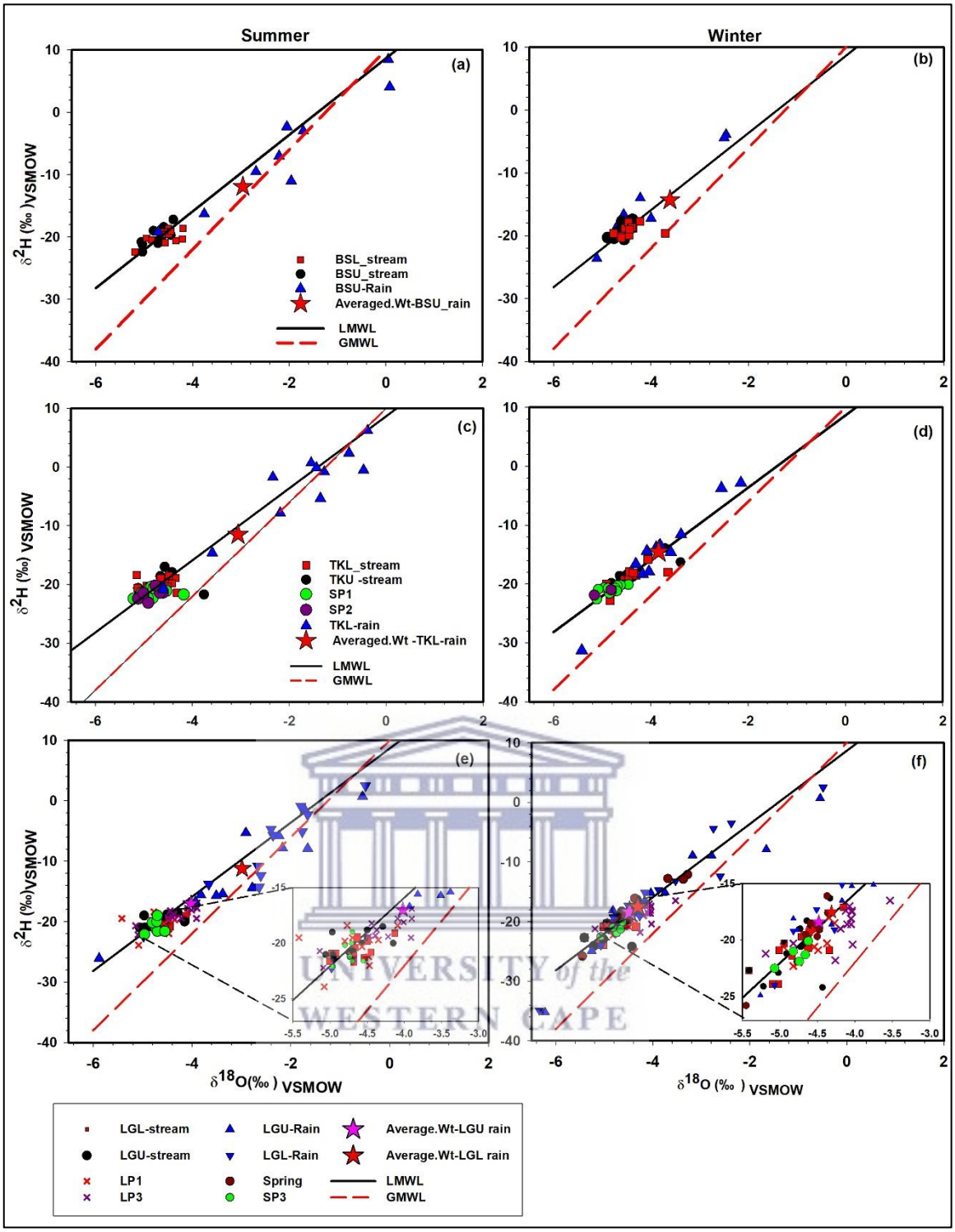

Figure.4.11. Dual $\delta^{18}O$ and $\delta^{2}H$ isotope plots of the stream (upstream and downstream), seeps (SP)/springs, piezometer (LP1 and LP3) and rainfall seasonal isotopic compositions for Bosboukloof (a,b), Tierkloof (c,d) and Langrivier (e,f). Including the amount-weighted average of each station.

A comparison of $\delta^{18}O$ and $\delta^{2}H$ compositions of streamflow, groundwater borehole, piezometer, seeps and TMG spring water samples with local rainfall (LMWL) and GMWL was used to make inferences about the sources of water at a location as shown in Figure.4.11 and Figure.4.13. As shown in Figure.4.11, most of the streamflow samples lie above the LMWL overlapping with the spring and seep samples in Langrivier and Tierkloof and they were all in a similar range as the groundwater (Figure.4.12). Though some of the streamflow samples show evaporative enrichment lying below the LMWL during the dry summer, particularly those from downstream in all study sites.

The lumped (all data, n= 25) comparison between Langrivier, Tierkloof and Bosboukloof stream samples (i.e., upstream-downstream site averages) during the study period showed some evidence of relative depletion in Langrivier compared to others (Figure.4.12 and Figure.4.13). The isotope values of streamflow samples in Langrivier also had a wider range compared to those for Bosboukloof and Tierkloof, especially during the wet winter (Figure.4.12). The corresponding $\delta^{18}O$ and $\delta^{2}H$ regression lines for the dry summer samples showed more evaporative enrichment and yielded a lower slope (<1) than the LMWL. The intercepts were mostly negative and lower than the LMWL of Harris et al. (2010). The wet winter of linear regression also showed impacts of evaporation with smaller slopes ranging from 4 to 5.61 across the individual study sites. The streamflow slopes for the wet winter correspond with those reported by Midgley and Scott (1997).

The streamflow isotopic values were mostly depleted compared to the amount-weighted average rainfall during both seasons, showing a similar range with the groundwater and LP1 sample isotopic values which reflects sub-surface water sources (Figure.4.12). Therefore, rainfall in the catchment had a minor effect on the streamflow. There were significant differences between the isotope ratios of the mid-slope and down-slope piezometers, LP1 and LP3 (p <0.05 for both $\delta^{18}O$ and $\delta^{2}H$, n= 26). The mid-slope soil water (LP1) isotopic compositions were similar to those of the streamflow samples in Langrivier. The down-slope piezometer soil water (LP3) was slightly enriched in $\delta^{18}O$ relative to all groundwater, streams, and mid-slope soil water (Figure.4.13). The LP3 samples lie between the LMWL and GMWL and the slopes of the regression lines were 2.72 in the dry summer and 5.17 in the wet winter (Figure.4.12). Due to the lack of piezometer water samples in Bosboukloof (i.e., the piezometer was consistently dry), the comparison of the streamflow samples with soil water could not be established.

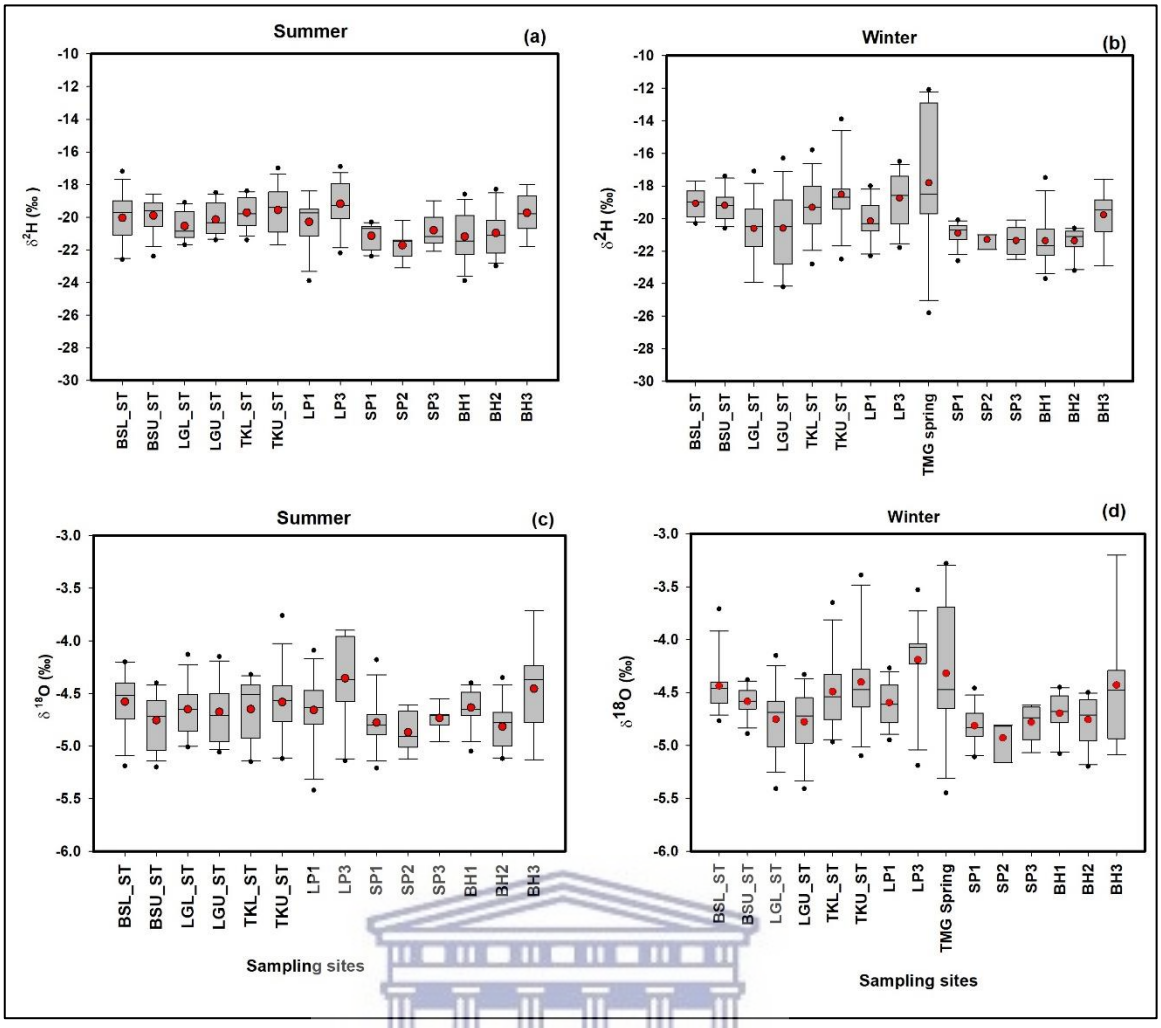

Figure.4.12. Box plots of the $\delta^{18}O$ and $\delta^{2}H$ isotopic compositions of streamflow (ST) upstream and downstream in Bosboukloof (BS), Tierkloof (TK) and Langrivier (LG), TMG spring, piezometers (LP), seep (SP) and groundwater boreholes (BH).

The mean isotopic values of the high elevation TMG perennial seeps (SP1 and SP2) in the Tierkloof sub-catchment overlapped with most of the borehole groundwater samples during both the wet and dry seasons (Figure.4.12 and Figure.4.13). The $\delta^{18}O$ and $\delta^{2}H$ values for SP1 were also depleted relative to amount-weighted rainfall during both the dry summer and wet winters, whereas those for SP2 reflected the isotopic ratios of the borehole groundwater samples (Figure.4.13). In comparison, the ephemeral TMG spring samples in Langrivier were more enriched than the groundwater, seep and stream samples (Figure.4.12). The TMG spring samples were mostly isotopically enriched plotting on the upper areas close to the amount-weighted means of the LMWL implying recharge from the winter rainfall. The samples gave a linear regression slope of 7 close to the LMWL and GMWL and that for the ephemeral seep (SP3) of 6.2.

The groundwater samples also were isotopically depleted compared to the amount-weighted rainfall averages for both the dry summer and wet winter. The groundwater samples were plotted between the LMWL and GMWL. The isotopic compositions of groundwater sampled from

boreholes during the wet winter were closer to amount-weighted averages of the lower (LGL-370 mamsl) and upper (LGU-680 mamsl) Langrivier rainfall samples. Interestingly, the differences in seasonal $\delta^{18}O$ and $\delta^{2}H$ means between the three boreholes (BH1, BH2 and BH3) were not statistically significant ($p > 0.05$) despite the difference in locations and elevation. The groundwater samples plotted between the LMWL and GMWL, implying that the winter rainfall recharged the groundwater.

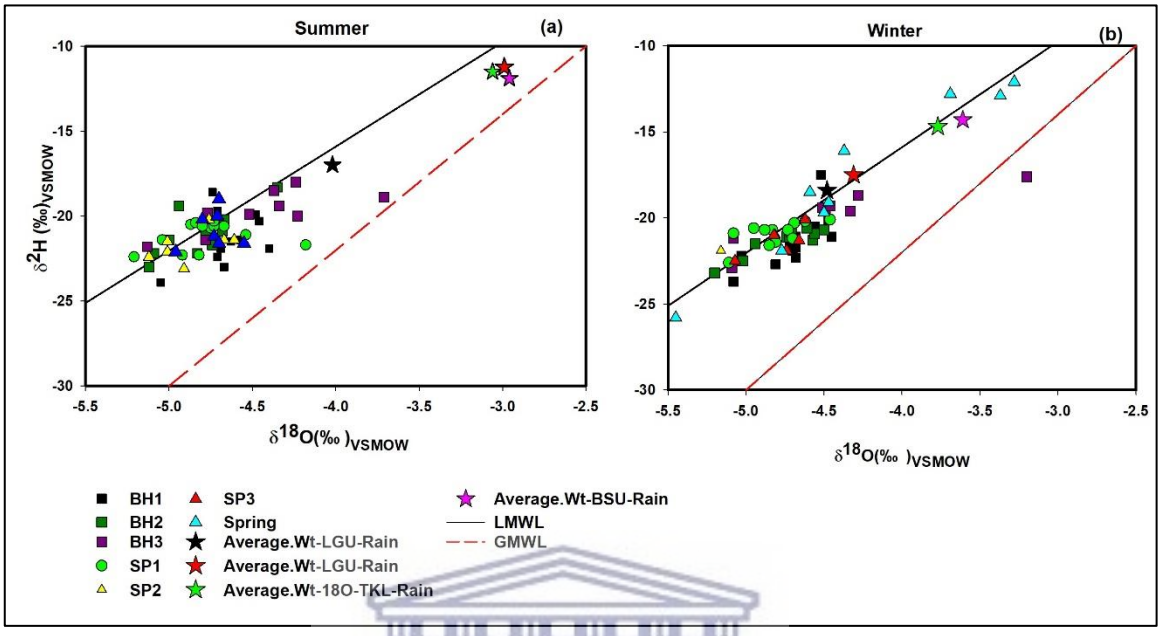

Figure.4.13. Dual isotope plots for boreholes (BH), spring and seeps (SP), including the average weighted rainfall isotopic ratios during the summer and winter seasons. BSU= Bosboukloof, TKU= Tierkloof, LGU= Langrivier Upper, LGL=Langrivier Lower rain gauge.

4.4. Discussion

4.4.1. Rainfall isotope characteristics and controlling factors

Past studies in isotope hydrology have demonstrated that the stable isotopic composition of precipitation in a specific region can be influenced by the local climatic conditions and the altitude of the rainfall (Dansgaard,1964; Rozanski et al., 1993, Gat, 2010).

In this study, the $\delta^{18}O$ and $\delta^{2}H$ values for all rainfall samples showed distinct seasonality whereby the wet winter averages were more depleted compared to the dry summer samples. A similar pattern was observed for the amount-weighted means. Harris et al. (2010) reported similar patterns from other parts across the TMG. This was attributed to the different weather systems causing different storms in the Western Cape (SAWB,1996). For instance, the anticyclonic events with warm moisture bring rain during the dry summer, whereas the cold frontal systems bring rain during the wet winter. Evidence of this was also observed from the low *d*-excess values during the dry summer compared to the high values during the wet winter. The former is commonly associated with

moisture derived from the Indian Ocean likely due to sub-cloud evaporation of the raindrops (Bershaw, 2018). The wet winter *d*-excess values were consistent with other studies within the TMG geological region (Weaver et al., 1999; Harris et al., 2010; Diamond, 2014), which was linked to the frontal depressions from the south Atlantic Ocean.

The seasonal rainfall showed a good correlation with altitude, as expected the higher isotope ratios were more depleted with increasing altitude (Figure.4.9). This trend is often observed when there is a notable topographic gradient (Gat, 2001). The observed values are comparable with those of Midgley and Scott (1994) in Jonkershoek who reported an altitude gradient of -0.32 ‰/100m elevation increase for $\delta^{18}O$. Diamond (2014), also reported an altitude effect between -0.075 to -0.34 ‰/ 100 m for $\delta^{18}O$, and between -0.48 and -2.2 ‰/100 m for $\delta^{2}H$ for the TMG geological region. This indicates the rain out effects of heavy isotopes with isotopic signature becoming more negative as the air mass progresses and cools towards higher elevations deeper into the valley (Dansgaard, 1964). Though other studies in the TMG region did not identify the amount of effect, which was attributed to the short data records (Diamond, 2014) and lack of consistency in sampling (Harris et al., 2010). As pointed out by Yurtsever and Gat (1981), the amount effect is pronounced in tropical regions, therefore, the presence of this effect in the TMG will require further investigations to validate these results.

The lack of long-term rainfall isotope data limits the understanding of the seasonal variations, and it is evident that the two-year sampling duration was insufficient to conclude the temperature effect. It is notable that, the sampling period followed a period of drought (2015-2017). Nevertheless, the current results were comparable with the long-term data set for this region (Harris et al., 2010) and the long-term Global Network of Isotopes in Precipitation (GNIP) Cape Town airport data (IAEA). Furthermore, long-term isotope data of rainfall and temperature are required to evaluate the effect of temperature in this catchment. Owning the short data records, it can be concluded that meaningful results could not be achieved, to reach a more definite conclusion.

4.4.2. Spatial variation in stream water sources and streamflow response

The combined application of hydrometric data and hydrochemical parameters tracer allowed for the identification of the seasonal variability in stream water sources and relative flow pathways across the Jonkershoek sub-catchments. Spatial patterns in rainfall (Buttle et al., 1998; Kendall and Coplen, 2001), the different water sources (Wu et al., 2017) and catchment lithologies (Uhlenbrook et al., 2002) have been found to be the main drivers of large spatial and temporal variations in streamflow $\delta^{18}O$ and $\delta^{2}H$ values and chemistry. The observed spatial variations in EC, Na and Cl may be attributed to the spatial heterogeneity in lithologies and different weathering conditions and geochemical processes of the bedrocks between the sub-catchment (Uhlenbrook et al., 2002).

In this study, the results showed significant spatial ($p \leq 0.05$) variability in streamflow isotope

compositions across the catchment. Similar patterns were observed for hydrochemical parameters (EC, Na and Cl), suggesting different flow lengths and internal mixing times (soil-rock interactions). This supports the assumption of physical and mineralogical heterogeneities in headwater catchments (Walker et al., 2003, Didszun and Uhlenbrook,2003). The samples in Bosboukloof were found to be more isotopically enriched, especially in $\delta^{18}O$, compared to Tierkloof and Langrivier. This suggests the contributions from a more isotopically enriched component soil water from the scree, indicating movement of water through the shallow surficial soils. Most enriched water samples were found downstream which could be explained by the cumulative evaporative effect (Saraiva Okello et al., 2018). Soil water tends to be more isotopically enriched due to evaporation processes in the soil related to the processes of soil-plant-atmosphere interface (Xu et al., 2020). Similar trends were observed in the piezometer water confirming sub-surface scree water as the contributing source to Bosboukloof streamflow.

Higher concentrations of EC, Na and Cl of the streamflow were also notable in Bosboukloof suggesting flow through a more mineralised saturated zone downslope and/or potentially longer travel through the soil-scree which allowed for geochemical processes such as mineral dissolution. The high concentration of Na^+ in Bosboukloof stream water indicates weathering of sodium-bearing rocks i.e., the Na-feldspar granite which makes up most of the scree. Thus, the source of Na^+ in these sub-catchments is attributed to the weathering and dissolution of the basement granites and silicates. These processes control the hydrochemical composition of the groundwater and piezometer samples as high concentrations of hydrochemical parameters were notable in water samples from these sources. The high Cl and EC observed in the stream water may have been due to the contact with rock minerals associated with high Cl or EC such as the Malmesbury shales and colluvium mixture. According to Guo et al. (2017), the evapotranspiration processes may result increase Cl concentrations in soil water.

The streamflow in Langrivier had more depleted $\delta^{18}O$ and $\delta^{2}H$ values on average, as well as the lowest average EC, Na and Cl than those of Bosboukloof and Tierkloof which may be explained by the difference in flow pathways. The low concentrations indicate flow through a less mineralised bedrock such as the TMG quartzite and/or shorter residence time resulting in less mineral dissolution (Song et al., 2006; Saraiva Okello et al., 2018). This may be the case in Langrivier, the hydrochemical concentrations especially EC and Cl were similar to those of the TMG spring. This may have several possible explanations or potentially contributing conditions. Firstly, greater proportional contributions from the high altitude less mineralised TMG perennial springs, likely from deeper groundwater discharge (Diamond, 2014) and wet winter interflow. Secondly, more rapid hydrological pathways with shorter rock water interaction time with the bedrock geology allowing less mineral dissolution. Lastly, the steeper and more incised nature of the Langrivier sub-catchment and stream supports at least the first two mechanisms. Furthermore, the hydrochemical parameters concentrations were higher than the stream samples indicating that the soil water was

less likely to be the source or flow path contributing to streamflow in this sub-catchment.

Spatial variability in the streamflow isotope ratios within a sub-catchment was more pronounced in the concentrations of the hydrochemical parameters for all sub-catchments. The downstream baseflow sample had higher values relative to the upstream. Owing to the geology and topography of the catchment, the streams originate from high altitudes less mineralised sources (TMG aquifer) and shift to more mineralised sub-surface flow pathways as they traverse to the stream outlet. This was evident from the high concentrations in the soil water from the piezometers which had concentrations close to the downstream samples confirming a mix of different sub-surface sources, particularly in Tierkloof and Bosboukloof. However, the sampled water from the piezometers in the Langrivier sub-catchment reflected the occurrence of the evaporation process plotting below the LMWL, while the EC. Cl and Na concentrations were higher than the stream samples suggesting limited or no contribution from soil water.

The borehole groundwater and stream water samples exhibited large differences in hydrochemical parameters for all sub-catchments. This indicated that the stream water in the sub-catchments was less likely to be from the borehole groundwater or granite shale aquifer. The similarities in isotopes and hydrochemical parameters between the stream and TMG spring water samples suggest possible contributions from the TMG aquifer either as spring discharge or baseflow. The high concentration of Na^+ and Cl^- in the borehole groundwater may be explained by the bedrock geology and the results of weathering processes mainly of feldspar and silicate, dissolution of feldspar-rich rocks, and cation exchange reactions (Farid et al.,2013; Madlala et al., 2018; Li et al., 2020). However, this was not reflected in the stream water samples. The general low ionic concentration in the TMG groundwater is attributed to the leaching of minerals and flushing of salts due to high rainfall at high elevations (Smart and Tedroux,2002). Furthermore, the high rainfall > 1000 mm/a may results in the dilution of old groundwater with new rainfall (Wu, 2009). Further research is needed in future to assess the contribution of granite-shale aquifer and the connectivity to the streams (i.e., point of surface and groundwater interaction).

4.4.3. Temporal variations in water sources and flow pathways

Previous studies had reported temporal variations in stable isotope patterns (Midgley and Scott, 1997) and hydrochemical parameters in the Jonkershoek (Britton et al.,1993). The isotopic values and hydrochemical concentrations results showed seasonal variations in contributing water sources across the sub-catchments (Figure.4.3 and Figure.4.11). Furthermore, the results showed that the hydrological functioning of the streams in the sub-catchments is the response to seasonal precipitation patterns in mountainous catchments. The seasonal changes were more pronounced in the streamwater compared to the groundwater, springs, seeps and piezometers. Similar findings were observed in other headwater catchments (e.g., Nienie et al., 2017; Young Jung et al., 2021). According to Penna et al., (2011), the main contributing water source to streamflow in headwater

catchments is the saturated riparian zone in the dry season. Therefore, the seasonal changes in solute concentrations and isotopic composition in the streams are likely influenced by the hydrological conditions of the soil layers (Jung et al., 2021).

The isotopic values were on average depleted during the dry summer and showed a gradual increase at the start of the wet winter. As expected, the rainfall isotopic signatures were damped during the peak of the wet winter (June-Sep). Most of the isotopic compositions of the streamflow and those from various sampled water sources overlapped during the wet winter (Figure.4.12 and Figure.4.13). Similar behaviour was observed for EC, Na and Cl values indicating flushing and then dilution effect of more mineralised water sources across the sub-catchments (Figure.4.6). This allows for multiple potential sources for wet winter baseflow, such as perennial spring discharge, displaced old soil water (Midgley and Scott, 1997; Blume et al., 2002), and recent rainfall translated as shallow subsurface flow. The TMG perennial and ephemeral spring flow to streams were physically observed on the mid-slopes in the wet winter and this was supported by the similarities in $\delta^{18}O$ and $\delta^{2}H$, EC, Na and Cl values between the TMG spring and streamflow samples. This indicates that TMG groundwater flows through the fractured zones via preferential flow pathways and is discharged as springs or seeps into the stream during both the dry and wet seasons (Roets et al., 2018). However, contributions from soils and granite shale groundwater particularly in BH1, BH2 and BH3 need further examination. The flow paths of borehole groundwater to the stream during both the wet and dry seasons couldn't be interpreted from the available data set.

The overlap of the isotopic compositions of the streamflow and the perennial TMG spring samples during the dry summer corroborates the hypothesis that baseflow is sustained by TMG groundwater discharging as springs at higher altitudes with more depleted isotopic ratios than dry summer rainfall. This was also confirmed by the similarities in water chemistry between the TMG springs and streamflow in Tierkloof and Langrivier. Similar patterns have been suggested and observed for the other TMG catchments confirming substantial storage (Saayman et al., 2003; Roets et al., 2008; Diamond, 2014). This is consistent with the locations of channel initiation, which are near the geological transition from the fractured TMG quartzite to the underlying shale and granite basement. However, the granite-shale (BH1) samples had notably higher concentrations (EC, Na and Cl) than either the TMG springs, streamflow or the soil water (Figure.4.5). The difference between the granite-shale and TMG quartzite groundwater is expected given the weathering processes of the differing rock minerals.

Studies elsewhere across the world (Kendall and Coplen, 2001; Wu et al., 2018), have found the difference in isotopic compositions of streamflow to reflect the spatial and temporal variations of groundwater in the area. The comparison of the $\delta^{18}O$ and $\delta^{2}H$ values between the streamflow and borehole groundwater samples showed similar values during the wet winter and the dry summer. However, the streamflow sample EC and Na values were generally close to the TMG spring and soil water values but a few magnitudes less than that of borehole groundwater, indicating little if

any contribution from granite-shale aquifers outflow in either sub-catchment. This indicated that groundwater that contributes to streamflow might not be from the same aquifer as the groundwater sampled from the boreholes. It is notable, that this could not be resolved from the stable isotope data, which showed an overlap between the streamflow, TMG springs, and granite-shale aquifer samples.

The dissimilarity between the rainfall and streamflow isotopic compositions in the three sites during the dry summer suggests that there is a little or negligible contribution of summer rain to the stream baseflows, and rainfall does not contribute directly to the streamflow in this catchment (Figure.4.12). The streamflow hydrograph showed that the dry summer rainfall had minimal impact on runoff with few small peaks and lower baseflow levels compared to the wet winter. This is attributed to the fact that most of the summer rainfall evaporates without producing runoff or recharging the groundwater. This occurs because of the relatively dry soils as a result of higher summer evapotranspiration (ET) rates and is a common pattern in semi-arid regions (Tekleab et al., 2014; Suarez et al., 2015). Moreover, in the dry summer, streamflow EC showed no response to small rainfall events (<10 mm) likely due to the reduced soil moisture, whereby most of the rainfall event water likely infiltrated and, been held in unsaturated soil storage, and much would have evaporated (Suarez et al., 2015).

These observations demonstrate how antecedent conditions control runoff responses and stream water chemistry in this catchment similar to the findings of Britton et al. (1993) in Swartboskloof also a sub-catchment of the Jonkershoek Valley. The more continuous wet winter rainfall is more likely to increase soil saturation and to the point of triggering subsurface flows, as seen in soil water displacement suggested by the geochemical results and the ephemeral spring flow. This indicates that the shallow soil water was relatively immobile during the dry summer and remobilized following the high rainfall during the wet season (Anderson et al., 1997).

4.4.4. Conceptual model: Stream water sources and flow pathways

Uhlenbrook et al., (2002) and Mosquera et al., (2016) demonstrated the value of stable isotope and hydrogeochemistry in conceptualising catchment processes. The integration of hydrometric, stable isotope and hydrochemical is used to conceptualise flow pathways for this area, which is shown in Figure.4.14. The conceptual model suggests the following processes:

a. The dry summer baseflow is sustained by the continuous discharge of TMG groundwater emerging as springs at higher elevations, which was indicated by the similarities in isotopic compositions and the hydrochemical parameters between the perennial spring and streamflow across the sub-catchments. The constant spring discharge is facilitated by the fractured nature of the aquifer. Furthermore, similar to the conceptual model for the nearby Zachariashoek catchment Saayman et al (2003) the large water storage capacity within the unsaturated or saturated zones in the Jonkershoek sustains the streams as delayed flow during baseflow conditions. However, in

Bosboukloof the high concentrations of hydrochemical parameters and generally enriched isotopic compositions compared to the other sites suggests the dominance of shallow sub-surface storage this could be water from/through the scree-soil on the mountain slopes.

b. The wet winter flow had increased baseflow sourced from TMG spring discharge at higher altitudes and perched water tables, indicated by the occurrence of seeps and ephemeral springs along the slopes, and displacement of soil water by incoming rainwater. The latter was supported by an increase in EC, Na and Cl concentrations at the initial stages of the wet winter across the sub-catchments. The isotopic data and EC of the stream samples showed dilution and an overlap with groundwater and rainfall samples as the wet winter progressed, which may suggest some more direct rainfall runoff input as rapid interflow. Interflow, in this case, is potentially rainwater that makes it to the stream along the shorter flow paths without a chemistry change.

These findings provide additional information to the existing conceptual models of TMG catchments (Saayman et al., 2003, Roets et al., 2008; Colvin et al., 2009) of the TMG by highlighting the great importance of interflow (spring and soil water) during the wet winter in the headwater catchments. However, based on the results of the stable isotope and hydrochemistry, no evidence of surface runoff contribution was found in the sub-catchments as illustrated in the conceptual models of Saayman et al., (2003). However, further work is needed to investigate the rainfall-runoff processes in these catchments during storm events and across inter-annual variability. A comparison of the hydrologic response at an event scale will be conducted in the subsequent section (Chapter 6) to support these findings.

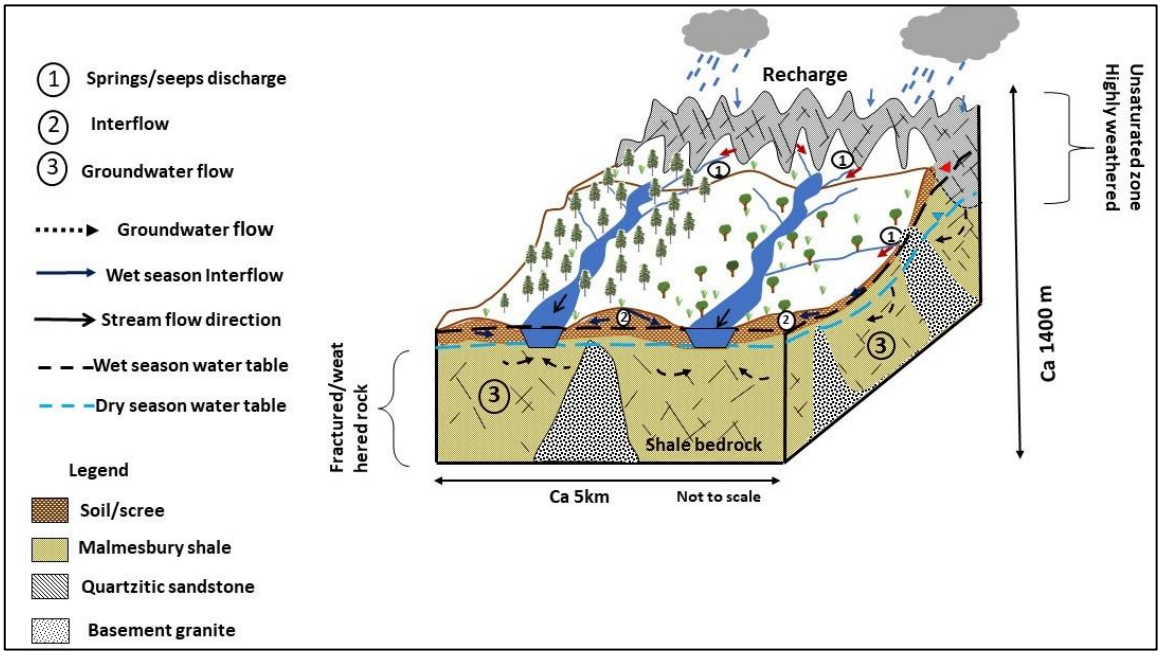

Figure.4.14. Conceptual model of the main seasonal streamflow generating processes. Mountain zone: The rock fractured quartzitic/sandstones vs foothill zone: highly weathered shales and granites and scree downhill.

4.4.5. Implication for local water resource management

The main goal was to study stable isotope and hydrochemical parameter patterns in various water sources and to understand the interaction between precipitation, surface, and groundwater in headwater catchments. Seasonal rainfall plays a significant role in shaping the magnitude and timing of streamflow in the catchment (He et al., 2020). Therefore, understanding the Spatio-temporal variations of rainfall isotopic compositions is highly necessary for understanding the dynamics of water resources in the catchment. Tracer-aided hydrological studies have the potential to reveal spatial and temporal variations in water sources and flow processes. This is because they integrate small-scale variability to give an effective indication of catchment –scale processes, this information can be used for calibration or validation of catchment hydrological models to be used in the implementation of local water resources management strategies (Kendall and Cadwell., 1998; Penna et al., 2015, Tekleab et al., 2015).

The findings suggest deep groundwater contributions from the TMG aquifer as spring discharge at high altitudes and mixing of water in the landscape (scree-soil) in some sub-catchments. This implies connectivity between the streams and the TMG aquifer. The stable isotope analysis showed seasonality with little or no rainfall direct rainfall contributions during the dry summer implying insufficient recharge during this period. This is likely to result in declines in the groundwater levels and could be a major concern in catchments such as the Jonkershoek whereby streamflow during low flow conditions is sustained by baseflows (Saayman et al., 2003). Moreover, this could challenge the sustainable management of water resources in this catchment. It is important to note

that these catchments are often inhabitat, hence the groundwater is pumped frequently for domestic supply. The high water demand during the dry summer may lead to over-abstraction. Moreover, the flow from this catchment also feeds major rivers which supply water for domestic use and irrigation downstream. Therefore, any changes upstream could have negative impacts on the water supply downstream. Long-term series of isotopic compositions and hydrochemical data of streamflow and rainfall also help understand the impacts of changes in the hydrological cycle on a larger scale during the current and future conditions.

4.5. Conclusions

In this study, hydrometric time-series analysis coupled with hydrochemical and stable water isotope approaches were applied to assess the spatiotemporal variations in stream water sources and identify flow paths governing streamflow generating mechanisms during baseflow conditions at the sub-catchment scale. The spatiotemporal variations in hydrochemical parameters EC, Na^+ and Cl^-, and stable water isotope patterns provided information on the flow pathways and stream water sources. All the stream samples showed lower solute concentrations and more depleted isotopic compositions during both the dry and wet seasons

The spatio-temporal variations in geochemical concentrations were larger than for stable isotopes. The spatial variability in hydrochemical concentrations between the upstream and downstream in Bosboukloof and Tierkloof was notably larger than in Langrivier, suggesting additional flow pathways and/or subsurface water components in these two catchments. The streamflow in Bosbouskloof reflects shallow sub-surface flows through the scree material and weathered zones. The observed spatial variations in the geochemistry of surface water across the sub-catchments reflect the difference in catchment physiographic characteristics such as geology, topography, and vegetation type and their influence on runoff processes. There is a need for further investigations to help clarify the integration between these factors influencing runoff processes.

The less variable isotopic compositions between upstream and downstream sites could be interpreted as limited subsurface water additions to the stream along this path in baseflow conditions or contributions of water with similar isotopic compositions to those feeding the headwaters. The combined measurements of EC supported the latter in the case of Bosboukloof. Similarities in isotopic trends between the groundwater, the spring and stream water suggest that in the dry summer, baseflow/streamflow is primarily sustained through TMG groundwater and interflow discharge as springs and seeps at high altitudes. During the wet winter, high flows were additionally fed by ephemeral springs and the seeps higher up in the catchment. The effects of seasonality in streamflow and rainfall were also more evident in EC and chloride compared to the stable isotopes.

The stable isotopes of the stream and TMG groundwater from springs as well as the borehole groundwater were similar indicating that groundwater contributes to streamflow. The major differences in EC and Cl concentrations between borehole groundwater, piezometer and stream samples indicate that groundwater and piezometer water quality is affected by the chemical weathering processes, evaporation and cation exchange. The differences in hydrochemistry between the TMG springs, borehole groundwater and the streamflow sample suggested the occurrence of two different bedrock groundwater aquifers: an aquifer within the TMG bedrock and another in the granite-shale bedrock. The fractured TMG aquifer feeds most of the cold springs which contribute to streamflow, while the granite-shale aquifer contributes to the chemistry of borehole groundwater. However, the study was not able to reveal information on the timing and quantity of different water sources and flow paths or the contribution of the borehole groundwater. This suggests the need for a more detailed study understand runoff components, particularly at the event scale during both the dry and wet seasons as well as the connectivity between the surface and borehole groundwater.

The lack of long-term rainfall isotope data limited our understanding of the seasonal variations, particularly since the sampling followed a period of drought (2015-2017). However, the findings did indicate isotopic compositions of rainfall in this catchment are controlled by the topography, and the seasonal rainfall amount plays a significant role in controlling the isotopic compositions of rainfall but not the streamflow. This knowledge is essential for the understanding of streamflow responses to climatic changes in the catchment. Hence, there is a great need for long-term monitoring and high-frequency collection of isotopes and hydrochemical data to provide deeper knowledge of the hydrological processes in this catchment. Nonetheless, the combination of hydrochemical and stable water isotopes with hydrometric data gave invaluable information which could be used to improve the conceptual model of flow paths in the catchments and other TMG catchments with similar characteristics.

CHAPTER 5: EVALUATING THE SPATIAL AND TEMPORAL VARIATION IN BASEFLOW ESTIMATES USING NUMERICAL DIGITAL FILTERS AND TRACER-BASED HYDROGRAPH SEPARATION.

This study aims to quantify baseflow and characterise its contribution to the stream in several catchments in the TMG fractured geology. This chapter presents the baseflow estimations in the Jonkershoek catchments based on the application of different baseflow separation methods, numerical filtering and tracer-based separation (i.e., conductivity mass balance). The case studies were three sub-catchments of the Jonkershoek Valley. The two-parameter Eckhardt recursive digital filter method (RDF) was applied to separate hydrographs into fast and slow flow components. The RDF provides a method for continuous hydrograph separation. Unless continuous chemistry data is available, the conductivity mass balance (CMB) is used to provide a snapshot estimate of the contribution of various sources to streamflow at the time of sampling. In this case, the CMB results for a set of sampling dates (2018-2020) were applied using electrical conductivity (EC) to calibrate the RDF parameter, BFI_{max}. The calibrated RDF was then used to extract the baseflow index (BFI) for different timesteps for the case-study catchments. Lastly, the non-parametric Mann-Kendall statistical test was applied to detect changes in long- (1946-2019) annual BFIs.

5.1. Introduction

An understanding of processes and factors accounting for spatiotemporal variations of baseflows is necessary for water resources management, particularly in semi-arid regions (Mazvimavi et al, 2004). This knowledge is relevant for managing surface water supply, conjunctive use of surface and groundwater, water quality, and ecological integrity (Roets et al., 2008; Liu et al., 2019). Most of the southern part of the Western Cape Province (WC) experiences a Mediterranean climate typified by long dry summers. Consequently, most of the rivers are non-perennial. Thus, the baseflows of rivers draining areas with Table Mountain sandstones play a crucial role in maintaining the stability of streamflow, as the primary source of streamflow between rainfall events. The magnitude of baseflow may vary greatly due to climatic, geographic, and environmental factors. Therefore, baseflow quantification and characterization are fundamental in assessing the long-term effects of climatic and anthropogenic influence (irrigation and land use changes) on water supply (Hughes and Smakhtin, 1996, Chen and Teegavarapu, 2020). It can further provide critical information for the validation and calibration of hydrologic and climate models (Lott and Stewart, 2016). However, processes and factors accounting for spatiotemporal variability of baseflows in these rivers are not understood.

In the Table Mountain Group (TMG) geological region, most of the rivers that contribute to regional water supply are fed by headwater streams in highly fractured Peninsula Formation sandstone

dominated mountainous terrain. These headwater streams benefit from groundwater discharges that emerge as springs and this supports baseflow sustaining the streamflow during periods of low flows/dry summer and droughts (Saayman et al., 2003a; Hartnady and Jones, 2007; Roets et al., 2008). Streamflow timing and quantity are influenced by many factors such as climate change and human-induced activities (e.g., land use change, industrialization etc.) and catchment characteristics. The large variability in rainfall and recent recurring drought conditions have presented a challenging situation. Declines in available water resources pose a great challenge to meeting the growing demand for irrigation and domestic supply. Therefore, studying the hydrological processes, such as baseflow characteristics in the TMG mountain catchments is fundamental for regional water management.

Recently, there has been an increasing interest in understanding the importance of baseflow contribution in South African catchments. In South Africa baseflow accounts for > 20% of the total runoff which is < 2 % of the rainfall (Vegter and Pitman, 2003). Baseflow averages of 75 % to 90 % of total flows have been reported for small catchments of the southwestern Cape and account on average for nearly 28% of the rainfall (Midgley and Scott, 1994; Brendenkamp et al., 1995). A study by Welderufael and Woyesssa (2010), applied different baseflow separation methods in the Modder River quaternary catchment (central South Africa) and reported averages between 43% and 75% baseflow contribution to streamflow, indicating a minimal contribution of annual rainfall to direct runoff. Jia (2007) performed continuous baseflow separation using the recursive digital filter method for streamflow data across the TMG. The results showed mean annual baseflow ranging from 6 to 33.5 mm with BFI between 3.9 and 30.3 % for TMG outcrop areas.

Madlala et al. (2018) performed a baseflow separation in the Berg River catchment, a neighbouring catchment to the Jonkershoek with a similar TMG geological setting. Using the numerical digital filter method, the study estimated 37.9% sub-surface water contributions to annual discharge in the Berg River. This value was close to that reported by Le Maitre and Colvin, (2008) of 30.74 to 36.9 % for fractured metasedimentary aquifers of South Africa which included the TMG. However, a few studies on baseflow estimation exist in the TMG catchments as many of the studies are concentrated in other parts of the country. These investigations are required in small headwater TMG geological regions such as the Jonkershoek which are the main contributors to large river systems that supply the Cape region.

The separation of baseflow from other components of the streamflow has been an integral part of most hydrological research to understand the groundwater contribution to streamflow. Commonly, the streamflow is divided into two components. First, the baseflow is defined as the delayed response to rainfall events which can involve shallow and deep sub-surface pathways, water from river banks, floodplains, and aquifers, which sustains the river between rainfall events (Cartwright et al.,2014; Rimmer and Hartmann ,2014; Raffensperger et al., 2017). The second component, the quickflow is the result of processes that respond quickly to rainfall events which may consist of overland flow, precipitation falling on the channel water surface, shallow-subsurface flow or interflow, and based on the catchment characteristics (Koskelo et al., 2012; Stewart, 2015).

The accurate separation of baseflow from other flow components is necessary to reveal its variation which can serve as a reliable indicator of changes in streamflow, low flow predictions, groundwater levels and quantity (Liu et al., 2019). Though, establishing techniques that can accurately separate baseflow from quick flow across different catchments is challenging (Nathan and McMahon, 1990; Duncan, 2019). Early researchers developed a variety of methods, which did not involve extensive fieldwork and are cost-effective. These include manual separation, automated digital filter and tracer mass balance methods (Mei et al., 2015; Shao et al., 2020). The most favoured approaches include numerical filtering methods such as recursive digital filters (RDF) using one parameter (e.g., Lynn and Hollick, 1979; Chapman, 1991, 1999) or two parameters(e.g., Eckhardt, 2005).

The Eckhardt (2005) two-parameter RDF has become the most utilized method compared to one parameter. An intercomparison study by Lim et al (2005) using 50 gauging stations in Indiana (USA), found that both RDF methods were highly correlated, and they both produced satisfactory results with a Nash-Sutcliffe coefficient value of 0.90. These methods are assumed to offer a quick way to separate the streamflow hydrograph compared to manual separation. The digital filtering methods can easily process long-term daily streamflow data. The RDF method filters out the low and high-frequency signals of the daily streamflow data assuming the quick flow have high-frequency signals and that baseflow have a low-frequency signal (Eckhardt, 2005). However, these methods are considered subjective and have no physical bases (Partington et al., 2013; Lott and Stewart, 2016). Therefore, they are likely to result in inaccuracies such as overestimation or underestimation in the estimated baseflows (Nathan and McMahon, 1990; Rutledge, 1998).

To address some of these shortcomings, recent advances in baseflow separation methods have involved the utilization of chemical hydrograph separation or chemical mass balance (CMB) methods which are considered to have a more physical basis compared to the graphical methods (Zhang et al., 2013; Cartwright et al., Lott and Stewart, 2016; Zhang et al., 2017; Kouanda et al., 2018; Shao et al., 2020). These studies have demonstrated the potential of combining the chemical mass method based on stream; hydrogeochemical datasets such as electrical conductivity (EC), silica or chloride and digital filters to improve baseflow estimation. Unlike RDF, CMB is objective because it is based on the measured concentrations of the stream water which are related to physical and chemical processes within the catchment (Stewart et al., 2007; Zhang et al., 2013).

However, many studies across the world (e.g., Lott and Stewart, 2016; Saraiva Okello et al., 2018; Kouanda et al., 2018) showed that the results of the CMB can be used to validate and calibrate the digital filters, as they are considered to indicate the catchment behaviour in terms of contributing flow paths based on real-time field measurements. According To Eckhardt (2008; 2011), the filtering parameter values can influence the calculated baseflow index. Therefore, the calibration with tracer-based hydrograph separation such as the chemical mass balance is fundamental to finding the adequate value for the filter parameters. The approach assumes that the EC in the groundwater and surface runoff are distinguishable due to the different flow paths, the concentration in baseflow will be greater than

that of surface runoff assuming the longer reaction time with mineral soil depending on the geology and residence time. More detailed examples of the use of this approach are provided in (Zhang et al., 2013; Rimmer and Hartmann, 2014; Lott and Stewart, 2016; Kouanda et al., 2018; Cartwright and Miller, 2021).

Cartwright et al. (2014), used both the chemical mass balance method and RDF to estimate baseflow their findings showed that RDF tends to produce higher baseflow values compared to CMB. They concluded that the estimated baseflows from numerical methods aggregate much of the water from delayed sources. Nathan and McMahon, (1990) made similar assumptions. On the other hand, the CMB aggregate delayed transient water stored with surface runoff component due to similar geochemical signatures. Kouanda et al. (2018), conducted a comparison study between various digital filter methods and the CMB method in Samendeni catchment, Burkina Faso. They found that the digital filter methods tend to produce a higher base flow index (BFI) compared to CMB. However, once calibrated, the digital filter methods reproduced BFI values that were close to those of the CMB. This supports the findings by Eckhardt (2011) that filter parameters are sensitive hence trace-based methods should be applied to validate the results of the digital filtering methods.

The selection of representative samples for baseflow EC as well as the duration and frequency of sampling to appropriately calibrate a baseflow has always been a concern. For instance, Kronholm and Capel, (2015) used the median of shallow groundwater, the highest in the stream excluding outliers or the specific conductance observed during the lowest streamflow to estimate the baseflow concentrations/slow flow, whereas Kouanda et al. (2018), Saraiva Okello (2018) and Lott and Stewart, (2016) used the highest/maximum observed EC in the streamflow as baseflow EC. The value of the quick flow component was estimated to be the lowest specific conductance observed with the peak flow. However, the CMB method may be deemed impractical in some regions due to the challenges of acquiring long-term geochemical data mainly due to a lack of financial capacities for hydrological monitoring and the inaccessibility of some sites. Hence, it has been underutilized in sub-Saharan regions with only a limited number of studies available (e.g., Saraiva Okello et al., 2015; Kouanda et al., 2018).

The present study aims to apply different techniques to quantify baseflow in the fractured rock catchment of the TMG using the Jonkershoek catchment as a case study. In addition, other hydrological aspects of the sub-catchments were addressed. The main objectives are (1) to quantify baseflow using the baseflow index (BFI) as a proxy at an annual, monthly and seasonal time, (2) to investigate the spatial and temporal variation in baseflow characteristics across the sub-catchments of the Jonkershoek catchment (3) to assess if conductivity mass balance (CMB) method can improve baseflow estimation in a TMG catchment with fractured rocks and affected by land use change. This study will provide a basis for future recommendations for baseflow separation in the TMG geological region and similar catchments. Understanding the contribution of baseflow and its variability with climate can enable the development of effective adaptation strategies to cope with climate change impacts such as droughts and provide an important decision support tool to assist in regional water management plans.

5.2. Study site

Detailed information on the selected study sites is presented in Figure.4.1. Figure.5.1 and Table.5.1 further describes the variation in morphology, land cover, rainfall and streamflow, and the long-term hydrometric records of ideal study sites

5.3. Data and Methods

5.3.1. Data source and collection

The long-term hydrological data including streamflow and rainfall of over 70 years spanning from 1946-2019 were obtained from the South African Environmental Observation Network (SAEON) (https://ecologi.shinyapps.io/Jonkershoek_Hydro/). The study catchments have V-notch gauging weirs located downstream just above the stream confluence with the main Jonkershoek River (Figure.4.1). Pressure transducers (Campbell Scientific) record the stage at the weirs at one-hour intervals (SAEON). The same period (1946-2019) of data records from each gauge was used for analysis. The rainfall was measured by SAEON using TE525 Texas Electronics (Dallas, Texas, USA) rain gauges with HOBO loggers that record event-based rainfall (0.25 mm resolution) and hourly temperature in Bosboukloof, Tierkloof and Langrivier as shown in Figure.4.1. The specific conductance (electrical conductivity referenced to 25º C, µS/cm) of the streamflow was measured monthly both during the summer (dry) and winter (wet) seasons from January 2018 to March 2020 at the three sub-catchments. In some instances, measurements were taken twice a month, the stream sampling sites are shown in Chapter 4 (Figure.4.1). The EC measurements were collected during non-rainfall days considered as baseflow conditions. Rainfall EC was measured from the collected cumulative rainfall water samples shown in Chapter 4. A multi-parameter water property probe (YSI Professional Plus, YSI Inc) was used for the measurements. The potential evapotranspiration was calculated using Hargreaves and Samani, (1982).

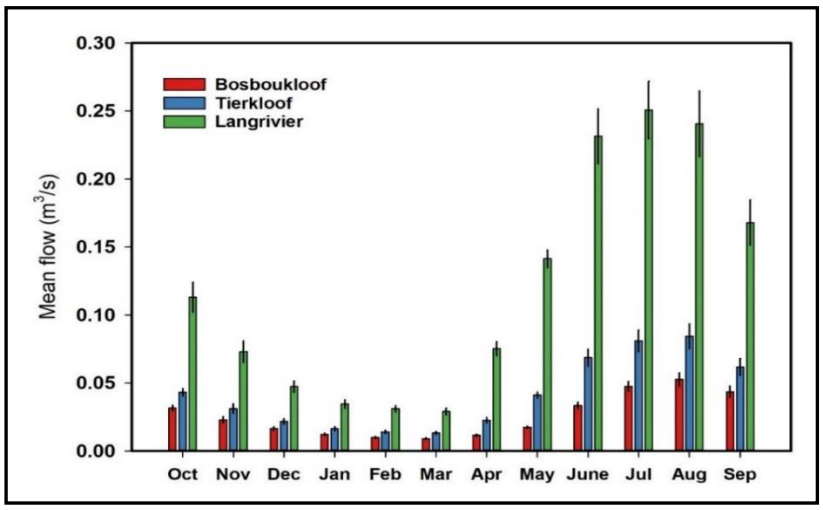

Figure.5.1. The long-term mean monthly flow for the three sub-catchments for the period 1946-2019 hydrological years with standard error bars.

Table.5.1. Summary of catchment physiographic and hydroclimatic characteristics for the observation period, hydrological years 2018-2019. Physiographic characteristics were adapted from (van Wyk, 1987 cited in Slingby et al., 2021).

	Bosboukloof	**Tierkloof**	**Langrivier**
Area ($km^{2)}$	2.0	1.57	2.45
Stream length (km)	1.53	1.80	2.43
Max elevation (mamsl)	1067	1530	1460
Min elevation (mamsl)	274	296	346
Mean elevation (m)	543	900	950
Mean channel slope %	26	49	40
Geology	Quartzitic sandstone, shale bands, weathered granite and extensive scree and talus.	Quartzitic sandstone, shale-bands, weathered granite and scree	Quartzitic sandstone, shale-bands, weathered granite and scree
TMG outcrop cover (% of the area)	12	26	41
Mean daily flow (m^3/s)	0.014	0.031	0.0715
Min daily flow (m^3/s)	0.0013	0.0043	0.0107
Max daily flow ($m^{3/}s$)	0.098	0.693	1.700
Mean annual runoff (mm/a)	232	558.6	962
Long-term MAR (mm/a)*	409	880.7	1461.5
Mean annual precipitation (mm/a)	1200	1139	1317
Long-term MAP (mm/a)*	1104	1244	1539
Mean annual PET (mm/a)**	1333	1414	1428
Min temperature	10.9	11.5	11.4
Max temperature	22.4	23.9	24.4

*MAP (Mean Annual Rainfall)/Mean Annual Runoff (MAR), long-term; 1946-2019 ** Calculated using Hargreaves & Samani(1982) method using air temperature recorded in each sub-catchment.

5.3.2. Baseflow separation methods

Several procedures of quality control were performed before performing hydrograph separation. This included screening the streamflow data for bias and identifying missing data. Streamflow data gaps of less than 30 days were infilled according to the methods described by (Hughes and Smakhtin, 1996). However, many studies follow the suggestion by Ladson et al. (2013), that the BFI should be determined from raw data only (i.e., original data not filled). Hence, the missing data of over a month were not infilled and the raw data was used for the separation. For this study site, missing records were from 2008 to 2011 which exceeded 30 days, therefore, the data was not filled.

5.3.2.1. Recursive digital filtering methods (RDF)

Various digital filtering algorithms are available for hydrograph separation, however, the recursive digital filter RDF proposed by (Eckhardt, 2005) has been widely used for separating streamflow into components of baseflow (the slow or low-frequency signals) and quick flow (fast or high-frequency signals). Currently, no baseflow separation technique is universally accepted as each has advantages and disadvantages. The performance of the various methods varies with hydrological and hydrogeological characteristics i.e., different soil types, antecedent moisture conditions and rainfall events (Koskelo et al., 2012; Partington et al., 2012). Therefore, it is often necessary to apply more than one filter and calibrate it according to the site characteristics. In this study two-parameter or Eckhardt digital method (Eckhardt, 2005) was selected to separate baseflow. The advantage of this method is that it incorporates both the reduction in streamflow and baseflow when quick flow ceases (Bosch et al., 2017).

The general equation for hydrograph separation is described by:

$$Q_j = Q_{Bj} + Q_{Sj} \qquad (5.1)$$

where Q_j is the daily discharge (m^3/s) at the sampling point, Q_{Bj} is the baseflow contribution (m^3/s) and Q_{sj} is the quickflow contribution (m^3/s) at daily time step *j*.

The two-parameter Eckhardt method (Eckhardt, 2005, 2008) separates the high and low-frequency signals. The filter requires two parameters: a recession constant, *a*, and BFI_{max}, the maximum calculable long-term ratio of baseflow to total streamflow. The RDF assumes that the outflow from an aquifer is linearly proportional to its storage and may often overestimate baseflow in large watersheds because of longer travel times to the catchment outlet resulting in dispersion of runoff peak (Miller et al., 2016). The two-parameter filter is described by the following equation:

$$Q_{Bj} = \frac{(1-BFI_{max})aQ_{Bj-1}+(1-a)BFI_{max}Q_j}{1-aBFI_{max}}; \qquad Q_{Bj} \leq Q_j \qquad (5.2)$$

$$1 > BFI_{max} > = 0$$

where Q_{Bj} (m^3/s) is the baseflow flux on day j, Q_j is the total discharge (m^3/s) on day j. BFI_{max} and a are the filter parameters. The BFI_{max} is the maximum value of the baseflow index (i.e., the ratio of baseflow to streamflow). The value is dimensionless and always varies from 0 to 1. When $BFI_{max} = 0$ then:

$$Q_{Bj} = aQ_{Bj-1} \tag{5.3}$$

which indicates that a is a recession constant. To perform the two-parameter digital filter technique, these parameters must first be estimated. However, estimation of the filtering parameters can be challenging as they are rarely the same across sites and directly affect the baseflow separation results (Liu et al., 2019).

5.3.2.2. Recession constant (*a* parameter)

Recession analysis aims to model the decrease of streamflow during periods without rainfall to define aquifer properties such as the parameters descriptive of water storage in the catchment in a porous or fractured medium (Stewart, 2015). The recession constant provides essential information on the water storage and releases characteristics within the sub-catchment. The recession constant varies from 0 to l and indicates the rate of depletion of flow, linked to the seasonal and environmental influence, topography, drainage pattern and soil and geological types (Mazvimavi, 2003; Yang et al., 2018). Several methods have been proposed for the estimation of the linear recession parameter "*a"* (Nathan and McMahon, 1990; Tallaksen, 1995; Rutledge, 1998; Eckhardt, 2005). However, for this study considering the influence of sub-catchment characteristics in Jonkershoek, several methods were applied to estimate the recession constant namely, the correlation method, the master recession curve and mean value.

Previous studies in South Africa found recession constant $a = 0.925$ to be suitable for digital filtering (Hughes et al., 2003; Welderufael and Woyesssa, 2010; Madlala et al., 2018). The recession constant a vary for different components. The values are typically in the ranges of 0.2 to 0.8 for surface runoff, 0.7- 0.94 for interflow and 0.93 to 0.995 for baseflow (Nathan and McMahon, 1990). Owing to the complexity and discrepancies between these methods, it was suggested that more than one method should be used to allow the identification of the specific catchment characteristics.

Here the filter parameter a was estimated using the daily streamflow data spanning from 1946 to 2019 by the correlation method (Tallaksen, 1995; Eckhardt, 2008), mean value and master recession curve exponent (MRC) (Eckhardt, 2005; Wenninger et al., 2008). Only dry summer period daily streamflow data (October- March) for each year was used to reduce the effect of the variability of the recession behaviour affected by catchment wetness and saturated aquifer thickness (Chen et al., 2012). The streamflow recession periods were identified as periods of decreasing streamflow for at least 10 to 15 days consecutive days. The length of the recession periods included in the analysis was selected based on the method being applied, as described below.

Assuming a linear relationship between storage and outflow:

$$S=kQ \tag{5.6}$$

where S is the storage, Q is the outflow and *k* is the recession coefficient. The streamflow recession can be described by equation (5.7), whereby the streamflow is assumed to recede exponentially during a period without groundwater recharge or direct runoff (Chapmann, 1999).

$$Q_j = Q_0 e^{-\alpha j} = Q_0 k^j \tag{5.7}$$

Where Q_j is the flow ($m^3\ s^{-1}$) at a given time *j* (*j* days), Q_0 is the initial flow ($m^3\ s^{-1}$) at the beginning of the dry summer (recession), j_0, and $k = e^{-\alpha}$ is the recession constant and α is the recession rate (day^{-1}) of the dry period. The inverse if the recession rate (α) expresses recession length in days ($K = 1/\alpha$) e.g., 45 days equates to $\alpha = 0.022\ days^{-1}$ and K = 0.978 (Rutledge, 1998). The recession constant can be found as the slope of the semi-logarithmic plot of a recession. The k is also referred to as *a* in RDF.

For the correlation method, a plot of discharge at one time (Q_j) against discharge one-time interval later (Q_{j+1}) was constructed for the recession periods and the slope of the regression line through the origins is considered the recession constant *a* also referred to as *k*. As described in (Tallaksen, 1995; Kissel and Schmalz, 2020), the first days of the recession were discarded to exclude the influence of direct runoff. For this study, the first 3 days were excluded (three-day lag interval) and it can be hypothesised that the direct runoff is quick in these steep terrain and small headwater catchments. The minimum recession length was set to 10 days due to the long data records of 71 years still ensuring that enough recessions are available to yield a strong analysis.

The MRCs were constructed using the method described by (Eckhardt, 2005; Rimmer and Hartmann, 2014) and the resulting *a* were compared. To construct the MRC, the average daily streamflow for the dry summers from 1946 to 2020 were overlapped based on the day of the year (DOY) from October to March (day 1 to 183), whereby the first day of October was considered day 1 and the last day of March day considered 182 or 183 depending on whether the year had 365 or 366 days. The recession constant was then calculated as described by the exponential decay equation (5.6). The recession curve is presented in a semi-logarithmic plot in such a way that the discharge (LnQ_t) is plotted against t (DOY) on the normal abscissa (Chen et al., 2012). Recession constants for the MRC were estimated using Equations (5.6) and (5.7). Lastly, the mean value of $Q_j + 1/Q_j$ during the dry period was estimated. The resulting recession constants from the MRC, correlation and mean method were averaged. The average "*a"* in each sub-catchment was applied to perform the digital filter baseflow separation.

5.3.2.3. Estimation of BFI_{max}

The maximum baseflow index (BFI_{max}) is a non-measurable parameter. In many instances the BFI_{max} cannot be estimated or identified before the separation, hence Eckhardt (2005) proposed values linked

to catchment hydrological and hydrogeological characteristics to minimize the subjective influence of the parameter. The proposed values are BFI_{max} = 0.80 for perennial streams with a porous aquifer, BFI_{max} = 0.50 for ephemeral streams with porous aquifers and BFI_{max} = 0.25 for perennial streams with hard rock aquifers. Eckhardt (2008) also suggested that optimization using tracers can provide data for better calibration of BFI_{max}. For this study, BFI_{max} was estimated using the backwards-filtering approach (Collischonn and Fan, 2013) implemented in the USGSGW toolbox (Barlow et al., 2015). The method estimates the BFI_{max} for each hydrological year (i.e., 365 days cycles). The advantage of this technique is that it is objective, and determines the parameters of the algorithms based on the flow characteristics, seasonal variations and storm events in each site (Bosch et al., 2017). More details on this method are provided in (Collischonn and Fan, 2013). Backwards filtering also assumes that the groundwater discharge is linearly proportional to storage given by Equation (4).

$$Q_{Bj-1} = \frac{Q_{Bj}}{a}, Q_{Bj-1} < Q_{j-1} \tag{5.4}$$

Where Q_{Bj} and Q_{Bj-1} are baseflow at time step j and j-1, respectively, and a is the recession constant. The BFI_{max} value can be found by dividing the sum of the calculated daily base-flow values by the sum of daily streamflow values.

$$BFI_{max} = \frac{\sum_{j=1}^{N} Q_{Bj}}{\sum_{j=1}^{N} Q_j} \tag{5.5}$$

5.3.2.4. Hydrograph separation and baseflow estimation

The two-parameter RDF hydrograph separation was computed using the average of the calculated "*a"* parameter and the BFI_{max} was estimated using the backward filtering method in the USGS GW toolbox. The suitability of the estimated filter parameters was determined using sensitivity analysis (Eckhardt, 2011). The sensitivity index (S) for the long-term data was calculated as the ratio between the relative error of BFI and that of the respective parameter either the *a* or BFI_{max} which signifies that the relative error of X per cent in *a* or BFI_{max} estimation causes a relative error of X per cent in BFI. Unlike the recession constant that can be determined by several recession analysis methods, the BFI_{max} cannot be derived from streamflow measurements alone. Therefore, the value of BFI_{max} will be more uncertain than the value of *a*. More detailed information on this analysis is provided in (Eckhardt, 2005, 2011). Sensitivity indices for *a* and BFI_{max} were simultaneously computed with the BFI values.

The continuous baseflow separations for daily streamflow time series were computed for the period 1946-2019 with emphasis on 2018 to 2019 and summer 2020, this period was chosen as it represents the years of the period of the research and the availability of geochemical data. The daily baseflow estimates were aggregated to annual, seasonal and monthly time scales. Additionally, the continuous hydrograph separation for long-term data was performed for the annual and seasonal periods using the daily streamflow time series from 1946-2019. Due to the missing data of 3 years, the time series was split into two periods 1946-2008 and 2011-2019 to determine the long-term baseflow index. The

hydrological year 2020 also had missing data (July to September). Therefore, 2020 data was used to represent only the dry summer. The baseflow separation was conducted as described in Figure.5.2.

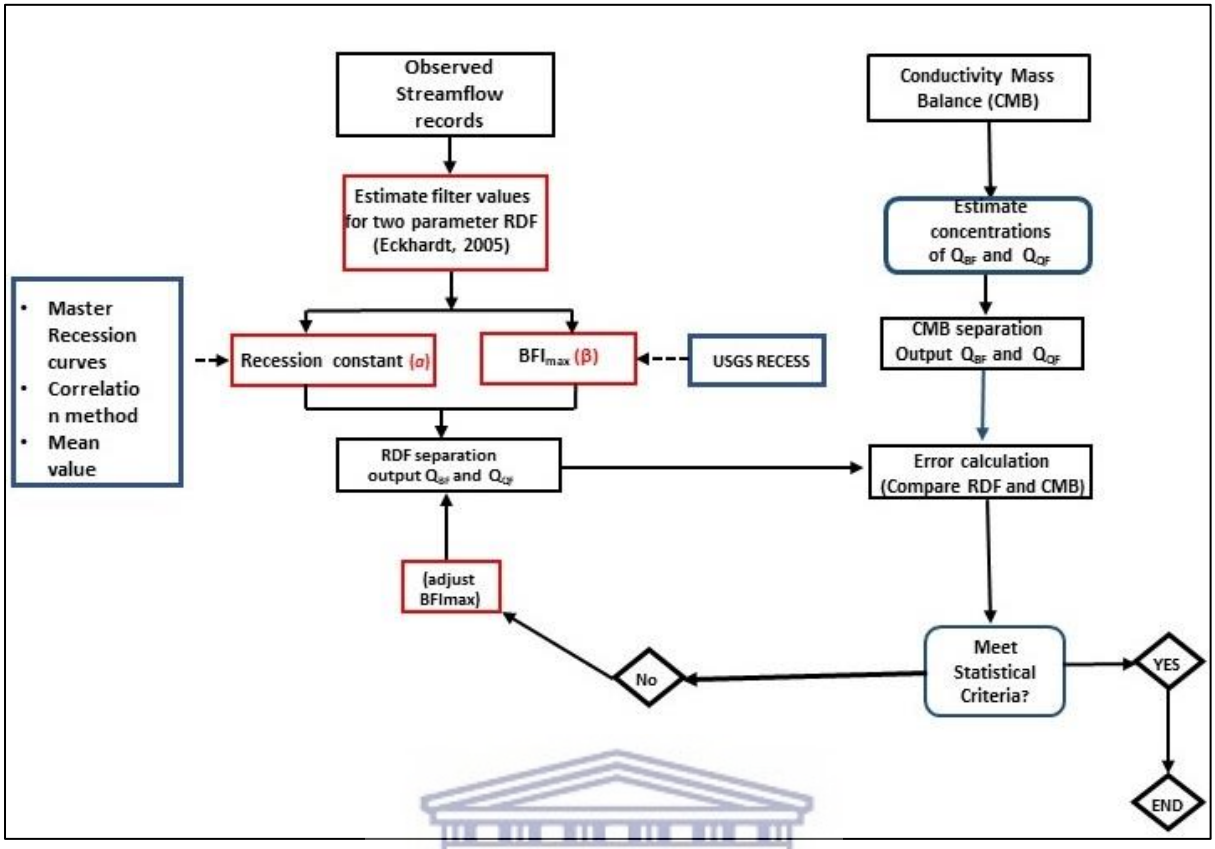

Figure.5.2. Summary of the methodology for baseflow separation (Modified after Rimmer and Hartmann, 2014).

5.3.3. Conductivity Mass Balance (CMB)/Mass balance filtering

Estimation of a reliable or accurate value for the BFI_{max} filtering parameter can be challenging as it is are rarely the same across catchments (Zhang et al., 2013). Hence Eckhardt (2005) proposed that the RDF methods should be validated using tracer-based hydrograph separation methods. Several studies (Zhang et al., 2013; Cartwright et al., 2014; Rimmer and Hartman., 2014; Saraiva Okello et al., 2018) have used the conductivity mass balance (CMB) method to determine BFI_{max} values based on local field data rather than generalisation. Eckhardt's (2011) sensitivity analysis found that the recession constant "*a"* had more influence on the baseflow index, however, the BFI_{max} was uncertain (Table.5.6). Therefore, Eckhardt (2008) suggested that to obtain a more refined BFI_{max} value, the researcher should consider tracer approaches to calibrate the BFI_{max} value. The validity of the RDF, and the tracer-chemical mass balance is assumed to produce more representative baseflow estimates compared to the RDF, however, it is limited to the times when chemical data was collected. In this study, the calibration or optimization of BFI_{max} was performed using the streamflow electrical conductivity as a tracer.

The potential EC values for the baseflow and quickflow components were estimated according to Saraiva Okello et al. (2018) and Kronholm and Cape (2015). The EC values of the baseflow component

(C_{QB}) were assumed to be the maximum EC value measured at the streamflow representing all sub-surface flow paths during the low-flow conditions. If the water entering the downstream and upstream are a mix of similar sources with the same concentrations, the downstream samples were used for each sub-catchment. In this catchment, the different areas near the downstream may influence the streamflow chemistry at the weir. This is evident in the high EC concentrations downstream compared to the upstream. The baseflow values were 67.1µS/cm, 49.1 µS/cm and 36.4 µS/cm excluding the outliers for Bosboukloof, Tierkloof and Langrivier, respectively.

The quickflow component was estimated to be the lowest EC value during the high flow season in winter, during this period the EC values are relatively low due to dilution and flushing by new rainfall water (Mokua et al., 2020). Langrivier sub-catchment had the lowest EC values of less than 20 µS/cm during the high flow season, challenging reasonable hydrograph separation. The streamflow EC value was close to the lowest value of winter rainfall in this catchment. For this reason, the lowest EC value of 20 µS/cm during the high flow seasons was used for all the sub-catchments. The conductivities and ionic concentrations of the total streamflow are known to have a consistent and statistically significant log-linear relationship with discharge over orders of magnitude ranges of discharge and periods for individual stream gauges (Stewart et al., 2007). Therefore, the baseflow and quick flow concentrations were assumed to remain constant throughout the observation period.

The conductivity mass balance method was calculated following Equation 5.8 (Kish et al., 2010; Zhang et al., 2013; Cartwright et al., 2014; Miller et al., 2015) to optimize the value of BFI_{max}.

$$Q_{BF} = Q\left[\frac{C_{QT}-C_{QF}}{C_{BF}-C_{QF}}\right] \qquad (5.8)$$

Q is the measured streamflow discharge (m^3/s), C_{QT} is the measured specific conductance of the streamflow (µS/cm) at a given timestep, C_{BF} and C_{QF} are the estimated specific conductance (µS/cm) of baseflow discharge and for the quickflow component, respectively. The conductivity mass balance or the chemical hydrography separation was performed for the sampled times during the hydrological years 2018 to 2020.

5.3.4. Calibration of the recursive digital filter parameters.

To calibrate the Eckhardt digital filter parameter the Rimmer and Hartmann (2014) and Lott and Stewart (2016) approaches were followed (Figure.5.2). The optimization of BFI_{max} was conducted for the period 2018 to 2020 for the days where EC values were measured. The BFI values obtained from the RDF methods were compared with those derived by the CMB. The calibration was achieved by adjusting the selected BFI_{max} values until the error between the BFIs derived by the CMB and RDF for the sampling days was at a minimum.

The accuracy of the simulated (RDF) BFI values was examined by employing several indicators of goodness of fit, using the CMB (Observed) method results as a constraint. The applied indicators were

the percentage of bias (PBIAS), coefficient of determination (R^2), root mean square error (RMSE) and correlation coefficient were calculated as suggested by (Singh et al., 2005; Moriasi et al., 2007; Lee et al., 2018) using Equations (5.9-5.11). The percentage bias (PBIAS) measures the average tendency of the simulated data to be larger or smaller than the observed, negative values indicate model underestimation bias and positive values indicate model overestimation bias (Gupta et., 1999). The RMSE indicates the magnitude of the average error given the units of the constituents of interests and values close to 0 indicate a perfect fit while increasing RMSE values indicate an increasingly poor match. The coefficient of determination (R^2) measures the degree of collinearity between observations and simulations.

$$R^2 = \frac{(\sum_{i=1}^{n}(Y_{obs,i} - \bar{Y}_{obs}) - (Y_{sim,i} - \bar{Y}_{sim,i}))^2}{\sum_{i=1}^{n}(Y_{obs,i} - \bar{Y}_{obs})^2 \sum_{i=1}^{n}(Y_{sim,i} - \bar{Y}_{sim})^2} \quad (5.9)$$

$$RMSE = \sqrt{\frac{\sum_{i=1}^{n}(Y_{sim,i} - Y_{obs,i})^2}{n}} \quad (5.10)$$

$$PBIAS = \left[\frac{\sum_{i=1}^{n}(Y_{sim,i} - Y_{obs,i}) * (100)}{\sum_{i=1}^{n} Y_{obs,i}}\right] \quad (5.11)$$

where, *n* is the number of the observations in the period under consideration, $Y_{sim,i}$ and $Y_{obs,i}$ represent the is the *i*-th simulated (RDF) or the observed (CMB) value, respectively. $\bar{Y}_{sim,i}$ is the mean of the simulated values and $\bar{Y}_{obs,I}$ is the mean of the observed values.

The statistical student's paired t-test was performed to test if there were significant differences between the means BFI values of the RDF and CMB. The t-test was performed using a 95% confidence interval (i.e., *p*-value ≥ 0.05). The baseflow separation was repeated as described in Figure.5.2. if the values of the statistical tests and the goodness of fit did not meet the criteria of PBIAS≤ ±10%, RMSE value less than half of the standard deviation of the observed data, *p*-value ≥ 0.05 and $R^2 > 0.5$ (Golmohammadi et al., 2014; Moriasi et al., 2007). If the calibration was considered satisfactory, meeting at least two of these criteria then the calculated daily BFI values were aggregated to annual, monthly and seasonal BFIs for each sub-catchment. The Mann-Kendall (MK) (Mann, 1945; Kendall, 1955) statistical test was used to detect statistically significant trends in the long-term BFI over 75 years (1946-2020). The significance level of the test was set at 95 % confidence intervals

5.4. Results

5.4.1. Flow and hydrochemical characteristics

Figure.5.3 presents the time series of the daily discharge and measured EC on sampled days and Table.5.2. contains the summary of the respective means, ranges and standard deviations of rainfall, flow, and measured EC for each sub-catchment over the sampling period. The sub-catchments had highly spatially and temporally variable discharge. The discharges exhibited strong seasonality, the flow was the lowest in dry summer months from October to March and increased during the wet winter

months (April and September). Compared to 2018, 2019 had the highest winter flow with maximum values of 0.98, 0.55 and 1.7 m^3/s in Bosboukloof, Tierkloof and Langrivier, respectively (Figure.5.3). Overall, for the sampled period the highest flows occurred in wet winter 2019 which also recorded a higher rainfall with occasional storm events of up to 80 and 90 mm/day. In contrast, the highest recorded daily winter rainfall was 58 mm/day in 2018. The flow in Bosboukloof was much lower compared to Tierkloof and Langrivier, daily values ranged from 0.0014 to 0.098 m^3/s (Table.5.2). In Tierkloof, the average daily discharge ranged from 0.004 to 0.534 m^3/s which is much higher than in Bosboukloof but less than at Langrivier, which had values ranging from 0.012 to 1.7 m^3/s.

As observed for discharge the EC values showed strong seasonality (Figure.5.3). The EC values were higher during the dry summer and increased steadily toward the beginning of the wet winter (May) and then decreased gradually as the wet season progresses. The lowest EC values were recorded during the periods of very high flows or later in the wet winter season, whereas the higher EC values were mainly recorded during the dry summer or the period of very low flow. Overall, the range of EC in Bosboukloof (42.9 to 67.8 µS/cm) was higher than in Tierkloof (31.3 to 49 µS/cm) and Langrivier which exhibited the lowest EC values compared to the other two sites ranging from 23 to 34.6 µS/cm (Table.5.2).

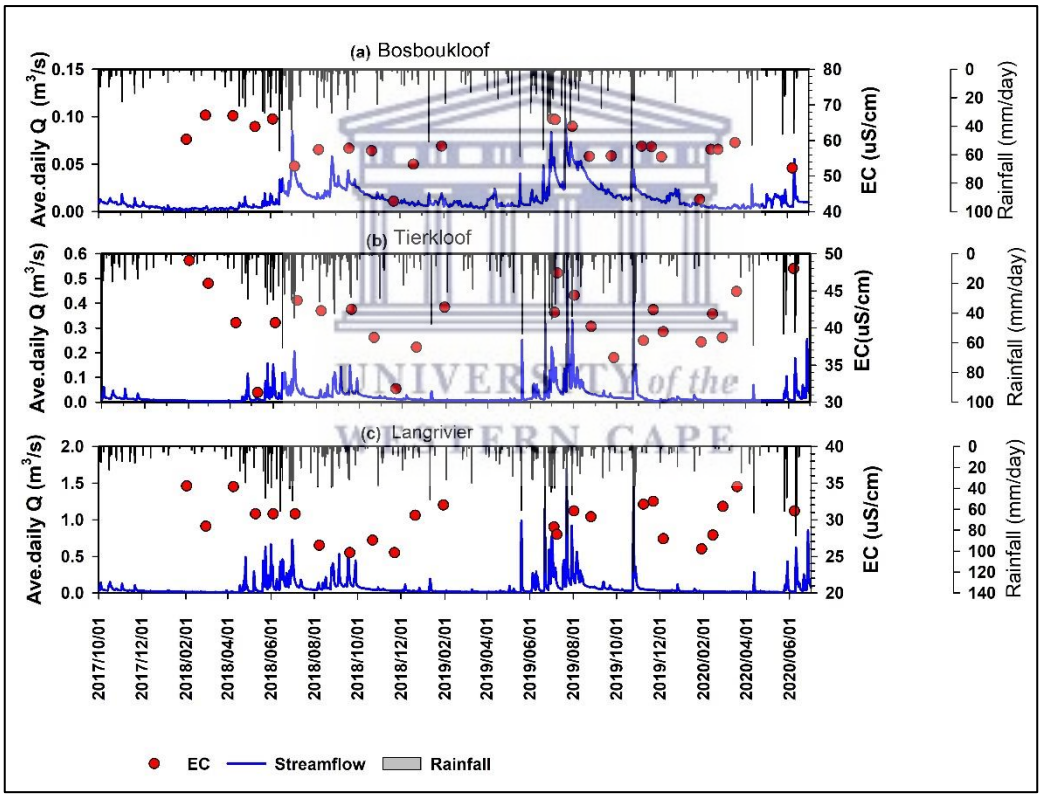

Figure.5.3. Temporal variations in daily flow, rainfall and EC concentrations between 2018-2020. (a) Bosboukloof, (b) Tierkloof and (c) Langrivier. (Note the different discharge and EC scales across the sub-catchments).

Table.5.2. Minimum, maximum, mean daily discharge, EC and rainfall values including standard deviations for the analysis period (2018-2020).

Parameter	Bosboukloof				Tierkloof				Langrivier			
	Min	Max	Mean	Stdev	Min	Max	Mean	Stdev	Min	Max	Mean	Stdev
Discharge	0.0014	0.098	0.014	0.013	0.004	0.534	0.024	0.039	0.012	1.70	0.071	0.12
EC	43.0	67.1	58.6	6.2	31.3	49.1	41.1	4.4	23.0	34.6	30.0	3.29
Rainfall	0.00	93.0	2.66	8.11	0.00	92.4	2.98	8.88	0.00	120.4	2.82	8.72

5.4.2. Recursive digital filter baseflow separation

5.4.2.1. Recession analysis α parameter characteristics

Three different recession analysis techniques were applied to obtain the recession constant (*a*) filter parameter for the period between 1946-2020, using the annual dry period generalised as the 183 days from October to March each year. The results are presented in both Figure.5.4 and Table.5.3**.** Here, the recession constant was determined using the master recession curve exponent (MRC), the correlation method, and the mean value as described in (Rimmer and Hartmann, 2014; Saraiva Okello et al., 2018). For the correlation method, the regression lines through the origin of the scatter plot produced estimated recession constant values of 0.968, 0.957 and 0.953 for the Bosboukloof, Tierkloof and Langrivier, respectively (Figure.5.4.(a-c)). The Q_{j+1} was strongly correlated with Q_j across the sub-catchments at r^2= 0.99.

For the MRC all the recession curves are nearly linear, however, the lower portion of the recession curves was somewhat convex-shaped, revealing a degree of non-linearity (Figure.5.4.(d-f)). The MRCs produced similar recession constants across catchments, with strong correlation coefficients for the fitted curves of r^2 = 0.989 (α = 0.009) for Bosboukloof, r^2 = 0.966 (α = 0.010) for Tierkloof and r^2= 0.977 (α = 0.0122) in Langrivier (Figure.5.4). Therefore, the determined recession constants (k) were 0.991, 0.990 and 0.987 for Bosboukloof, Tierkloof and Langrivier, respectively. The mean values method produced very similar recession constants of between 0.962 and 0.967 across the sub-catchments. Expressing the value in days (K) based on the average recession constant of the different estimates, Bosboukloof and Tierkloof exhibited longer recessions 38 and 34 days, respectively, while Langrivier appeared shorter, with 30 days.

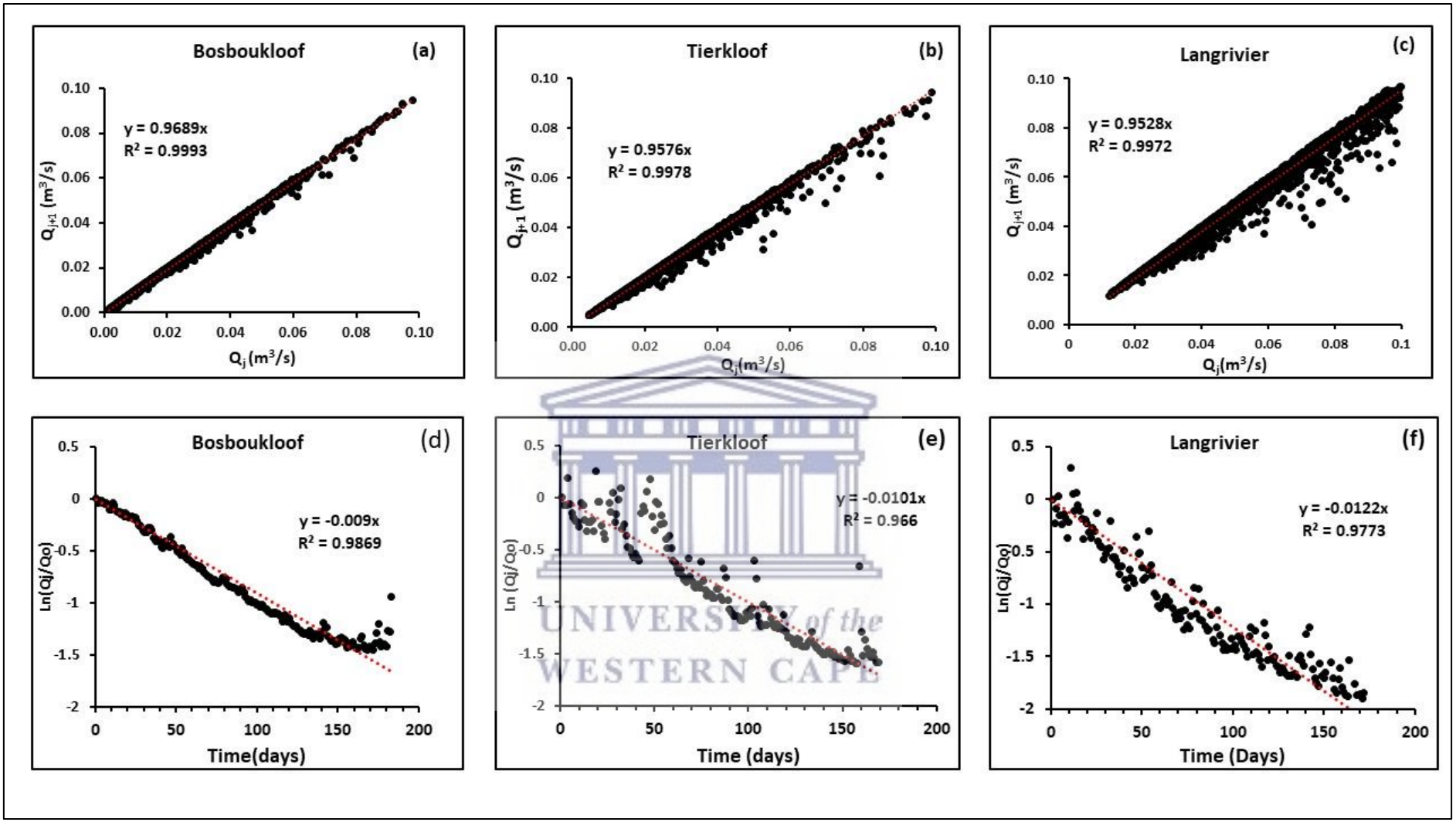

Figure.5.4. Plots of the calculated recession constants for the correlation methods (a) Bosboukloof, (b) Tierkloof and (c) Langrivier. The MRC α (d) Bosboukloof, (e) Tierkloof and (f) Langrivier

Table.5.3. Results of the long-term recession constant *a* for Bosboukloof, Tierkloof and Langrivier. Including the K in days based on the average.

	Recession constant (*a*) from different methods				
	Master recession curve	**Correlation method**	**Mean $(Q_{j+1})/Q_j$**	**Average (*a*)**	**K in days**
Bosboukloof	0.989, R^2=0.95	0.968, R^2=0.999	0.967	0.974	38
Tierkloof	0.986, R^2= 0.97	0.957, R^2= 0.997	0.967	0.971	34
Langrivier	0.987, R^2= 0.89	0.953, R^2= 0.997	0.962	0.967	30

5.4.2.2. The BFI_{max} parameter

The backward-moving filter was used to estimate the BFI_{max} parameters. The results of this estimation process are presented in Table.5.4. The long-term annual values at three study sites were highly variable both spatial and temporally.

The estimated mean annual BFI_{max} value in Bosboukloof was greater compared to Tierkloof and Langrivier (Table.5.4). In Bosboukloof, the mean annual BFI_{max} ranged from 0.61 to 0.99 with an average of 0.89. In the Tierkloof sub-catchment, the mean annual BFI_{max} parameter ranged from 0.56 to 0.79 with a mean of 0.68. The Langrivier sub-catchment exhibited lower BFI_{max} values than those in Bosboukloof and Tierkloof. The annual value ranged from 0.27 to 0.68, with a mean value of 0.54. The coefficient of variation (CV) of the mean BFI_{max} values was < 15 % and showed spatial and temporal variation (Table.5.4). Bosboukloof and Tierkloof had the lowest mean annual CV, 5.44 and 5.40 % compared to Langrivier which was higher with a value of 12.5. The estimated mean BFI_{max} values were used for baseflow separation for all three sub-catchments.

Table.5.4. Estimated long-term BFI_{max} for the three sub-catchments for the analysis period (1946-2019).

		BFI_{max}				
	Period	**Min**	**Max**	**Mean**	**Std.dev**	**CV %**
Bosboukloof	Annual	0.60	0.99	0.86	0.05	5.44
Tierkloof	Annual	0.56	0.79	0.68	0.04	5.40
Langrivier	Annual	0.27	0.68	0.54	0.07	12.5

5.4.3. Calibration of the digital filter parameters and conductivity mass balance

Conductivity mass balance (CMB) or tracer-based hydrograph separation was applied to calibrate the initially estimated BFI_{max} filter parameters. Figure.5.5 and Figure.5.6 shows the results of the comparison between the uncalibrated recursive digital filter (RDF) and CMB method for the three sub-catchments.

5.4.3.1. Comparison of the uncalibrated RDF and CMB method

Table.5.5 presents the comparison of the results between uncalibrated and calibrated digital filter BFI with the CMB method BFI for the sampling days. The estimates of baseflow and quickflow were calculated for the sampling days (2018-2020). Using the original mean estimated BFI_{max} and the averaged recession constant (a) in each study site, the uncalibrated RDF produced higher mean BFI values than the CMB for the sampling days across all sub-catchments. The results of the uncalibrated RDF and CMB methods for Tierkloof and Langrivier were significantly different ($p < 0.05$) (Table.5.5). In contrast, the differences between the two methods were not significant for Bosboukloof ($p > 0.05$). For Bosboukloof, the original estimated BFI_{max} of 0.86 produced a BFI value ranging from 0.65 to 1.0 and a slightly higher mean (0.89) for the recursive digital filter compared to the wider range recorded for the CMB method (0.49 to 1.0, mean: 0.82). At Tierkloof, the mean BFI values for the two methods were different with 0.81 for RDF and a slightly lower value of 0.76 for the CMB method. The range of BFI values for the CMB method was wider from 0.39 to 1.00 compared to the RDF of 0.62 to 1.00. In Langrivier, the difference between the mean BFI value of the uncalibrated RDF and CMB method was large with values of 0.67 and 0.51, respectively. The uncalibrated RDF and CMB methods showed highly variable BFIs for different sampling days, particularly between the high flow and low flow days. The BFI values in Langrivier had a wider range for both methods compared to the other two sites. The BFI values ranged from 0.38 to 1.00 and 0.21 to 1.00 for uncalibrated RDF and CMB, respectively.

In addition, the average baseflow discharge (Q_b) for the sampling days using uncalibrated RDF varied from those of the CMB method, particularly for Langrivier (Figure.5.6). However, the differences between the estimated mean values calculated with uncalibrated RDF and CMB method were small and not significant with p-value 0.431 and 0.852 for all sub-catchments.

The linear regression between the BFI values of the uncalibrated RDF and the CMB method showed no relationship of $r^2 = 0.01$ ($p = 0.026$, n = 25) for Bosboukloof and Tierkloof (Figure.5.5). Conversely, the relationship between the BFI values of uncalibrated RDF and the CMB method for the sampling days in Langrivier showed a positive but weak correlation coefficient of $r^2 = 0.11$($p = 0.325$) (Figure.5.5. e and f). The baseflow discharge showed strong correlations of $r^2 = 0.93$ ($p < 0.05$, n =25) for Bosboukloof, $r^2 = 0.95$ ($p < 0.05$, n= 25) for Tierkloof and $r^2 = 0.77$ ($p = 0.002$, n = 24) for Langrivier. Statistically significant differences were observed between the BFI values for the uncalibrated RDF and the CMB method in both Tierkloof and Langrivier (Table.5.5).

Table.5.5. Summary of the goodness of fit indicators results between the uncalibrated or calibrated recursive digital filter and CMB method daily BFI values, BFI (n=27). Analysis period (2018-2019,2020).

		BFI_{max}	RDF mean BFI	CMB mean BFI	*p*-value	RMSE	R^2	PBIAS (%)
Bosboukloof								
All sample	Uncalibrated	0.86	0.89	0.82	0.164	0.16	0.01	3.2
	Calibrated	0.85	0.83	0.82	0.263	0.19	0.06	1.2
Tierkloof								
All samples	Uncalilbrated	0.68	0.81	0.76	0.042	0.22	0.01	8.8
	Calibrated	0.65	0.75	0.76	0.974	0.27	0.11	9.2
Langrivier								
All samples	Uncalibrated	0.54	0.67	0.51	0.040	0.25	0.101	9.6
	Calibrated	0.40	0.50	0.51	0.971	0.24	0.174	-0.3

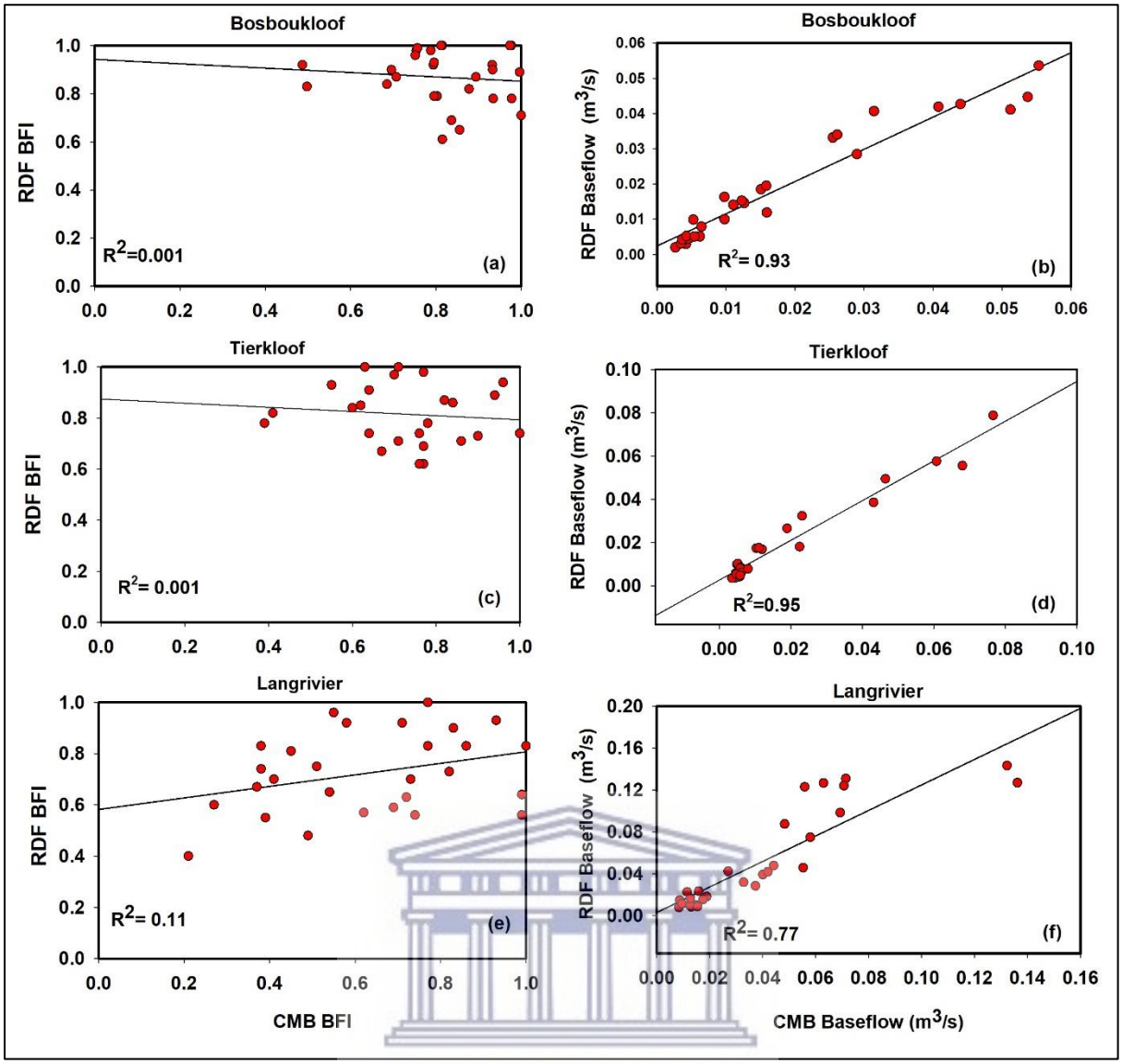

Figure.5.5. Relationship between the BFI/ baseflow discharge estimated uncalibrated Recursive Digital Filter (RDF) and the CMB method for sampling days (2018-2020).

5.4.3.2. Comparison between calibrated RDF and CMB method

The uncalibrated digital filter BFI values were found to be higher than the CMB estimated value across the three study sites (Table.5.5). Attempting to optimize the BFI_{max} parameter using the CMB results, resulted in improvements in the RDF prediction (Figure.5.6). However, no improvement was observed for Bosboukloof where the uncalibrated and calibrated mean BFI values were the same. The RDF estimated mean BFI values across all the sample days improved changing from 0.88 to 0.83, very close to the CMB value of 0.82 (Figure.5.6 and Table.5.5). In Tierkloof the mean BFI estimated using the uncalibrated RDF (0.81) was found to be slightly higher than that of CMB for all sample days. By slightly adjusting the BFI_{max} values to 0.65 from 0.68 the BFI of the RDF were like that of the CMB method. Once calibrated, the mean BFI values for the sampling days were 0.75 for calibrated RDF and 0.76 for CMB. The adjusted BFI_{max} in Langrivier showed significant improvement in the recursive digital filter outputs. By calibrating the BFI_{max} parameter and adjusting the value from 0.54 to 0.40, the

RDF newly estimated mean BFI values were similar to that of the CMB method at 0.50. Once the RDF was calibrated the mean baseflow estimates improvements were significant across the sub-catchments with $p > 0.05$ (Figure.5.6).

The relationship between the BFI values calculated using the calibrated RDF and CMB method for sampled days showed no improvement for Bosboukloof and Langrivier. The coefficient of determination was $r^2 = 0.005$ and $r^2 = 0.18$, respectively. Conversely, for Tierkloof the two methods showed minor improvement from $r^2 = 0.01$ to $r^2 = 0.11$ ($p = 0.432$, n =25). The PBIAS showed improvements, particularly for Langrivier from 9.8 to -0.3 %. The calibrated BFI_{max} values Bosboukloof and Tierkloof showed an overestimation of the baseflow index with PBIAS of 1.2 % and 9.2 %, respectively. Nonetheless, these values were still within the range of PBIAS $\leq \pm$ 10% which can be considered a successful calibration according to Moriasi et al., (2007). However, not many improvements were recorded for the RMSE across the sub-catchments, especially for Bosboukloof and Tierkloof whereby the value showed an increase (Table.5.5). Baseflow discharge estimated using the calibrated RDF was strongly correlated with that of the CMB method for all sub-catchments, coefficient of determination between $r^2 = 0.79$ and 0.99 (Figure.5.7). In general, no significant differences were observed between the BFI values and baseflow for the two methods after calibration for all investigated sub-catchments ($p > 0.05$).

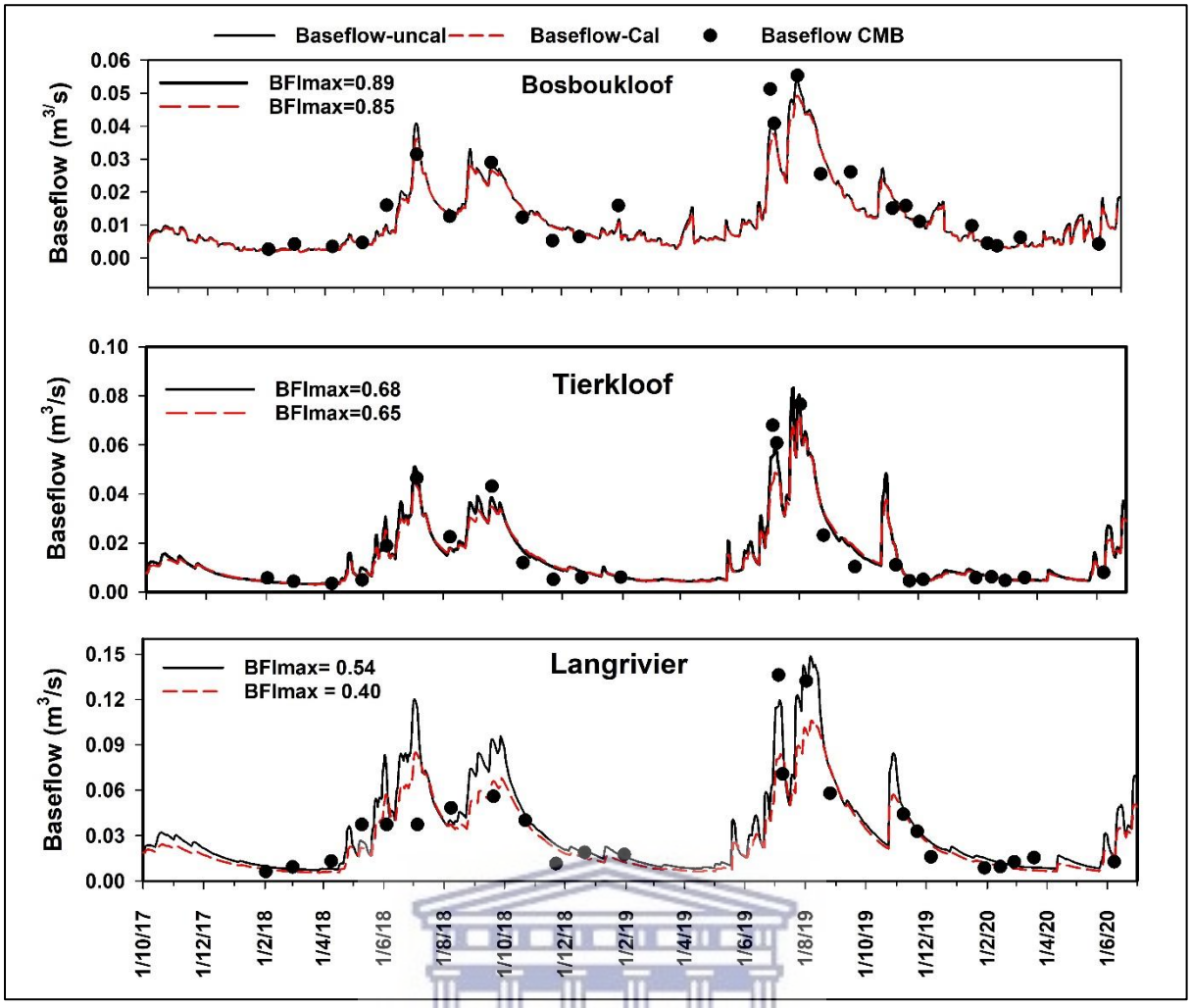

Figure.5.6. Comparison of baseflows discharge on daily basis estimated using uncalibrated digital filter and those based on the use of CMB method. Cal = calibrated, uncal = uncalibrated.

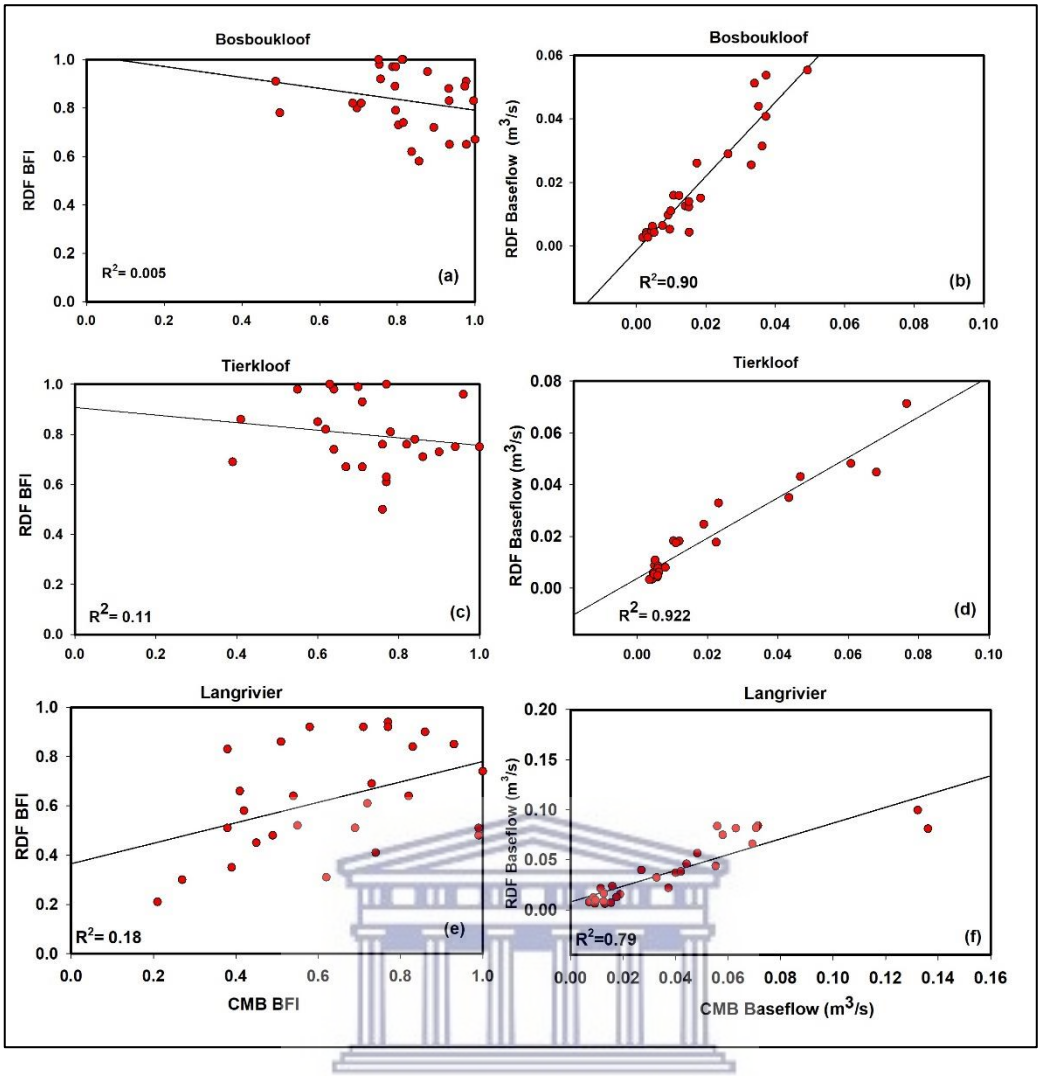

Figure.5.7. Relationship between the BFI or baseflow discharge estimated using calibrated Recursive Digital Filter (RDF) vs CMB method for the sampling days (2018-2020).

5.4.4. Sensitivity analysis of the long-term baseflow estimation

The adjusted filter parameters BFI_{max} for the sub-catchments were applied to compute the daily baseflow estimates for the long-term data (Table.5.7). The results are presented in Table.5.6 shows that both the recession constant (*a*) BFI_{max} influenced the estimated BFI values. However, the BFI_{max} appeared to have a greater impact compared to the recession constant (*a*) and the BFI was more sensitive to the BFI_{max}. The estimated annual BFI values using the uncalibrated RDF were respectively 0.85 for Bosboukloof, 0.63 for Tierkloof and 0.48 for Langrivier. Once the BFI_{max} was calibrated, the annual average in Langrivier decreased from 0.48 to 0.38, whereas minor improvements were observed for Bosboukloof and Tierkloof (Table.5.7). Maximum differences between the uncalibrated and calibrated RDF models were observed for the mean monthly baseflow and BFI values (Figure.5.8 and Figure.5.9). The greatest improvements mean monthly BFI and baseflow discharge were notable in Bosboukloof and Langrivier. The average baseflow discharge values were higher for the uncalibrated RDF especially for the wet winter months of July, August and September and dry summer months January, October,

and November. The average monthly baseflow discharge and BFI values showed minor variations for the dry summer months from February to March (Figure.5.8 and Figure.5.9).

Table.5.6. The sensitivity indices for the original and optimised RDF parameter BFI_{max} for the long-term dataset (1946-2019).

	Uncalibrated					Calibrated			
	(α)	BFI_{max} (β)	S (BFI|*a*)	S (BFI|BFI_{max})	BFI	BFI_{max}	S (BFI|*a*)	S (BFI|BFI_{max})	BFI
Bosboukloof									
Annual	0.974	0.86	-0.28	0.27	0.85	0.80	-0.08	0.09	0.84
Tierkloof									
Annual	0.971	0.68	-0.21	0.12	0.63	0.65	-0.17	0.09	0.60
Langrivier									
Annual	0.967	0.54	-0.29	0.09	0.48	0.40	-0.08	0.05	0.38

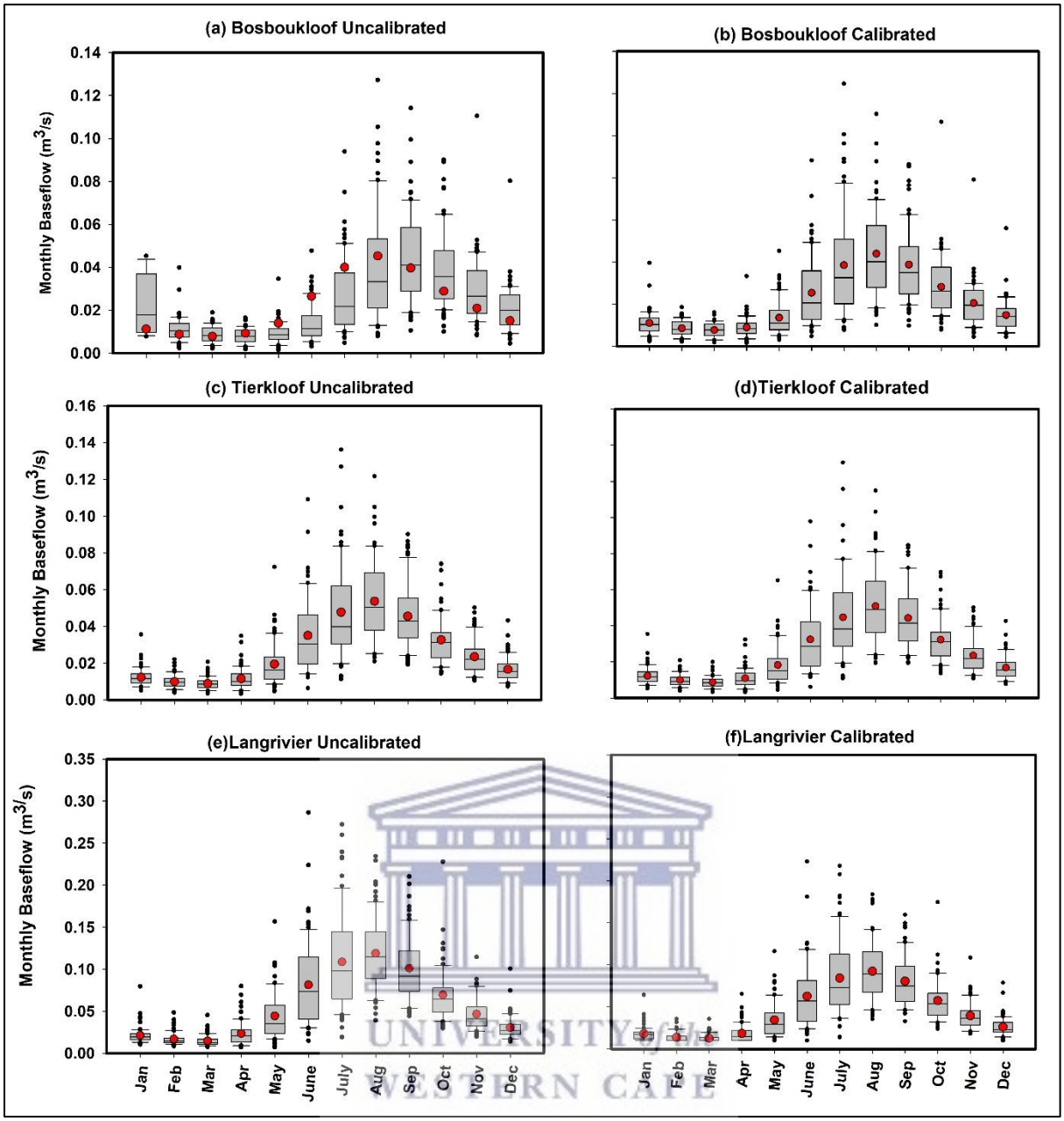

Figure.5.8. Boxplots comparison between the uncalibrated and calibrated RDF for the long-term (1946-2019) average monthly baseflow discharge (m^3/s) for (a,b) Bosboukloof, (c,d)Tierkloof and (e,f)Langrivier.

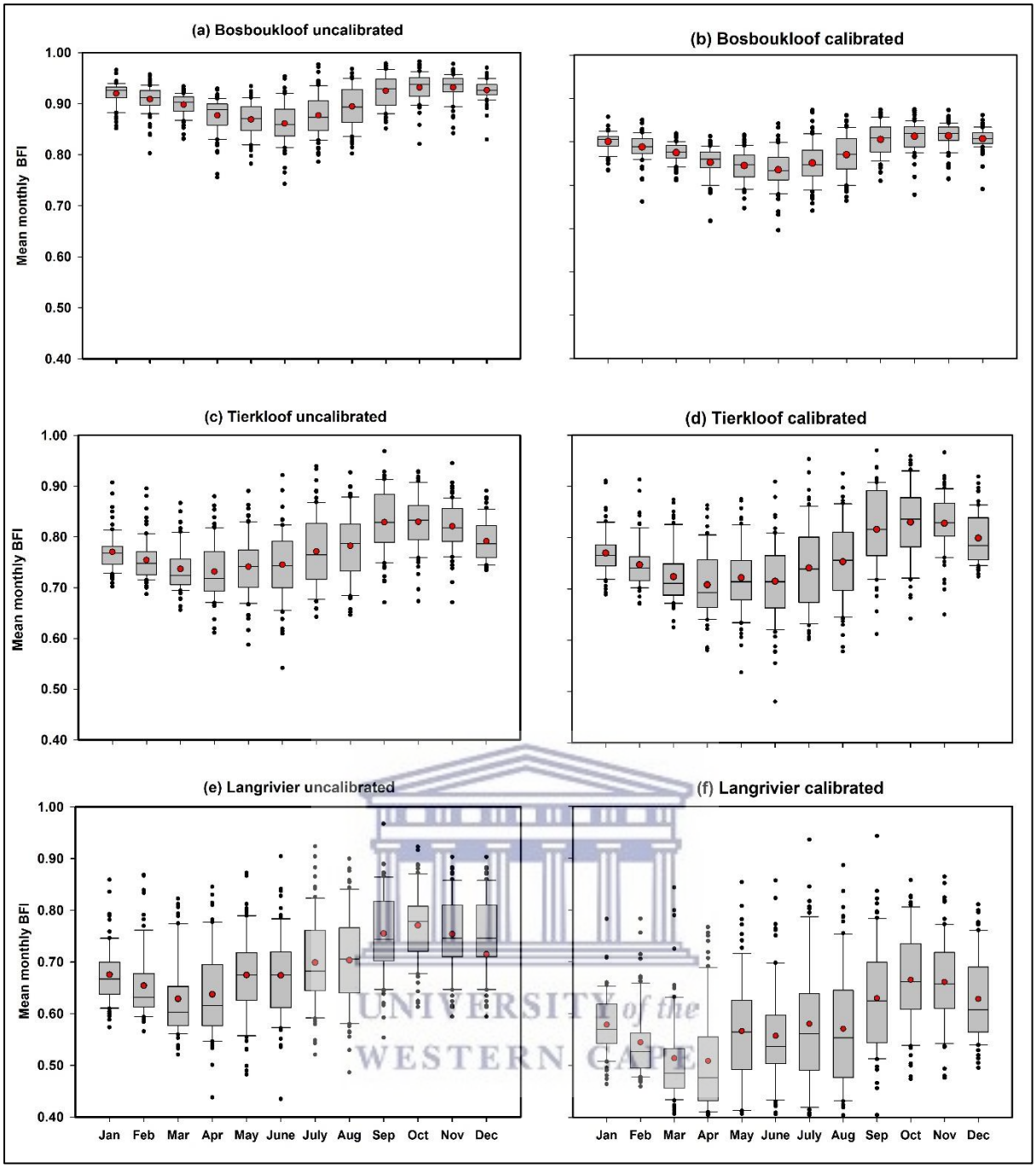

Figure.5.9. Boxplots comparison between the uncalibrated and calibrated RDF for the long-term (1946-2019) average monthly BFI for (a,b) Bosboukloof, (c,d)Tierkloof and (e,f)Langrivier.

5.4.5. Long-term spatial and temporal BFI patterns

5.4.5.1. Annual scale

The results of the calibrated RDF using the long-term daily data were aggregated to monthly, seasonal, and annual average baseflow and quickflow estimates. A detailed list of the long-term seasonal and annual BFI averages is presented in Appendix C, (Table.C.1-3). Figure.5.10 presents the spatial and temporal variations in the estimated mean annual baseflow index. Based on the calibrated RDF model the BFI estimates showed marked spatial variation across all catchments. However, the BFI values showed minor temporal variations, particularly in Bosboukloof when compared to the other site (Figure.5.10). The order of the long-term mean annual BFI values was Bosboukloof > Tierkloof > Langrivier. The range for the BFI in Bosboukloof was small at 0.75 to 0.89 with a mean value of 0.88. At Tierkloof the BFI had a range of 0.55 to 0.64 and a mean of 0.63. In contrast, Langrivier had a wider range of 0.25 to 0.41 with a mean of 0.38 (Appendix C, Table.C.1-3). The *CV* also showed spatial variation in annual BFI at 3.57 % in Bosboukloof, 3.04 % in Tierkloof and 7.02 % in Langrivier. Moreover, no trends were detected in the annual and seasonal BFI values across the sub-catchments.

The average annual baseflow discharge (1946-2019) varied spatially. The highest baseflows were observed in 1977 for all the individual sub-catchments (Figure.5.11). Baseflow discharge showed large fluctuations between high and low flows. The mean annual baseflow discharge was respectively 0.022 m^3/s (423 mm/year) for Bosboukloof constituting 88 % of the total flow. At Tierkloof the mean annual baseflow discharge was 0.025 m^3/s (537 mm/year) with a contribution of 63 % of total flow. Langrivier and 0.045 m^3/s (372 mm/year) with quickflow of 0.074 (920 mm/year) m^3/s which was the highest of all sub-catchments (Figure.5.11).

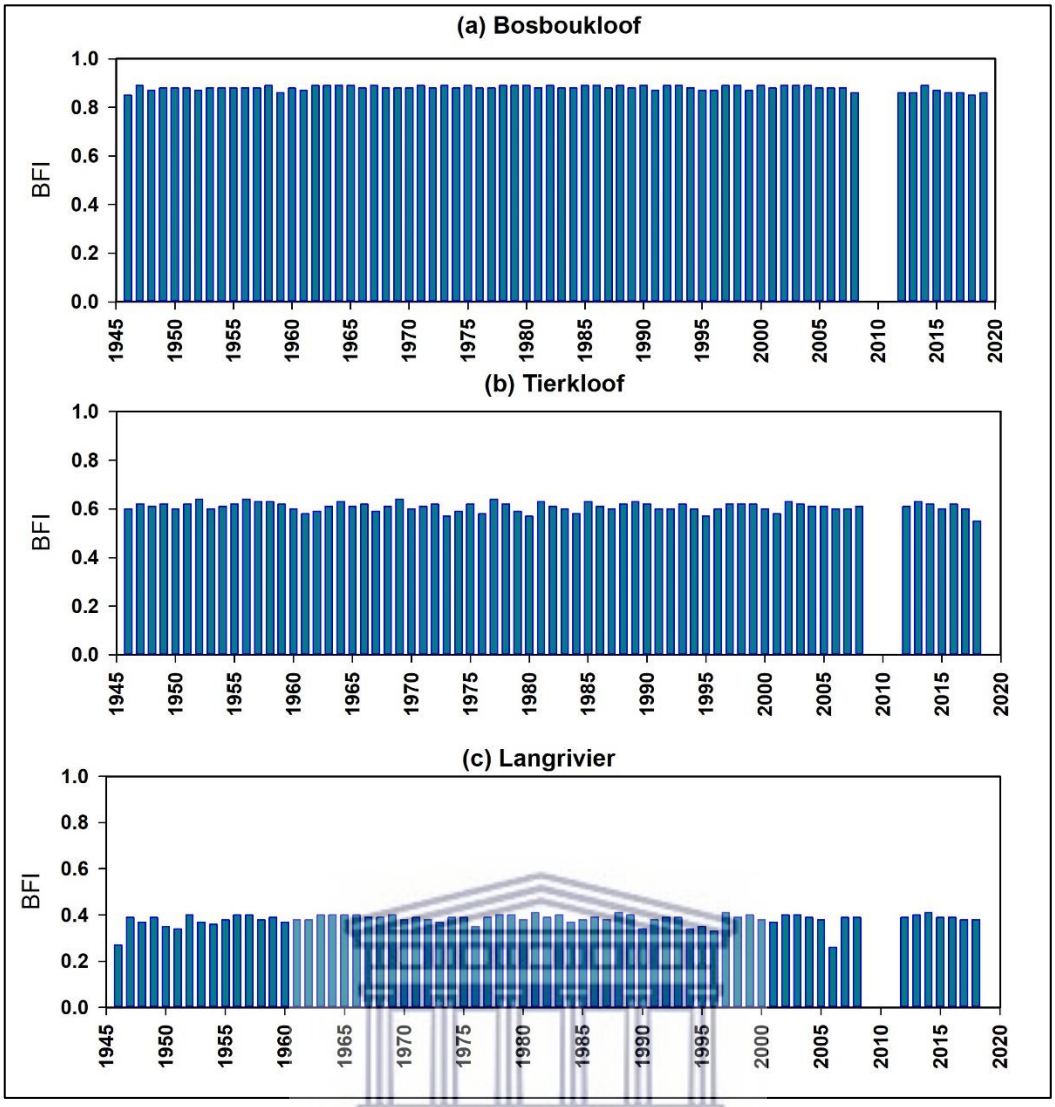

Figure.5.10. Temporal variations in annual BFI estimates based on calibrated RDF method for (a) Bosboukloof, (b) Tierkloof and (c) Langrivier sub-catchments, for the period 1946-2019.

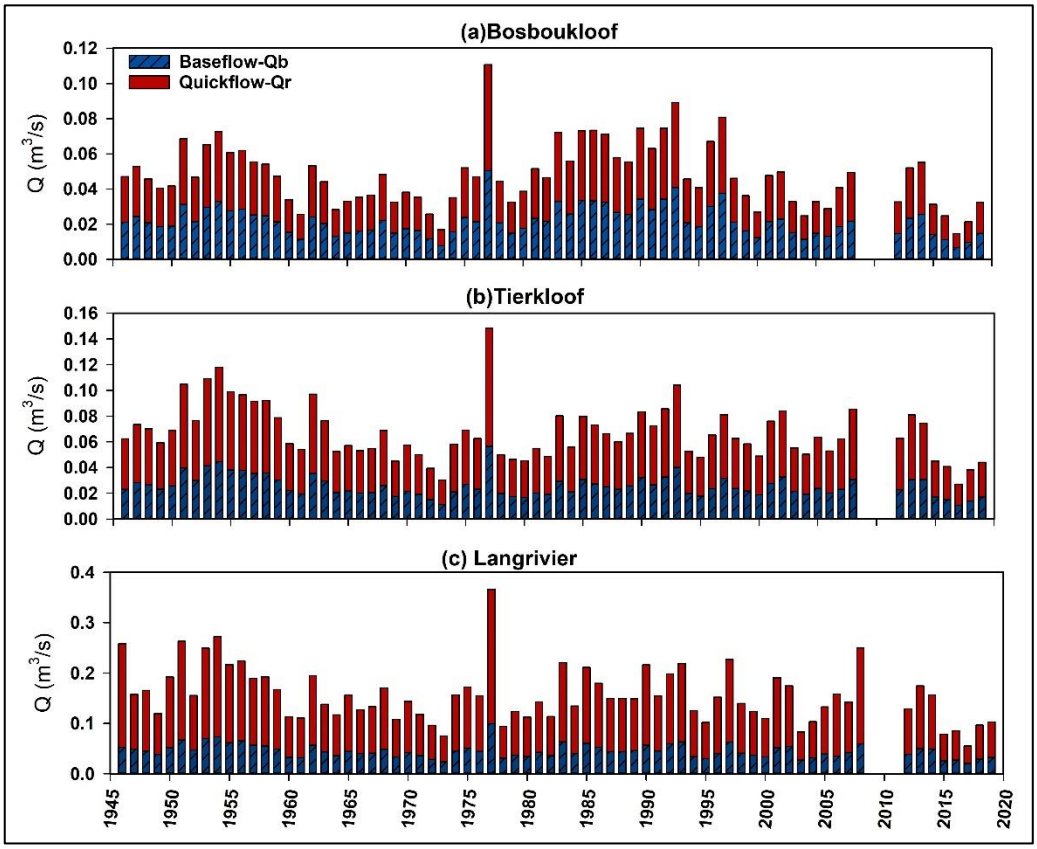

Figure.5.11. Annual variations of quickflows and baseflows discharge (m^3/s) during the 1946-2019 period. Note the scale difference.

5.4.5.2. Monthly and seasonal scale

The long-term average BFI values and baseflow estimates revealed general large spatial variations and seasonality. The dry summer (Oct – Mar) had higher average BFI values relative to the wet winter (Apr – Sep). Minimal differences were found between the annual and the wet winter BFI. Similar to the annual BFI results, Bosboukloof showed the highest seasonal BFI value compared to the other site. In Bosboukloof, the dry summer average BFI ranged from 0.82 to 0.94 constituting 89 % of the total flow (Appendix C, Table.C.1). At Tierkloof the dry summer average BFI had a wider range from 0.44 to 0.82, with a baseflow contribution of about 73 % to total flow. Langrivier had the lowest dry summer average BFI compared to the other sub-catchments, the BFI ranged from 0.37 to 0.62 with baseflow contributions of 50 % total flow. The wet winter average BFI range in Bosboukloof showed minimum variation with that for the dry summer ranging from 0.78 – 0.84, constituting 82 % of the total flow. Conversely, the wet winter average BFI at Tierkloof was lower, ranging from 0.53 to 0.64 contributing 60 % of the total flow. Langrivier had the smallest BFI range (0.22 to 0.38) and the lowest proportion of baseflow of 34 %.

The largest baseflow and quickflow discharge occurred during the wet months of May to September and decreased during the dry summer months from October to March (Figure.5.13). Baseflow peaks were detected during the wet winter months of July and August, which were consistent with the findings of Hughes et al (2003). The lowest quickflow discharge occurred in Bosboukloof followed by Tierkloof,

while Langrivier had the highest quickflow, especially from May to September. The highest average monthly BFI values were recorded from September to March, with baseflow contributions between 84 to 91 % at Bosboukloof, 67 to 75 % at Tierkloof and 48 to 55 % to total flow at Langrivier (Figure.5.12). The lowest average monthly BFI values occurred during the wet winter months from April to August. The decrease in BFI from the high dry summer months values to the low wet winter months values was more pronounced in Tierkloof and Langrivier compared to Bosboukloof. The baseflow contributions to total flow between April and August were the highest at Bosboukloof ranging from 73 to 79 %. At Tierkloof the baseflow contribution to total streamflow during this period ranged from 43 to 60 %. As expected, in Langrivier the proportion of baseflow to total streamflow between April and August was the lowest compared to the other sites, between 24 and 38 %.

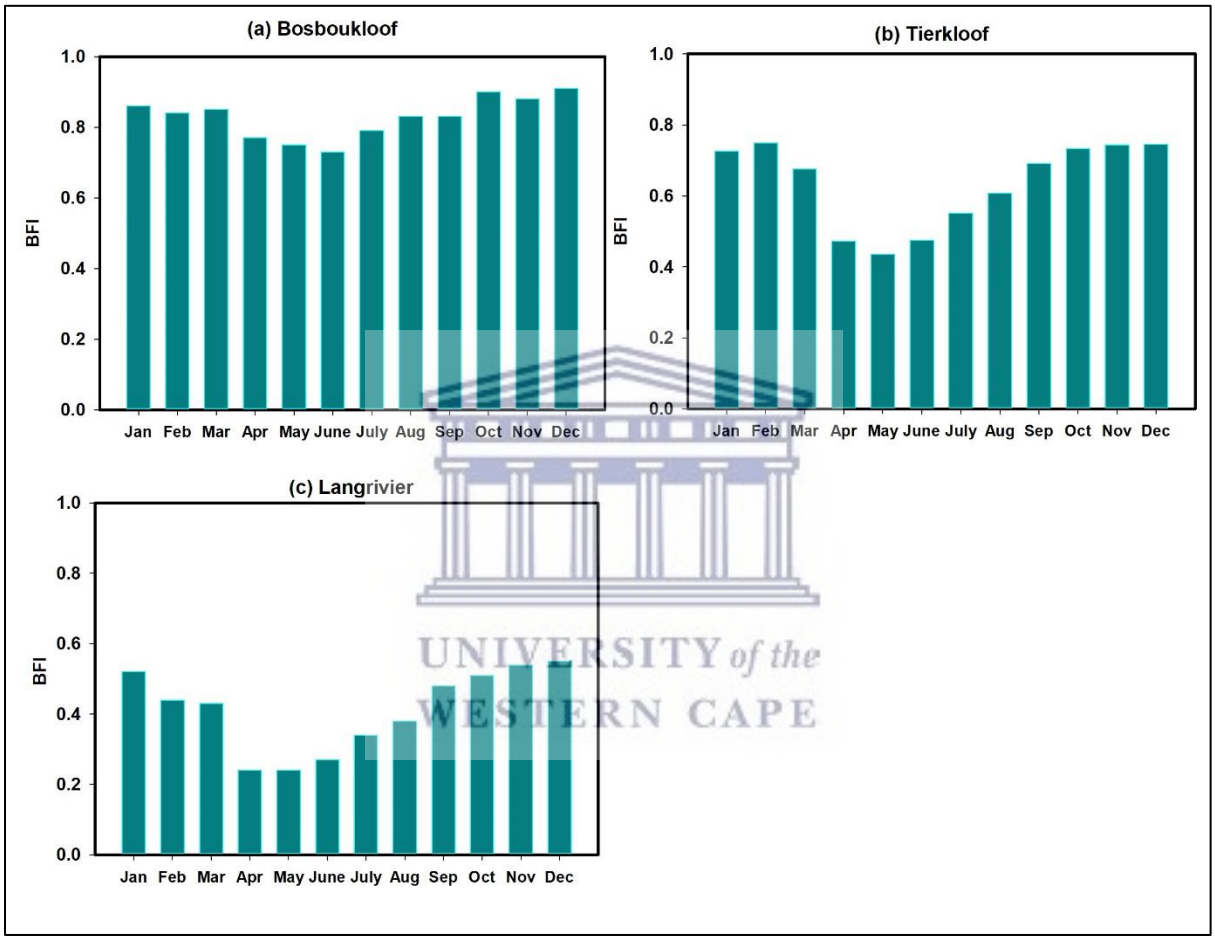

Figure.5.12. Average monthly BFI values during the 1946-2019 period at (a) Bosboukloof, (b) Tierkloof and (c) Langrivier.

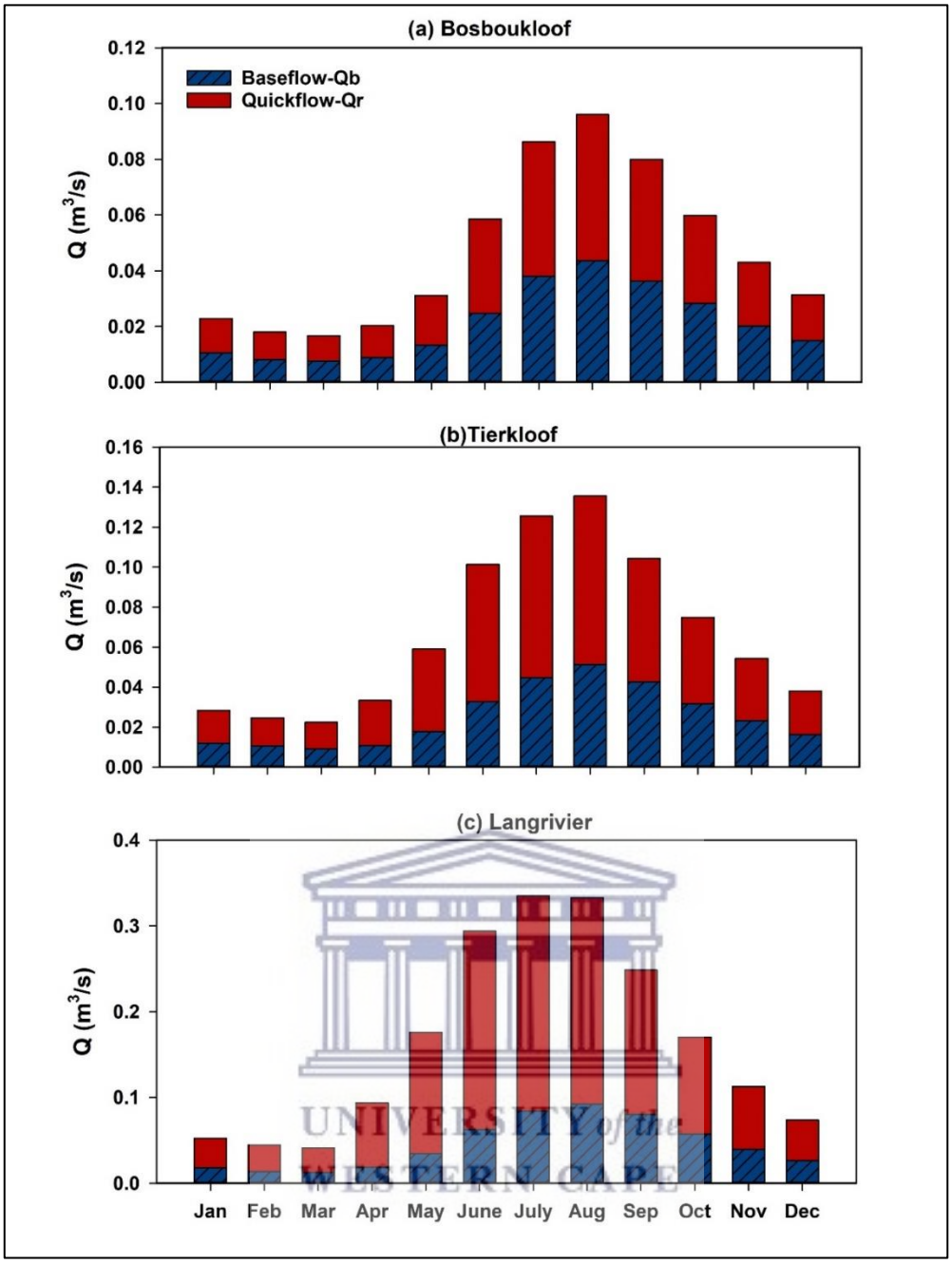

Figure.5.13. Average monthly quickflow (Qr) and baseflow (Qb) based on the calibrated RDF model for the hydrological years 1946-2019 for the three sub-catchments (a) Bosboukloof, (b) Tierkloof and (c) Langrivier. Note the scale difference in Langrivier.

Additionally, the Mann Kendall (MK) statistical test was applied to the long-term BFI data to detect changing trends and Sen's slope (Q) in average monthly baseflow contribution. The MK test results are presented in Table.5.7. Significant decreasing trends were common in June (Z_{MK} = -2.39 to -2.13) across all catchments. Significant decreasing trends were also detected in October and November coinciding with the observed decrease in baseflow and quickflow discharge (Figure.5.13 and Table.5.7). Overall, no statistically significant trends were found for most of the monthly BFIs.

Table.5.7. Results of the Mann –Kendall test for the mean monthly and annual BFI during the analysis period (1946-2019). The bolded letter indicates the significant trends.

Period	**Bosboukloof**	**signific.**	**Tierkloof**	**signific.**	**Langrivier**	**signific.**
Annual	-0.24		-1.07		-0.93	
Summer	-1.84		0.88		-1.76	
Winter	-0.21		-0.77		-0.60	
Months						
Jan	-1.34		-0.26		-0.60	
Feb	-0.70		0.77		0.01	
Mar	-1.23		-0.38		0.05	
Apr	-0.93		0.19		-0.74	
May	0.46		-0.49		-1.37	
June	**-2.29**	*** Decr**	**-2.13**	*** Decr**	**-2.39**	*** Decr**
July	-0.51		-0.05		-0.54	
Aug	0.03		0.54		-0.50	
Sep	0.21		0.85		-1.00	
Oct	**2.35**	*** Incr**	**2.41**	*** Incr**	1.00	
Nov	-0.18		-1.26		**-2.57**	*** Decr**
Dec	-0.19		-0.40		-1.54	

Level of significance: * if trend $\alpha = 0.05$, if no symbol the significance is greater than 0.

5.5. Discussion

5.5.1. The validity of the recursive digital filter and conductivity mass balance methods

The recursive digital filter method (Eckhardt, 2005) was applied to separate the stream hydrograph into the slow and fast components in three sub-catchments. The RDF output of the long-term data showed that sensitivity indices of estimated BFI_{max} were generally lower than that for the recession constant (*a)* see Table.5.6. The absolute value of the sensitivity index for *a* was greater, indicating that BFI is more affected by the recession constant (*a)*. As pointed out by Eckhardt (2011), despite the BFI being more sensitive to the recession constant, the BFI_{max} value is more uncertain, therefore, this uncertainty motivated the calibration of the BFI_{max} parameter. The calibration of the RDF method was obtained by comparing the results of the CMB method with the RDF.

The calibrated BFI_{max} value showed significant improvement in the two-parameter RDF output whereby most of the estimated BFI indexes showed better agreement with the CMB method results (Table.5.5). This was most evident in the Langrivier sub-catchment which showed large differences of nearly 10 % between the calibrated and uncalibrated RDF outputs. However, the goodness of fit analysis showed poor performance between the RDF and the CMB method results, across all sub-catchments. The poor performance of the statistics could be linked to (1) variability in measured EC values caused by dilution and mixing during high flow periods which may sometimes not be accounted for in the digital filter (Longobardi et al., 2019), (2) the relatively sparse and (3) short-term EC data, therefore the temporal variability was not accounted for.

Subsequently, the calibrated BFI_{max} values were used to predict the long-term baseflow across the three study sites. The comparison of the CMB and uncalibrated RDF outputs also showed that the uncalibrated RDF tends to estimate greater BFI values. The largest differences were recorded in Langrivier. This indicates the importance of estimating BFI_{max} value for individual sub-catchment as to applying the suggested values by Eckhardt (2011) for perennial streams and Smakhtin, (2001) for South African catchments. This is critical for baseflow separation considering spatial irregularities of fracturing or weathering of the bedrock; therefore, the system may not be entirely porous across the sub-catchments. Further investigations are required to gain an understanding of the relationship between catchment characteristics and BFI_{max}.

Our findings were in line with those by (Cartwright et al., 2014; Lott and Stewart, 2016; Saraiva Okello et al., 2018; Kouanda et al., 2018), who estimated baseflow using digital filters and conductivity mass balance and found that uncalibrated RDF predicted slightly higher baseflow than CMB. The difference in outputs of the two methods is because the digital filter considers most of the water from delayed sources as baseflow, while the CMB method potentially aggregates most of the delayed transient water stores with surface runoff (Cartwright et al., 2014). The CMB is inherently responsive to the physical and chemical processes and flow paths in the catchment (Miller et al., 2014). Thus, it is important to calibrate the digital filters against the chemical mass balance to improve the results of the hydrograph separation (Stewart et al., 2007; Cartwright et al., 2014; Lott and Stewart, 2016; Kouanda et al., 2018).

In this study, large differences between the estimated and the calibrated BF_{max} were found in Langrivier. This suggests that the RDF method should not be used without calibration as it can lead to uncertainties. This poses a challenge for most catchments that do not have long-term water quality data. However, other RDF methods such as the one-parameter filters (Lyne and Hollick,1979) should be considered where tracer data are not available. Lim et al. (2005) found that both the one-parameter and two-parameter digital filters were highly correlated for 50 gauging stations in Indiana with NSE 0.90. Furthermore, Longobardi et al. (2019) found that the one-parameter digital filter can be accurately calibrated using the recession events during a low flow season in a small (3 km ^{2}), forested and sandstone-dominated catchment. Their results for the calibrated one and two-parameter digital filters were comparable to the mass balance filter and were considered suitable for estimation of the annual baseflow.

5.5.2. Spatial variations of digital filter parameters

The filter parameters exhibited spatial variation across the sub-catchments, particularly the BFI_{max}. Bosboukloof and Tierkloof had higher estimated recession constants (*a)*, while estimates for Langrivier were lower. According to Jia (2007), lower *a* value produces smaller estimated baseflow volumes in the TMG streams. The sub-catchments displayed recession constants ranging from 0.967 to 0.974 which were consistent with those estimated by Jia (2007), but lower than those of Smakthin and Watkins (1997) and Hughes et al. (2003) for South African catchments.

Bosboukloof and Tierkloof showed longer, slower recessions compared to Langrivier. Bosboukloof yielded a longer average recession (k = 38 days) indicating slower drainage, potentially from the deep aquifer and other delayed flow pathways. The slower drainage in Bosboukloof and Tierkloof is likely driven by the shallow slopes covered by a deeper accumulation of scree-talus compared to Langrivier with shallow scree. Chen et al. (2012) observed a similar pattern in Wujiang River, south China showing that slow recessions could represent the steady-state flow from lower permeability media and the geomorphic characteristics of the sub-surface water storage at the valley bottom. A study by Hughes (1997) found that the baseflow recession analysis for most South African catchments could be explained by the type and proportion of the lithologies. The study concluded that the catchments with more than one type of bedrock lithologies may exhibit different structures which can either disrupt or enhance baseflow recession. This may be the case in Jonkershoek which is dominated by fractured granite and shale bedrock and nature may vary in each sub-catchment. Conversely, in Langrivier the fast recession may be due to the influence of the catchment topography on baseflow production e.g.,, the incised drainage dominated by steep channel slopes (41%), low water storage capacity and the highly fractured nature of the bedrock geology in the sub-catchment allows for rapid flow paths that would increase largely during the wet winter and recedes relatively quickly producing the observed steeper recession.

The calibrated BFI_{max} for Bosboukloof closely agrees with the suggested value of ~0.80 (Eckhardt, 2005) for the perennial stream and porous aquifer. Moreover, the calibrated BFI_{max} in Bosboukloof and Tierkloof were also within the ranges of values similar to those estimated by Collischonn and Fan, (2013) of 0.52 to 0.95 for porous aquifers in Brazil dominated by sedimentary packages of sandstones with high permeability and primary porosity. However, the low calibrated BFI_{max} in Langrivier did not agree with those suggested by Eckhardt (2005). The TMG outcrop in this sub-catchment is more exposed compared to the other sites, suggesting more direct flow paths from the upstream to the channel outlet. Thus, the different values imply the influence of other catchment characteristics such as drainage patterns, topography and hydrogeological characteristics (e.g., fractures, degree of bedrock geology weathering). Further study on spatial variability and potential effects of catchment characteristics on BFI_{max} is still required for quantification of baseflow and improved water resource management in this catchment. The results of this study confirm that variations in catchment characteristics should be taken into consideration when defining/estimating filter parameters.

5.5.3. Spatial and temporal variations in baseflow characteristics

Annual BFI

The outputs of the Eckhardt-two parameters digital filtering suggested distinct spatial patterns in the annual baseflow across the sub-catchments (Figure.5.10). However, the temporal variations were minor across the sites, especially in Bosboukloof This indicates that most of the sub-catchments are dominated by sub-surface flow mainly through the fractured TMG bedrock and the scree-soil material (Saayman

et al., 2003). The fractures, faults and steep slopes with thin soils allow rapid transmission of water to the deep sub-surface storage, the deep groundwater is steadily discharged as springs feeding the streamflow during low flow conditions. This was evident in the observed similarities between the TMG bedrock groundwater/springs and streamflow stable isotopes during the dry season as illustrated in Chapter 4 and Mokua et al. (2020).

The variability across the three sub-catchments could be explained by factors such as topography, spatial irregularities in geological structures (e.g fractures) and vegetation cover (Bloomfield et al., 2009; Price, 2011). The sub-catchments with more scree-talus material cover and pine forest, Bosboukloof and Tierkloof, had higher baseflow proportions, than Langrivier, which has a larger area of steep rocky cliffs. The scree-talus is likely to have high infiltration rates and act as a shallow aquifer providing an additional source of baseflow (Harris and Diamond, 2013). Rumsey et al. (2015) reported an association between the soil, slope and baseflow yields in the Upper Colorado River Basin. The PCA analysis showed a strong positive weighting (52%) where sites with greater baseflow yield plotted. van Tol (2020), also showed that catchment hillslope characteristics (slope angle) and rate of evapotranspiration control the duration and magnitude of the sub-surface flows in most South African catchments. Therefore, the deep scree-soil with high water retention and shallow slopes are likely to be the key controlling factors of the magnitude and timing of baseflow in Bosboukloof.

Langrivier had the highest inter-annual BFI variability. The BFI values are in agreement with those of previous studies in the small catchments of the southwestern Cape region of South Africa (Brendenkamp et al., 1995). However, they were higher than those of the quaternary catchments (average scale: 400 km^2) of the TMG outcrop area (Jia, 2007) which ranged from 0.30 to 0.48 and the value of 0.30 estimated for the fractured metasedimentary rock in general (LeMaitre and Colvin, 2008). The low BFI in Langrivier could potentially be explained by the steep topography suggesting that rainfall is likely to be transmitted faster to the stream via both surface flow and preferential pathways through the fractured rock (Hewlett and Bosch, 1984), increasing the proportion of quickflow. The estimated low average annual baseflow contribution in Langrivier agrees with the findings of Madlala et al. (2018) in the nearby Berg River catchment (TMG) for fractured meta-sedimentary catchments of South Africa. However, these estimations were made using different digital filtering techniques i.e., Lynn and Hollick (1979. Therefore, the comparison should be made with caution due to differences in algorithms.

Figure.5.1 and Table.5.1 showed that Bosboukloof generates the lowest mean annual baseflow of 342 mm/year compared to 511 mm/year for Tierkloof and 578 mm/year for Langrivier. This was expected considering the low mean annual runoff (MAR) of Bosboukloof. The higher baseflow volumes in Tierkloof and Langrivier could be attributed to their larger TMG outcrops and higher rainfall amount in the upper steep areas of this catchment, leading to higher mean annual precipitation. Santhi et al.(2008) found that landscape characteristics such as relief and gradient are highly correlated with BFI (R^2 = 0.79) and baseflow volume (R^2 = 0.93) in small catchments (200 km^2) in the US, respectively.

High baseflow was also found to be correlated to the amount of rainfall. Considering landcover, a positive relationship between BFI and pine forest area was reported by (Pramono et al., 2017) in the Kedungbulus sub-watershed (Indonesia), who found that higher BFI (0.75) was associated with a pine forest area of 75 % while pine forest area of 43% produced lower BFI of 0.55. However, when considering baseflow volume, Price et al. (2011) found a positive correlation between higher forest cover and lower baseflow, which was attributed to the high evapotranspiration and infiltration rates of the forest. This could be the case in the Jonkershoek where the afforested Bosboukloof and Tierkloof had a low baseflow volume compared to the non-afforested Langrivier. The infiltrating water is likely to recharge the high draining scree-cover and shallow weathered bedrock, and the pines tap into this groundwater, reducing baseflow.

Annual BFI values showed only minor temporal variations, with Bosboukloof and Tierkloof showing the least variability (Figure.5.11). Baseflow is consistently a major component of streamflow in these sub-catchments. Langrivier on the other hand had a higher proportion of quickflow. These results could be viewed as a contradiction to previous research, as peak flows during storm events in this catchment have shown to be dominated by "old water' (e.g., Midgley and Scott,1997; Mokua et al., 2020). These findings indicate that the quickflow may include rapid sub-surface flows from the shallow weathered zones that push older stored water into the stream. Therefore, the assumption that rain chemistry represents quick flow may not be a good fit for this site, hence the poor correlation between CMB and RDF.

Monthly Baseflow Index

Similar to the annual BFI estimates, these values exhibit large spatial variation and seasonality. All three sub-catchments had higher proportional contributions from baseflow in the dry summer (Oct-Mar) compared to wet winter (Apr-Sep), as expected given the seasonality of rainfall. Baseflow peaks were detected during the wet winter months of July and August but over 50 % of the dry season flow was attributed to baseflow (BFI > 0.5). According to Kelly et al. (2019), the high BFI indicates permeable catchment conditions, whereby the catchment water is stored during the wet season and is discharged to the streams during the dry season. Also, the drier antecedent conditions could have resulted in lower quickflow generation during episodic summer events, which would increase BFI. In Bosboukloof and Tierkloof, the pines have been found to have impacted the dry season flow to a greater extent compared to the annual and wet season runoff, potentially due to high evapotranspiration rates (Scott et al., 2000).

The larger baseflow volume during the wet season months (July-Sep) indicates wetter antecedent conditions in the scree-soil cover below the TMG and likely lower evapotranspiration (ET) from both pines and fynbos. As a result, the more quick flow was generated by the steep upper catchment areas during the wet season, hence lower BFI. This is consistent with other research that suggests catchment wetness and/or water storage capacity is an important control on baseflow (Yao et al., 2021). The high

BFI observed during the dry season across the sub-catchments indicates the importance of baseflow in maintaining dry season flows.

5.5.4. Implications on the water resources management in the TMG aquifer regions

Information on the magnitude and characteristics of baseflow contributions to streamflow within the TMG catchments is fundamental for the development and validation of catchment hydrological and climate models (Van Wageningen and Du Plessis, 2007; Du Plessis and Schloms, 2017). The models are used in decisions support for policymakers and water managers to ensure sustainable development of water resources in the Cape region under the changing climate and environment. Moreover, the use of hydrochemistry provided important additional information on flow pathways that can be used to parameterize and calibrate hydrological models, especially rainfall-runoff models (Birkle and Soulsby 2015; Piovano et al., 2019).

The results observed for Bosboukloof and Tierkloof were relatively higher than those of the previous studies in the TMG geological area (Hughes et al., 2003; Jia, 2007; LeMaitre and Colvin, 2008; Madlala et al., 2018). The variation may be attributed to the difference in storage (LeMaitre and Colvin, 2008), land use/cover (Wang et al., 2014), bedrock geology (Longobardi and Villian, 2008) and topography (Price, 2011). The baseflow estimates in Langrivier were in close agreement with those of the previous studies in the TMG outcrop areas (Jia, 2007; LeMaitre and Colvin, 2008; Madlala et al., 2018) implying similar catchment characteristics. For example, Langrivier is characterized by steep topography, in combination with the bare slopes and indigenous vegetation cover which can be considered one of the common features in most TMG outcrop areas.

The comparison of BFIs is generally not recommended across studies as different baseflow separation techniques will provide different estimates. These algorithms may define baseflow and the quickflow components differently. Considering that the application CMB method integrates variability in the flow paths and the heterogeneity in catchment properties compared to the digital filters. The results of this study could potentially be extrapolated to other TMG geological with similar characteristics. The calibration of the digital filters provided important insight into the catchment processes. However, it is recommended that other tracer-based methods including stable isotopes and major ions besides those considered in this study should be evaluated. Tracer-based may provide accurate information on chemical signatures of water sources and provide reference to calibrate the non-tracer-based baseflow separation methods for future studies.

5.6. Conclusions

The direct measurement of the baseflow component within a catchment is difficult, making the accuracy of different baseflow separation methods problematic. This study applied the two-parameter Eckhardt digital filter method and the conductivity mass balance method using EC measured over two years to estimate baseflow in three sub-catchments. Firstly, the long-term streamflow (1946-2019) was utilized

to estimate the values of the filtering parameters and secondly, the short-term EC data (2018-2020) was used to test and calibrate these parameters. The analysis showed that the estimated BFI values using digital filter parameters were sensitive and the uncalibrated RDF produced higher baseflow estimations compared to the CMB method. The application of the CMB method as a constraint to calibrate the filter parameters improved the baseflow estimates, and calibrated RDF baseflow index values were in closer agreement with the values CMB method. However, while the two methods produced similar average baseflow estimates, the correlation remained low. The dominant contribution of 'old water' even in storm responses has been observed in these streams (Midgley and Scott, 1994).

RDF outputs indicated spatial variations in annual and monthly BFIs across the sub-catchments. This is likely to be a function of several factors such as the heterogeneity in bedrock geology, topography and vegetation cover across the sub-catchments. The results suggest that more than half the annual and summer streamflow in Bosboukloof and Tierkloof is derived from baseflow. Although Langrivier's flow was dominated by quickflow, baseflow accounted for half of the flow in summer on average. This highlights the importance of baseflow in sustaining the streamflow during the dry season in the Jonkershoek catchment. The seasonal variability shown in the monthly BFI and baseflow amounts can be attributed to low rainfall and high ET rates during summer. The results demonstrate that a high degree of variability can exist in the contribution of baseflow between neighbouring headwater streams, likely linked to catchment geomorphic characteristics and land cover. Further evaluation of how streamflow responds during events is required to provide more insight into the spatiotemporal variations of hydrological processes particular those related to runoff generation including surface-groundwater interactions.

The findings showed that CMB is an effective and inexpensive tool to estimate baseflow, however, its application was limited by the lack of high-frequency EC data in this case. Even though the CMB method proved to be suitable for RDF calibration, EC can provide challenges and may not be a suitable calibration tracer for some catchments with low concentrations and short data sets which may lead to uncertainties in the mass balance methods and calibration of the RDF. Therefore, we recommend that the CMB method should be accompanied by uncertainty analysis to improve the resulting BFI estimations. Nevertheless, the finding indicates that the incorporation of digital filter and CMB methods may generate more reliable baseflow estimates than RDF alone, although long-term and high-frequency monitoring of tracer data is recommended for future research. Overall, the results improved the understanding of baseflow characteristics in a TMG catchment. This study could form a base for future research on the baseflow characteristic in the TMG and it can contribute to informed water resources management, especially when it comes to determining the possible implications of climate and land use change.

CHAPTER 6: STORM EVENT RUNOFF GENERATING PROCESS BASED ON HYDROGRAPH SEPARATION METHODS IN TWO HEADWATER SUB-CATCHMENTS.

This chapter characterizes runoff generation processes based on the combination of tracer-based hydrograph separation and hydro-meteorological observations during a winter storm event in 2019. The case studies were two adjacent sub-catchments of the Jonkershoek catchment namely, Bosboukloof and Tierkloof. The two- and three-component hydrochemical and isotope hydrograph separations are applied to identify runoff components, and evaluate the relative contributions of different geographic and temporally defined water source end-members during a storm event to explore likely flow pathways. The end-member mixing analysis (EMMA) is employed to identify end members. The results of the hydrograph separation for the event were translated into conceptual models for the respective sub-catchments.

6.1. Introduction

A sound understanding of catchment internal processes, in particular, runoff generating processes is important for the predictive capabilities of hydrologic modelling, and conceptualisation under different conditions. This will allow for better parameterization of hydrological models used for the conservation and management of surface water and groundwater resources in mountainous headwater catchments (Wenninger et al., 2008). This knowledge is essential for the evaluation of critical issues regarding water availability and sustainability for socio-economic purposes and ecological needs (Genereaux and Hooper, 1998; Uhlenbrook et al., 2002). This is crucial in semi-arid and arid, and Mediterranean-type climate regions which are naturally prone to droughts and floods as a consequence of several global change drivers (Bougharioua et al., 2014; Misra, 2014).

Accurate quantification of water resources and allocation critically depends on a sound understanding of runoff generating processes and water flow pathways in a catchment (Camacho Suarez et al., 2015). Hydrograph separation techniques using stable isotopes and hydrochemical tracers have resulted in major advances in the understanding and conceptualizing of runoff generation mechanisms in many mountainous catchments across a range of climatic conditions during storm events (Hoeg et al., 2000; Uhlenbrook et al., 2002, 2004; Mul et al., 2008; Penna et al., 2015). The technique integrates tracer and hydrometric measurements into hydrograph separation and can allow estimation of residence time, identifying flow paths and runoff components as well as the relative contributions (Klaus and McDonnell, 2013; Camacho Suarez et al., 2015; Penna et al., 2015). However, the use of these approaches in the arid and semi-arid regions of Sub-Saharan Africa, particularly in South Africa is still limited. These techniques have not well been assessed in fractured rock geology such as in the Table Mountain Group (TMG) catchments. This is due to the lack of financial resources to build proper monitoring infrastructure, maintenance of equipment and physical access to sites (Mazvimavi, 2003).

This challenges the acquisition of climatic and hydrometric datasets to cover the right Spatio-temporal of catchment characteristics (Tekleab, 2015).

Tracer studies in the Jonkershoek in particular stable isotope and hydrochemistry revealed large spatial and seasonal variability of stream water sources and flow pathways in baseflow (Mokua et al., 2020). Further analysis of baseflow separation showed that the total streamflow is dominated by sub-surface flow and minor quickflow in some sub-catchments while others were dominated by quickflow (see Chapter 5). The variations of components and flow pathways were linked to the differences in catchment physiographic characteristics. Similar observations were made in other headwater catchments across the world (Soulsby et al., 2004; Didzun and Uhlenbrook, 2008; Blöschl et al., 2013). Didzun and Uhlenbrook (2008), used hydrochemical analysis to investigate the dominant runoff processes during six events in catchments from 0.015 km^2 to 250 km^2 in Dreisam catchment, southwest Germany. They reported that most of the observed differences in hydrological could be related to changes in topography and other catchment characteristics (e.g., soil, land use, geology).

Several studies have demonstrated that runoff generation processes can vary spatially and temporally and are affected by catchment properties, suggesting that mechanisms at the hillslope scale, flow pathways and flow path length may vary from those at the catchment scale. In some cases, at a hillslope scale, runoff generation is controlled by sub-surface structures, surface topography and vegetation cover. The sub-surface structures promote preferential flow pathways, and surface topography such as steepness, soil and vegetation cover which influence effective rainfall input. In contrast, at the catchment scale, factors such as structural elements (e.g., size of contributing area and storage), landscape organization, geology and stream characteristics such as river incision and drainage density play a major role in controlling runoff generation (McGlynn et al., 2004; Camacho Suarez et al., 2015; Sun et al., 2017).

In the TMG area, Moon and Dardis (1998) cited in Roets et al. (2008) identified the underlying geological structure and drainage patterns of rivers as controlling factors of streamflow generation. A conceptual model by Roets et al. (2008) indicated that runoff generation mechanisms in the TMG outcrop areas vary spatially (i.e., from headwater to low reaches) and temporally (i.e., low and high flow periods) and that sub-surface flow processes play a major role in runoff generation all year round. The conceptual model suggests that runoff is controlled by geological features such as fracture networks and the weathered bedrock zone which serves as a reservoir that stores water during the rainy season. These authors concluded that groundwater flow, shallow sub-surface flow (i.e., interflow, translatory flow), and surface runoff were the dominant processes. The analysis of stream water sources in the Jonkershoek revealed two deep groundwater sources namely, the granite/shale and the TMG bedrock groundwater. However, it was found that most of the streamflow is sourced from the TMG bedrock, and the tracer data could not reveal the hydraulic connectivity between the stream channel and granite/shale groundwater (see chapter 4, Mokua et al., 2020). Furthermore, according to Versfeld

(1981) and Hewlett and Bosch (1984), overland flow plays a minor role in stormflow production in the Jonkershoek and is of minor importance in the mountain catchments of the fynbos biome.

Interflow is considered the key component and accounts for most of the baseflow in the TMG mountainous catchments favoured by the geomorphologic and hydrogeological conditions of the catchments (Xu et al., 2003). The process can occur in several ways which include impermeable soil horizons hindering downward percolation of water, fractured zones, partially saturated flow formed via a perched water table and preferential flow paths in soils (Xu et al., 2003). The role of interflow as the major streamflow generating component in the Jonkershoek sub-catchment was illustrated by Mokua et al. (2020). The tracer study found that streamflow interflow including ephemeral and perennial TMG springs was the main contributing source of streamflow during the wet and dry seasons.

Past investigations in the Jonkershoek and other TMG outcrop areas revealed two components, delayed subsurface flows and direct runoff (which includes overland flow) (Britton, 1993; Midgley and. Scott, 1994; Bugan et al., 2012). The findings of Midgley and Scott, (1994), sampled isotopes in headwater streams of the Jonkershoek catchment during six events. The isotope hydrograph separation suggests that stormflow was dominated by "old" water, with "event water" accounting for 8.5% or less of the stormflow across the catchment. They concluded that stormflow in the catchment was dominated by rapidly displaced "old water". The "pre-event/"old " water refers to the water present in the catchment before the rain event, which consists of soil water and groundwater, while "event" refers to rain falling during a storm or event of interest. water (Sklash and Farvolden, 1979). However, their study only investigated time-source (i.e., event and pre-event water) components and did not look further into geographic sources (e.g., groundwater flow, perched saturated flow etc). Therefore, this study will add geochemical tracers to examine possible geographic source contributions and to account for additional runoff components during a storm event.

Britton et al. (1997), studied the hydrochemical (pH, HCO^{-}_{3}, Cl^{-}, PO_4^{3-} -P, NO^{-}_{3} –N and TDS) response during 4 storm events in Swartboskloof tributary to the Jonkershoek and found that, during winter storms, runoff predominantly resulted from direct runoff, whereas, during the summer storms, delayed interflows were dominant. Bugan et al. (2012) used stable isotopes and a water balance model to perform hydrograph separation in Sandspruit, a low rainfall catchment located within the larger Berg River dominated by the TMG geology, and they concluded that streamflow was driven by interflow from the soil horizon which accounted for 94.68 % of total and overland flow accounted only 4.92 %, with a minimal groundwater contribution. They further stated the streamflow is more dependent on the temporal distribution of rainfall rather than the annual rainfall volume which was supported by the poor correlation between the average rainfall and annual streamflow. The current study will build on this existing literature and theories/concepts from hydrological process understanding in the TMG.

Based on the above literature review, published work on runoff generation in the TMG aquifer catchments can be considered scarce, especially given the diversity of findings over the few studies that

have been conducted. There is a need to further understand factors controlling runoff generation, particularly during storm events. Little work exists thus far on the integrated application of hydrometric data and with environmental tracers (stable isotopes and hydrochemical parameters) to examine sub-surface flow paths and differentiates sources contributing to streamflow in this region (Saayman et al., 2003). Hence testing the suitability of these techniques may contribute to resolving some of the existing questions. The existing questions are,

(i) Are the chemistry and stable isotopes different enough to distinguish between the different end-members, especially the different aquifers?

(ii) do the storm runoff components and their relative contributions vary across the neighbouring TMG headwater catchments?

To provide a better understanding of the spatial and temporal mechanism of stormflow generation, rainfall-runoff processes (i.e., how the water moves within the sub-catchments during rainfall events), were investigated during a winter storm event. To achieve this aim, integrated analysis of isotopic, hydrochemical, hydrometric and meteorological data was applied to address three objectives: i) to identify and quantify runoff generating components in two headwater sub-catchments using hydrograph separation based on steady-state mass balance equations of water and tracer fluxes, ii) to understand how streamflow components vary in response to rainfall events across the two sub-catchments with different vegetation and geomorphology, iii) to develop a conceptual model of the catchment response to the event,(iv) test the suitability of tracer-based hydrograph separation techniques in small headwater sub-catchment in the TMG.

6.2. Study site

The study was conducted in Bosboukloof and Langrivier see Figure.2.1.The two sites were selected due to the heterogeneity in their landscape, hydroclimatic factors (rainfall and discharge), hydrochemistry and land cover as shown by Mokua et al. (2020), as well as the easy access to install monitoring equipment at the sampling sites. These study sites exhibit large spatial variations in rainfall and streamflow which are influenced by topography, geology and land use (Wicht, 1934; Mokua et al., 2020). The variations in hydrometric and hydrochemistry between these sub-catchments were demonstrated in the previous chapter (sections 4.3.2 and 4.3.3).

The average daily flow for 2019 in Langrivier was 0.072 m^3/s higher compared to 0.014 m^3/s for Bosboukloof with a relatively quick storm response compared to the slow response compared to Bosboukloof. The perennial springs from the TMG fractured sandstone aquifer contribute to the stream discharge throughout the year. However, streamflow is highly seasonal with the highest flows occurring during the winter season (Table.6.1). Furthermore, spatial variations in streamflow hydrochemistry and isotopic ratios ($\delta^{18}O$ and $\delta^{2}H$) were reported by (Mokua et al., 2020). Bosboukloof has relatively high EC, Na and Cl concentrations compared to Langrivier which has concentrations similar to those of the

TMG springs (Figure.4.12 and Table.4.5). The streamflow in Bosboukloof is isotopically enriched relative to those in Langrivier (Mokua et al., 2020).

As illustrated in **Chapter 2**, the geology of the two study sites does not vary much. The actual area of the granites in most of the sub-catchments does not exceed 133 km^2 (Fry, 1987). The upper part of the catchment is capped by a thick sedimentary succession of highly deeply fractured quartzitic sandstones of the TMG Peninsula Formation. However, the weathering and erosion of the TMG outcrop across the catchment resulted in the exposure of the bedrock granites and shale, especially in Bosboukloof. The slope cover in Bosboukloof comprises permeable talus scree material made up of sandstone clasts and containing granite fragments that also filled the streambeds (Fry,1987; Söhnge, 1988). In contrast, slope cover in Langrivier comprises poorly developed shallow soils with a mix of weathered granite, sandstones and shale debris. More details on the study sites are provided in **Chapter 2**. There are no major alluvium deposits or floodplains in the sub-catchments.

Table.6.1. Summary of hydro-meteorological characteristics of the study sub-catchments for the hydrological year 2019. Mean Annual rainfall (P), mean annual runoff (Qt), and annual temperature (T).

Sub-catchment	Area (km^2)	P (mm/a)			Qt (mm/a)			T (ºC)
		Total	Summer	Winter	Total	Summer	Winter	
Bosboukloof	2.00	1168	235.0	932.3	278	83	196	16.8
Langrivier	2.45	1364	354.2	1024.7	968	197	771	17.8

6.3. Material and methods

6.3.1. Hydrometric and soil data monitoring

For this study, at least 3 storm events sampling was planned which includes a summer event sampling to investigate runoff generating processes between 2019 and 2020. However, due to several issues which include the COVID19 pandemic lockdown, logistical limitations and finance this aim could not be achieved. Also, the rainfall intensity (> 2 mm/h) and timing anticipated for the summer event in 2019/2020 were not sufficient to allow event sampling as proposed by Munoz-Villers and McDonnell (2012). Therefore, a single rainfall event was investigated during the rainy winter season of 2019. The monitoring period was carried out during the winter period from the 5^{th} to 9^{th} July 2019. The sampled rain event occurred on the 6^{th} - 7^{th} July. According to Muñoz-Villers and McDonnell, (2012), an individual rainfall event is defined as a period with more than 0.2 mm of rainfall separated from other events by at least three hours with no rainfall. Under this definition, the sampled rain event lasted approximately 12 hrs. Streamflow was measured by a 90º V-notch gauging weir located downstream in each sub-catchment outlet at 10-minute intervals during the event. Rainfall amounts were measured with tipping bucket rain gauges, model TR-5251 (Texas Electronic Inc, USA) located near the weirs at hourly intervals with a resolution of 0.25 mm. A more detailed description of the monitoring

instruments in this catchment is provided in Chapter 4 and also by (Slingsby et al., 2021). Rain gauges 11B in Bosboukloof and 8B in Langrivier were used for the analysis as they were close to the weirs and had complete data (Figure.2. 2 and Figure.2.4).

Shallow groundwater levels were measured in a piezometer located downstream (370 mamsl) near the weir using a pressure transducer (Level logger model 3001, Solinst Canada Ltd) paired with a barometric logger to compensate for atmospheric pressure (Barologger, Solinst Canada Ltd). Additionally, groundwater levels were measured from two boreholes (BH1 and BH3) at 30 minutes intervals using pressure transducers similar to those installed in the piezometers. However, water chemistry at these boreholes could not be manually sampled during the rainfall event as they are located outside the catchment, > 5 km distance from the weirs and could not be easily accessed. The boreholes are located at different elevations with varying geological formations, BH1 is located upslope (280 mamsl) within the highly weathered and fractured granite and shales, whereas BH3 (224 mamsl) is located within the floodplain comprising of alluvium underlain by weathered granite bedrock along the main Jonkershoek River as illustrated in Figure.4.1

Soil moisture was recorded as volumetric water content (VWC) at each sub-catchments at hourly intervals. Each site was equipped with five (5) ECH$_2$O EC-5 (dielectric aqua sensor) soil moisture probes (Decagon Devices, Inc., USA) installed at different depths 30 cm apart (15 to 145 cm) along the streambank, ~ 5 m from the channel. According to the manufacturer, these sensors have an accuracy of ± 0.03 m^3/m^3 for mineral soils and ±0.02 m^3/m^3 for any porous medium. The sensors were calibrated according to the specific soil types in each sub-catchment. The soil moisture data from 14 April 2019 in Bosboukloof was missing due to the vandalism of the data logger. Also, the probes at a depth of 145 cm in Langrivier failed, resulting in missing data from April 2019 onwards including the sampled period. Hence this compromised the estimate of the antecedent soil moisture at this depth

6.3.2. Sampling

Rainfall, shallow sub-surface water from piezometers, groundwater, and spring and stream water was sampled for tracer concentrations (Table.6.2 and Figure.4.1). For pre-event (baseflow/low flow) conditions (05. July 2019), samples were collected from various locations within the catchments, groundwater from two boreholes (BH1 and BH3), one piezometer in each sub-catchment (BPZ in Bosboukloof and LP3 in Langrivier), TMG spring, two perennial seeps located upslope in Langrivier and Tierkloof, and streamflow from both upstream and downstream of the gauging stations. Pre-event samples were collected a day before the expected rain event and post-event samples were collected a day after. Both could be considered baseflow condition samples given the fast response and recession times of these catchments. Two samples were collected on each occasion, one sample in the morning (between 10h00 and 11h30) and the other in the afternoon (between 13h00 and 15h00).

During the event, stream samples were collected from rainfall, piezometer and stream near the weirs. Grab samples from streams were collected hourly, taken in 200 ml and 50 ml high-density polyethene

(HDPE) bottles with septa insert cap to minimize evaporation. The 200 ml samples were collected for hydrochemical analysis, while the 50 ml samples were for stable water isotope analysis. Due to a lack of access to the higher elevation rain gauges during the event, rainwater samples during the event were collected near the lower elevation rain gauges using a specially designed sequential volume sampler equipped with 50 ml plastic bottles and a funnel 13.5 cm connected to polyvinyl chloride (PVC) tube paired with the tipping bucket rain gauge (Figure.6.1). The sampler for sequential filling of a series of 50 ml bottles without cross-contamination. Bulk rainwater was also sampled with a cumulative rainwater sampler near the rain gauges. The cumulative samplers were designed and modified according to the IAEA standards (International Atomic Energy Agency) and equipped with a 13.5 cm diameter funnel attached to a 2.3 L plastic bottle by a PVC tube. The samples were sealed with parafilm tape to prevent evaporation during storage and transportation to the laboratory. Water physicochemical parameters such as electrical conductivity (EC) as specific conductance, pH, temperature (T) and dissolved oxygen (DO) were measured in-situ for the stream water, piezometer, spring and rainwater using the handheld multiparameter probe (YSI, USA).

Table.6.2. Samples collected during event sampling before and after the event 5- 9 July 2019.

Sample type	Bosboukloof	Langrivier	Jonkershoek, other sites	Sampling dates
Rainwater				
Pre-event Bulk	1	1		05/07/2019
Event Bulk	1	1		06 to 07/07/2019
Event sequential	4	6		06 – 07/07/2019
Stream water				
Pre-event	2	2		05/07/2019
Event	16	19		06-07/07/2019
Post-event	1	1		09/07/2019
Piezometer				
Non-event	5	3		05 and 09/07/2019
Event		8		06 to 07/07/2019
Borehole groundwater	2		2	05 and 09/07/2019
Seep		1	2	05 and 09/07/2019
TMG spring		2		05 and 09/07/2019

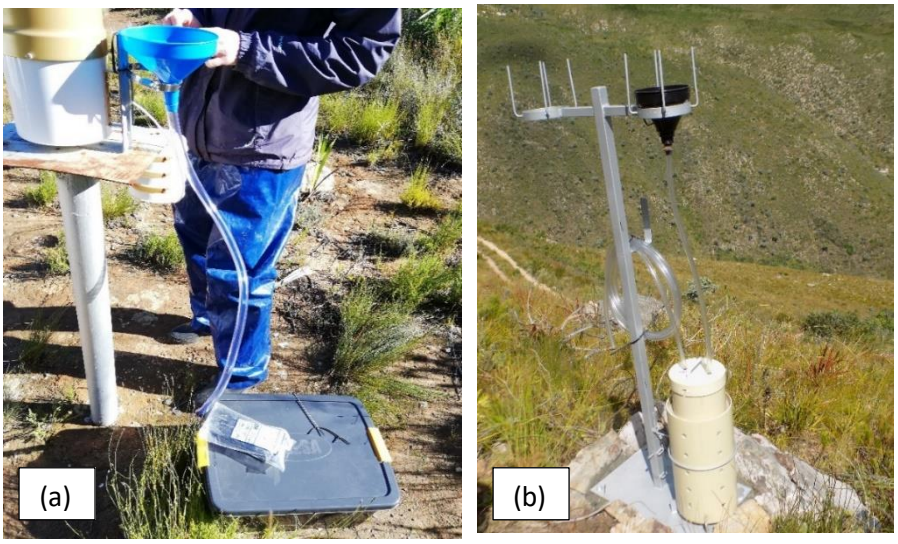

Figure.6.1. Sequential rainwater sample near a tipping bucket rain gauge and (b) the bulk rainwater

According to McDonnell et al. (1990), the isotopic composition of storm/rainfall is rarely constant throughout an event. Large variations may occur over a short period during the event due to factors such as temperature, evaporation and air mass vapor which influence the isotopic compositions of rainfall. Therefore, the incremental mean which is weighted by average hourly rainfall intensity during the sampling increment was used to calculate $\delta^{18}O$ and $\delta^{2}H$ which provide some adjustment of the isotopic composition for the changing rainfall (McDonnell et al., 1990; Zhao et al., 2019). The incremental mean of the rainfall isotopic value is expressed as:

$$\delta D = \frac{\sum_{i=1}^{n} P_i \delta_i}{\sum_{i=1}^{n} P_i} \qquad (6.1)$$

where δ_i is the isotopic content of the event water at time step *i* obtained by sequential sampling, P_i is the average millimetres per hour of rainfall intensity during time step *i*, and *n* is the number of samples.

Additionally, the weighted - mean isotopic composition of the pre-event streamflow samples was calculated using Eq. (2)

$$\delta^{18}O = \frac{\sum_{i=1}^{n} Q_i \delta_i}{\sum_{i=1}^{n} Q_i} \qquad (6.2)$$

where, Q_i is the daily discharge (m^3/s) and δ_i (‰) is the isotopic composition of the streamflow and *n* is the number of observations.

Hydrochemical analyses were performed at the Department of Environment and Water Science laboratory (EWS), University of the Western Cape (UWC). Due to the low ionic concentrations of the water within this catchment, the samples were only analysed for Na^+ and Cl^{-1} which were within the detection limits of the instruments. Other major ions (Ca, Mg, SiO2, K,) were not considered due to

relatively low ionic concentrations in the stream, based on a preliminary analysis carried out at Bemlab (Cape Town) (Appendix B). The streams in Jonkershoek are near pristine, therefore, the groundwater, spring and stream samples were considered clean with no pollutants. Samples from the piezometers were filtered with 0.45 µm filters before analyses.

6.3.3. Hydrograph separation

6.3.3.1. Two-component

The two-component hydrograph separation was used to separate the stream hydrograph into time source and geographic source components. The two-component hydrograph separation involved the use of a single tracer, either the stable isotope (^{18}O or ^{2}H) (McDonnell et al., 1990; Uhlenbrook et al., 2002) or hydrochemical tracers EC, Cl^- and Na^+ (Uhlenbrook et al., 2002; Mul et al., 2008; Wenninger et al., 2008). The stable isotopes (^{18}O or ^{2}H) were used to separate the hydrograph into time source components, i.e., pre-event and event water, while the hydrochemical tracers (EC, Na^+ and Cl^-) were used to divide the hydrograph into contributions from different geographic sources (e.g., deep groundwater, shallow sub-surface water etc).

Assuming the components vary with time the mass balance equation is expressed as follows (Sklash and Fervolden, 1979):

$$Q_{T(t)} = Q_{p(t)} + Q_{e(t)} \quad (6.3)$$

$$Q_{T(t)} C_{T(t)} = Q_{p(t)} C_{p(t)} + Q_{e(t)} C_{e(t)} \quad (6.4)$$

where $Q_{T(t)}$, is the total streamflow, $Q_{p(t)}$ is the flow contribution of pre-event water (soil and groundwater) and $Q_{e(t)}$ is the flow contribution from event water at time step *t*; and *c* is the isotopic composition and the subscripts, *T(t), p (t),* and *e (t)* refers to the total streamflow, the pre-event, and event component at time step *t*, respectively. The event water composition($C_{e(t)}$) was obtained from the calculation of the incremental mean weighting method for rainfall isotopic compositions Eq.6.2 (McDonnell et al., 1990). The pre-event ($C_{P(t)}$) was characterised by stream samples collected before the event during baseflow conditions (i.e.,, fed by groundwater storage or other delayed sources) while event water was represented by rainfall samples collected downstream inside the sub-catchment during the event.

Combining equations (6.3) and (6.4) the contribution of the event water and pre-event water to the total runoff can be estimated by:

$$Q_{e(t)} = Q_{T(t)} \left(\frac{C_{T(t)} - C_{p(t)}}{C_{e(t)} - C_{p(t)}} \right) \quad (6.5)$$

$$Q_{P(t)} = Q_{T(t)} \left(\frac{C_{T(t)} - C_{e(t)}}{C_{p(T)} - C_{e(t)}} \right) \quad (6.6)$$

The general assumptions to be met for the successful application of the hydrograph separations are (Sklash and Farvolden, 1979; Hoeg et al., 2000; Hrachowitz et al., 2010):

1. There must be significant differences in tracer concentrations of the different components.
2. The tracer concentration should remain constant in space and time, or any variations can be accounted for (i.e., the fluctuation in concentrations of the components from beginning to end of the storm is measurable).
3. The contribution of an additional component (i.e., vadose zone) must be negligible, or the tracer signature must be similar to that of the groundwater component.
4. The tracers must behave conservatively and mix well.
5. The tracer concentrations of the components are not collinear.

6.3.3.2. End-Member selection

The selection of suitable tracers and end members to be applied in the three-component hydrograph separation was performed using mixing triplots. The approach is used to estimate the proportion of different end-members based on stable isotopes and hydrochemical parameters. The tracers were plotted against streamflow to determine dilution and hysteresis effect as suggested by Camacho Suarez et al (2015).

Mixing triplots were constructed for each streamflow sample using pair of conservative tracers, for example, $\delta^{18}O$ and $\delta^{2}H$, $\delta^{2}H$ and EC, $\delta^{18}O$ and EC or Na^{+} or Cl^{-}. For the separation to be viable, the stream sample concentrations must be located within the triangular value range defined by the specified end-member samples. The tracer measurement error threshold was assumed at ±5%. According to Cullen (n.d), no meaningful separation can be achieved if the end members are overlapped or too close to each other which leads to high sensitivity and small errors.

Several potential end members were assessed across the investigated sub-catchments. This includes deep bedrock groundwater (i.e., borehole BH3 and BH1) samples from the granite aquifer and TMG springs samples (TMG aquifer groundwater), piezometers and seepage from scree-soil as shallow sub-surface flow (SSF), and direct runoff (i.e., all pathways where rainwater of the specific event was discharged to the stream without chemistry change, this includes rapid interflow via rock fractures) were tested to select suitable end-members in both sub-catchments (Table.4.2). However, for Bosboukloof the TMG spring samples and the piezometer did not fit within the mixing triangle with the direct runoff. Therefore, they were not considered suitable end-members for the analysis in Bosboukloof. Also, in Langrivier, the granite/shale groundwater samples did not plot within the triangle, hence they were excluded as end members in Langrivier.

The selected end members for the three-component hydrograph separation in Bosboukloof were the shallow sub-surface flow, granite-shale groundwater and direct runoff. The shallow sub-surface flow

was represented by the ephemeral seepage from scree and soil exposed along the roadcuts in the neighbouring sub-catchment Tierkloof sampled before the event. The seepage samples showed tracer concentrations almost similar to those of the piezometer in Langrivier indicating a mix of near-surface water and perched water at the soil -bedrock interface, the flow generally occurs from mid-to-end of the wet winter. The piezometer samples in Bosboukloof could not be used for the hydrograph separation due to the similarity in tracer concentrations with the stream samples which violates assumption (1) of the hydrograph separation. The third end member was the granite-shale bedrock groundwater at BH1 which is characterised by flow from the highly weathered granite-shale aquifer.

The selected end members in Langrivier were direct runoff, shallow-subsurface flow and TMG bedrock groundwater. The shallow sub-surface flow was characterised by the piezometer (LP3) samples. The piezometer samples were considered to be intermediate components from the perched shallow saturated layer and/or delayed translatory flow in the unsaturated zone (Roets et al., 2008; Camacho Suarez et al., 2015). The second end-member was the TMG bedrock groundwater considered to be TMG spring discharge from the deep highly fractured TMG aquifer sampled before the event.

6.3.3.3. Three-component hydrograph separation

Past hydrological studies (Wels et al., 1991; De Walle et al., 1998) have urged that the streamflow hydrograph is made up of more than two components. Assuming that the storm flows in this catchment is a mix of more than two components, the three-component hydrograph separation was also used to evaluate the possibility of additional runoff components during the event. The three-component hydrograph separation considers streamflow as a multi-component process (Ogunkonya and Jenkins, 1993; Mei and Anagnostou, 2015). The three-component hydrograph separation was applied for the separation of streamflow into various geographic water source components, direct runoff, shallow sub-surface flow and bedrock groundwater. In this study, the separation was applied using a combination of isotopic and hydrochemical tracers shown by the mixing plots (Figure.6.8). The mass balance equation for the three-component hydrograph separation can be expressed as follows:

$$Q_{T(t)}C_{T(t)} = Q_{r(t)}C_{r(t)} + Q_{ssf(t)}C_{ssf(t)} + Q_{gw(t)}C_{gw(t)} \quad (6.7)$$

where $Q_{T(t)}$, $Q_{r(t)}$, $Q_{ssf(t)}$ and $Q_{gw(t)}$ are the assumed components of total runoff, direct runoff, shallow sub-surface storm flow (SSF) and bedrock groundwater at time step *t*, respectively. The respective tracer concentrations correspond to $C_{T(t)}$, $C_{r(t)}$, $C_{ssf(t)}$ and $C_{gw(t)}$ at time step *t*. Since groundwater from boreholes could not be sampled during the event due to logistical issues, the concentrations for C_{gw} were inferred from TMG spring and BH1 granite shale groundwater samples collected before the event. Different components were selected for each sub-catchment based on the availability of tracer data and differences in tracer concentrations to meet the hydrograph separation assumptions. The hydrograph separation was based on assumptions in section 6.3.3.1.

6.3.3.4. Uncertainty calculation

The uncertainty propagation technique by Genereux, (1998) is commonly applied to estimate the uncertainties in hydrograph separation due to tracer or analytical measurement uncertainties using Gaussian error estimator for two- and three-component separations (Muñoz-Villers and McDonnell, 2012a; Tekleab, et al., 2014; Zhou et al., 2016). Assuming that the uncertainty in each variable is independent of the uncertainty in the others, the relative error W_f of the contribution of a specific runoff component is related to the uncertainty in each variable by the following equation:

$$W_y = \sqrt{\left(\frac{\partial y}{\partial x_1} W_{x1}\right)^2 + \left(\frac{\partial y}{\partial x_2} W_{x2}\right)^2 + \ldots\ldots + \left(\frac{\partial y}{\partial x_n} W_{xn}\right)^2} \qquad (6.8)$$

where W represents the uncertainty in the variables specified in the subscripts (i.e., Wy is the uncertainty in y), assuming that y is a function of several variables $x_1, x_2, \ldots, x_n$, $\frac{\partial y}{\partial x_n}$ is the derivative of function y in terms of variable x_n and assuming the uncertainty in each variable is independent of the uncertainty in the others (Genereux, 1998).

The incorporation of Eq. (6.7) into Eq. (6.8) gives the propagated total uncertainty related to the different components calculated using Eq. (6.9).

$$W_{fp} = \sqrt{\left[\frac{C_{e(t)} - C_{T(t)}}{(C_{e(t)} - C_{p(t)})} W_{C_P}\right]^2 + \left[\frac{C_{T(t)} - C_{p(t)}}{(C_{e(t)} - C_{p(t)})} W_{C_e}\right]^2 + \left[\frac{-1}{(C_{e(t)} - C_{p(t)})} W_{C_T}\right]^2} \qquad (6.9)$$

where W represents the uncertainty in the concentration value for the pre-event (f_p) and event (f_e) specified in the subscript, c is the concentration of the corresponding tracer, e represents the event water, p represents pre-event water and T represents total flow. The relative error is given as a percentage. The uncertainty of W_e (event water), W_{Cp} (pre-event water) and W_{CT} (stream water) for $\delta^{18}O$, $\delta^{2}H$ and EC. The uncertainties related to each set component were computed by using the standard deviation multiplied by the t values from the student's t distribution at a 95 % confidence level (Genereux, 1998, He et al., 2020). Assuming that there was minimal, or no measurement uncertainty introduced during sampling, the W_{CT} was set using the laboratory precisions of the stable isotope analysis at 0.5‰ for $\delta^{18}O$ and 1.5 ‰ for $\delta^{2}H$ as suggested by Genereaux (1998). The uncertainty of each geographic source (i.e., shallow sub-surface flow, direct runoff and bedrock groundwater) was estimated similar approach.

6.3.3.5. Antecedent conditions analyses

Additionally, the Antecedent Precipitation Index (API) was estimated for the rain event at both sub-catchments using the rainfall measured from the lower rain gauge near the weir. This index assumes an exponential decay function for the influence of rainfall after it occurs, to represent the rate of soil moisture depletion during periods of no rainfall (Linsley et al., 1975). The API is defined as follows:

$$API = \sum_{t=1}^{-i} P_t \, k^{-t} \quad (6.11)$$

where P_t is the total rainfall amount in t days (mm/h), i is the number of days before the storm event and k is the decay constant. The empirical decay *(k*) is usually between 0.85 and 0.98 (Linsley et al., 1975). Therefore, in this study, the assigned *k* value of 0.90 was applied based on the study by Smakhtin and Watkins, (1997) for South African headwater catchments. The long-term average winter API was used to put the storm API value into context.

In addition, the rainfall frequency analysis (RFA) was computed to estimate the rainfall rate/ volume for the return period of an event of this magnitude in the Jonkershoek catchment. The calculation was done using the long-term daily rainfall from 2011 to 2019 which includes the study period. The long-term daily rainfall from 1946-2019 could not be used due to missing data between 2008 and 2011 which could hamper the accurate estimation of events. According to Gado et al. (2012), an accurate evaluation of the time series mean of the selected stations should be stationary.

6.4. Results

6.4.1. Rainfall characteristics

A summary of the event characteristics is shown in Table.6.3. There was marked spatial variability in rainfall intensity between the two sub-catchments during the event. The average hourly rainfall intensity was 1.56 mm/h (total: 21.9 mm) in Bosboukloof and 3.5 mm/h (total: 42.2 mm) in Langrivier. Medium events of this magnitude (20-45 mm/day) have return intervals of 4.4 and 9 times a year, producing average flows of 0.06-0.08 m^3/s and 0.42 to 0.65 m^3/s in Bosboukloof and Langrivier, respectively (Figure.6.2).

The event duration between two sub-catchments had a difference of 2 hrs. The rainfall in Bosboukloof started early (11: 00 am) with a drizzle and increased gradually with a total duration of 14 hrs, whereas Langrivier had a shorter duration (12 h) which intensified after 4 hrs. The sampled rain event followed relatively mild antecedent conditions during the winter period. The antecedent rainfall was higher in Langrivier, with an API_7 of 89 mm, compared to Bosboukloof, with an API_7 of 62 mm (Table.6.3). The API values were above the long-term winter of 49.2 mm and 47 mm in Bosboukloof and Langrivier, respectively. No event soil moisture data was available for Bosboukloof, however, Langrivier showed a profile antecedent soil moisture condition of 51 %, 7 days since the last rainfall (API_7 89 mm) which was wetter compared to the winter average of 35%.

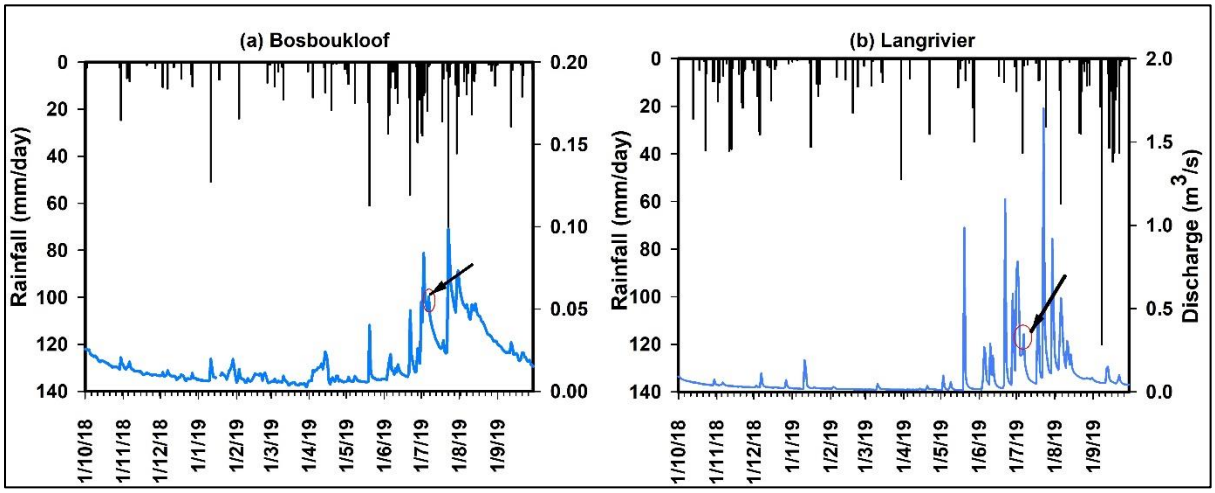

Figure.6.2. Daily rainfall and discharge for (a) Bosboukloof (11B) and (b) Langrivier (8B) for the year 2019. The sampled rain event is indicated by the red circles and arrow.

Table.6.3.Characteristics of the monitored 6-7 July 2019 event in Bosboukloof and Langrivier.

	Bosboukloof	**Langrivier**
Rainfall		
Date of rain event	6- 7 July 2019	6-7 July 2019
Rain start and end time	12:00 - 01:00	13:00 - 00:00
Total rainfall depth (mm)	21.9	42.2
Average rain intensity (mm/h)	1.56	3.53
Maximum rain intensity (mm/h)	3.0	7.11
Duration of rain event (h)	14	12
Time to peak rainfall (h)	10	6
Runoff		
Total runoff volume, (mm)[a]	1.43	6.34
Peak flow (m^3/s)	0.08	0.95
Lag time (h)[b]	2*, 1**	4
Time to peak flow after rainfall started (h)	12	10
API_7 (mm)	62	89
Long-term winter API (mm)	49.2	47

[a]start to the end of the event, [b] from peak rainfall to peak flow, Bosboukloof : *lag time first peak rainfall to the first peak flow, ** lag time from second peak rainfall to the second peak flow in Bosboukloof

6.4.2. Hydrological responses during the event

The time series of rainfall and streamflow showed high responsiveness of streamflow and the environmental tracers to rainfall inputs (Figure.6.3 and Figure.6.4). The two sub-catchments exhibited large differences in event rainfall-runoff responses. There was clear variation in lag times and peak flows between the investigated sub-catchments. The average hourly intensity was lower in Bosboukloof which generated lower peak flow (Table.6.3). The discharge in Bosboukloof responded rapidly to rainfall producing two discharge peaks that followed rainfall intensity variations. The double peaks

showed a response to the brief decrease/change in rainfall intensity. The first peak discharge (22:00,0.073 m^3/s) had a lag of 2 hours since the beginning of the event / first rainfall peak (Figure.6.3.a). The second peak occurred at 00:00 (0.077 $m^{3/}s$) with 1 hour lag from the second rainfall peak**.** The overall lag to the maximum peak (second peak) flow was 11 hrs since the beginning of the rain event. The streamflow had a slower recession compared to Langrivier which receded sharply.

Langrivier had a higher average rainfall intensity which produced a high peak flow (0.95 m^3/s, 1.2 mm/h) recorded at 00:00 almost 10 hours after the rain has started. The lag time between the rainfall and discharge peaks was longer in Langrivier, almost 4 hrs, but showed a sharp rise with the increase in rainfall intensity. The discharge rate returned to the pre-event baseflow conditions (0.122 m^3/s) 34 hours after the rainfall ended and 28 hrs after peak flow.

The 24 hr rain events of this magnitude generally produce 24-hour streamflow averages of 0.05 m^3/s in Bosboukloof and 0.08 m^3/s in Langrivier depending on the antecedent rainfall, which was within the same ranges as those for the samples event. The estimated event runoff coefficients were 0.06 in Bosboukloof and 0.15 in Langrivier. These values were calculated from lower rain gauges near the weirs, therefore the coefficients serve as an indication and may be overestimated or underestimated.

The water table of the granite-shale groundwater (BH3) and the piezometer located near the weir in Langrivier showed a delayed response to rainfall compared to the streamflow, the peak response at BH3 lagged by more than 12 hours (on the 7th July; 09:00) since the beginning of the event. The groundwater levels showed a steady rise of almost 10 cm from 2.61 m to 2.51 m.b.g.l, although the rise receded quickly after a few hours (Figure.6.4.b). The groundwater table at BH1 remained constant and did not show any level response to rainfall inputs (Figure.6.3.b). The recorded slow piezometer response to rainfall inputs had a lag time of more than 12 hours and receded monotonically over two days. The water table also increased from 2.36 to 2.26 m.b.g.l.

The soil moisture response and content in Langrivier varied with depth (Figure.6.4.e). The shallow soil layers were drier compared to the deeper layer throughout the event. The average hourly moisture content was 17.0 % (15 cm), 13.5% (45 cm), 16.8 % (75 cm) and 24.6 % (105 cm) before the event. During the event, the moisture content had a minor increase 18.3 %, 14.0 %, 17.2 % and 25.0 % at 15 cm, 45 cm, 75 cm and 105 cm depths, respectively. As expected, the shallow layers (15 cm and 45 cm) showed a quick response to peak rainfall with lags between 1 and 2 hrs compared to the deeper soil layers. The deeper soil layers (75cm and 105 cm) showed a delayed response of nearly 10 hrs.

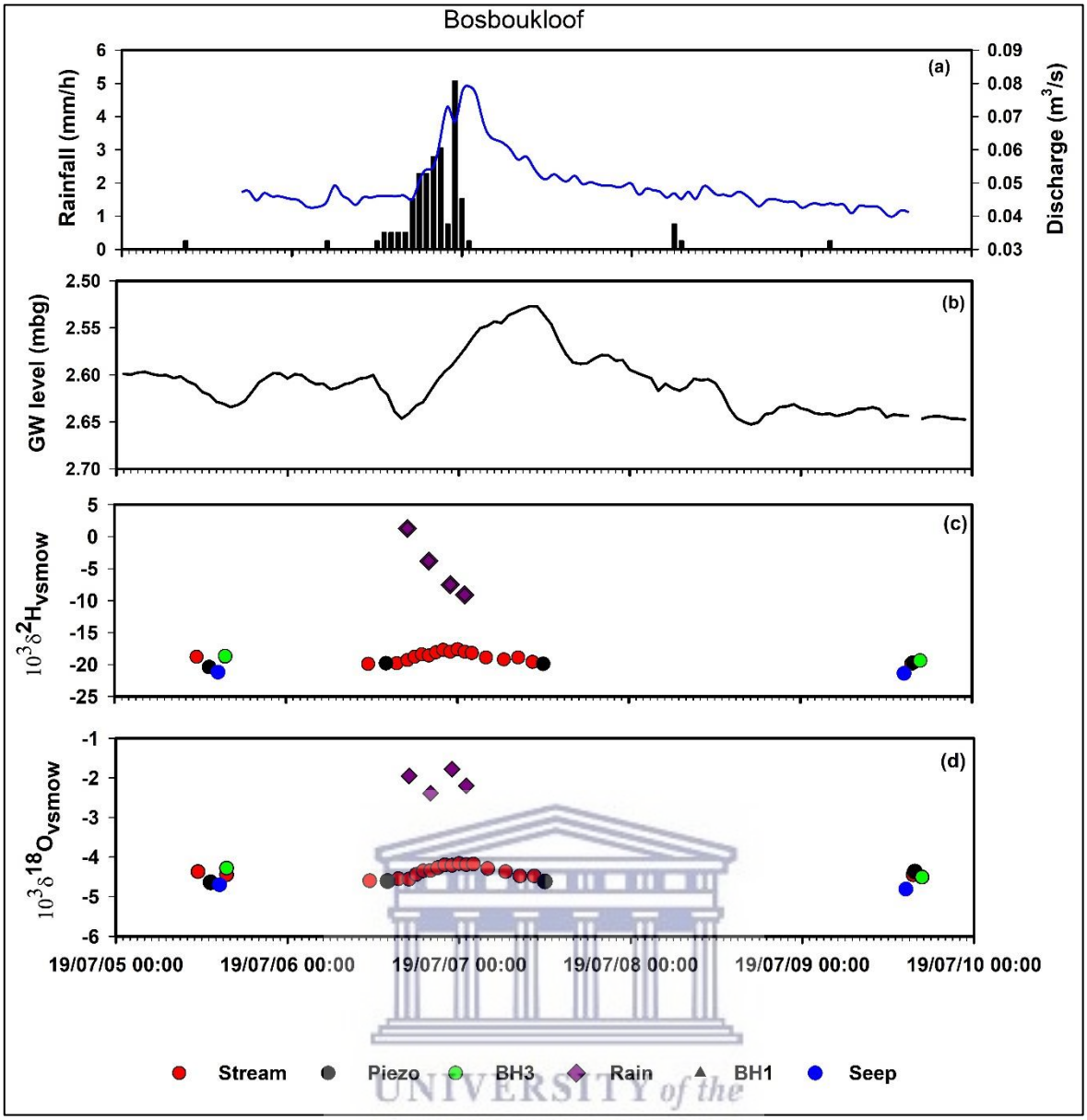

Figure.6.3. Temporal variations of (a) rainfall and discharge (m^3/s), (b) water levels at BH3, (c) and (d) isotopic compositions δ^2H (‰) and $\delta^{18}O$ (‰) of stream, piezometer, groundwater, spring and incremental rainwater samples for Bosboukloof.

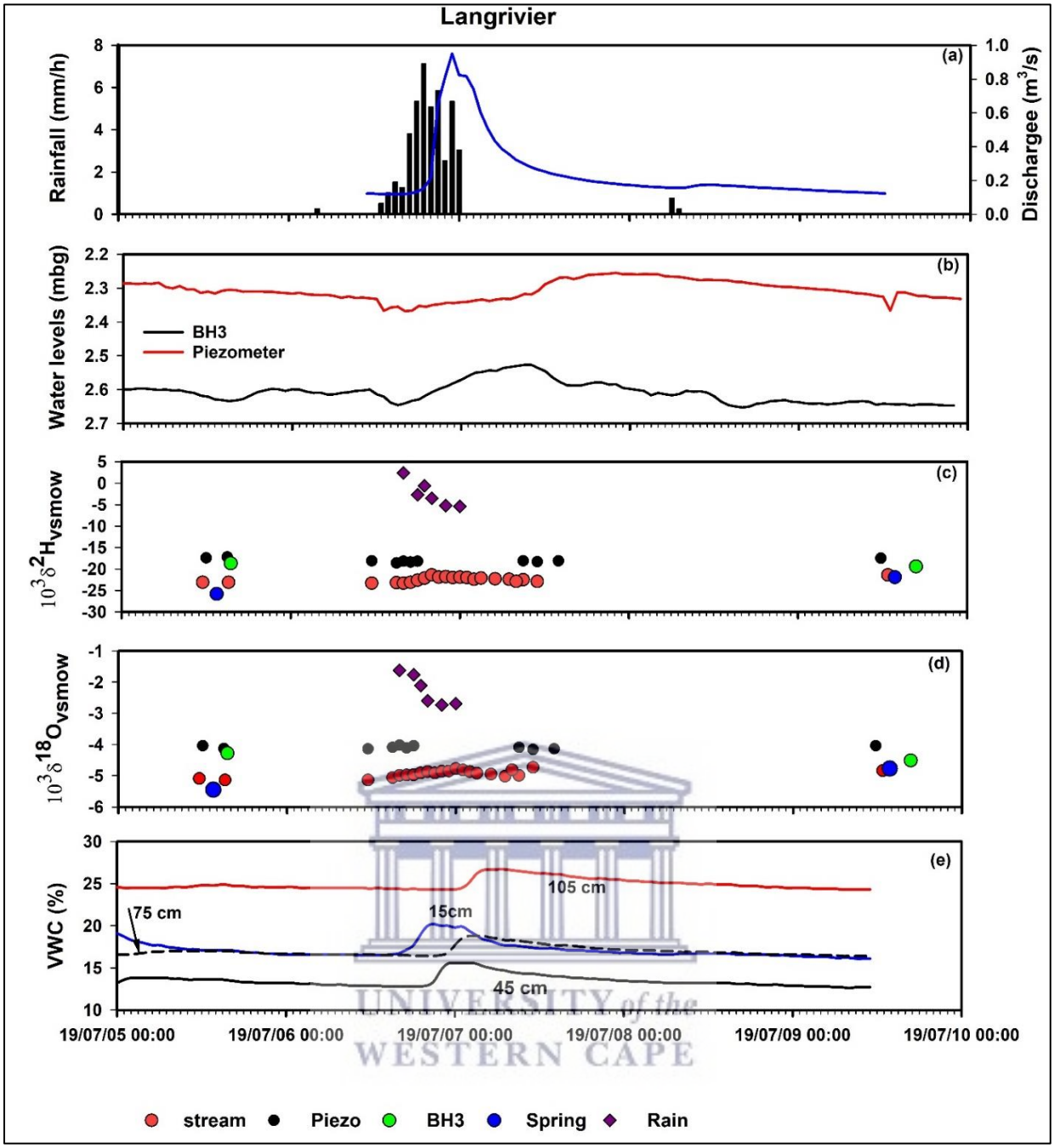

Figure.6.4. Temporal variations in (a) rainfall (mm/h) and hourly discharge (m^3/s), (b) hourly water levels from piezometer and BH3, (c) and (d) isotopic composition δ^2H (‰) and $\delta^{18}O$ (‰) of stream, piezometer, groundwater, spring and incremental rainwater samples and (e) average hourly soil moisture content for Langrivier.

6.4.3. Isotopes and hydrochemical response

The isotopic ratios of $\delta^{18}O$ and $\delta^{2}H$ and the hydrochemical parameters (EC, Na, and Cl) of streamflow showed temporal variations and large responses to rainfall inputs across the sub-catchments. The temporal changes in concentrations during the event are shown in (Figure.6.4 and Figure.6.6). A full list of the samples is provided in Table.D.1 and

Table.D.2 in Appendix D. The isotope ratios of the stream samples were more depleted than the incremental weighted means of the sequential rainfall samples in both sub-catchments (Figure.6.5). The incremental mean isotope ratios for the whole event were -2.08 ‰ for $\delta^{18}O$ and -5.7 ‰ for $\delta^{2}H$ in Bosboukloof, and -2.30 ‰ for $\delta^{18}O$ and -2.9 ‰ for $\delta^{2}H$ in Langrivier. The event streamflow sample weighted means were -4.32 ‰ for $\delta^{18}O$ ‰ and -18.5 ‰ for $\delta^{2}H$ in Bosboukloof, and -4.88 ‰ for $\delta^{18}O$ and -22.18 ‰ for $\delta^{2}H$ in Langrivier.

The $\delta^{18}O$ values of the stream water in Bosboukloof showed a progressive increase towards more enrichment (from -4.55‰ to -4.17 ‰) with increasing rainfall and discharge. A subsequent steady decrease to more depleted values was observed during the recession. A similar trend was detected for $\delta^{2}H$ with an increase from -19.9‰ to a less negative of -17.7‰. The concentrations of hydrochemical parameters of streamflow also showed dilution responses with the increase in rainfall intensity and discharge. However, unlike the isotope values, the concentrations decreased from a background value of 78 µS/cm to 58 µS/cm during peak flow (Figure.6.6.a). A steady increase in concentration occurred during the recession period. Sodium (Na^{+}) concentrations increased from 8.5 to 13 mg/l and decreased gradually during the first peak flow. An increase occurred later during the second peak to 14 mg/l followed by a gradual decrease as the flow receded (Figure.6.6.c). Contrary to EC and sodium, no clear trend in stream chloride (Cl^{-}) concentrations was detected for Bosboukloof.

Large fluctuations were observed but minor dilution responses were evident during peak flow. The trend in piezometer hydrochemical parameters was less pronounced, though the concentrations were in the same range as the stream samples. The borehole samples showed an increase in chloride concentration and a decrease in sodium concentration after the event. Overall, the streamflow isotopic signatures overlapped with the groundwater, piezometer and seep values during baseflow conditions.

The stream water $\delta^{18}O$ and $\delta^{2}H$ values in Langrivier were isotopically depleted compared to those in Bosboukloof more especially for $\delta^{2}H$. The values increased with increasing rainfall intensity and discharge, from -5.14 ‰ to -4.66 ‰ during peak flow. Albeit they were still isotopically depleted relative to the rainfall isotope ratios. The sequential rain samples exhibited an opposite depleting trend as the rainfall intensified. These samples overlapped with the spring and were in the same range as the groundwater samples (Figure.6.4.(c,d) and Figure.6.5). The piezometer (LP3) $\delta^{18}O$ and $\delta^{2}H$ values were more isotopically enriched and showed a gradual increase in response to rainfall input. Like Bosboukloof, Langrivier streamflow EC, Na and Cl showed distinct dilution responses towards peak discharge. There was an initial rise in concentrations with rainfall intensity and discharge, with EC

increasing to 38 µS/cm followed by a decrease to 18 µS/cm with the time steps towards peak flow (Figure.6.6.b). A gradual increase was observed during the recession to the baseflow values of 28 µS/cm. On the other hand, the sodium concentrations in the stream water increased from 5.4 to 6.8 mg/l at the beginning of the event, dilution was observed as the rainfall intensified until peak discharge accompanied by fluctuations that occurred as the rainfall and discharge increased. Moreover, the concentrations increased two days after the event.

The streamflow chloride concentrations showed a clear decreasing trend with increasing rainfall and discharge, dilution indicated by a smooth decrease in concentrations was observed during peak flow whereby the values dropped from 9.2 to 4.4 mg/l. Of the groundwater sampling sites, only the Langrivier piezometer (LP3) could be sampled during the event and was only accessible for the first few hours. Nonetheless, this information provided some information on the shallow sub-surface flow response in the sub-catchment. The geochemical tracer concentration showed an increasing trend towards peak flow and after peak flow for all the parameters, however, the missing peak flow samples obscured a clear analysis of the trends.

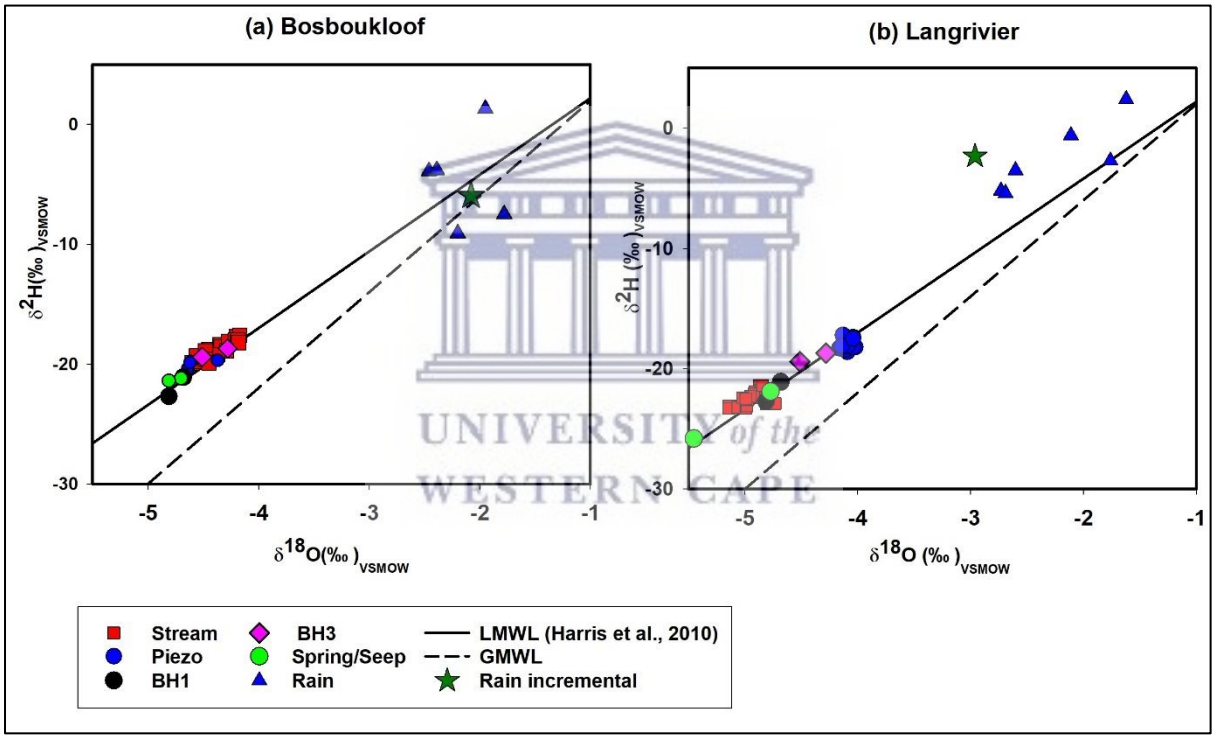

Figure.6.5. Dual isotope plot for the sample collected during the 6-7 July 2019 event in (a) Bosboukloof and (b) Langrivier, including the incremental weighted isotope values.

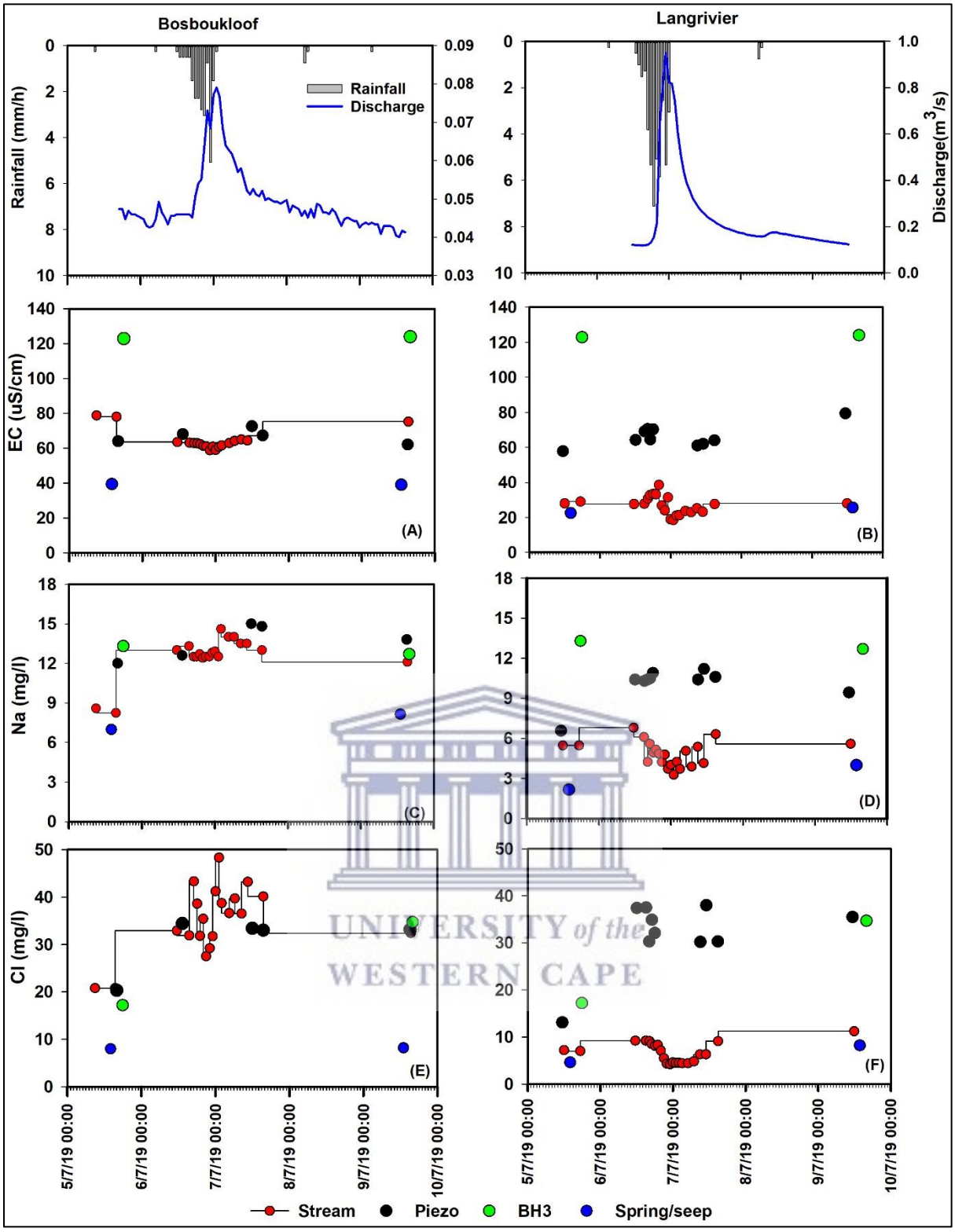

Figure.6.6. Temporal variations of hydrochemical parameter (EC. Na and Cl) responses during the 6-7 July 2019 event.

6.4.6. Hydrograph separation

6.4.6.1. Time source contributions

The two-component hydrograph separation was done to separate the stream hydrograph into pre-event (i.e., stream samples before the event) and event (i.e., event rainfall) components and estimate their relative contributions using $\delta^{18}O$ and $\delta^{2}H$. Figure.6.7 presents the results of the two-component hydrograph separation for the two study sites. The respective incremental weighted means $\delta^{18}O$ and $\delta^{2}H$ were used to represent the event water isotopic compositions to compute the hydrograph separation. The isotope-based hydrograph separation gave similar pre-event and event water contributions across the sub-catchments. Using $\delta^{18}O$ and $\delta^{2}H$, the contribution of event water rose from 0% at the early stages of the event to 12 % during peak flow. Overall, the average event water contribution was extremely small accounting for 4 % of the total flow. Conversely, pre-event contribution decreased gradually at every time step during the rise followed by a smooth increase during the recession. The pre-event contribution was dominant on the rising (95 to 100 %) and the falling limbs and declined slightly to 88 % at peak discharge.

Using the Gaussian error estimator, the overall uncertainty using $\delta^{18}O$ for pre-event (W_{fp}) and event (W_{fe}) fraction was small at 5% in both sub-catchments. The $\delta^{2}H$ error was proportionally larger compared to the $\delta^{18}O$ error at 19.1% and 22 % for both Bosboukloof and Langrivier, respectively Table.6.4. The uncertainties for the isotope-based hydrograph separations showed a general decrease towards peak discharge for every time step.

Table.6.4. Pre-event and event water contributions for two-component hydrograph separation using $\delta^{2}H$ (‰) or $\delta^{18}O$ (‰), as tracers and the corresponding uncertainty of pre-event water (W_{fp}) as a percentage (%).f_e =fraction of event, f_p= fraction of pre-event.

	Bosboukloof		Langrivier	
	$\delta^{18}O$	**$\delta^{2}H$**	**$\delta^{18}O$**	**$\delta^{2}H$**
f_e (%)	6	4	5	2
f_p (%)	94	96	95	98
W_{fp} (%)	4.6	19.1	5.1	22

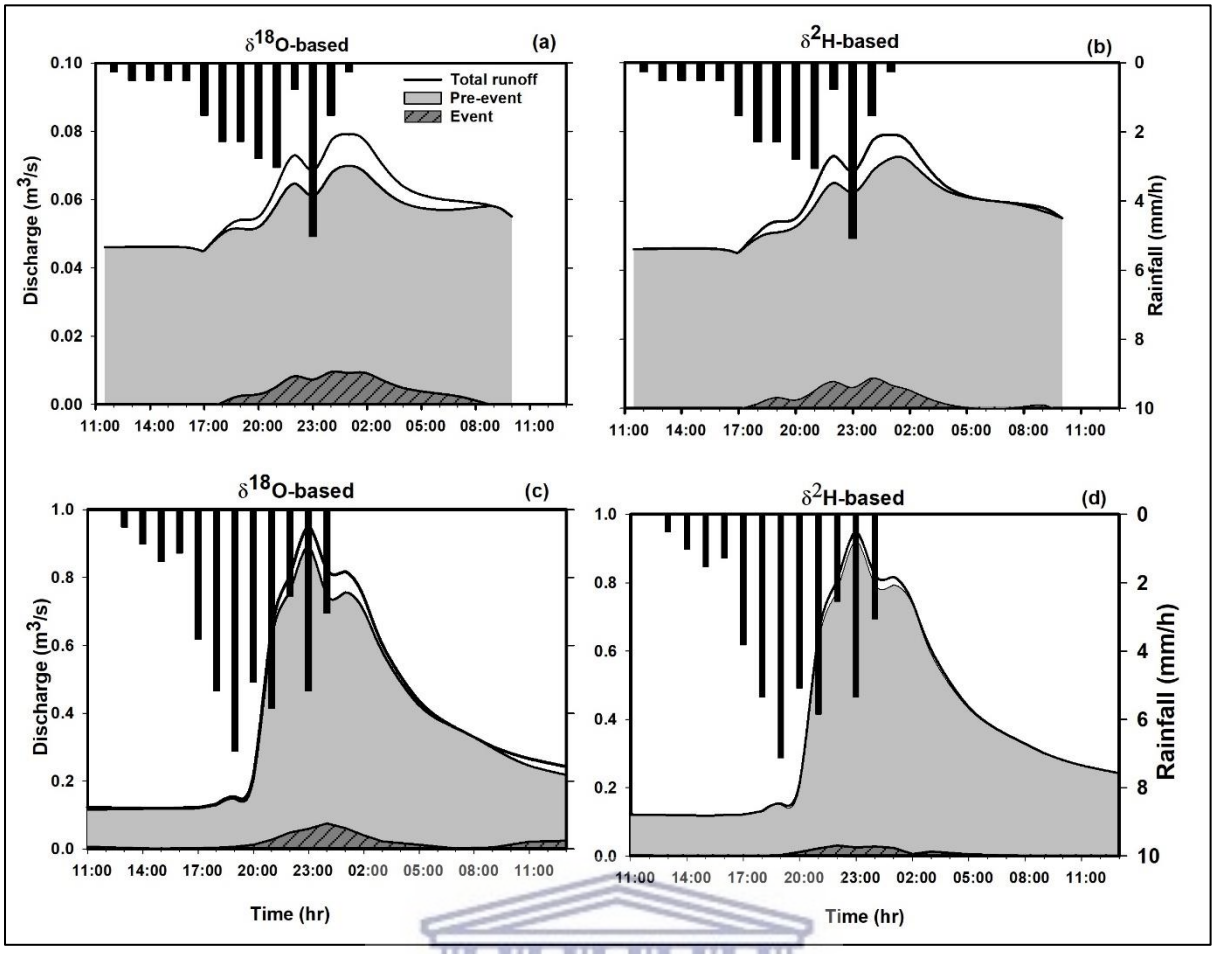

Figure.6.7. Isotope-based two-component hydrograph separation in (a-b) Bosboukloof and (c-d) Langrivier. Black dots indicate sampling times.

6.4.6.2. Geographic sources hydrograph separation

Three-component hydrograph separation

The mixing plots were used to identify the suitable end-members contributing to streamflow during the event. The model showed that $\delta^{18}O$ – EC/Na and $\delta^{2}H$ – EC/Na were the conservative suitable to perform the hydrograph separation. The identified suitable end-members were direct runoff, granite-shale bedrock groundwater and shallow sub-surface flow (ephemeral seep samples) in Bosboukloof (Figure.6.8.(a-b)). The large differences between the granite-shale borehole groundwater and Langrivier streamflow solute concentrations led to a failure of the three-component hydrograph separation. In contrast, the suitable end-members in Langrivier were direct runoff, TMG bedrock groundwater (TMG spring) and shallow sub-surface flow (Piezometer samples).

Figure.6.9 shows the graphical presentation of the three-component hydrograph separations for the event. In Bosboukloof the streamflow samples fell within the mixing triangle clustered near the shallow sub-surface flow (SSF) end-member (Figure.6.8.(a-b)). Figure.6.9 shows that the rising limb of the hydrograph was mainly constituted by SSF (65.7% for $\delta^{18}O$-EC, 61.9% for $\delta^{2}H$-EC) (Table.6.5), the contribution decreased slightly to 58% at peak discharge from 76 % at the beginning of the event. The

first peaks of direct runoff and shallow sub-surface flow coincided with the first and second peak discharge. The direct runoff input increased from 4 to 22 % at both peaks. Contrastingly, the granite-shale bedrock groundwater did not show any specific trend and generally remained constant at ~22 %, the contribution increased slightly, by nearly 1% towards recession.

Conversely, the $\delta^{18}O/^{2}H$-Na based separation in Bosboukloof suggested the dominance of granite-shale bedrock groundwater which rose from 41% to a maximum peak discharge of 53% (Appendix D, Figure.D. 1.). The SSF dominated the rising limb mostly until just before the first peak, decreasing from 55% to 33%. The falling limb was composed of bedrock groundwater which also dominated at peak discharge and to a smaller extent by SSF. The contribution of SSF subsequently increased during the recession. The direct runoff input increased towards peak discharge (from 3 to 21 %). For the $\delta^{18}O/\delta^{2}H$ separation, the samples did not fall within the concentration ranges of the source end-members. This was likely due to the size of potential analytical error compared to the relatively small differences in concentration. Similarly, combinations with Cl could not be used for the separations as the stream samples were not bound within the concentration range of the end members. The overall differences between the EC- and Na-based separation were large for the SSF and bedrock groundwater.

In Langrivier the three-component hydrograph separation presented was based on $\delta^{18}O$-Na and $\delta^{2}H$-Na (Figure.6.9.(c-d)). The mixing plot showed that all the stream samples were within the triangle concentration range of the end-members, and most of the samples clustered around the bedrock groundwater (Figure.6.8.(c-d)). The storm flow was composed of TMG bedrock groundwater flow, followed by direct runoff and minor inputs from SSF (Table.6.5). The TMG bedrock groundwater contributions ranged between 72-84% for both $\delta^{18}O$-Na and $\delta^{2}H$-Na. The groundwater constituted the rising and falling limbs while the direct runoff lagged, and the contribution increased steadily hourly with rainfall intensity towards peak flow. The direct runoff peak coincided with that of the TMG bedrock groundwater. The direct runoff inputs rose from 9 % to 17% during peak discharge, followed by a gradual decrease. The average contributions of direct runoff during the event were 13.2 and 15.1 % to total stormflow for the $\delta^{18}O$-Na and $\delta^{2}H$-Na, respectively. The average contribution of SSF was 4% for both the $\delta^{18}O$-Na and $\delta^{2}H$-Na. Overall Langrivier had a higher bedrock groundwater contribution compared to Bosboukloof during the event.

The hydrograph separation with other tracer combinations ($\delta^{18}O$-$\delta^{2}H$) showed up to 60% groundwater contribution with higher SSF contributions of 27% compared to the Na-based separations (Not presented). The samples for the Cl-based separations did not fall within the concentration ranges of the source end-members, hence they were not considered for the hydrograph separation in both Bosboukloof and Langrivier.

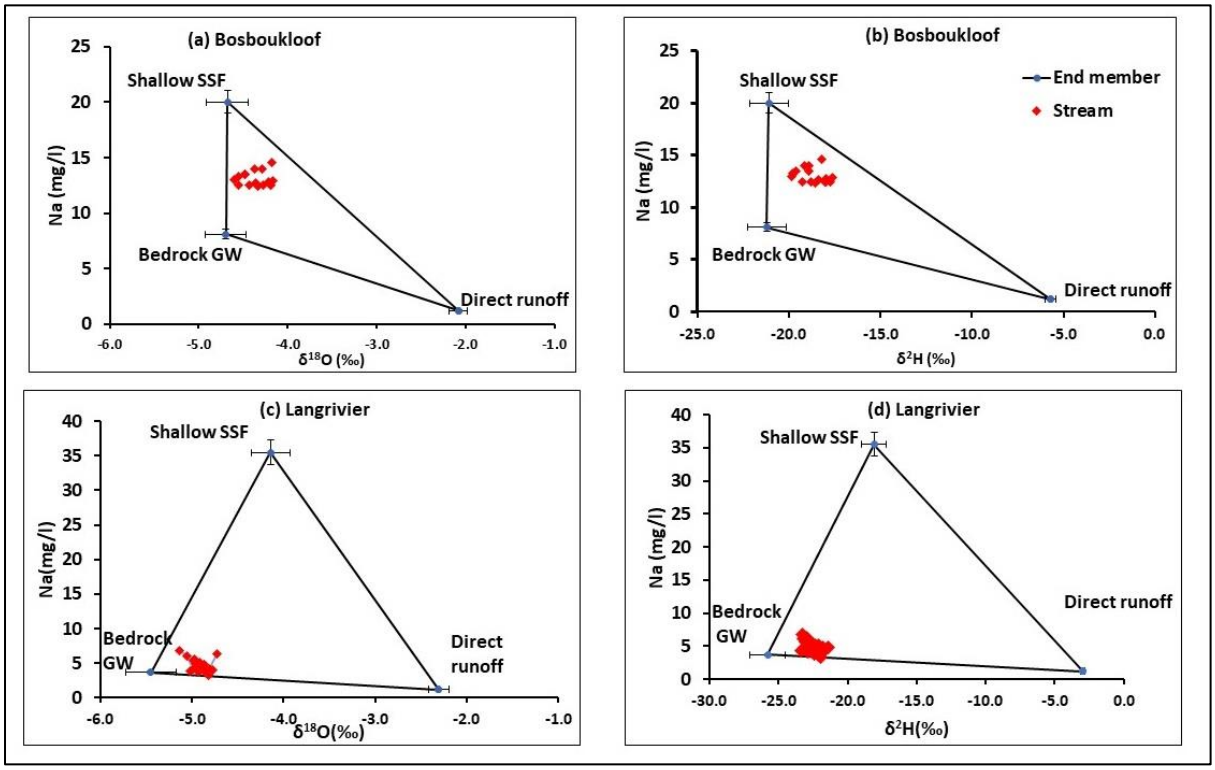

Figure.6.8. Mixing diagrams for (a- b) Bosboukloof using $\delta^{18}O$/ $\delta^{2}H$ and EC and (c-d) Langrivier and $\delta^{18}O$/ $\delta^{2}H$ and Na derived using samples collected during the 6-7 July 2019 event.

Table.6.5. Mean percentages (%) end-member contributions for Bosboukloof and Langrivier during the 6-7 July 2019 event.

End-member	**Bosboukloof**				**Langrivier**	
	$\delta^{18}O$- EC	$\delta^{2}H$-EC	$\delta^{18}O$-Na	$\delta^{2}H$-Na	$\delta^{18}O$-Na	$\delta^{2}H$-Na
Direct runoff, %	13.0	16.2	12.7	15.9	13.2	15.1
Shallow SSF, %	65.7	61.9	39.3	34.1	4.0	4.5
Bedrock groundwater, %	21.3	21.9	47.9	49.9	82.4	80.4

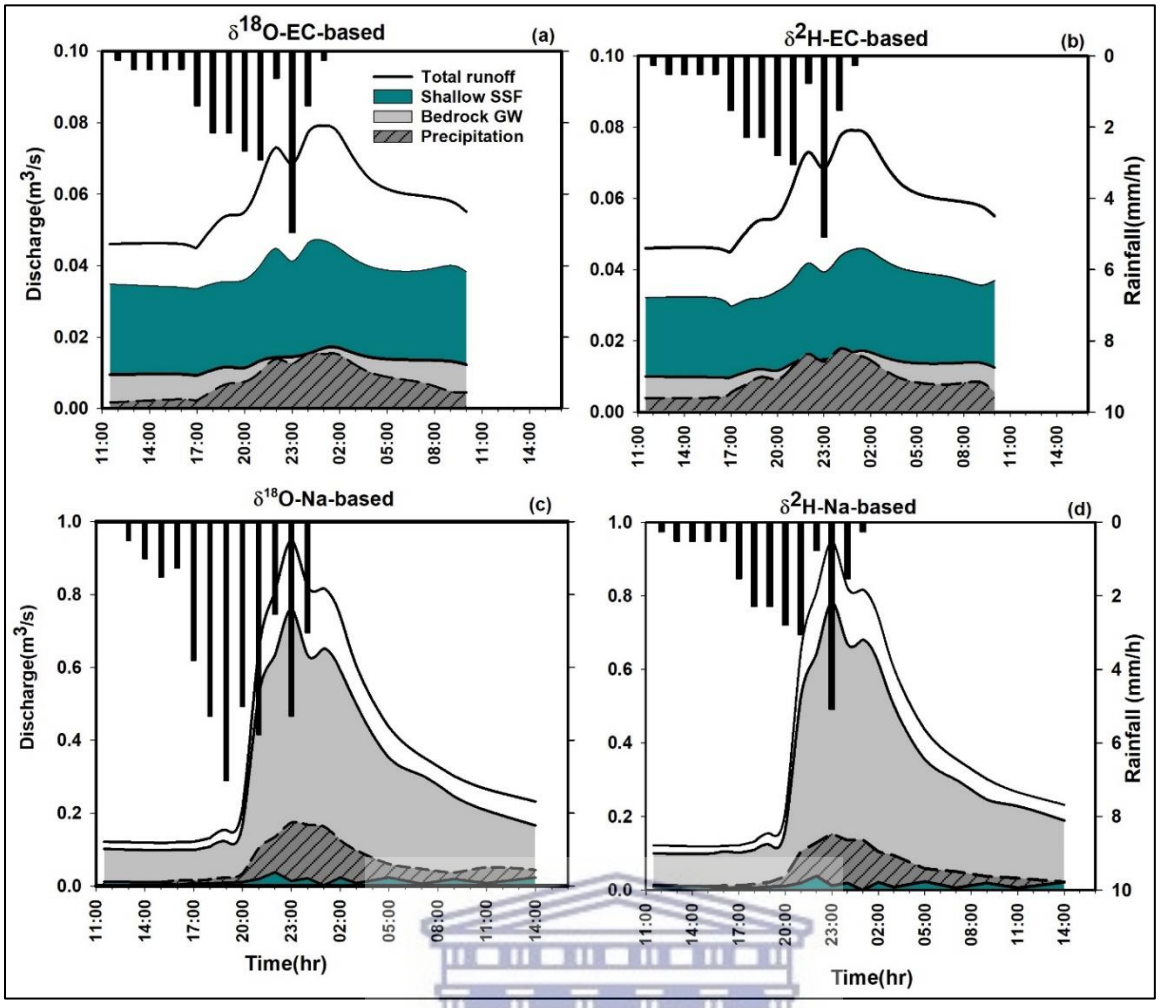

Figure.6.9. Three component hydrograph separation is based on (a-b) $\delta^{18}O/\delta^{2}H$ - EC in Bosboukloof and (c-d) $\delta^{18}O/^{2}H$ -Na in Langrivier. Black dots are the sampling times.

6.5. Discussion

6.5.1. Runoff generation processes in the Jonkershoek sub-catchments

The application of isotopic and geochemical tracers combined with the hydrometric measurements enabled the separation of the winter storm hydrograph into respective contributing components and flow paths. The examination of the event revealed that the majority of the storm hydrograph was dominated by sub-surface stormflow in line with findings from early studies in mountainous catchments (e.g., Sklash and Fervolden, 1976; Anderson and Burt, 1978, Midgley and Scott, 1994) and enabled conceptualisation of the flow processes (Figure.6.10 and Figure.6.11). The dominant end-members varied across the sub-catchments, the order of contribution was shallow sub-surface flow (SSF), granite-shale bedrock groundwater and direct runoff in Bosboukloof. Conversely, the majority of the storm flow in Langrivier originated from the TMG bedrock groundwater, followed by direct runoff and minor contributions from the SSF (Figure.6.11).

The hydrograph separation suggests that SSF in Bosboukloof was quickly activated and decreased hourly, whereas the granite-shale bedrock groundwater contributions were more constant throughout

the event, though less dominant than the SSF (Figure.6.9.(a-b)). This implies that flow from the freely draining scree-talus soil layers dominated the rising limb hydrograph which triggered a quicker runoff response than in Langrivier. This flow is driven for example, by long periods of soil saturation, especially during the wet winter and/or rapid infiltration of new water via vertical preferential flow (e.g., macropores/pipe flow) and can instigate rapid near-surface lateral discharge (seepages) displacing perched water at the soil-bedrock interface downslope (Anderson and Burt, 1978; McDonnell, 1990; Uchida et al., 2003; van Tol, 2020). These preferential flows can rapidly deliver water into the stream while the latter occurs when the soil reaches a certain saturation threshold to allow rapid mobility of the soil water and is usually delayed under dry conditions (Penna et al., 2011, 2015). The shallow sub-surface water flow was likely driven by similar processes in Langrivier, however, it was not as rapid and pronounced as in Bosboukloof.

Based on the elevation of the borehole and the depth of the groundwater level, there is possible interconnectivity between the stream and granite-shale bedrock aquifer. This explains the observed contribution of the granite-shale groundwater in Bosboukloof. Therefore, the hydrologic connectivity (hillslope- stream) is likely to be driven by the steep topography and the deeply weathered bedrock allowing transmission of water to the stream during events. However, further investigations are required to evaluate to assess the connectivity between hillslope, granite-shale groundwater and stream in this catchment. On the other hand, the observations in Langrivier indicate that the TMG bedrock groundwater contribution occurred as TMG springs and seepages. The discharge may occur as rejected recharge re-emerging laterally through the fractures via preferential pathways or at the soil-rock interface (Hughes, 2010; Roets et al., 2008).

Moreover, the vertical percolation and recharge of the deeper layers of the TMG aquifer also control discharge from hillslope (springs and seepages). This discharge is controlled mainly by the connectivity/alignment of the fractures (Lin et al., 2014). These water fluxes are likely to reach the stream quickly in Langrivier due to the steep topography and nearly bare slopes. This was supported by the rapid rise from the contribution from TMG bedrock groundwater and direct runoff observed in the chemical hydrograph separation for the event.

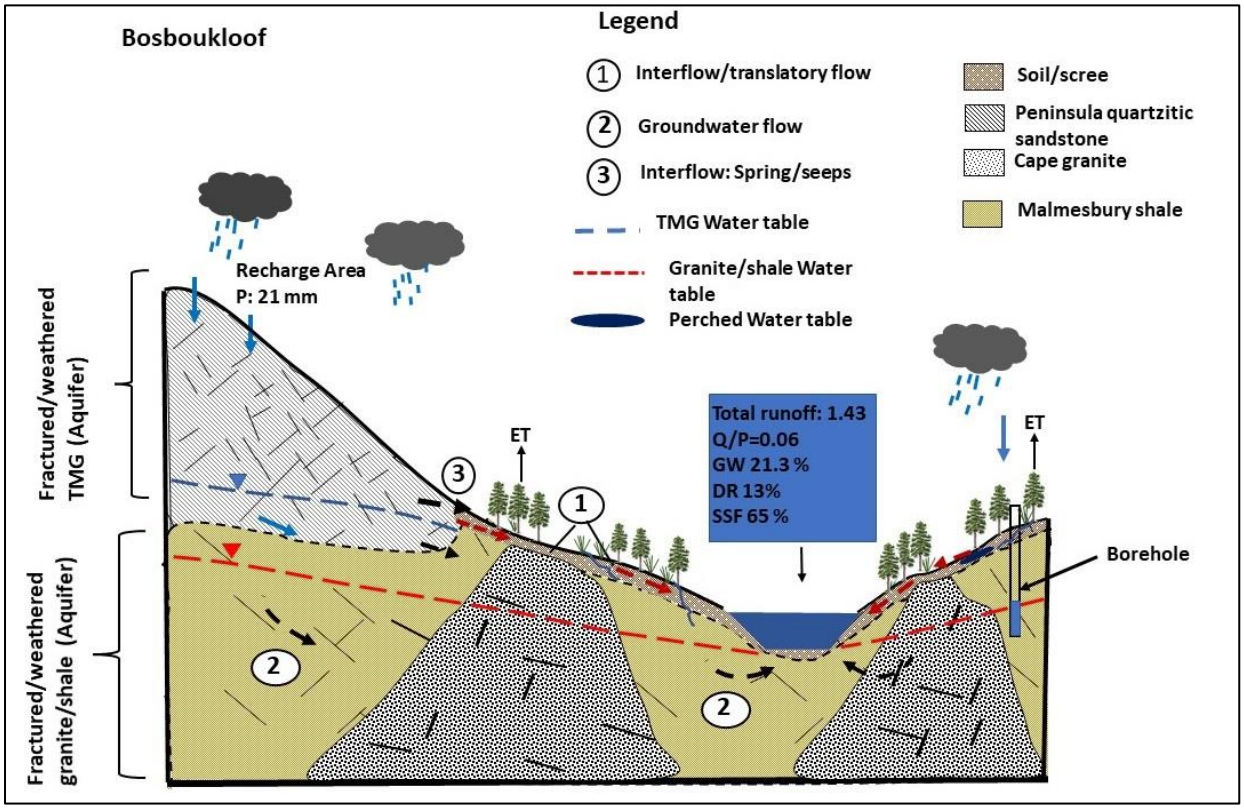

Figure.6.10. Longitudinal profile of runoff generation processes in Bosboukloof. Terms: Q, discharge, P: Rainfall, ET: evapotranspiration, DR: Direct runoff, GW: Granite-shale bedrock groundwater and SSF: Shallow sub-surface flow. The red arrows are the dominant flow path.

The increase in direct runoff contribution during peak flow, especially in Langrivier indicates the rapid mixing of event water (either as direct channel precipitation or rapid interflow) with bedrock groundwater or minor overland flow on the rocky parts of the catchment. The presence of overland flow was reported in the Swartboskloof sub-catchment (Jonkershoek) by Britton et al. (1993) during winter flood events of 152 and 201 mm/day. According to other studies in the semi-arid regions of Southern Africa (e.g., Mul et al., 2008; Camacho Suarez, et al., 2015), the generation of overland flow/surface runoff depends mainly on the antecedent conditions and rainfall intensity. For instance, Mul et al. (2008), showed that a small flood event (rainfall: ~10 mm/day) produced surface runoff of < 5 % in mountainous Makanya catchment, Tanzania, whereas a flood event with rainfall of 175-100 mm/day produced 50 % surface runoff during peak (Mul et al., 2009). Therefore, it can be assumed that moderate events such as this are less likely to produce Hortonian overland flow in these sub-catchments.

Unlike in Langrivier, the TMG bedrock groundwater in Bosboukloof may not reach the stream directly during the event, hence it did not appear as a suitable end-member. The TMG-sourced water in this sub-catchment is likely to flow through deep scree-talus before reaching the channel, which likely results in the water being more mixed with higher solute concentrations. Therefore, no evidence of TMG groundwater contribution was found in Bosboukloof.

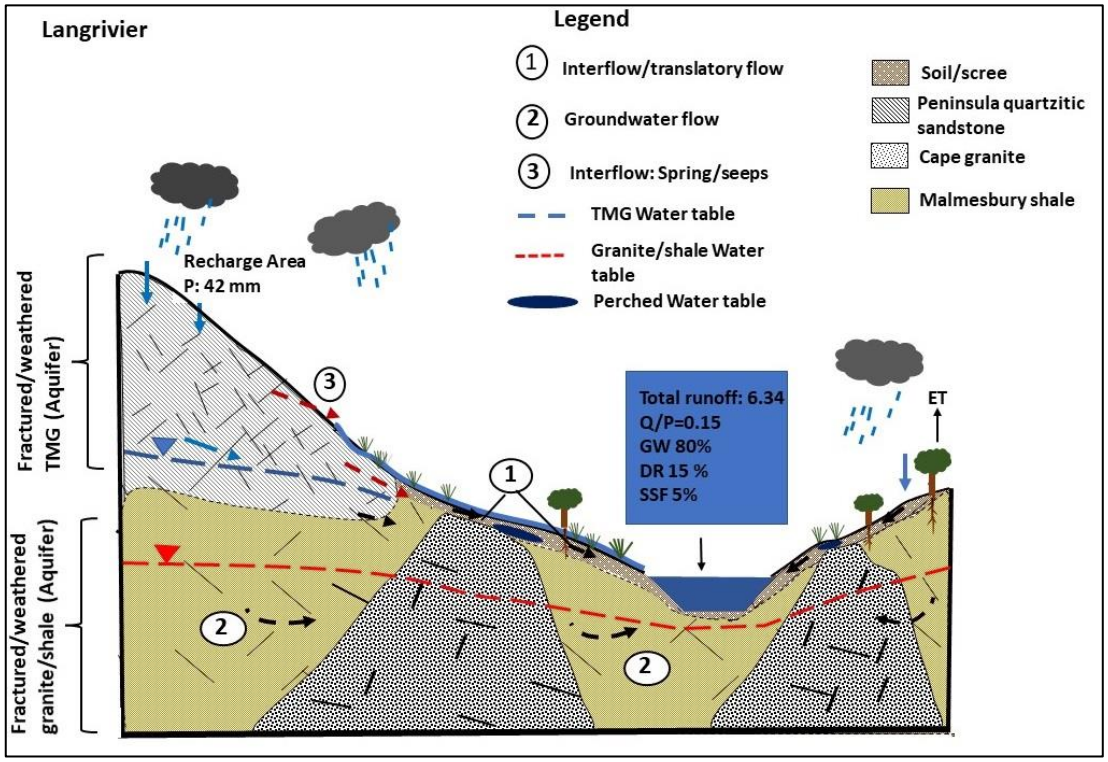

Figure.6.11. Longitudinal profile of runoff generation processes in Langrivier. Terms: Q, discharge, P: Rainfall, DR: Direct runoff, ET: evapotranspiration, GW: TMG bedrock groundwater and SSF: Shallow sub-surface flow. The red arrows indicate dominant flow paths.

6.5.2. The role of pre-event/event water and comparison with other headwater catchments

The overall results of this study, confirm the previous findings in these sub-catchments and other similar catchments on the important role of sub-surface flow pathways/pre-event water contribution during storm events (Britton et al., 1993; Midgley and Scott, 1994, Bugan et al., 2012). The two-component hydrograph separations revealed that the stormflow was supplied mainly by pre-event water accounting for more than ~90% of the total stormflow and event water which accounted for < 10% across the sub-catchments (Figure.6.7). The results were in line with Midgley and Scott (1994), who found pre-event /old water contributions of 90 % while new water constituted 10 % of the total stormflow from 6 winter events in this catchment. This agrees with the early findings by Sklash and Fervolden (1979) and Buttle (1998) which revealed that stormflow in headwater catchments is supplied largely by pre-event water moving via the sub-surface routes to the channel, as a result of groundwater ridging or translatory flow. Also in the Jonkershoek catchment, Midgley and Scott (1994) linked the pre-event water sources to translatory flow. Their results showed dilution response of isotopic signature of stormflow by more isotopically enriched water, indicating mixing with the displaced soil water after a certain amount of saturation was reached.

The dominance of pre-event water has been reported to be a function of antecedent conditions (Britton et al., 1993, Camacho Suarez et al, 2015, Muñoz-Villers and McDonnell, 2012). Britton et al. (1993)

also showed the majority of the winter stormflow in the Swartboskloof sub-catchment of the Jonkershoek was driven by the antecedent conditions. The high soil moisture levels and high storage deficits reduce infiltration resulting in short percolation and lag times between the start of rainfall and the rise of the hydrograph producing large direct runoff which included delayed flows. However, for these sub-catchments, an in-depth understanding of the role/effects of antecedent conditions during both the wet and dry summer events still requires further investigation.

The observed increase in event water fractions with rainfall intensity across the sub-catchments was in line with the findings of Renshaw et al. (2003), Kværner and Kløve, (2006) in Mink Brook forested headwater catchment (USA) and Fischer et al. (2017) in Zwäckentobel headwater catchment (Zurich). According to Renshaw et al., (2003), the increase in event water fractions can be attributed to the changing flow paths during the event. This implies the delivery of new water to the stream because of direct channel precipitation or rapid interflow along preferential flow pathways through the fractured rock.

The observed differences between the event water fractions during peak flow (~5 %) across the sub-catchment, could be attributed to the distinct differences in catchment characteristics such as hillslope geology and vegetation cover. For example, the forested slope vegetation in Bosboukloof can intercept rainfall before it reaches the ground reducing surface runoff or can enhance infiltration and recharge by slowing down runoff. In the Langrivier sub-catchment, the steep slope and less dense vegetation can rapidly deliver water directly to the channel during an event. However, Langrivier showed a smaller flow response (0.419 m^3/s) during this event compared to the long-term average for this event size (0.657 m^3/s). Hewlett and Bosch, (1984) found that, unlike Bosboukloof, Langrivier showed little correlation between peak size and rainfall intensity which was not expected because of the high average response, largest storms, little water storage capacity and the higher proportion (30 %) of a nearly bare rock surface which are known for rapid delivery of water. They concluded that rainfall intensity is not an important factor in stormflow production in this densely vegetated sub-catchment (Hewlett and Bosch, 1984). Therefore, it can be assumed that the soil layer, texture and weathered bedrock geology are the main controlling factors of storm response.

6.5.2. Applicability of hydrochemical and stable isotope tracers

Hydrochemical tracers generally represent deeper sub-surface sources as a combined measure of dissolved ions in the water, the concentrations are controlled by dissolution processes on mineral ions and weathering processes of bedrock geology (Laudon and Slaymaker, 1997; Ladouche et al., 2001; Hugenschmidt et al., 2014). In this catchment, the source of chloride and sodium could be associated with weathering and dissolution of plagioclase minerals from feldspar rich granites upslope (Cape granite) or scree-talus derived from the granites. The hydrochemical tracers behaved differently across the study sites depending on the selected end-members suggesting heterogeneity in lithologies. For

example, Cl could not be used for source separation between end –members samples used due to the large similarities in concentrations between the samples.

The application of hydrochemical tracers in hydrograph separation, especially EC has been controversial and met with scepticism due to its non-conservative behaviour compared to isotopic tracers. However, in some studies, it has been claimed successively to be a good proxy for isotopes producing similar results (Blume et al., 2008; Penna et al., 2011). It has also been reported to underestimate (Meriano et al., 2011) or overestimate (Blume et al., 2008) pre-event/event water fraction. For this study, EC-based separation was found to produce large uncertainties (~60 %) compared to Na and Cl. The large uncertainties were attributed to site-specific conditions such as the spatial heterogeneity related to the different flow paths or lithologies and weathering conditions (Uhlenbrook et al., 2002). Furthermore, it can be assumed that the sampling was not sufficient to account for the spatial variations in flow pathways.

Hydrograph separation using Na showed small uncertainty errors compared to those involving EC. Therefore, Na should be considered for hydrograph separation in future studies in other TMG outcrop areas. The behaviour of these non-conservative tracers will depend on specific catchment characteristics and the hydrological functioning of the catchments. Thus, it is also important that they are assessed in other TMG catchments. The stable isotopes successively allowed for the separation of the respective time source components and three-component hydrograph separation producing smaller uncertainty, especially for ^{18}O which could be attributed to their conservative nature. Therefore, it is advised that the use of a hydrochemical tracer in hydrograph separation in this catchment should be assessed against the stable isotopes due to their limitations.

6.6. Conclusion

Knowledge of runoff generation processes is crucial as they provide information on the spatiotemporal variations in hydrological processes which support the development of catchment conceptual models. Although characterization of flow pathways and source areas can be challenging in fractured geology headwater catchments, the application of hydrometric data integrated with tracers allowed for the identification and quantification of runoff generation processes for a medium-magnitude winter event. The data provided evidence of the contribution of soil water to streamflow during rain events. The results showed that different tracers provide different information on runoff components or flow paths in each sub-catchment and the estimated fraction of the stream components were tracer specific. The isotopes, Na and Cl were found to produce lower uncertainty for the hydrograph separation compared to EC. Therefore, sodium and chloride were found to be suitable for geographic source separation. However, this does not dismiss the potential of EC as a tracer, but it should be applied with caution allowing for larger margins of error.

The hydrograph separation results revealed noticeable spatial variations in runoff response between the two sub-catchments with shorter lag time in Bosboukloof compared to long lag time in Langrivier which

were linked to delays during recharge and/or infiltration rainwater to the deeper layers. The results of the 2-component separation pre-event vs event (rain) water using stable isotopes of suggested pre-event water. Three-component hydrograph separations were done to quantify the relative contributions from direct runoff, shallow sub-surface flow and bedrock groundwater discharge. The outputs indicated that shallow sub-surface flows and TMG bedrock groundwater discharge were the dominant runoff generating components during the event in Bosboukloof and Langrivier, respectively. The spatial variation in dominant processes were related to catchment characteristics e.g., geology, vegetation and topography. This resulted in the dominance of lateral sub-surface flow components (e.g., soil-scree water) in Bosboukloof compared to Langrivier. Direct runoff dominated peak flow (15 %) at both study sites, which suggested the contribution of direct channel precipitation or rapid interflow through the highly fractured rock, especially in Langrivier.

The finding highlighted the important role of interflow and translatory flow in these sub-catchments during winter storm events. Furthermore, they were consistent with other studies on runoff generating processes in Southern Africa and forested headwater catchments elsewhere in the world. Overall, this study provided one piece of the puzzle in building a bigger picture on understanding the different runoff components and flow pathways that govern runoff production during the winter event in the small mountainous catchments of the TMG outcrop areas. The results provided an improved understanding of runoff generating processes and surface water-groundwater interaction in the TMG headwater catchments and highlighted the complexity of studying these processes in spatially heterogeneous geology and using hydrochemical tracers in the nearly pristine stream water. Moreover, they will provide a baseline for these kinds of hydrological studies in the future in the TMG geological region and similar regions which will be beneficial for local water sources planning and management under the changing climatic conditions.

CHAPTER 7: CONCLUSIONS AND RECOMMENDATIONS

7.1. Conclusions

The main aim of this study was to characterize streamflow generating mechanisms under changing environmental and climatic conditions in the Jonkershoek catchment. Understanding these processes is crucial for the sustainable management of headwater catchments within the TMG geological region and has implications for the management of water resources in the Cape region. Though the understanding of these hydrological processes is crucial in this water-scarce region, financial constraints, the complex geology and topography affect the collection of high-resolution data. Unfortunately, important data such as environmental isotope tracers and hydrochemistry which are known to be useful for understanding mechanisms of streamflow generation are often not available. Therefore, these kinds of hydrological studies have been limited in the TMG geological region.

Previous studies in the Jonkershoek used hydrometric data, with one prior study applying environmental tracer data in storm events (Midgley and Scott, 1994). The current study used a novel multi-method approach combining environmental isotopes and hydrochemical data (from streams, groundwater boreholes, springs and seeps, piezometers and rainfall) alongside hydrochemistry data and various statistical methods for better understanding and characterisation of hydrological processes and the quantification of flow components in the catchment. The following conclusions were drawn from this study.

Trends in hydro-climatic variables and drought assessment (Chapter 3)

The evaluation of the long-term trends in rainfall and streamflow time series (1946-2019) for the three sub-catchments of the Jonkershoek, identified significant decreasing trends in annual rainfall and streamflow for most of the stations. Bosboukloof, the catchment with the longest history of pine plantation and the lowest runoff, was an exception; despite a declining rainfall trend, no significant trends in streamflow were found. The detected decreasing trends were consistent with the meteorological and hydrological droughts at the end of the time-series identified using the Standardized Precipitation Index (SPI) and Standardized Streamflow Index (SSI), respectively. The homogeneity tests showed non-consistent change points and downwards shifts for both rainfall and streamflow time series in Tierkloof and Langrivier. The change points were consistent with the afforestation period in Tierkloof and were partially linked to climate trends, supported by the rainfall declines across all sub-catchments.

The different catchments showed different patterns in their responsiveness to periods of high and low rainfall. The correlations between the SPI value and SSI showed spatial variations, with shorter SPI accumulation in Langrivier (1-3 months) and longer (12-months) SPI- accumulation in Bosboukloof. This result shows that the difference in catchment storage due to irregularities in fracturing, the rugged

topography and uneven spatial distribution of scree-soil on the slopes are the key factors controlling the spatial variations.

The sub-catchments showed a great response to land-cover changes compared to climate declining rainfall. The Indicators of Hydrologic Alterations (IHA) revealed significant decreasing trends in flow attributes over the analysis period 1946-2019. The magnitude of multi-day annual extremes (1-,7- and 30- days) showed a substantial decrease across the investigated sub-catchments, particularly in Tierkloof and Langrivier. Furthermore, the assessment of the impacts of afforestation versus clear-felling on streamflow regimes in Bosboukloof and Tierkloof showed that afforestation altered the magnitude and timing of flow extremes. More pronounced alterations were noticed in the multi-day-maximums annual extremes, median monthly flows and the baseflow index. In contrast, the maximum flows and mean monthly flow showed a substantial increase in response to clear-felling which were attributed to the decrease in evapotranspiration rates and water usage by the pine plantations.

Spatial and temporal patterns in stable isotopes and hydrochemical parameters to reveal the seasonality in water sources during baseflow conditions (Chapter 4)

The spatiotemporal variation in stable water isotopes and hydrochemistry combined with hydrometric time series were applied to characterize the seasonality in flow paths and streamwater sources. Both the rainfall and water samples from various sources except borehole groundwater exhibited seasonality. This suggests that the streamflow responded to seasonal precipitation. The stream water sample was more depleted during the wet season events close to rainfall composition indicating recharge by non-evaporated rainfall. During summer, there were overlaps in the $\delta^{18}O$ and $\delta^{2}H$ isotopic signature of the streamflow and both the TMG bedrock groundwater (springs) and granite-shale bedrock groundwater (boreholes samples). However, there was no strong relationship between the streamflow $\delta^{18}O$ and $\delta^{2}H$ values with those of the monthly rainfall indicating that rainfall during this period did not significantly recharge sources feeding baseflow. It was concluded that in the dry summer season the baseflow is dominated by the TMG bedrock groundwater emerging at high elevations (i.e., TMG springs). The wet winter season streamflow was attributed to interflow including water emerging at ephemeral and enhanced discharge at perennial TMG springs. The seasonal variation in EC, Na and Cl across the sub-catchments suggests the displacement of old water by new event water.

The isotopic compositions and concentrations of hydrochemical parameters of stream water showed spatial variations. The hydrochemical compositions increased from upstream to downstream suggesting the introduction of new source components along the flow paths. The spatial variability in rainfall and streamflow isotopic compositions and hydrochemical responses across the sub-catchments was accompanied by evidence of differing flow path contributions supporting baseflow in each sub-catchment. Furthermore, the stream water sample in Bosboukloof had high concentrations of EC and chloride and was isotopically enriched compared to Tierkloof and Langrivier indicating flow through

sub-surface scree-soil with a high evaporation effect and had been subjected to the processes of mineral dissolution and cation exchange.

The hydrochemical concentration differences between the borehole groundwater and streamflow samples were too large to link the baseflows to the granite-shale bedrock groundwater. The groundwater and piezometer water quality were controlled by geochemical processes such as weathering of feldspar minerals from the bedrock granite, mineral dissolution of silicates and feldspars, evaporation which increased EC and Cl concentrations as well as cation exchange reactions. This in part indicates that the hydrochemistry data was not sufficient to account for spatiotemporal variability in processes or there were uncertainties in sample distribution. Based on these results it was concluded that two different bedrock groundwater aquifers occur in this catchment, an aquifer within the TMG bedrock and another in the granite-shale bedrock.

The rainfall isotopic composition exhibited seasonality. The seasonality in the rainfall isotopic ratios suggested different moisture sources during the dry summer and wet winter seasons. Altitude and the amount effect were identified as the major controlling factors of the rainfall isotopic compositions. However, this was not reflected in the stream water samples indicating that less or no direct contribution from seasonal rainfall.

Evaluating the spatial and temporal variation in baseflow estimates based on digital filters and tracer-based baseflow separation methods. (Chapter 5)

The separation of daily streamflow into fast and slow components over the period 1946-2019 using two-parameter recursive digital filter method (RDF), has shown that the resulting BFI values were more sensitive to the recession constant parameter, however, the BFI_{max} was more uncertain. The electrical conductivity data collected during 2018-2020 allowed the optimization of the filter parameter BFI_{max} and improved the baseflow estimation. The optimized BFI_{max} values can serve as a reference for further studies in the TMG geological region.

The estimated baseflow showed spatial variations and minor temporal variations. The spatial variations were linked to the rugged and variable topography and irregularities in fracturing that control the release of baseflow. The long-term average baseflow contributions to total streamflow were 86%, 61% and 38 %, for Bosboukloof, Tierkloof and Langrivier respectively. The BFI values indicated large spatial variations. High BFI values occurred in Bosboukloof and Tierkloof, especially during the dry summer season. Langrivier had low BFI values and a higher proportion of direct runoff throughout the year compared to Tierkloof and Bosboukloof, particularly during the high flow winter season. Decreasing trends in BFI values and baseflow discharge occurred during the low flow dry summer months (Oct to Dec). The declines in baseflow volume over time indicate declines in groundwater discharge over time due to a decrease in groundwater level which is linked to the declining trends in winter rainfall identified in Chapter 3. Given that Bosboukloof is afforested with pines may tap into the deep groundwater sources this sub-catchment appears to be more vulnerable compared to the Langrivier and Tierkloof. The

observed seasonality can have a significant impact on water resources for regions that rely on baseflows and other similar headwater catchments.

Understanding runoff generating processes using tracer-based hydrograph separation methods (Chapter 6)

Investigation of runoff generating processes was conducted in two sub-sub-catchments during a single small-medium magnitude winter event with return intervals of 4 to 9 times a year. Stable isotopes proved to be suitable tracers for quantifying time source components (two-component hydrograph separation, HS). A combination of stable isotope and hydrochemistry enabled the identification and quantification of runoff components (e.g., shallow sub-surface flow, direct runoff and bedrock groundwater discharge) employing a three-component hydrograph separation.

Sub-surface flows and pre-event water were the dominant runoff components in both Langrivier and Bosboukloof. Interflow and translatory flow (i.e., scree soil water, at soil-bedrock interface, fractures flow) were found to be the major flow pathways responsible for the stormflow across the sub-catchments. The three-component hydrograph separation revealed spatial variations in runoff components and hydrological responses. The dominant runoff generating processes during the event response in Bosboukloof appeared to be shallow sub-surface flow (~65%), followed by the granite-shale bedrock groundwater discharge (~ 30 %) while direct runoff contribution was minor < 15 %. Conversely, in Langrivier, the dominant components were TMG bedrock groundwater (~80%), direct runoff (15 %) and shallow sub-surface flow (5 %). The spatial difference in the hydrologic processes likely reflects the influence of the difference in land cover (i.e., pines vs fynbos) and topography on catchment response during the storm event. In Bosboukloof, the afforested sub-catchment, the pines are likely to increase interception in storms and increase ET resulting in driers antecedent soil conditions and lower groundwater table, hence reduced direct runoff compared to Langrivier.

The findings indicate the potential of tracer-based hydrograph separation to characterise runoff generation components in Jonkershoek suggests the connectivity between the stream and granite-shale aquifer in Bosboukloof sub-catchments which could not be identified from the simple evaluation of stable isotope and hydrochemistry in Chapter 4. The high-frequency sampling and choice of end members appeared to have sufficient to reflect catchment processes during a storm event. The integration of isotopes and hydrochemistry improved the findings of previous studies in this catchment (e.g., Midgley and Scott,1994; Britton et al., 1998) by identifying runoff components and relative flow pathways.

7.2. Knowledge contribution

The study contributes knowledge of runoff generating processes in small mountainous catchments (< 5km^2) dominated by the Table Mountain Group (TMG) fractured geology system and other Mediterranean-type climate catchments using a multi-method approach. The Jonkershoek catchment

(146 km^2) is characterized by steep mountainous terrains with fractured geology which increases the complexities of understanding hydrological processes. Their diverse topographic characteristics have resulted in high variability in streamflow and rainfall. These mountains are dominated by baseflow from the TMG aquifer discharged as high elevation springs and seeps as well as interflow through the weathered bedrock rock and fracture networks. However, detailed studies on factors accounting for the spatial and temporal variability in hydrological are still lacking. Understanding the processes and factors accounting for the spatial and temporal variations of streamflows in this area is critical. This information can be used to build appropriate conceptual and numerical models of this catchment's functioning to support the management of water resources. It is crucial to understand the processes governing streamflow generation and water flow regimes associated with precipitation patterns in headwater catchments for proper management of water resources at the sub-catchment scale which can later be translated to the catchment scale. The findings of the study improved the understanding of streamflow generating processes in a mountain catchment with geology dominated by the Table Mountain Group.

The study highlighted that large spatial and temporal variability in water flow paths, streamflow components, and magnitude of streamflow and baseflows can exist across small spatial scales (i.e., 2 km^2 apart). It illustrated how various catchment physiographic characteristics such as topography, soil characteristics and vegetation cover are likely to influence runoff generating mechanisms. Lastly, it revealed the impacts of land-use changes such as afforestation and climate variability of streamflows. Conceptual models indicating various runoff generating processes both on seasonal and event-based scales were developed for the three sub-catchments. The developed conceptual models will be considered for other catchments within the TMG and other catchments with similar characteristics across the world. The new data such as the stable water isotopes and water quality could be used in future for water quality assessments such as chemical transport and sources of water pollution, evaluating the impacts of climate variability on water resources related to changes in precipitation patterns in mountainous areas are highly sensitive to these changes.

7.3. Recommendations

This study is the first to investigate the spatial and temporal variations in runoff generation and quantify runoff components based on the integrated use of hydrometric, stable isotopes and hydrochemical data in the Jonkershoek catchment. The data generated and the approach used can further be adopted in other TMG catchments or other catchments with similar hydrological and hydrogeological characteristics. The results laid a foundation for future research and the development of the improved hydrological model. Further studies aimed at improving process understanding, particularly those involving the spatiotemporal variations in runoff generation are recommended. The following recommendations are made:

- From the results, it was evident that afforestation has large effects on streamflow generation in the catchment. It is recommended that afforestation is carried out in such a manner that can allow the headwater streams to maintain their natural flow. Additional, regular clearing is required to ensure recovery of streamflow. Therefore, the different stakes holders such as hydrologists, forestry management and the Department of Water and Sanitation (DWS) must collaborate to ensure plantation cycles are planned in such a manner that should not alter the baseflow of streams and streamflow yields.
- The application of stable water isotopes and hydrochemical measurements were effective indicators for identifying stream water sources and flow paths. However, two years of sampling and monthly sampling frequency were not sufficient to reveal the temporal characteristics of stable isotopes and hydrochemistry. Therefore, long- term and high-frequency monitoring of stable isotopes and hydrochemistry from various sources are recommended to account for the temporal variability. This knowledge is crucial for understanding the behaviour of the catchment under changing conditions and improving water resource management.
- Installation of groundwater monitoring boreholes close to the gauges is recommended for the monitoring of water levels, chemistry and stable isotopes to improve process understanding.
- High-density sampling is also recommended to account for the spatial variability as well as improve the quantification and identification of runoff generating components. It can further help reduce the uncertainties in tracer-based methods and improve calibrations.
- Despite the proximity and similar lithological types in the sub-catchment, large spatial variations in hydrologic responses, runoff components and hydrochemistry were evident. It is therefore recommended that catchment water resources management practices take into account these differences in catchment characteristics.
- It is recommended that more than one storm event be sampled, preferably during both the dry summer and wet winter to account for the spatiotemporal variations in the hydrological response and runoff components.
- To improve the calibration of the recursive digital filter method, other tracers including stable isotopes and major ions besides those considered in this study should be tested as they may provide accurate information on chemical signatures of water sources and provide reference to calibrate the non-tracer based baseflow separation methods for future studies. This kind of study should be conducted in other TMG catchments to validate these conclusions.

8. References

Ahmad, I., Tang, D., Wang, T., Wang, M. and Wagan, B.. (2015). Precipitation trends over time using Mann-Kendall and spearman's Rho tests in SWAT river basin, Pakistan, *Advances in Meteorology.*, 2015,pp.1-13. doi: 10.1155/2015/431860.

Alexandersson, H. and Moberg, A. (1997). Homogenization of Swedish temperature data. Part I: Homogeneity test for linear trends, *International Journal of Climatology.*, 17(1), pp. 25–34. doi: 10.1002/(sici)1097-0088(199701)17:1<25:aid-joc103>3.3.co;2-a.

Ali, R., McFarlane.D., Varma, S., Dawes, Emelyanova, I. and Hodgson.G. (2012). Potential climate change impacts on the water balance of regional unconfined aquifer systems in south-western Australia, *Hydrology and Earth System Sciences.*, 16(12), pp. 4581–4601. doi: 10.5194/hess-16-4581-2012.

Anderson, M.G. and Burt, T.P. (1978). The role of topography in controlling throughflow generation. *Earth-Surface Processes*., 3 (4): 331-344.

Anderson, S. P., Dietrich, W.E., Montgometry, D.R., Torres, Conrad, M.E. and Loaque, K. (1997). Subsurface flow paths in a steep, unchanneled catchment. *Water Resources Research.*, 33(12), pp. 2637–2653. doi: 10.1029/97WR02595.

Asano, Y. and Uchida, T. (2018). The roles of channels and hillslopes in rainfall/run-off lag times during intense storms in a steep catchment, *Hydrological Processes.*, 32(6), pp. 713–728. doi: 10.1002/hyp.11443.

Barker, L. J. Hannaford, J., Chiverton, A. and Svensson, C. (2016). From meteorological to hydrological drought using standardised indicators, *Hydrology and Earth System Sciences*., 20(6), pp. 2483–2505.

Barlow, P. M., Cunningham, W.L., Zhai, T. and Gray, M.(2015). U.S. Geological Survey Groundwater Toolbox, a graphical and mapping interface for analysis of hydrologic data (Version 1.0) — User guide for estimation of base flow, runoff, and groundwater recharge from streamflow data, U.S. Geological Survey Techniques and Methods, (book 3, chap. B10), pp. 27.

Bershaw, J. (2018). Controls on deuterium excess across Asia, *Geosciences (Switzerland).*, 8(7). doi: 10.3390/geosciences8070257.

Betancur, T., Palacio T., C. A. and Escobar M., J. F. (2012). Conceptual Models in Hydrogeology, Methodology and Results, *Hydrogeology - A Global Perspective.*, (July 2014). doi: 10.5772/28155.

Beven, K. J. (2012). *Rainfall-Runoff Modelling, the primer*. Second edition. Lancaster, UK: WILEY - BLACKWELL,pp. 6-15

Birkel, C. Tetzlaff, D., Dunn, S.M., and Soulsby, C. (2011).Using lumped conceptual rainfall-runoff models to simulate daily isotope variability with fractionation in a nested mesoscale catchment, *Advances in Water Resources*., 34(3), pp. 383–394. doi: 10.1016/j.advwatres.2010.12.006.

Birkel, C. Tetzlaff, D., Dunn, S.M., and Soulsby, C. (2011). Using time domain and geographic source tracers to conceptualize streamflow generation processes in lumped rainfall-runoff models, *Water Resources Research*., 47(2), pp. 1–15. doi: 10.1029/2010WR009547.

Birkel, C. and Soulsby, C. (2015). Advancing tracer-aided rainfall – runoff modelling : a review of progress, problems and unrealised potential, *Hydrological Processes*., 29(July), pp. 5227–5240. doi: 10.1002/hyp.10594.

Blake, D., Mlisa, A. and Hartnady, C. (2010). Large scale quantification of aquifer storage and volumes from the Peninsula and Skurweberg Formations in the southwestern Cape, *Water SA.*, 36(2), pp. 177–184.

Blowes, D.W. and Gillham, R.W. (1988). The generation and quality of streamflow on inactive uranium tailings near Elliot Lake, Ontario. *Journal of Hydrology*., 97(1-2), pp. 1-22

Blume, T., Zehe, E. and Bronstert, A. (2008). Investigation of runoff generation in a pristine, poorly gauged catchment in the Chilean Andes II: Qualitative and quantitative use of tracers at three spatial scales, *Hydrological Processes*., 22(November 2008), pp. 3676–3688. doi: 10.1002/hyp.

Bosch, D. D. Arnold, J.G., Allen, P.G. and Lim, K. (2017). Temporal variations in baseflow for the Little River experimental watershed in South Georgia, USA, *Journal of Hydrology: Regional Studies*., 10, pp. 110–121. doi: 10.1016/j.ejrh.2017.02.002.

Botai, C. M., Botai, J. O. and Adeola, A. M. (2018). Spatial distribution of temporal precipitation contrasts in South Africa, *South African Journal of Science*., 114(7–8), pp. 70–78. doi: 10.17159/sajs.2018/20170391.

Bohte, R., Mul, M.L., Savenije, H.H.G., Uhlenbrook, S. and Kessler, T. (2010). Hydrograph separation and scale dependency of natural tracers in a semi-arid catchment, *Hydrology and Earth System Sciences.*,7, pp. 1343-1372.

Boughariou, E. Bouri, S., Khanfir, H. and Zarhloule, Y. (2014). Impacts of climate change on water resources in arid and semi-arid regions: Chaffar Sector, Eastern Tunisia, *Desalination and Water Treatment.*, 52 (10–12), pp. 2082–2093. doi: 10.1080/19443994.2013.822322.

Brendenkamp,D.B., Botha, L.J., Van Tonder,G.J. and Van Rensburg, H.J. (1995). Manual on quantitative estimation of groundwater recharge and aquifer storativity.WRC Report No. 73/95.Water Research Commission, Pretoria.

Britton, D. L., Day, J.A. and Henshall-Howard, M-P. (1993). Hydrochemical response during storm

events in a South African mountain catchment: the influence of antecedent conditions,*Hydrobiologia.*, 250, pp. 143–151.

Brown, V.A., McDonnell, J.J., Burns, D.A. and Kendall.C. (1999). The role of event water, a rapid shallow component, and catchment size in summer stormflow. *Journal of Hydrology.*, 217,pp.171-190.

Bruijnzeel, L.A. (2004). Hydrological functions of tropical forests: not seeing the soil for the trees? *Agriculture, Ecosystems and Environment*., 104, pp. 185-228

Bugan, R., Jovanovic, N. Z. and Clercq, W. P. De (2012). The water balance of a seasonal stream in the semi-arid Western Cape (South Africa), *Water SA.*, 38(2), pp. 201–212.

Buishand, T.A. (1982). Some methods for testing the homogeneity of rainfall records, *Journal of hydrology*., 58, pp. 11-27

Burls, N. J., Blamey, R.C., Cash, B.A., Swenson, E.T., al Fahad, A., Bopape, M-J, M., Straus, D.M. and Reason, C.J.C.(2019). The Cape Town "Day Zero" drought and Hadley cell expansion, *Climate and Atmospheric Science.*, 2(1), pp. 1–8. doi: 10.1038/s41612-019-0084-6.

Buttle, J. M. (1998). Fundamentals of Small Catchment hydrology, In Isotope Tracers in Catchment. Kendall, C. and McDonnell, J.J. (eds). Amsterdam, New York: Elsevier Ltd. doi: 10.1016/B978-0-444-81546-0.50001-X.pp. 2-49

Camacho Suarez, V. V., Saraiva Okello, A. M. L., Wenninger, J.W. and Uhlenbrook, S. (2015).Understanding runoff processes in a semi-arid environment through isotope and hydrochemical hydrograph separations, *Hydrology and Earth System Sciences.*, 19(10), pp. 4183–4199. doi: 10.5194/hess-19-4183-2015.

Cartwright, I., Gilfedder, B. and Hofmann, H. (2014).Contrasts between estimates of baseflow help discern multiple sources of water contributing to rivers, *Hydrology and Earth System Sciences.*, 18(1), pp. 15–30. doi: 10.5194/hess-18-15-2014.

Cartwright, I. and Miller, M. P. (2021). Temporal and spatial variations in river specific conductivity: Implications for understanding sources of river water and hydrograph separations, *Journal of Hydrology.*, 593, p. 125895. doi: 10.1016/j.jhydrol.2020.125895.

Castillo Rápalo, L.M., Uliana, E.M., Moreira, M.C., da Silva, D.D., de Melo Ribeiro, C.B., da Cruz,I.F. and dos Reis Pereira, D. (2021). Effects of land use and-cover changes on streamflow regime in Brazial Savannah, *Journal of Hydrology.*, 38, pp.100934

Chapman, T. (1999). A comparison of algorithms for stream flow recession and baseflow separation, *Hydrological Processes.*, 13(5), pp. 701–714.

Chapman, T. G. (1991). Comment on "Evaluation of automated techniques for base flow and recession analyses" by R. J. Nathan and T. A. McMahon, *Water Resources Research.*, 27(7), pp. 1783–1784. doi: 10.1029/91WR01007.

Chen, H. and Teegavarapu, R. S. V. (2020). Comparative analysis of four baseflow separation methods in the south atlantic-gulf region of the U. S, *Water (Switzerland).*, 12(1). doi: 10.3390/w12010120.

Chen, X., Zhang, Y., Xue, X., Zhang, Z. and Wei,L. (2012). Estimation of baseflow recession constants and effective hydraulic parameters in the karst basins of southwest China, *Hydrology Research*., 43(1–2), pp. 102–112. doi: 10.2166/nh.2011.136.

Clark, B. and Ractliffe, G. (2007). Berg River baseline monitoring programme. The Freshwater Consulting Group, DWAF Report No. P WMA 19/G10/00/2107, Department of Water and Affairs and Forestry, South Africa, 5 (October), p. 111.

Collischonn, W. and Fan, F. M. (2013). Defining parameters for Eckhardt's digital baseflow filter, *Hydrological Processes.*, 27(18), pp. 2614–2622. doi: 10.1002/hyp.9391.

Colvin, C., Riemann, K., Brown, C., Le Maitre, D., Mlisa, A., Blake. D., Aston, T., Maherry, A., Engelbrecht, J., Pemberton, C., Magoba, R., Soltau, L. and Prinsloo,E. (2009). Ecological and environmental impacts of large scale development in the Table Mountain Group (TMG) Aquifer System, WRC Report 1327/1/08, Water Research Commission, Pretoria.

Congjian, S., Li, X., Chen, Y., Li, W., Stotler, R. L. and Zhang, Y. (2016).Isotopic time series partitioning of streamflow components under regional climate change in the Urumqi River, northwest China, *Hydrological Sciences Journal*., 61(8), pp. 1443–1459.

Craig, H. (1961). Isotopic variations in meteoric waters, *Science.*, 133, pp. 1702–1703.

Cullen, J. (n.d). The use of End Member Mixing Analysis in identifying the relative contribution of different runoff pathways. It's potential value for future catchment management studies. *Environment Agency Wales*., pp. 64-73.

Day, J. A. and King, J.M.(1995). Geographical patterns and their origins, in the dominance of major ions in South Africa, *South African Journal of Science*., 91, pp. 299-306.

Dansgaard, B. W. (1964). Stable isotopes in precipitation,*Tellus.*, 16, pp. 436-468

DeWalle, D.R.., Swistock, B.R. and Sharpe, W. E.(1988). Three-component tracer for stormflow on a small Appalachian forested catchment, *Journal of Hydrology.*, 104 (1-4), pp. 301-310

Diamond, R. E. (2014). Stable isotope hydrology of the Table Mountain Group. [PhD. Thesis], University of Cape Town, Cape Town. doi: 10.1016/j.apmr.2007.05.004.

Didszun, J. and Uhlenbrook, S. (2008). Scaling of dominant runoff generation processes: Nested

catchments approach using multiple tracers, *Water Resources Research*., 44(2), pp. 1–15. doi: 10.1029/2006WR005242.

Duah, A. A. (2010). Sustainable utilization of Table Mountian Group aquifers [PhD Thesis]. University of the Western Cape, Bellville.

Duncan, H. P. (2019). Baseflow separation – A practical approach, *Journal of Hydrology*, 575(November 2018)., pp. 308–313. doi: 10.1016/j.jhydrol.2019.05.040.

du Plessis, J. A. and Schloms, B. (2017). An investigation into the evidence of seasonal rainfall pattern shifts in the Western Cape, South Africa, *Journal of the South African Institution of Civil Engineering*., 59(4), pp. 47–55. doi: 10.17159/2309-8775/2017/v59n4a5.

du Plessis, J.A. and van Zyl, H. (2021): The effect of veld fires on the hydrological responses of streamflow. Water SA., 47 (2), pp. 185-193.

Dye, P., Moses, G., Vilakazi, P., Ndlela, R. and Royappen, M. (2001). Comparative water use of wattle thickets and indigenous plant communities at riparian sites in the Western Cape and KwaZulu-Natal, *Water SA.*, 27(4), pp. 529–538.

Eckhardt, K. (2005). How to construct recursive digital filters for baseflow separation, *Hydrological Processes.*, 19, pp. 507–515. doi: 10.1002/hyp.5675.

Eckhardt, K. (2008). A comparison of baseflow indices, which were calculated with seven different baseflow separation methods, *Journal of Hydrology.*, 352(1–2), pp. 168–173.

Eckhardt, K. (2011). Technical Note: Analytical sensitivity analysis of a two-parameter recursive digital baseflow separation filter, *Hydrology and Earth System Sciences Discussions*., 8(5), pp. 9469–9480. doi: 10.5194/hessd-8-9469-2011.

Farid, I., Trabelsi,R., Zouari, K. and Beji, R. (2013). Geochemical and isotopic study of surface and groundwaters in Ain Bou Mourra basin, central Tunisia, *Quaternary International*., 303, pp. 210–227. doi: 10.1016/j.quaint.2013.04.021.

Fenicia, F., McDonnell, J. J. and Savenije, H. H. G. (2008). Learning from model improvement: On the contribution of complementary data to process understanding, *Water Resources Research*., 44(6), pp. 1–13. doi: 10.1029/2007WR006386.

Fischer, B. M. C., Meerveld, H. J. I. Van and Seibert, J. (2017). Spatial variability in the isotopic composition of rainfall in a small headwater catchment and its effect on hydrograph separation, *Journal of Hydrology*., 547, pp. 755–769. doi: 10.1016/j.jhydrol.2017.01.045.

Foks, S. S., Raffensperger, J.P., Penn, C.A. and Driscoll, J.M. (2019). Estimation of base flow by optimal hydrograph separation for the conterminous United States and implications for national-extent hydrologic models, *Water (Switzerland).*, 11(8). doi: 10.3390/w11081629.

Frisbee, M..D. (2010). Streamflow generation processes and residence times in a large, mountainous watershed in the southern rocky mountains of Colorado, [PhD Thesis], New Mexico Institute of Mining and Technology, Socorro, New Mexico.

Fry, M, St.L. (1987). A detailed characterization of soils under different fynbos-climate-geology combinations in the Southe western Cape.M.Sc. Thesis, University of Stellenbosch, Maitland, South Africa.

Gale, B.A. The effect of regulation by two impoundments on an acid, Blackwater, Cape Mountain Stream.[PhD Thesis], University of Cape Town, Cape Town.

Gebremicael, T. G., Mohamed, Y. A. and Van der Zaag, P. (2019). Attributing the hydrological impact of different land use types and their long-term dynamics through combining parsimonious hydrological modelling, alteration analysis and PLSR analysis, *Science of the Total Environment.*, 660, pp. 1155–1167. doi: 10.1016/j.scitotenv.2019.01.085.

Genereux, D. (1998). Quantifying uncertainty in tracer-based hydrograph separations, *Water Resources Research.*, 34(4), pp. 915–919.

Gilbert, R. O. (1988). Statistical Methods for Environmental Pollution Monitoring, *Biometrics.*, 44(1), p. 319. doi: 10.2307/2531935.

Gilvear, D.J., Heal, K.V. and Stephen.A. (2002). Hydrology and ecological quality of Scottish river ecosystems,*Science of the Total Environment*. 294, pp.131-159

Giustini, F., Brilli, M. and Patera, A. (2016). Mapping oxygen stable isotopes of precipitation in Italy, *Journal of Hydrology: Regional Studies.*, 8, pp. 162–181.

Gonzales, A. L. , Nonner,J., Heijkers, J. and Uhlenbrook, S. (2009). Comparison of different base flow separation methods in a lowland catchment, *Hydrology and Earth System Sciences.*, 13(11), pp. 2055–2068. doi: 10.5194/hess-13-2055-2009.

Gröning, M., Lutz, H.O., Roller-Lutz, Z., Klalik, M., Gourcy, L. and Pöltenstein, L. (2012). A simple rain collector preventing water re-evaporation dedicated for δ18O and δ2H analysis of cumulative precipitation samples, *Journal of Hydrology*, 448-449, pp. 195-200.

Grubbs, F.E. (1950).Sample criteria for testing outlying observations. *The annals of Mathematical Statistics*, vol 21 (1),pp.27-58

Grubbs,F.E and Beck,G. (1972). Extension of sample sizes and percentage points for significance tests of outlying observations. *Technometrics*,vol 14,pp. 847-854

Guastini, E., Zuecco, G., Errico, A., Castelli, G., Bresci, E., Preti,F. and Penna, D. (2019). How does streamflow response vary with spatial scale ? Analysis of controls in three nested Alpine catchments, *Journal of Hydrology*,570, pp. 705–718.

Gupta, H. V., Sorooshian, S. and Yapo, P. O. (1999). Status of Automatic Calibration for Hydrologic Models: Comparison with Multilevel Expert Calibration, *Journal of Hydrologic Engineering*, 4(2), pp. 135–143. doi: 10.1061/(asce)1084-0699(1999)4:2(135).

Hafi, Z. B. and Ali, A. A. M. (2019). Available online www.jsaer.com Research Article Analysis of Temporal Trends and Variability of Rainfall Series in Northeastern Libya, *Journal of Scientific and Engineering Research*, 6(4), pp. 89–99.

Haga, H., Matsumoto, Y., Matsutani, J., Fujita, M., Nishida, K. and Sakamoto, Y. (2005). Flow paths, rainfall properties, and antecedent soil moisture controlling lags to peak discharge in a granitic unchanneled catchment', *Water Resources Research*, 41(12), pp. 1–14. doi: 10.1029/2005WR004236.

Hamed, K. H. and Rao, R. (1998). A modified Mann-Kendall trend test for autocorrelated data', *Journal of Clinical Oncology*, (204), pp. 182–196. doi: 10.1200/jco.2018.36.15_suppl.522.

Harris, C., Burgers, C., Miller, J. and Rawoot, F. (2010). O- and H-isotope record of Cape Town rainfall from 1996 to 2008, and its application to recharge studies of table mountain groundwater, South Africa, *South African Journal of Geology*, 113(1), pp. 33–56. doi: 10.2113/gssajg.113.1.33.

Harris, C., Oom, B. M. and Diamond, R. E. (1999). A preliminary investigation of the oxygen and hydrogen isotope hydrology of the greater Cape Town area and an assessment of the potential for using stable isotopes as tracers', *Water SA*, 25(1), pp. 15–24.

Hartnady, C. J. and Jones, M. Q. (2007). Geothermal Studies of the Table Mountain Group Aquifer Systems. WRC Report 1403/1/7, pp.1-2, Water Research Commission, Pretoria.

Hewlett, J. D. and Bosch, J. M. (1984). The dependence of storm flows on rainfall intensity and vegetal cover in South Africa, *Journal of Hydrology*, 75(1–4), pp. 365–381.

He, Z., Unger-Shayesteh, K., Vorogushyn, S., Weise, S.M., Duethmann, D., Kalashnikova, O., Gafurov, A. and Merz, B. (2020). Comparing Bayesian and traditional end-member mixing approaches fro hydrohraph separation in glacierized basin. *Hydro. Earth Syst.Sci*, 24, pp.3289-3309.

Hewlett, J. D. and Hibbert, A. R. (1967). Factors Affecting the Response of Small watershed to precipitation in Humid areas, *Forest Hydrology*, 1, pp. 275–290.

Hoeg, S., Uhlenbrook, S. and Leibundgut, C. (2000). Hydrograph separation in a mountainous catchment - combining hydrochemical and isotopic tracers, *Hydrological Processes.*, 14(7), pp. 1199–1216. doi: 10.1002/(SICI)1099-1085(200005)14:7<1199::AID-HYP35>3.0.CO;2-K.

Hooper, R. P., Christophersen, N. and Peters, N. E. (1990). After more than a decade of acid deposition research, quantitative representation of the chemical mechanisms that control streamwater chemistry remains uncertain and elusive. Coupled hydrological and chemical models (hydrochemical models) have been, *Program.*, 116.

Hooper, R. P. and Shoemaker, C. A. (1986). A Comparison of Chemical and Isotopic Hydrograph Separation, *Water Resources Research*.., 22(10), pp. 1444–1454. doi: 10.1029/WR022i010p01444.

Hrachowitz, M., Bohte, R., Mul, M.L., Bogaard, T.A., Savenije, H.H.G. and Uhlenbrook, S. (2011). On the value of combined event runoff and tracer analysis to improve understanding of catchment functioning in a data-scarce semi-arid area, *Hydrology and Earth System Sciences.*, 15(6), pp. 2007–2024. doi: 10.5194/hess-15-2007-2011.

Hu, Y., Maskey, S., Uhlenbrook, S. and Zhao, H. (2011). Streamflow trends and climate linkages in the source region of the Yellow River, China, *Hydrological Processes.*, 25(22), pp. 3399–3411. doi: 10.1002/hyp.8069.

Hugenschmidt, C., Ingwersen, J., Sangchan, W., Sukvanachaikul, Y., Duffner, A., Uhlenbrook, S. and Streck, T. (2014). A three-component hydrograph separation based on geochemical tracers in a tropical mountainous headwater catchment in northern Thailand, *Hydrology and Earth System Sciences.*, 18(2), pp. 525–537. doi: 10.5194/hess-18-525-2014.

Hughes, D. A. (2010). Unsaturated zone fracture flow contributions to stream flow: Evidence for the process in South Africa and its importance, *Hydrological Processes.*, 24(6), pp. 767–774. doi: 10.1002/hyp.7521.

Hughes, D. A., Hannart, P. and Watkins, D. (2003). Continuous baseflow separation from time series of daily and monthly streamflow data, *Water SA.*, 29(1), pp. 43–48.

Hughes G.O.(1997). An analysis of baseflow recession in the Republic of South Africa. [Msc Thesis], University of Natal,Pietermaritzburg.

Hughes, D. A. and Smakhtin, V. (1996). Daily flow time series patching or extension:a spatial interpolation approach based on flow duration curves, *Hydrological Sciences Journal.*, 41(6), pp. 851–871. doi: 10.1080/02626669609491555.

Hussain, F., Nabi, G. and Boota, M. W. (2015). Rainfall Trend Analysis By Using the Mann-Kendall Test & Sen ' S Slope Estimates : a Case Study of District Chakwal Rain Gauge Barani Area, Northen Punjab Province, Pakistan, *Science International (Lahore).*, 27(January), pp. 2–9.

International Atomic Energy Agency, (2002). A new device for monthly rainfall sampling for GNIP.Water & Environmental Newsletter, International Atomic Energy Agency. Special Issue on Global Network of Isotopes in Precipitation, (16), pp.5.

International Atomic Energy Agency,(2009). IAEA-WMO Programme on isotopic composition of precipitation: Global Network of Isotope In Precipitation (GNIP) Technical procedure sampling.

Intergovernmental Panel on Climate Change (IPCC).Climate change (2007). Solomom, S., Qin, D., Manning, M., Marquis, M., Averty.K., Tignor, M.B., Miller, H.l. and Chen, Z (eds). The Physical

Science Basis. Fourth Assessment Report (AR4).

Jia, H. (2007). Groundwater resource evaluation in Table Mountain Group aquifer systems. [PhD Thesis], The University of the Western Cape, Bellville.

James, A. L. and Roulet, N. T. (2007). Investigating hydrological connectivity and its association with threshold change in runoff response in a temperate forested watershed, *Hydrological Processes.*, 21(March), pp. 3391–3408. doi: 10.1002/hyp.

Jung, YY., Koh, DC., Shin,WJ., Kwon, HI., Oh, YH. and Lee, KS. 2021. Assessing seasonal variations in water sources of streamflow in a temperate mesoscale catchment with granitic bedrocks using hydrochemistry and stable isotopes, *Journal of Hydrology: Regional Studies*., 38, pp. 100940

Jury, M.R. (2020). Climate trends in the Cape Town area, South Africa, *Water SA.*, 46 (3), pp. 438-447.

Kang, H. M. and Yusof, F. (2012). Homogeneity Tests on Daily Rainfall Series in Peninsular Malaysia, *International Journal of Contemporary Mathematical Sciences.*, 7(1), pp. 9–22.

Kannan, N., Anandhi, A. and Jeong, J. (2018). Estimation of stream health using flow-based indices, *Hydrology.*, 5(1). doi: 10.3390/hydrology5010020.

Kazemzadeh, M. and Malekian, A. (2018). Homogeneity analysis of streamflow records in arid and semi-arid regions of northwestern Iran, *Journal of Arid Land*., 10(4), pp. 493–506. doi: 10.1007/s40333-018-0064-4.

Kelly, L., Kalin, R.M., Bertram, D., Kanjaye, M., Nkhata, M. and Sibande, H.(2019). Quantification of Temporal Variations in Base Flow Index Using Sporadic River Data: Application to the Bua Catchment, Malawi, *Water*., 11, pp.2-17.

Kendall, C. and Coplen, T. B. (2001). Distribution of oxygen-18 and deuterium in river waters across the United States, *Hydrological Processes.*, 15(7), pp. 1363–1393. doi: 10.1002/hyp.217.

Kendall, M.G. (1975). *Rank Correlation Methods* (4th ed). 2nd Impression, London Griffin.pp.

Kim, B. S., Kim, B. K. and Kwon, H. H. (2011). Assessment of the impact of climate change on the flow regime of the Han River basin using indicators of hydrologic alteration, *Hydrological Processes*., 25, pp.691-704.

Kish, G.; Stringer, C.; Stewart, M.; Rains, M.; Torres, A. (2010). Prepared in cooperation with the Southwest Florida Water Management District A Geochemical Mass-Balance Method for Base-Flow Separation, Upper Hillsborough River Watershed, West-Central Florida, *2003-2005 and 2009*. US Geological Survey, Report 2010-5092.

Kissel, M. and Schmalz, B. (2020). Comparison of baseflow separation methods in the German low mountain range, *Water (Switzerland)*., 12(6). doi: 10.3390/w12061740.

Klaus, J. and McDonnell, J. J. (2013). Hydrograph separation using stable isotopes: Review and evaluation, *Journal of Hydrology*., 505, pp. 47–64. doi: 10.1016/j.jhydrol.2013.09.006.

Kocsis, T., Kovács-Székely, I. and Anda, A. (2020). Homogeneity tests and non-parametric analyses of tendencies in precipitation time series in Keszthely, Western Hungary, *Theoretical and Applied Climatology*., 139(3–4), pp. 849–859. doi: 10.1007/s00704-019-03014-4.

Koskelo, A. I., Fischer, T.R., Utz, R.M. and Jordan, T.E. (2012). A new precipitation-based method of baseflow separation and event identification for small watersheds (< 50 km^2), *Journal of Hydrology*., 450–451, pp. 267–278. doi: 10.1016/j.jhydrol.2012.04.055.

Kouanda, B., Coulibaly, P., Niang, D., Fowe, T., Karambiri, H. and Paturel, J.E. (2018). Analysis of the Performance of Base Flow Separation Methods Using Chemistry and Statistics in Sudano-Sahelian Watershed, Burkina Faso, *Hydrology: Current Research.*, 09(02). doi: 10.4172/2157-7587.1000300.

Kronholm, S. C. and Capel, P. D. (2015). A comparison of high-resolution specific conductance-based end-member mixing analysis and a graphical method for baseflow separation of four streams in hydrologically challenging agricultural watersheds, *Hydrological Processes.*, 29(11), pp. 2521–2533. doi: 10.1002/hyp.10378.

Kruger, F.J. and Wicht, C. (1976). Vegetation and water supply in Mountain Catchments of South Africa, *Council of Habitats ,Conference Mountain environments of South Africa.*, pp. 1–12.

Kruger, F. J. and Bennett, B. M. (2013) 'Wood and water: a historical assessment of South Africa's past and present forestry policies as they relate to water conservation, *Transactions of the Royal Society of South Africa*., 68(3), pp. 163–174. doi: 10.1080/0035919X.2013.833144.

Kværner, J. and Kløve, B. (2006). Tracing sources of summer streamflow in boreal headwaters using isotopic signatures and water geochemical components, *Journal of Hydrology.*, 331(1–2), pp. 186–204. doi: 10.1016/j.jhydrol.2006.05.008.

Łabędzki, L. (2007). Estimation of local drought frequency in central Poland using the standardized precipitation index SPI, *Irrigation and Drainage.*, 56(1), pp. 67–77. doi: 10.1002/ird.285.

Ladouche, B. Probst,A.,Viville, D., Idir, S., Loubet, M., Probst, J.-L. and Bariac, T. (2001). Hydrograph separation using isotopic, chemical and hydrological approaches (Strengbach catchment, France), *Journal of Hydrology.*, 242(3–4), pp. 255–274. doi: 10.1016/S0022-1694(00)00391-7.

Laudon, H. and Slaymaker, O. (1997). Hydrograph separation using stable isotopes, silica and electrical conductivity: An alpine example, *Journal of Hydrology.*, 201(1–4), pp. 82–101. doi: 10.1016/S0022-1694(97)00030-9.

Lee, J., Kim, J., Jang, W.S., Lim, K.J. and Engel, B.A. (2018). Assessment of baseflow estimates considering recession characteristics in SWAT, *Water (Switzerland).*, 10(4), pp. 1–14. doi:

10.3390/w10040371.

Le Maitre, D. C. and Colvin, C. A. (2008). Assessment of the contribution of groundwater discharges to rivers using monthly flow statistics and flow seasonality, *Water SA.*, 34(5), pp. 549–564. doi: 10.4314/wsa.v34i5.180652.

Lesch, W. and Scott, D. F. (1997). The response in water yield to the thinning of Pinus radiata, Pinus patula and Eucalyptus grandis plantations, *Forest Ecology and Management.*, 99 (3), pp. 295–307. doi: 10.1016/S0378-1127(97)00045-5.

L, J., Wang, W., Wang, D., Li, J. and Dong, J. (2020). Hydrochemical and stable isotope characteristics of lake water and groundwater in the Beiluhe Basin Qinghai-Tibet Plateau, Water., 12, pp. 2269

Lin, L. (2007). Hydraulic properties of the Table Mountain Group (TMG) aquifers. [PhD Thesis], University of the Western Cape, Bellville.

Lin, L., Lin, H. and Xu, Y. (2014). Characterisation of fracture network and groundwater preferential flow path in the Table Mountain Group (TMG) sandstones, South Africa, *Water SA.*, 40(2), pp. 263–272.

Liotta, M., Favara, R. and Valenza, M. (2006). Isotopic composition of the precipitations in the central Mediterranean: Origin marks and orographic precipitation effects, *Journal of Geophysical Research Atmospheres.*, 111(19), pp. 1–12. doi: 10.1029/2005JD006818.

Liu, Z., Liu, S., Ye, J., Sheng, F., You, K., Xiong, X. and Lai, G. (2019). Application of a digital filter method to separate baseflow in the small watershed of Pengchongjian in Southern China, *Forests.*, 10(12). doi: 10.3390/F10121065.

Lorenzo-Lacruz, J. Vincente-Serrano, S.M., Gonzalez-Hidalgo, J.C., Lopez-Moreno, J.I. and Cortesi, N. (2013). Hydrological drought response to meteorological drought in the Iberian Peninsula, *Climate Research.*, 58(2), pp. 117–131. doi: 10.3354/cr01177.

Lott, D. A. and Stewart, M. T. (2016). Baseflow separation: A comparison of analytical and mass balance methods, *Journal of Hydrology*., 535, pp. 525–533. doi: 10.1016/j.jhydrol.2016.01.063.

Love, D., Uhlenbrook, S., Twomlow, S. and van der Zaag, P.(2010). Changing hydroclimatic and discharge patterns in the northern Limpopo Basin, Zimbabwe, *Water SA.*, 36(3), pp. 335–350.

Ma, Z., Kang, S., Zhang, L., Tong, L. and Su, X. (2008). Analysis of impacts of climate variability and human activity on streamflow for a river basin in arid region of northwest China, *Journal of Hydrology.*, 352(3–4), pp. 239–249. doi: 10.1016/j.jhydrol.2007.12.022.

Madlala, T. E. (2015). Determination of groundwater-surface water interaction, upper Berg River catchment, South Africa. Msc [Thesis], University of the Western Cape, Bellville.

Madlala, T., Oberholster, T. K. P. and Xu, Y. (2018). Application of multi - method approach to assess groundwater – surface water interactions, for catchment management, *International Journal of Environmental Science and Technology*. https://doi.org/10.1007/s13762-018-1819-3

Mahlalela, P. T., Blamey, R. C. and Reason, C. J. C. (2019). Mechanisms behind early winter rainfall variability in the southwestern Cape, South Africa, *Climate Dynamics*., 53(1–2), pp. 21–39. doi: 10.1007/s00382-018-4571-y.

Mann, H. B. (1945). Nonparametric Tests Against Trend, *Econometrica.*, 13(3), pp. 245–259.

Mathews, R. and Richter, B. D. (2007). Application of the indicators of hydrologic alteration software in environmental flow setting, *Journal of the American Water Resources Association*., 43(6), pp. 1400–1413. doi: 10.1111/j.1752-1688.2007.00099.x.

Mazvimavi, D. and Wolski (2010). Investigating changes over time of annual rainfall in Zimbabwe, *Hydrology and Earth System Sciences.*, 14(12), pp. 2671–2679. doi: 10.5194/hess-14-2671-2010.

McDonnell, J. J. (1990). A Rationale for Old Water Discharge Through Macropores in a Steep, Humid Catchment, *Water Resources Research.*, 26(11), pp. 2821–2832. doi: 10.1029/WR026i011p02821.

McDonnell, J. J., Bonell, M., Stewart, M.K. and Pearce, A.J. (1990). Deuterium variations in storm rainfall: Implications for stream hydrograph separation, *Water Resources Research*., 26(3), pp. 455–458. doi: 10.1029/WR026i003p00455.

McGlynn, B. L., McDonnell., J.J., Siebert, J. and Kendall, C. (2004). Scale effects on headwater catchment runoff timing, flow sources, and groundwater-streamflow relations, *Water Resources Research.*, 40(March), pp. 1–14.

McGuire, K. J. and McDonnell, J. J. (2006). A review and evaluation of catchment transit time modeling, *Journal of Hydrology*., 330(3–4), pp. 543–563. doi: 10.1016/j.jhydrol.2006.04.020.

Mckee, T. B., Doesken, N. J. and Kleist, J. (1993). The relationship of drought frequency and duration to time scales. In: Proceedings of the Ninth Conference on Applied Climatology, *American Metereological Society.*, (Boston), pp. 179–184.

Mei, Y. and Anagnostou, E. N. (2015). A hydrograph separation method based on information from rainfall and runoff records, *Journal of Hydrology*., 523, pp. 636–649. doi: 10.1016/j.jhydrol.2015.01.083.

Midgley, J.J. Scott, D. (1994). The use of stable isotopes of water (D and 18O) in hydrological studies in the Jonkershoek Valley, *Water SA.*, 20(2), pp. 151–154.

Midgley, J. and Schafer, G. (1992). Correlates of water colour in streams rising in Southern Cape catchments vegetated by fynbos and/or forest, *Water SA.*, 18(2), pp. 93–100.

Millares, A., Polo, M. J. and Losada, M. A. (2009) . The hydrological response of baseflow in fractured mountain areas, *Hydrology and Earth System Sciences Discussions*., 6(2), pp. 3359–3384. doi: 10.5194/hessd-6-3359-2009.

Miller, J. A., Dunford, A.J., Swana, K.A., Palcsu, L., Butler, M. and Clarke, C.E. (2017). Stable isotope and noble gas constraints on the source and residence time of spring water from the Table Mountain Group Aquifer, Paarl, South Africa and implications for large scale abstraction, *Journal of Hydrology*., 551, pp. 100–115. doi: 10.1016/j.jhydrol.2017.05.036.

Miller, M. P., Susong, D.D., Shope, C.L., Heilweil, V.M. and Stolp, B.J. (2014). Continuous estimation of baseflow in snowmelt-dominated streams and rivers in the Upper Colorado River Basin: A Chemical Hydrograph Separation Approach, *Water Resources Research.*, 50(8), pp. 6986–6999. doi: 10.1002/2013WR014939.

Milly, P. C. D., Dunne, K. A. and Vecchia, A. V. (2005). Global pattern of trends in streamflow and water availability in a changing climate, *Nature*., 438(7066), 347–350, doi:10.1038/nature04312, 2005.

Misra, A. K. (2014). Climate change and challenges of water and food security, *International Journal of Sustainable Built Environment*., 3(1), pp. 153–165. doi: 10.1016/j.ijsbe.2014.04.006.

Mohuba, S. C., Abiye, T.A., Demlie, M.B., Modiba, M.J. (2020). Hydrogeological Characterization of the Thyspunt Area, Eastern Cape Province, South Africa, *Hydrology*., 7(49), pp. 1–20.

Mokua, R. A., Glenday, J., Nel, J.M. and Butler, M. (2020). Combined use of stable isotopes and hydrochemical characteristics to determine streamflow sources in the Jonkershoek catchment, South Africa, *Isotopes in Environmental and Health Studies*., 0(0), pp. 1–22. doi: 10.1080/10256016.2020.1760861.

Moriasi, D., Arnold, J.G., van Liew, M.W., Binger, R.L., Harmel, R.D. and Veith, T.L. (2007). Model evaluation guidelines for systematic quantification of accuracy in Watershed simulations, *American Society of Agricultural and Biological Engineers*., 50(3), pp. 885–900. doi: 10.1234/590.

Mosquera, G. M., Célleri, R., Lazo, P.X., Vaché, K.B., Perakis, S.S. and Crespo, P. (2016). Combined use of isotopic and hydrometric data to conceptualize ecohydrological processes in a high-elevation tropical ecosystem, *Hydrological Processes*., 30(17), pp. 2930–2947. doi: 10.1002/hyp.10927.

Mul, M. L., Muitiibwa, R.K., Uhlenbrook, S. and Savenije, H.H.G.(2008). Hydrograph separation using hydrochemical tracers in the Makanya catchment, Tanzania, *Physics and Chemistry of the Earth*., 33(1–2), pp. 151–156. doi: 10.1016/j.pce.2007.04.015.

Mul, M. L., Savenije, H. H. G. and Uhlenbrook, S. (2009). Spatial rainfall variability and runoff response during an extreme event in a semi-arid catchment in the South Pare Mountains, *Hydrology and Earth System Sciences*., 13, pp. 1659–1670.

Muñoz-Villers, L. E. and McDonnell, J. J. (2012). Runoff generation in a steep, tropical montane cloud forest catchment on permeable volcanic substrate, *Water Resources Research*., 48(9). doi: 10.1029/2011WR011316.

Nathan, R. J. and McMahon, T. A. (1990). Evaluation of automated techniques for base flow and recession analyses, *Water Resources Research*., 26(7), pp. 1465–1473.

Ngcobo, S., Jewitt, G.P.W., Stuart-Hill, S.I. and Warburton. M. L. (2013). Impacts of global change on southern African water resources systems, *Current Opinion in Environmental Sustainability*., 5(6), pp. 655–666. doi: 10.1016/j.cosust.2013.10.002.

Nienie, A.B., Sivalingam,P., Laffite, A., Ngelinkoto,P., Otamonga, JP., Matand, A., Mulaji, C.K., Mubedi, J.I., Mpiana, P.T. and Poté. (2017). Seasonal variability of quality by physicochemical indexes and traceable metal in suburban area in Kikwit, Democratic Republic of Congo, *International soil and water conservation Research*., 5, pp.158-165.

Nkiaka, E., Nawaz, N. R. and Lovett, J. C. (2017). Using standardized indicators to analyse dry/wet conditions and their application for monitoring drought/floods: a study in the Logone catchment, Lake Chad basin, *Hydrological Sciences Journal*., 62(16), pp. 2720–2736.

Ogunkonya, O.O. and Jenkins, A. .(1993). Analysis of storm hydrograph and flow pathways using three-component hydrograph separation, *Journal of Hydrology*., (142), pp. 71–88.

Otto, F. E. L.,Wolski, P., Lehner, F., Tebaldi, C., van Oldenborgh, G., Hogesteeger, S., Sighn, R., Holden, P., Fučkar, N.S., Odoulami, R. and New, M.(2018). Anthropogenic influence on the drivers of the Western Cape drought 2015-2017, *Environmental Research Letters.*, 13(12). doi: 10.1088/1748-9326/aae9f9.

Partington, D., Brunner, P. Simmons, C.T., Werner, A.D., Therrien, R., Maier, H.R. and Dandy, G.C. (2012). Evaluation of outputs from automated baseflow separation methods against simulated baseflow from a physically based, surface water-groundwater flow model, *Journal of Hydrology.*, 458–459, pp. 28–39. doi: 10.1016/j.jhydrol.2012.06.029.

Partington, D., Brunner,P., Frei, S., Simmons, C.T., Werner, A.D., Therrien, R.,Maier, H.R., Dandy, G.C. and Fleckenstein, J.H. (2013). Interpreting streamflow generation mechanisms from integrated surface-subsurface flow models of a riparian wetland and catchment, *Water Resources Research*., 49(9), pp. 5501–5519. doi: 10.1002/wrcr.20405.

Parsons, R. (2002). Recharge of Table Mountain Group aquifer systems, In Pietersen, K. and Parsons, R. (eds) A synthesis of the hydrogeology of the table mountain group-formation of the research strategy.WRC report no. TT 158/01, 205-208.Water Research Commission, Pretoria.

Penna, D., Tromp-van Meerveld, H.J., Gobbi, A., Broga, M. and Dalla Fontana, G.(2011) The influence of soil moisture on threshold runoff generation processes in an alpine headwater catchment, *Hydrology*

and Earth System Sciences., 15(3), pp. 689–702. doi: 10.5194/hess-15-689-2011.

Penna, D., van Meerveld, H.J., Oliviero, O., Zuecco, G., Assendelft, R.S., Dalla Fontana, G., and Borga, M.. (2015) Seasonal changes in runoff generation in a small forested mountain catchment, *Hydrological Processes.*, 29(8), pp. 2027–2042. doi: 10.1002/hyp.10347.

Pettitt, A.N.(1979). A Non-Parametric Approach to the change -point problem, *Applied Statistics*., 28 (2), pp 126-135

Pfister, L.,Martinez-Carreras, N., Hissler, C., Klaus, J., Carrer, G.E., Stewart, M.K. and McDonnell, J.J. (2017). Bedrock geology controls on catchment storage, mixing, and release: A comparative analysis of 16 nested catchments, *Hydrological Processes.*, 31(10), pp. 1828–1845. doi: 10.1002/hyp.11134.

Pinder, G.F., Jones, J. F. (1969). Determination of the Ground- Water Component of Peak Discharge from the Chemistry of Total Runoff, *Water Resource.Research*., pp. 438–445.

Pramono, I, B., Budiastuti, M.Th, S., Gunawan, T. and Wiryanto (2017). Base Flow from Various Area of Pine Forest at Kedungbulus Sub Watershed, Kebumen District, Central Java, Indonesia, *International Journal of Developments and Sustainability*., 6, pp. 99–114.

Price, K. (2011). Effects of watershed topography, soils, land use, and climate on baseflow hydrology in humid regions: A review, *Progress in Physical Geography.*, 35(4), pp. 465–492. doi: 10.1177/0309133311402714.

Price, K., C. Rhett Jackson, C.R., Parker, A.J., Reitan, T., Dowd, J. and Cyterski.M..(2011). Effects of Watershed Land Use and Geomorphology on Stream Low Flows during Severe Drought Conditions in the Southern Blue Ridge Mountains, Georgia and North Carolina, United States, *Water Resource Research,* 47 (2), pp. 2516-2534.

Raffensperger, J. P., Baker, A.C., Blomquist, J.D., and Hopple, J.A. (2017). Optimal hydrograph separation using a recursive digital filter constrained by chemical mass balance, with application to selected Chesapeake Bay watersheds. National Water Quality Program Assessment Project, U.S. Geological Survey. Scientific Investigations Report 2017-5034. doi: 10.1007/s002650050467.

Rebelo, A.G., Boucher, C., Helme, N., Mucina, L. and Rutherford, C. (2006). Fynbos Biome Project. Sterlitzia, 19, pp. 55-56.

Renshaw, C. E., Feng, X., Sinclair, K.J. and Dums, R.H. (2003). The use of stream flow routing for direct channel precipitation with isotopically-based hydrograph separations: The role of new water in stormflow generation, *Journal of Hydrology.*, 273(1–4), pp. 205–216. doi: 10.1016/S0022-1694(02)00392-X.

Richter, B. D., Baumgartner, J.V., Braun, D.P. and Powell, J. (1998). Spatial assessment hydrologic

alteration within a river network, *Regulated Rivers Research and Management*., 14, pp. 329–340.

Rijsberman, F. R. (2006). Water scarcity: Fact or fiction?, *Agricultural Water Management.*, 80(1–3 SPEC. ISS.), pp. 5–22. doi: 10.1016/j.agwat.2005.07.001.

Rimmer, A. and Hartmann, A. (2014). Optimal hydrograph separation filter to evaluate transport routines of hydrological models, *Journal of Hydrology*., 514, pp. 249–257. doi: 10.1016/j.jhydrol.2014.04.033.

Rodgers, P., Soulsby, C., Waldron, S. and Tetzlaff, D. (2005). Using stable isotope tracers to identify hydrological flow paths, residence times and landscape controls in a mesoscale catchment, *Hydrology and Earth System Sciences Discussions*., 2(1), pp. 1–35. doi: 10.5194/hessd-2-1-2005.

Roets, W., Xu, Y., Raitt, L., El-Kahloun, M., Meire, P., Calitz, F., Batelaan, O., Anibas, C., Parideans, K., Vandenbroucke, T., Verhoest, N.E.C. and Brendonck, L. (2008). Determining discharges from the Table Mountain Group (TMG) aquifer to wetlands in the Southern Cape, South Africa, *Hydrobiologia*., 607(1), pp. 175–186. doi: 10.1007/s10750-008-9389-x.

Roets, W., Xu, Y., Raitt, L. and Brendonck, L. (2008). Groundwater discharges to aquatic ecosystems associated with the Table Mountain Group (TMG) aquifer: A conceptual model, *Water SA*., 34(1), pp. 77–88.

Rosewarne, P. (2002). Hydrogeological characteristics of the Table Mountain Group aquifer.In: Pietersen, K. and Parsons, R. (eds) A synthesis of the hydrogeology of the table mountain group-formation of the research strategy.WRC report no. TT 158/01, 205-208. Water Research Commission, Pretoria.

Rouault, M. and Richard, Y. (2003). Intensity and spatial extension of drought in South Africa at different time scales, *Water SA*., 29(4), pp. 489–500. doi: 10.4314/wsa.v29i4.5057.

Rumsey, C. A., Miller, M. P. and Sexstone, G. A. (2020). Relating hydroclimatic change to streamflow, baseflow, and hydrologic partitioning in the Upper Rio Grande Basin, 1980 to 2015, *Journal of Hydrology.*, 584. doi: 10.1016/j.jhydrol.2020.124715.

Rust, I. C. (1967) On the sedimentation of the Table Mountain Group in the Western Cape Province.[D.Sc. Thesis], Stellenbosch University, unpublished.

Rutledge, A. T. (1998). Computer programs for describing the recession of ground-water discharge and for estimating mean ground-water recharge and discharge from streamflow records-Update, U.S. Geological Survey Water-Resources Investigations Report 98–4148, pp. 52.

Salmi, T., Määttä, A., Anttila, P., Tuija, R. and Ammell, T.(2002). Detecting trends of annual values of atmospheric pollutants by the Mann-Kendall test and Sen's slope estimates-The excel template application MAKESENS.Publication on air quality, 31. Finnish Meteorological Institute, Helsinki.

Saayman, I.C., Scott, D.F., Prinsloo, F.W., Moses, G., Weaver, J. M. C. (2003). Evaluation of the application of natural isotopes in the identification of the dominant streamflow generation mechanisms in TMG catchments. WRC Report no.1234/1/03, Water Research Commission, Pretoria.

SAEON (2019). South Africa Environmental Observation Network (SAEON) Observation Database,. doi: .1037//0033-2909.I26.1.78.

Santhi, C., Allen, P.M., Muttiah, R. S.., Arnold, J. G. and Tuppad, P. (2008). Regional Estimation of Base Flow for the Conterminous United States by Hydrologic Landscape Regions, *Journal Hydrology*., 351, pp.139–53.

Saraiva Okello, A. M. L., Masih, I., Uhlenbrook, S., Jewitt, G.W.P., Van der Zaag, P. and Riddell, E. (2015). Drivers of spatial and temporal variability of streamflow in the Incomati River basin, *Hydrology and Earth System Sciences.*, 19(2), pp. 657–673. doi: 10.5194/hess-19-657-2015.

Saraiva Okello, A. M. L., Uhlenbrook, S., Jewitt, G.P.W., Masih, I., Riddell, E.S. and Van der Zaag, P.(2018). Hydrograph separation using tracers and digital filters to quantify runoff components in a semi-arid mesoscale catchment, *Hydrological Processes.*, 32(10), pp. 1334–1350. doi: 10.1002/hyp.11491.

Saraiva Okello, A. M. L. (2018). Improved hydrological understanding of semi-arid subtropical transboundary basin using multiple techniques: The Incomati River Basin. [PhD Thesis], Delft University of Technology, The Netherlands.

Schulze, R. E. (2011). Approaches towards practical adaptive management options for selected water-related sectors in South Africa in a context of climate change, *Water SA.*, 37(5), pp. 621–646. doi: 10.4314/wsa.v37i5.1.

Scott, D. F. (1994). The hydrological effects of fire in South African mountain catchments, [PhD thesis], University of Natal, Pietermaritzburg. doi: 10.1016/0022-1694(93)90119-T.

Scott, D. F. (1997).The contrasting effects of wildfire and clear-felling on the hydrology of a small catchment, *Hydrological Processes.*, 11(May 1995), pp. 543–555.

Scott, D. F., Prinsloo, F.W., Moses, G., Mehlomakulu, M. and Simmers, A.D.A. (2000). A re-analysis of the South African catchment afforestation experimental data, WRC report no. 810/1/00, Water Research Commission, Pretoria. pp.1-138.

Scott, D. F. and Prinsloo, F. W. (2008). Longer-term effects of pine and eucalypt plantations on streamflow, 44(July), *Water Resources Research*., 44.,pp. 1–8. doi: 10.1029/2007WR006781.

Scott, D.F. and Gush, M. B. (2017). Forest management and water in the Republic of South Africa, In Garcia-Chevisich, P. B., Neary, D.G., Scott, D.F., Benyon, R.G. and Reyna, T (eds), Forest management and impact on water resources: A review of 13 countries, UNESCO, pp. 159-165

Shao, G., Zhang, D., Guan, Y., Sadat, M.A. and Huang, F. (2020). Application of Different Separation Methods to Investigate the Baseflow Characteristics of a Semi-Arid, Northwestern China, *Water*., 12(434), pp. 1–22.

Sidle, R. C., Tsuboyama,Y., Noguchi, S., Hosoda, I., Fujieda, M. and Shimizu, T. (1995). Seasonal hydrologic response at various spatial scales in a small forested catchment, Hitachi Ohta, Japan, *Journal of Hydrology*., 168, pp. 227–250.

da Silva, R. M., Santos, C.A.G., Moreira, M., Corte-Real, J., Silva, V.C.L. and Medeiros, I.C. (2015). Rainfall and river flow trends using Mann–Kendall and Sen's slope estimator statistical tests in the Cobres River basin, *Natural Hazards.*, 77(2), pp. 1205–1221. doi: 10.1007/s11069-015-1644-7.

Singh, J., Knapp, H.V. and Demissie, M.(2005). Hydrological modeling of the Iroquois River watershed using HSPF and SWAT, *Journal of the American Water Resources Association*., 41(2), pp. 343–360. doi: 10.1111/j.1752-1688.2005.tb03740.x.

Sivapalan, M. (2003). Process complexity at hillslope scale, process simplicity at the watershed scale : is there a connection ?Hydrological Processes., 17, pp. 1037–1041. doi: 10.1002/hyp.5109.

Smart, M.C. and Tredoux,G. (2002). Groundwater quality and fitness for use. In: Pietersen, K. and Parsons, R. (eds) A synthesis of the hydrogeology of the table mountain group-formation of the research strategy.WRC report no. TT 158/01, Water Research Commission, Pretoria. pp.205-208.

Sklash, R.N, Farvolden, M. . (1979) 'Role of Groundwater in storm runoff, *Journal of Hydrology*., 43, pp. 45–65.

Sklash, M. G., Stewart, M. K. and Pearce, A. J. (1986) 'Storm Runoff Generation in Humid Headwater Catchments: 2. A Case Study of Hillslope and Low-Order Stream Response, *Water Resources Research.*, 22(8), pp. 1273–1282. doi: 10.1029/WR022i008p01273.

Slingsby, J. A., de Buys, A., Simmers, A.D.A., Prinsloo, E., Forsyth, G.G., Glenday, J. and Allsopp, N. (2021). Jonkershoek: Africa's oldest catchment experiment - 80 years and counting, *Hydrological Processes.*, pp. 0–3. doi: 10.1002/hyp.14101.

Smakhtin, V. U. (2001). Estimating continuous monthly baseflow time series and their possible applications in the context of the ecological reserve, *Water SA.*, 27(2), pp. 213–217.

Smakhtin, V. U. (2001). Low flow hydrology: A review, *Journal of Hydrology.*, 240(3–4), pp. 147–186. doi: 10.1016/S0022-1694(00)00340-1.

Smakhtin, V. Y. and Watkins, D. A. (1997). Low Flow Estimation in South Africa: Classification and Hydrological modelling of low flows in Southern Africa, WRC Report 494/1/97, Water Research Commission, Pretoria, pp. 1–573.

Spencer, S.A., Anderson, A.E., Silins, U. and Collins, A.L.(2021). Hillslope and groundwater

contributions to streamflow in a Rocky Mountain watershed underlain by glacial till and fractured sedimentary bedrock. *Hydrology of Earth System Sciences*., 25, pp. 237 -255.

Song, X., Xiangchao, L., Jun, X., Jingjie, Y.U. and Changyuan, T.(2006). A study of interaction between surface water and groundwater using environmental isotope in Huaisha River basin, *Science in China, Series D: Earth Sciences*., 49(12), pp. 1299–1310. doi: 10.1007/s11430-006-1299-z.

Soulsby, C., Rodgers, P., Smart, R., Dawson, J. and Dunn, S.(2003). A tracer-based assessment of hydrological pathways at different spatial scales in a mesoscale Scottish catchment, *Hydrological Processes.*, 17, pp. 759–777. doi: 10.1002/hyp.1163.

Soulsby, C., Neal, C., Laudon.H., Burns, D.A., Merot, P., Bonell.M., Dunn, S.M. and Tetzlaff,D. (2008). Catchment data for process conceptualization: simply not enough?, *Hydrological Processes.*, 22(2008), pp. 2057–2061. doi: 10.1002/hyp.

Stewart, M., Cimino, J. and Ross, M. (2007). Calibration of base flow separation methods with streamflow conductivity, *Ground Water*., 45(1), pp. 17–27. doi: 10.1111/j.1745-6584.2006.00263.x.

Stewart, M. K. (2015). Promising new baseflow separation and recession analysis methods applied to streamflow at Glendhu Catchment, New Zealand, *Hydrology and Earth System Sciences*., 19(6), pp. 2587–2603. doi: 10.5194/hess-19-2587-2015.

Stone, A. (1985). Swartboskloof groundwater investigation interim report of findings. Discussion document for Rhodes University, Forestry research and University of Cape Town meeting, 25 June 1985. Unpublished report.

Sueker, J. K. Ryan, J.N., Kendall, C. and Jarrett, R.D. (2000).Determination of hydrologic pathways during snowmelt for alpine/subalpine basins, Rocky Mountain National Park, Colorado, *Water Resources Research*., 36(1), pp. 63–75. doi: 10.1029/1999WR900296.

Sun, H., Kasahara, T., Otsuki, K., Saito, T., and Onda, Y. (2017). Spatio-temporal streamflow generation in a small, steep headwater catchment in western Japan, *Hydrological Sciences Journal*., 62(5), pp. 818–829. doi: 10.1080/02626667.2016.1266635.

Tallaksen, L. M. (1995). A review of baseflow recession analysis, *Journal of Hydrology*., 165(1–4), pp. 349–370. doi: 10.1016/0022-1694(94)02540-R.

Tashie, A., Pavelsky, T. and Emanuel, R. E. (2020). Spatial and Temporal Patterns in Baseflow Recession in the Continental United States, *Water Resources Research (Accepted Manuscript)*. doi: 10.1029/2019WR026425.

Tashie, A., Scaife, C. I. and Band, L. E. (2019).Transpiration and subsurface controls of streamflow recession characteristics, *Hydrological Processes.*, 33(19), pp. 2561–2575. doi: 10.1002/hyp.13530.

Taylor,V., Jewitt, G. and Schulze, R.(2003). Indicators of Hydrologic alterations for assessing

environmental flows for highly variable river. Unpublished.

Tekleab , S. (2015). Understanding catchment processes and hydrological modelling in the Abay/Upper Blue Nile basin, Ethiopia.[PhD Thesis], Delft University of Technology, The Netherlands.

Tekleab, S., Wenninger, J. and Uhlenbrook, S. (2014). Characterisation of stable isotopes to identify residence times and runoff components in two meso-scale catchments in the Abay/Upper Blue Nile basin, Ethiopia', *Hydrology and Earth System Sciences*., 18(6), pp. 2415–2431. doi: 10.5194/hess-18-2415-2014.

Tessema, N., Kebede, A. and Yadeta, D. (2020). Modeling the Effects of Climate Change on Streamflow Using Climate and Hydrological Models : The case of the Kesem Sub-basin of the Awash River Basin, Ethiopia., *International Journal of River Basin Management*, pp. 1–46.

Thamm, A. G. (2000). Lithostratigraphy of the Graafwater Formation (Table Mountain Group), *South African Committee for Stratigraphy - Lithostratigraphic Series.*, 35(May).

Thamm, A.G. and Johnson, M.R. (2006). The Cape Supergroup, in Johnson, M.R., Anhaeusser,C.R., and Thomas, R.J. (eds).The geology of South Africa. Geological Survey of South Africa, Council for Geoscience, Pretoria, pp.443-460

van Tol, J. (2020) 'Hydropedology in South Africa: Advances, applications and research opportunities', *South African Journal of Plant and Soil.*, 37(1), pp. 23–33. doi: 10.1080/02571862.2019.1640300.

Uchida, T., Asano, Y., Ohte, N. and Mazuyama.T. (2003). Seepage area and rate of bedrock groundwater discharge at a granitic unchanneled hillslope, *Water Resources Research.*, 39(1), pp. 1–12. doi: 10.1029/2002WR001298.

Uhlenbrook, S., Frey, M., Leibundgut, and Maloszewski, P. (2002). Hydrograph separations in a mesoscale mountainous basin at event and seasonal timescales, *Water Resources Research.*, 38(6), p. 1096.

Uhlenbrook, S., Roser, S. and Tilch, N. (2004). Hydrological process representation at the meso-scale: The potential of a distributed, conceptual catchment model, *Journal of Hydrology.*, 291(3–4), pp. 278–296. doi: 10.1016/j.jhydrol.2003.12.038.

van Wilgen, B.W. (1981). Some effects of fire frequency on the aerial plant biomass of Fynbos communities at Jonkershoek, Stellenbosch.*South African Forestry Journal.*, 118, pp. 42-55.

Vegter, J.R. and Pitman.W.V.(2003).Recharge and stream flow, in Xu, Y. and Beekman, H.E.(eds).Groundwater recharge and estimation in Southern Africa.UNESCO Paris., pp. 109-123.

Vicente-Serrano, S. M., Gonzalez-Hildalgo, J.C., de Luis, M. and Raventos, J. (2004). Drought patterns in the Mediterranean area: The Valencia region (eastern Spain), *Climate Research.*, 26(1), pp. 5–15. doi: 10.3354/cr026005.

Vitvar, T., Aggarwal, P. K. and Mcdonnell, J. J. (2003). A Review of Isotope Applications in Catchment Hydrology, pp. 151–169.

Van Wageningen, A. and Du Plessis, J. A. (2007). Are rainfall intensities changing, could climate change be blamed and what could be the impact for hydrologists, *Water SA*, 33(4), pp. 571–574.

Walker, J.F., Hunt , R., Bullen, T.D., Krabbenhoft, D.P., and Kendall,C. (2003). Variability of isotope and major ion chemistry in the Allequash Basin, Wisconsin. *Groundwater*., 41 (7), pp.883-894.

Warburton, M.L., Schulze, R.E. and Maharaj,M. (2005). Is South Africa's temperature changing? An analysis of trends from daily records, 1950-2000, in Schulze, R.E (ed)Climate change and water resources in Southern Africa: Studies on Scenarios, Impacts, Vulnerabilities and Adaptation.WRC Report 1430/1/05.Water Research Commission, Pretoria, pp. 275-295.

Weaver, J. M. C., Talma, A. S. and Cavé, L. C. (1999). Geochemistry and isotopes for resource evaluation in the fractured rock aquifers of the Table Mountain Group, WRC Report 481/1/99(481), Water Research Commission, Pretoria.

Welderufael, W. and Woyesssa, Y. (2010). Streamflow analysis and comparison of base flow separation method, *European Water.*, 31, pp. 3–12.

Wenninger, J.,Uhlenbrook, S., Lorentz, S. and Leibundgut, C.. (2008). Identification of runoff generation processes using combined hydrometric, tracer and geophysical methods in a headwater catchment in South Africa, *Hydrological Sciences Journal.*, 53(1), pp. 65–80. doi: 10.1623/hysj.53.1.65.

Wicht, C. (1934). A preliminary account of Rainfall in Jonkershoek, *Royal Society of South Africa*., XXII(28(b)), pp. 161–173.

Van Loon, A. F. and Laaha, G. (2015). Hydrological drought severity explained by climate and catchment characteristics, *Journal of Hydrology*., 526, pp. 3–14.

Van Wilgen, B. W. (1994). Some Effects of Fire Frequency on Fynbos at Jonkershoek, Stellenbosch, South Africa. Msc [Thesis], University of Cape Town, Cape Town.

Wolski, P., Conradie, S., Jack, C. and Tadross,M. (2020). Spatio-temporal patterns of rainfall trends and the 2015–2017 drought over the winter rainfall region of South Africa, *International Journal of Climatology*., 41(S1), pp. E1303–E1319. doi: 10.1002/joc.6768.

Wu, Y. (2005). Groundwater recharge estimation in Table Mountain Group Aquifer systems. [PhD Thesis], The University of the Western Cape, Bellville.

Xu, Y. and Beekman, H. E. (2003). Groundwater Recharge Estimation in Southern Africa, UNESCO IHP Series No 64. doi: 10.3109/00016486709127791.

Xu, Y., Lin, L. and Jia, H. (2009). Groundwater Flow Conceptualization and Storage Determination of the Table Mountain Group (TMG) Aquifers.WRC Report 1419/1/09, Water Research Commision, Pretoria.

Xu,D., Jiao-Jiao,H. and Yang-Yi,Z. (2020). Characterization of soil water by means of hydrogen and oxygen isotope ratio at dry-wet season under different soil layers in dry-hot valley of Jinsha River,*Open Chemistry*., 18, pp.822-832.

Yang, H., Choi, H. T. and Lim, H. (2018). Applicability assessment of estimation methods for baseflow recession constants in small forest catchments, *Water (Switzerland)*., 10(8). doi: 10.3390/w10081074.

Yang, W., Xiao, C. and Liang, X. (2019) .Technical note: Analytical sensitivity analysis and uncertainty estimation of baseflow index calculated by a two-component hydrograph separation method with conductivity as a tracer, *Hydrology and Earth System Sciences*., 23(2), pp. 1103–1112. doi: 10.5194/hess-23-1103-2019.

Yao, L., Sankarasubramanian, A. and Wang. D. (2021). Climatic and Landscape Controls on Long-Term Baseflow, *Water Resour. Resources.*, 57 (6), pp. 1–20, https://doi.org/10.1029/2020WR029284.

Yue, S., Pilo, P., Phinney, B. and Cavadias, G. (2002). The influence of autocorrelation on the ability to detect trend in hydrological series, *Hydrological Processes.*, 16(9), pp. 1807–1829. doi: 10.1002/hyp.1095.

Yue, S. and Hashino, M. (2003). Long-term trends of annual and monthly precipitation in Japan, *Journal of the American Water Resources Association*., 39(3), pp. 587–596. doi: 10.1111/j.1752-1688.2003.tb03677.x.

Yue, S. and Wang, C. Y. (2004). The Mann-Kendall test modified by effective sample size to detect trend in serially correlated hydrological series, *Water Resources Management*, 18(3), pp. 201–218. doi: 10.1023/B:WARM.0000043140.61082.60.

Zhang, J., Zhang, Y., Song, J. and Cheng, L.(2017). Evaluating relative merits of four baseflow separation methods in Eastern Australia, *Journal of Hydrology*., 549, pp. 252–263. doi: 10.1016/j.jhydrol.2017.04.004.

Zhang, N., Xia, Z., Zhang, S. and Jiang,H. (2012). Temporal and spatial characteristics of precipitation and droughts in the upper reaches of the Yangtze River basin (China) in recent five decades, *Journal of Hydroinformatics.*, 14(1), pp. 221–235. doi: 10.2166/hydro.2011.097.

Zhang, R., Li, Q., Chow, T.L., Li, S. and Danielescu, S. (2013). Baseflow separation in a small watershed in New Brunswick, Canada, using a recursive digital filter calibrated with the conductivity mass balance method, *Hydrological Processes.*, 27(18), pp. 2659–2665. doi: 10.1002/hyp.9417.

Zhang, X., Zhang, L., Zhao, J., Rustomji, P. and Hairsine, P. (2008). Responses of streamflow to changes in climate and land use/cover in the Loess Plateau, China, *Water Resources Research.*, 45(7), pp. 1–12. doi: 10.1029/2007WR006711.

Zhao, S., Hu, H., Harman, C.J., Tian, F., Tie, Q., Lui, Y. and Peng, Z. (2019). Understanding of storm runoff generation in a weathered, fractured granitoid headwater catchment in northern China, *Water (Switzerland).*, 11(1), pp. 1–22. doi: 10.3390/w11010123.

Zhou, J., Wu, J., Lui, S., Zeng, G., Qin, J., W. and Zhao, Q. (2015). Hydrograph Separation in the Headwaters of the Shule River Basin: Combining Water Chemistry and Stable Isotopes, *Advances in Meteorology*., 2015(January). doi: 10.1155/2015/830306.

Appendix A

Table.A. 1. Monthly streamflow Mann Kendall trend analysis. The statistically significant decreasing trends are in bold and

	Bosboukloof		**Tierkloof**		**Langrivier**	
Month	**Z_{MK}**	**Signf. trend**	**Z_{MK}**	**Signf. trend**	**Z_{MK}**	**Signf. trend**
Jan	**-1.85**	*	**-2.44**	*	-0.91	
February	**-2.32**	*	**-2.88**	*	**-2.01**	*
March	**-1.95**		**-2.87**	*	**-2.04**	*
April	**-2.30**	*	**-2.26**	*	**-2.28**	*
May	**-2.76**	*	**-2.25**	*	-1.82	
June	-0.99		-0.27		0.14	
July	-0.57		-0.60		-1.19	
August	-0.64		-1.90		-2.09	
September	-0.92		**-2.20**	*	**-1.85**	*
October	-1.45		**-3.48**	*	**-3.05**	*
November	-1.07		**-2.30**	*	-1.68	
December	**-1.96**	*	**-2.68**	*	-1.32	

Level of significance: * If trend at α=0.05; no symbol= the significance level is greater than 0.

Table.A.2. Monthly rainfall Mann Kendall trend analysis. The statistically significant decreasing trends are in bold and statistically significant increasing trends in red.

	Bosboukloof 5B		**Bosboukloof 11B**		**Tierkloof 9B**		**Tierkloof 13B**		**Langrivier 8B**		**Langrivier 14B**	
Month	**Z_{MK}**	**Signf. trend**	**Z_{MK}**	**Signf. trend**	**Z_{MK}**	**Signf. trend**	**Z_{MK}**	**Signf. trend**	**Z_{MK}**	**Signf. trend**	**Z_{MK}**	**Signf. trend**
Jan	0.31		0.76		0.62		0.21		0.21		0.59	
February	0		0.35		-0.15		0.11		-0.39		0.09	
March	-1.28		-0.16		-1.62		-0.62		-1.21		0.35	
April	**-2.09**	***, Decr**	-1.10		**-2.15**	***, Decr**	-1.23		**-1.90**	***,Decr**	-1.44	
May	**-3.05**	***, Decr**	**-2.32**	***, Decr**	**-2.82**	***, Decr**	**-2.31**	***, Decr**	**-3.00**	***, Decr**	**-2.51**	***, Decr**
June	-0.62		-0.06		0.64		0.16		0.33		-0.17	
July	**-1.99**	***, Decr**	-1.47		-1.50		-1.42		-1.06		**-1.84**	
August	-1.58		-0.64		0.08		-0.52		-1.47		-1.25	
September	**-1.85**		-1.30		-1.28		-1.18		-0.73		-1.27	
October	**-1.82**		**-2.13**	***, Decr**	**-2.42**	***, Decr**	**-2.04**	***, Decr**	**-2.48**	***, Decr**	**-2.50**	***, Decr**
November	**-2.04**	***, Decr**	-0.41		0.00		-0.22		-1.08		-0.51	
December	-0.79		-0.62		-0.39		-0.59		-0.37		-0.73	

Level of significance: * If trend at $\alpha = 0.05$; no symbol the significance level is greater than

Table.A.3. Summary of the Standardized Precipitation Index (SPI) and Standardized Streamflow Index (SSI) values for a 12-month time scale.

	SPI			SSI		
Hydrologic Year	**Bosboukloof**	**Tierkloof**	**Langrivier**	**Bosboukloof**	**Tierkloof**	**Langrivier**
1945	0.64	0.99	1.09			
1946	0.01	-0.21	0.05	0.2	-0.02	1.96
1947	-0.28	-0.22	0.11	0.42	0.42	0.14
1948	0.3	-0.36	-0.2	0.09	0.31	0.3
1949	-0.7	-0.94	-0.9	-0.26	-0.32	-0.59
1950	0.34	-0.35	-0.19	-0.15	0.27	0.8
1951	1.55	1.43	1.52	1.14	1.6	1.8
1952	0.14	-0.17	0.04	0.13	0.52	0.15
1953	0.96	0.67	1	1	1.73	1.53
1954	1.49	1.15	1.55	1.3	1.99	1.84
1955	1.31	0.95	1.06	0.82	1.38	1.18
1956	0.48	0.52	0.6	0.85	1.27	1.13
1957	1.11	0.76	1.04	0.59	1.11	0.67
1958	0.35	0.61	0.65	0.51	1.13	0.66
1959	0.59	0.25	0.37	0.19	0.65	0.24
1960	-0.42	-0.39	-0.32	-0.68	-0.28	-0.79
1961	-0.42	-0.67	-0.46	-1.39	-0.44	-0.67
1962	1.67	1.32	1.21	0.5	1.43	0.84
1963	-0.24	-0.26	0.17	-0.03	0.54	-0.23
1964	-0.42	-0.44	-0.14	-1.2	-0.7	-0.81
1965	0.27	-0.03	-0.04	-0.77	-0.38	-0.02
1966	0.14	0.06	0.16	-0.61	-0.61	-0.41
1967	0.21	-0.47	-0.33	-0.49	-0.49	-0.4
1968	0.58	0.80	0.62	0.22	0.24	0.32
1969	-0.65	-0.71	-0.65	-0.83	-1.18	-0.9
1970	0.23	0.26	0.28	-0.4	-0.32	-0.11
1971	-0.94	-0.89	-0.79	-0.62	-0.83	-0.74
1972	-0.46	-0.38	-0.38	-1.41	-1.59	-1.33
1973	-1.22	-1.55	-1.6	-2.55	-2.41	-1.9
1974	0.73	0.44	0.45	-0.55	-0.24	0.17
1975	0.15	0.46	0.35	0.39	0.2	0.27
1976	0.95	0.64	0.43	0.16	-0.02	0.19
1977	2.58	3.41	2.96	2.38	2.71	2.62
1978	-0.96	-1.24	-0.99	-0.05	-0.9	-1.27
1979	-0.24	-0.51	-0.3	-0.83	-1.04	-0.74
1980	-0.19	-0.25	-0.32	-0.34	-1.08	-0.8
1981	0.38	0.82	0.74	0.39	-0.45	0.01
1982	-0.4	-0.86	-0.91	0.07	-0.98	-0.96
1983	0.9	1.22	1.4	1.26	0.8	1.14
1984	0.2	-0.64	-0.56	0.58	-0.42	-0.28
1985	0.72	1.50	1.12	1.29	0.69	1.03
1986	0.13	0.51	0.77	1.32	0.46	0.54
1987	0.48	0.29	0.22	1.22	0.13	0.01

1988	-0.26	-0.09	0.1	0.67	-0.23	-0.09
1989	0.48	0.44	0.69	0.56	0.09	0
1990	0.47	0.32	0.6	1.33	0.81	1.13
1991	0.53	0.25	0.31	0.95	0.47	0.25
1992	0.09	0.83	0.4	1.34	0.94	0.76
1993	0.98	1.71	1.42	1.81	1.55	1.06
1994	-0.76	-0.86	-0.77	0.08	-0.62	-0.33
1995	0.38	-0.52	-0.57	-0.22	-0.9	-0.94
1996	0.62	0.53	0.5	1.12	0.17	0.17
1997	-0.21	0.60	0.53	1.51	0.71	1.23
1998	-0.8	-0.10	0.56	0.08	-0.06	-0.22
1999	-0.57	1.72	-0.18	-0.49	-0.28	-0.49
2000	-2	0.55	-1.28	-1.33	-0.88	-0.92
2001	0.6	0.93	0.41	0.22	0.65	0.85
2002	0.15	0.61	0.57	0.25	0.82	0.36
2003	1.5	-0.30	-0.47	-0.79	-0.53	-1.63
2004	-1.55	-0.92	-0.84	-1.54	-0.81	-1.08
2005	-0.59	0.08	0.07	-0.77	0	-0.25
2006	-0.77	-0.69	-0.55	-1.14	-0.64	0.45
2007	-0.18	0.54	0.41	-0.22	-0.05	-0.11
2008				0.36	1.04	1.63
2009						
2010						
2011						
2012	-0.76	-1.16	-0.81	-0.75	0.03	-0.25
2013	-0.56	-1.06	-0.56	0.45	0.77	0.43
2014	-1.3	-1.55	-1.36	0.53	0.32	-0.27
2015	-1.95	-2.39	-2.72	-0.87	-1.17	-1.9
2016	-2.16	-2.23	-2.43	-1.5	-1.42	-1.56
2017	-1.56	-2.96	-3.16	-2.86	-2.84	-2.67
2018	-0.63	-0.85	-0.54	-1.85	-1.59	-1.12
2019	-0.76	-0.65	-0.64	-0.81	-1.27	-1.11

Appendix B

Table B. 1. Preliminary water quality results for stream, piezometer and borehole sample in Jonkershoek.

bemlab
www.bemlab.co.za
Part of Full-Care

sanas
Testing Laboratory
T0654

16 Van der Berg Crescent
Gant's Centre
Strand

P O Box 684
Somerset Mall,
7137

Tel. (021) 853-1490
Fax (021) 853-1423

E-Mail admin@bemlab.co.za

Vat Reg. Nr. 4200161414

CERTIFICATE OF ANALYSES

Report Nr.: **WT005746.DOC**

Retang Mokua
University of Western Cape
Dept. Enviro and Water Sciences

Date received: **11-04-2019**
Time received: **09:05**

Sampled by Retang Mokua

Water Analyses Report

Origin	Lab. Nr.	pH @ 25°C	EC @ 25°C mS/m	Na mg/l	K mg/l	Ca mg/l	Mg mg/l	Cl mg/l	CO_3^{2-} mg/l	HCO_3^- mg/l	SO_4 mg/l	B mg/l	Cu mg/l	Zn mg/l	P mg/l	NH_4-N mg/l	NO_3-N mg/l	*F mg/l	*TDS mg/l
ST- LGL- 006a	5746	6.3	3	3.0	<0.47	0.6	0.5	11.9		7.5	<1.43	0.08	<0.02	<0.03	0.16	<0.28	<0.36	0.2	17.6
P2- LP3- 006a	5747	7.1	6	5.5	0.7	0.8	0.9	21.7		8.7	<1.43	<0.08	<0.02	<0.03	0.05	<0.28	<0.36	0.1	34.2
CN- BHU- 004a	5748	7.6	13	16.9	0.6	10.1	2.9	28.2		57.9	2	<0.08	<0.02	0.04	0.11	<0.28	<0.36	0.7	75.8

Origin	Lab. Nr.	Alkalinity as CaCo3 (mg/l)	Date Sampled	*Si mg/l	Temperature at reception (°C)	*Total Fe mg/l	*Total Mn mg/l	*Dissolved Fe mg/l	*Dissolved Mn mg/l	Date Analysed
ST- LGL- 006a	5746	<11.49	05/07/2019	0.85	21.4	0.22	0.01	0.03	0.00	15/04/2019
P2- LP3- 006a	5747	<11.49	05/07/2019	1.19	21.3	0.09	0.00	0.03	0.00	15/04/2019
CN- BHU- 004a	5748	48.55	05/07/2019	6.69	21.3	0.03	0.00	0.02	0.00	15/04/2019

** = Not SANAS Accredited*

Statement: The reported results may be applied only to samples received. Any recommendations included with this report are based on the assumption that the samples were representative of the source from which they were taken.

Notes:

To ensure sample integrity, samples are stored only for seven days after release of the report. Thereafter it is disposed of and a fresh sample will be required if additional analyses are requested.

Results marked with "**Not SANAS Accredited**" in this report are not included in the SANAS Schedule of Accreditation for this laboratory. These results relate to the items tested.

This test report shall not be reproduced except in full, without written approval of the laboratory.

Refer to website for uncertainty of measurement and referenced methods.

Sample condition: Samples received in good condition.

Table B. 2. Summary of the amount-weighted means for $\delta^{18}O$ and $\delta^{2}H$ for all rainfall stations including the regression coefficients and coefficient of determination.

Station	2018-2019 (n=22)		Summer (n=12)		Winter (n=10)		Regression and R^2 $\delta^{2}H=a\,\delta^{18}O + b$		Regression and R^2 $\delta^{2}H=a\,\delta^{18}O + b$	
	$\delta^{2}H$ (‰)	$\delta^{18}O$ (‰)	$\delta^{2}H$ (‰)	$\delta^{18}O$ (‰)	$\delta^{2}H$ (‰)	$\delta^{18}O$ (‰)	Wet	R^2	Dry	R^2
LGU-680	-28.4	-6.86	-16.9	-4.02	-18.4	-4.48	a=6.0, b=8.2	0.88	a=5.8, b=5.5	0.90
BSU-400	-15.5*	-3.69*	-11.2*	-2.99*	-17.5*	-4.31*	a=6.38, b=9.7	0.55	a=5.5, b=5.54	0.91
LGL-370	-16.8[a]	-4.03[a]	-11.9[a]	-2.96[a]	-14.3[a]	-3.61[a]	a=7.8,b=16	0.97	a=5.83, b=6.8	0.86
TKL-290	-14.7	-3.77	-11.5	-3.06	-14.5	-3.84	a=8.45, b=17.5	0.94	a=5.7, b=6.5	0.90

*n=17 (2018-2019), summer (n=8), winter (n=9), [a] n=11 (2018-2019), summer (n=11)
Winter (n=10)

Table B. 3. Minimum, maximum and standard deviations in EC, sodium and chloride for the downstream and upstream samples

		Bosboukloof			Langrivier			Tierkloof		
		Min	Max	Mean	Min	Max	Mean	Min	Max	Mean
Dry summer (n=13)										
Upper	EC(µS/cm)	34.6	50.8	44.5(±5.1)	17.5	36.2	24.5(±1.2)	24.7	44.5	34.5(±5.7)
	Na	6.3	11.4	9.3(±1.4)	2.9	6.7	5.8(±0.9)	4.3	10.7	6.8(±2.1)
	Cl	8.5	24.0	15.0(±5.3)	4.0	9.9	6.8(±6.8)	3.2	19.0	11.0(±1.4)
Lower	EC(µS/cm)	48.5	69.9	62.3(±6.8)	24.5	34.5	30.3(±3.2)	37.6	54.6	47.8(±5.1)
	Na	10.7	15.4	13.6(1.5)	5.1	9.1	6.7(±1.1)	3.2	15.0	9.5(±2.8)
	Cl	10.7	35.9	21.3(±7.7)	4.3	9.9	7.2(±1.6)	3.8	28.3	16.5(±6.9)
Wet winter (n=13)										
Upper	EC(µS/cm)	32.3	60.4	49.7(±6.9)	19.6	39.1	27.1(±6.5)	27.1	44.1	33.7(±5.0)
	Na	2.8	24.0	10.6(5.7)	1.86	7.2	4.6(±1.4)	2.35	9.23	6.4(±2.3)
	Cl	1.1	63.3	20.7(±16)	1.5	16.4	8.6 (±1.4)	0.3	25.3	13.5(±6.5)
Lower	EC(µS/cm)	59.8	77.8	69.9(±5.7)	25.5	37.6	30.5(±3.9)	22.7	60.7	48.1(±3.1)
	Na	7.5	24.1	14.3(±5.1)	4.0	7.9	6.4(±1.1)	4.6	14.5	9.2(±3.2)
	Cl	8.5	43.4	27.7(±10)	5.8	23.3	11.2(±6.4)	2.8	34.1	18.3(±9.5)

Appendix C

Table.C.1. Summary and descriptive statistics of baseflow characteristic Bosboukloof sub-catchment, mean annual and seasonal total flow (Qt), baseflow (Qb) and quick flow (Qr) in m^3/s and baseflow index (BFI).

	Annual				Summer				Winter			
WY	Qt (m^3/s)	Qb (m^3/s)	Qr (m^3/s)	BFI	Qt (m^3/s)	Qb (m^3/s)	Qr (m^3/s)	BFI	Qt (m^3/s)	Qb (m^3/s)	Qr (m^3/s)	BFI
1946	0.026	0.021	0.005	0.87	0.014	0.012	0.002	0.84	0.038	0.030	0.008	0.80
1947	0.028	0.024	0.004	0.88	0.021	0.019	0.002	0.91	0.035	0.029	0.006	0.83
1948	0.025	0.021	0.004	0.87	0.015	0.014	0.002	0.89	0.035	0.028	0.007	0.81
1949	0.022	0.019	0.003	0.87	0.023	0.021	0.002	0.89	0.021	0.017	0.004	0.82
1950	0.023	0.019	0.004	0.86	0.014	0.013	0.002	0.88	0.031	0.025	0.006	0.81
1951	0.037	0.031	0.006	0.86	0.017	0.015	0.002	0.89	0.058	0.048	0.010	0.82
1952	0.025	0.021	0.004	0.87	0.025	0.022	0.003	0.88	0.025	0.020	0.005	0.81
1953	0.036	0.030	0.006	0.86	0.017	0.016	0.002	0.90	0.054	0.044	0.010	0.82
1954	0.040	0.033	0.007	0.86	0.018	0.016	0.002	0.90	0.061	0.049	0.012	0.81
1955	0.033	0.028	0.005	0.86	0.023	0.020	0.002	0.89	0.043	0.035	0.008	0.81
1956	0.033	0.028	0.005	0.88	0.025	0.022	0.003	0.89	0.042	0.035	0.007	0.83
1957	0.030	0.025	0.005	0.86	0.017	0.015	0.002	0.90	0.043	0.035	0.008	0.81
1958	0.029	0.025	0.005	0.86	0.026	0.023	0.003	0.87	0.033	0.027	0.006	0.82
1959	0.026	0.021	0.005	0.85	0.016	0.013	0.002	0.86	0.036	0.029	0.007	0.81
1960	0.019	0.015	0.003	0.85	0.013	0.011	0.001	0.88	0.024	0.020	0.005	0.81
1961	0.014	0.011	0.003	0.85	0.008	0.007	0.001	0.89	0.020	0.016	0.004	0.79
1962	0.029	0.024	0.005	0.86	0.010	0.009	0.001	0.89	0.049	0.039	0.009	0.81
1963	0.024	0.020	0.004	0.87	0.024	0.021	0.002	0.90	0.024	0.019	0.005	0.81
1964	0.015	0.013	0.002	0.88	0.012	0.011	0.001	0.90	0.018	0.015	0.003	0.83
1965	0.018	0.015	0.003	0.87	0.012	0.010	0.002	0.86	0.024	0.020	0.004	0.83
1966	0.019	0.016	0.003	0.87	0.011	0.010	0.001	0.88	0.027	0.022	0.005	0.83
1967	0.020	0.017	0.003	0.86	0.011	0.010	0.001	0.91	0.029	0.023	0.006	0.81
1968	0.026	0.022	0.004	0.87	0.015	0.013	0.002	0.88	0.037	0.031	0.006	0.83
1969	0.017	0.015	0.002	0.89	0.017	0.015	0.002	0.89	0.018	0.015	0.003	0.83
1970	0.021	0.017	0.003	0.87	0.011	0.010	0.001	0.90	0.031	0.025	0.006	0.82
1971	0.019	0.016	0.003	0.88	0.017	0.015	0.002	0.90	0.021	0.018	0.004	0.83
1972	0.014	0.012	0.002	0.86	0.010	0.009	0.001	0.90	0.018	0.015	0.004	0.80
1973	0.009	0.008	0.001	0.86	0.008	0.007	0.001	0.92	0.010	0.008	0.002	0.80
1974	0.020	0.016	0.004	0.84	0.006	0.005	0.001	0.89	0.033	0.026	0.007	0.78
1975	0.028	0.024	0.004	0.87	0.018	0.017	0.002	0.90	0.038	0.031	0.006	0.83
1976	0.026	0.021	0.004	0.86	0.015	0.013	0.002	0.89	0.036	0.029	0.007	0.81
1977	0.060	0.050	0.010	0.87	0.029	0.026	0.003	0.88	0.091	0.075	0.016	0.83
1978	0.024	0.021	0.003	0.89	0.027	0.025	0.003	0.90	0.020	0.017	0.003	0.84
1979	0.018	0.015	0.003	0.88	0.014	0.012	0.002	0.89	0.021	0.018	0.004	0.83
1980	0.021	0.018	0.004	0.86	0.017	0.015	0.002	0.88	0.025	0.020	0.005	0.81

1981	0.028	0.023	0.005	0.88	0.017	0.015	0.002	0.87	0.039	0.032	0.007	0.82
1982	0.025	0.022	0.003	0.89	0.021	0.019	0.002	0.92	0.028	0.024	0.004	0.84
1983	0.039	0.033	0.006	0.87	0.018	0.016	0.002	0.88	0.060	0.050	0.010	0.83
1984	0.030	0.026	0.004	0.88	0.023	0.021	0.002	0.90	0.037	0.031	0.006	0.83
1985	0.040	0.034	0.006	0.87	0.029	0.025	0.004	0.88	0.050	0.042	0.009	0.83
1986	0.040	0.033	0.007	0.86	0.020	0.017	0.002	0.88	0.060	0.049	0.011	0.82
1987	0.039	0.033	0.006	0.87	0.024	0.021	0.002	0.90	0.054	0.044	0.010	0.82
1988	0.031	0.027	0.004	0.88	0.026	0.024	0.002	0.92	0.036	0.030	0.007	0.82
1989	0.030	0.025	0.004	0.88	0.020	0.018	0.002	0.89	0.040	0.033	0.007	0.83
1990	0.040	0.034	0.006	0.87	0.023	0.021	0.002	0.91	0.058	0.048	0.010	0.83
1991	0.035	0.028	0.006	0.85	0.018	0.016	0.002	0.90	0.051	0.040	0.011	0.79
1992	0.040	0.034	0.006	0.87	0.025	0.023	0.002	0.91	0.056	0.046	0.010	0.82
1993	0.048	0.041	0.008	0.87	0.026	0.023	0.003	0.89	0.071	0.059	0.012	0.83
1994	0.025	0.021	0.004	0.85	0.018	0.016	0.002	0.90	0.032	0.025	0.006	0.81
1995	0.022	0.019	0.004	0.87	0.012	0.010	0.001	0.88	0.033	0.027	0.006	0.82
1996	0.037	0.030	0.007	0.86	0.020	0.017	0.002	0.88	0.054	0.043	0.011	0.79
1997	0.043	0.038	0.006	0.88	0.058	0.052	0.006	0.89	0.028	0.023	0.005	0.83
1998	0.025	0.021	0.004	0.86	0.016	0.014	0.002	0.88	0.034	0.028	0.006	0.83
1999	0.020	0.016	0.004	0.87	0.015	0.013	0.003	0.84	0.025	0.020	0.005	0.80
2000	0.014	0.012	0.002	0.87	0.012	0.011	0.001	0.94	0.017	0.013	0.003	0.80
2001	0.026	0.021	0.005	0.86	0.008	0.008	0.001	0.93	0.044	0.035	0.009	0.79
2002	0.027	0.023	0.004	0.88	0.021	0.019	0.002	0.91	0.032	0.026	0.005	0.83
2003	0.018	0.015	0.003	0.87	0.016	0.014	0.002	0.88	0.019	0.016	0.003	0.83
2004	0.013	0.011	0.002	0.86	0.011	0.010	0.001	0.91	0.016	0.013	0.003	0.81
2005	0.018	0.015	0.003	0.86	0.008	0.007	0.001	0.88	0.028	0.023	0.005	0.81
2006	0.016	0.013	0.002	0.87	0.010	0.009	0.001	0.91	0.022	0.018	0.004	0.83
2007	0.022	0.019	0.004	0.85	0.010	0.009	0.001	0.89	0.034	0.028	0.006	0.82
2012	0.018	0.015	0.003	0.78	0.006	0.006	0.001	0.88	0.030	0.024	0.006	0.79
2013	0.029	0.023	0.005	0.78	0.018	0.016	0.002	0.89	0.039	0.031	0.008	0.79
2014	0.030	0.026	0.004	0.78	0.027	0.024	0.002	0.91	0.032	0.027	0.005	0.84
2015	0.017	0.014	0.003	0.79	0.017	0.014	0.003	0.82	0.017	0.014	0.003	0.82
2016	0.014	0.011	0.002	0.78	0.007	0.006	0.001	0.87	0.020	0.017	0.004	0.81
2017	0.008	0.007	0.001	0.76	0.007	0.007	0.001	0.88	0.009	0.007	0.002	0.78
2018	0.012	0.010	0.002	0.78	0.005	0.004	0.001	0.84	0.018	0.015	0.004	0.80
2019	0.018	0.015	0.003	0.77	0.011	0.009	0.001	0.88	0.025	0.020	0.004	0.82
2020					0.012	0.010	0.002	0.84				
Mean	**0.026**	**0.022**	**0.004**	**0.86**	**0.017**	**0.015**	**0.002**	**0.89**	**0.035**	**0.028**	**0.006**	**0.82**
min	0.008	0.007	0.001	0.76	0.005	0.004	0.001	0.82	0.009	0.007	0.002	0.78
max	0.060	0.050	0.010	0.89	0.058	0.052	0.006	0.94	0.091	0.075	0.016	0.84
Std	0.010	0.008	0.002	0.030	0.008	0.007	0.001	0.021	0.015	0.012	0.003	0.015
CV %	37.4	37.8	39.9	**3.57**	20.6	45.7	11.74	**2.36**	44.1	44.9	43.6	**1.80**

Table.C.2. Summary and descriptive statistics of flow characteristic Tierkloof sub-catchment, mean annual and seasonal total flow (Qt), baseflow (Qb) and quick flow (Qr) in m^3/s and baseflow index (BFI).

	Annual				**Summer**				**Winter**			
WY	**Qt**	**Qb**	**Qr**	**BFI**	**Qt**	**Qb**	**Qr**	**BFI**	**Qt**	**Qb**	**Qr**	**BFI**
1946	0.040	0.023	0.017	0.60	0.027	0.019	0.009	0.68	0.052	0.029	0.023	0.56
1947	0.046	0.028	0.017	0.62	0.025	0.018	0.007	0.73	0.066	0.041	0.025	0.62
1948	0.044	0.026	0.017	0.61	0.023	0.017	0.006	0.75	0.064	0.038	0.026	0.59
1949	0.036	0.023	0.013	0.62	0.031	0.023	0.007	0.76	0.041	0.025	0.016	0.61
1950	0.043	0.026	0.018	0.60	0.025	0.017	0.007	0.71	0.062	0.037	0.025	0.59
1951	0.065	0.040	0.026	0.62	0.027	0.020	0.007	0.73	0.103	0.064	0.040	0.62
1952	0.047	0.030	0.017	0.64	0.041	0.030	0.011	0.73	0.053	0.033	0.020	0.61
1953	0.068	0.041	0.027	0.60	0.031	0.024	0.008	0.76	0.105	0.063	0.041	0.61
1954	0.074	0.045	0.029	0.61	0.027	0.020	0.006	0.76	0.121	0.073	0.048	0.61
1955	0.061	0.038	0.023	0.62	0.037	0.027	0.010	0.72	0.084	0.053	0.031	0.63
1956	0.059	0.038	0.021	0.64	0.039	0.029	0.010	0.75	0.079	0.049	0.029	0.63
1957	0.056	0.035	0.021	0.63	0.026	0.020	0.006	0.76	0.086	0.054	0.032	0.63
1958	0.057	0.036	0.021	0.63	0.047	0.033	0.014	0.70	0.066	0.041	0.025	0.62
1959	0.049	0.030	0.018	0.62	0.026	0.019	0.007	0.75	0.071	0.044	0.027	0.62
1960	0.036	0.022	0.014	0.60	0.022	0.016	0.006	0.73	0.051	0.030	0.020	0.60
1961	0.035	0.019	0.015	0.58	0.014	0.010	0.004	0.74	0.055	0.031	0.025	0.55
1962	0.062	0.035	0.026	0.59	0.020	0.014	0.005	0.73	0.104	0.061	0.043	0.59
1963	0.047	0.030	0.018	0.61	0.041	0.031	0.010	0.75	0.053	0.031	0.023	0.57
1964	0.032	0.021	0.011	0.63	0.024	0.017	0.006	0.73	0.040	0.026	0.015	0.63
1965	0.036	0.022	0.014	0.61	0.025	0.016	0.009	0.64	0.046	0.029	0.018	0.62
1966	0.033	0.020	0.013	0.62	0.019	0.013	0.006	0.67	0.047	0.030	0.018	0.63
1967	0.034	0.021	0.013	0.59	0.014	0.012	0.003	0.81	0.054	0.032	0.022	0.59
1968	0.043	0.026	0.017	0.61	0.024	0.017	0.007	0.70	0.062	0.038	0.024	0.61
1969	0.028	0.018	0.010	0.64	0.024	0.017	0.007	0.72	0.031	0.019	0.012	0.61
1970	0.036	0.021	0.015	0.60	0.015	0.012	0.004	0.76	0.057	0.033	0.024	0.59
1971	0.031	0.019	0.012	0.61	0.020	0.015	0.004	0.78	0.042	0.025	0.017	0.60
1972	0.024	0.015	0.009	0.62	0.013	0.010	0.003	0.78	0.036	0.022	0.014	0.60
1973	0.019	0.011	0.008	0.57	0.013	0.010	0.003	0.78	0.025	0.013	0.012	0.53
1974	0.037	0.021	0.016	0.59	0.014	0.010	0.004	0.72	0.060	0.035	0.026	0.57
1975	0.043	0.027	0.016	0.62	0.023	0.018	0.006	0.76	0.062	0.038	0.023	0.62
1976	0.039	0.023	0.016	0.58	0.017	0.013	0.004	0.74	0.062	0.036	0.026	0.58
1977	0.092	0.057	0.035	0.64	0.045	0.031	0.014	0.69	0.139	0.088	0.051	0.63
1978	0.030	0.020	0.010	0.62	0.027	0.021	0.006	0.79	0.033	0.020	0.014	0.59
1979	0.029	0.017	0.011	0.59	0.018	0.014	0.005	0.75	0.040	0.023	0.017	0.57
1980	0.029	0.017	0.012	0.57	0.021	0.014	0.006	0.69	0.036	0.020	0.016	0.56
1981	0.035	0.020	0.014	0.63	0.022	0.014	0.008	0.63	0.047	0.029	0.019	0.60
1982	0.030	0.019	0.010	0.61	0.019	0.015	0.004	0.80	0.040	0.024	0.015	0.61
1983	0.051	0.029	0.022	0.60	0.020	0.013	0.007	0.66	0.082	0.048	0.033	0.59
1984	0.035	0.021	0.014	0.58	0.019	0.015	0.004	0.80	0.052	0.029	0.022	0.56

1985	0.049	0.031	0.019	0.63	0.036	0.024	0.012	0.66	0.063	0.040	0.023	0.64
1986	0.046	0.027	0.019	0.61	0.018	0.013	0.004	0.75	0.074	0.044	0.030	0.60
1987	0.042	0.025	0.017	0.60	0.020	0.016	0.004	0.80	0.063	0.036	0.027	0.58
1988	0.037	0.023	0.014	0.62	0.022	0.018	0.005	0.79	0.052	0.030	0.021	0.59
1989	0.041	0.026	0.015	0.63	0.022	0.016	0.006	0.72	0.060	0.039	0.022	0.64
1990	0.051	0.032	0.019	0.62	0.025	0.019	0.006	0.76	0.077	0.048	0.029	0.62
1991	0.046	0.027	0.020	0.60	0.017	0.013	0.004	0.76	0.075	0.042	0.032	0.57
1992	0.053	0.033	0.020	0.60	0.027	0.020	0.006	0.77	0.079	0.048	0.032	0.60
1993	0.064	0.040	0.024	0.62	0.035	0.025	0.010	0.72	0.094	0.059	0.035	0.63
1994	0.033	0.020	0.013	0.60	0.018	0.013	0.004	0.75	0.048	0.028	0.020	0.59
1995	0.030	0.018	0.013	0.57	0.012	0.009	0.003	0.76	0.048	0.028	0.020	0.58
1996	0.042	0.024	0.018	0.60	0.028	0.018	0.010	0.64	0.056	0.032	0.024	0.57
1997	0.050	0.032	0.018	0.62	0.049	0.035	0.015	0.71	0.050	0.030	0.020	0.61
1998	0.039	0.024	0.015	0.62	0.026	0.017	0.008	0.67	0.053	0.032	0.020	0.62
1999	0.037	0.022	0.015	0.62	0.020	0.015	0.005	0.73	0.053	0.031	0.022	0.58
2000	0.030	0.019	0.012	0.60	0.019	0.016	0.003	0.82	0.042	0.024	0.018	0.57
2001	0.049	0.028	0.021	0.58	0.013	0.011	0.002	0.82	0.084	0.047	0.037	0.56
2002	0.051	0.033	0.019	0.63	0.035	0.025	0.010	0.72	0.068	0.044	0.024	0.64
2003	0.034	0.021	0.012	0.62	0.029	0.020	0.009	0.70	0.039	0.024	0.015	0.62
2004	0.031	0.019	0.012	0.61	0.020	0.015	0.005	0.76	0.042	0.025	0.017	0.59
2005	0.040	0.024	0.016	0.61	0.018	0.013	0.005	0.72	0.062	0.037	0.025	0.60
2006	0.033	0.020	0.013	0.60	0.016	0.013	0.004	0.78	0.049	0.030	0.019	0.61
2007	0.039	0.023	0.016	0.60	0.017	0.012	0.005	0.72	0.062	0.037	0.025	0.60
2012	0.040	0.023	0.017	0.61	0.014	0.009	0.004	0.68	0.067	0.039	0.028	0.58
2013	0.051	0.031	0.020	0.61	0.028	0.022	0.006	0.78	0.074	0.043	0.031	0.58
2014	0.046	0.031	0.016	0.63	0.035	0.027	0.008	0.77	0.057	0.036	0.021	0.63
2015	0.028	0.017	0.011	0.62	0.021	0.015	0.006	0.69	0.035	0.021	0.014	0.60
2016	0.025	0.015	0.010	0.60	0.011	0.009	0.003	0.74	0.039	0.023	0.016	0.59
2017	0.017	0.011	0.006	0.62	0.012	0.009	0.003	0.78	0.022	0.013	0.009	0.60
2018	0.024	0.014	0.010	0.60	0.011	0.008	0.003	0.74	0.038	0.021	0.016	0.57
2019	0.029	0.017	0.012	0.55	0.012	0.010	0.002	0.81	0.045	0.026	0.020	0.57
2020					0.015	0.006	0.008	0.44				
Mean	**0.042**	**0.025**	**0.016**	**0.61**	**0.023**	**0.017**	**0.006**	**0.73**	**0.060**	**0.036**	**0.024**	**0.60**
Min	0.017	0.011	0.006	0.55	0.010	0.006	0.002	0.44	0.022	0.013	0.009	0.53
Max	0.092	0.057	0.035	0.64	0.049	0.034	0.014	0.82	0.139	0.088	0.051	0.64
Std dev	0.013	0.008	0.005	0.018	0.0088	0.004	0.004	0.027	0.022	0.003	0.013	0.018
CV %	31.8	32.25	31.8	3.04	37.6	36.7	38.9	7.66	36.4	37.9	35	4.06

Table.C.3. Summary and descriptive statistics of flow characteristics in Langrivier sub-catchment, mean annual and seasonal total flow (Qt), baseflow (Qb) and quick flow (Qr) in m^3/s and baseflow index (BFI).

	Annual				**Summer**				**Winter**			
WY	**Qt**	**Qb**	**Qr**	**BFI**	**Qt**	**Qb**	**Qr**	**BFI**	**Qt**	**Qb**	**Qr**	**BFI**
1946	0.206	0.052	0.165	0.27	0.048	0.026	0.022	0.54	0.385	0.083	0.302	0.22
1947	0.108	0.049	0.071	0.39	0.046	0.023	0.023	0.50	0.193	0.070	0.122	0.36
1948	0.120	0.045	0.083	0.37	0.045	0.023	0.022	0.51	0.207	0.067	0.140	0.32
1949	0.081	0.038	0.052	0.39	0.065	0.033	0.033	0.50	0.122	0.042	0.080	0.34
1950	0.140	0.052	0.096	0.35	0.066	0.031	0.035	0.47	0.229	0.073	0.156	0.32
1951	0.195	0.067	0.135	0.34	0.055	0.027	0.027	0.50	0.352	0.108	0.244	0.31
1952	0.108	0.047	0.072	0.40	0.084	0.041	0.043	0.49	0.156	0.053	0.103	0.34
1953	0.179	0.070	0.117	0.37	0.060	0.031	0.029	0.52	0.315	0.105	0.209	0.34
1954	0.199	0.073	0.135	0.36	0.043	0.022	0.021	0.50	0.373	0.122	0.251	0.33
1955	0.155	0.062	0.105	0.38	0.091	0.034	0.057	0.37	0.242	0.087	0.155	0.36
1956	0.158	0.066	0.098	0.40	0.079	0.040	0.039	0.50	0.250	0.090	0.160	0.36
1957	0.133	0.057	0.085	0.40	0.048	0.023	0.024	0.49	0.235	0.088	0.147	0.37
1958	0.137	0.055	0.086	0.38	0.096	0.047	0.049	0.49	0.187	0.065	0.121	0.35
1959	0.119	0.049	0.075	0.39	0.056	0.028	0.028	0.51	0.190	0.069	0.121	0.36
1960	0.081	0.033	0.054	0.37	0.042	0.021	0.021	0.49	0.133	0.045	0.087	0.34
1961	0.079	0.032	0.060	0.38	0.027	0.014	0.013	0.52	0.154	0.049	0.105	0.32
1962	0.138	0.057	0.093	0.38	0.043	0.019	0.024	0.44	0.255	0.088	0.167	0.34
1963	0.095	0.043	0.063	0.40	0.083	0.043	0.040	0.52	0.129	0.044	0.085	0.34
1964	0.081	0.036	0.051	0.40	0.055	0.025	0.030	0.46	0.119	0.044	0.075	0.37
1965	0.112	0.044	0.068	0.40	0.074	0.033	0.041	0.45	0.152	0.058	0.094	0.38
1966	0.087	0.040	0.060	0.40	0.052	0.026	0.026	0.50	0.148	0.055	0.093	0.37
1967	0.092	0.041	0.059	0.39	0.039	0.024	0.015	0.62	0.160	0.059	0.101	0.37
1968	0.122	0.048	0.077	0.39	0.065	0.032	0.033	0.50	0.188	0.068	0.120	0.36
1969	0.075	0.033	0.052	0.40	0.065	0.032	0.032	0.50	0.105	0.037	0.069	0.35
1970	0.101	0.042	0.068	0.38	0.045	0.023	0.022	0.51	0.175	0.060	0.116	0.34
1971	0.082	0.036	0.053	0.39	0.049	0.024	0.025	0.49	0.131	0.046	0.084	0.36
1972	0.068	0.028	0.045	0.38	0.034	0.017	0.017	0.51	0.114	0.039	0.075	0.34
1973	0.051	0.024	0.038	0.37	0.036	0.017	0.019	0.48	0.087	0.029	0.059	0.33
1974	0.112	0.045	0.077	0.39	0.044	0.022	0.022	0.50	0.197	0.067	0.129	0.34
1975	0.121	0.051	0.073	0.39	0.059	0.029	0.030	0.49	0.190	0.071	0.120	0.37
1976	0.111	0.044	0.077	0.35	0.042	0.021	0.021	0.51	0.199	0.067	0.132	0.34
1977	0.266	0.100	0.167	0.39	0.122	0.058	0.063	0.48	0.411	0.146	0.265	0.35
1978	0.063	0.031	0.045	0.40	0.049	0.026	0.024	0.52	0.102	0.035	0.066	0.35
1979	0.087	0.037	0.054	0.40	0.054	0.027	0.027	0.50	0.125	0.047	0.078	0.38
1980	0.078	0.034	0.051	0.38	0.064	0.032	0.031	0.51	0.112	0.041	0.071	0.36
1981	0.100	0.043	0.072	0.41	0.074	0.034	0.039	0.46	0.155	0.054	0.101	0.35
1982	0.077	0.036	0.047	0.39	0.048	0.025	0.023	0.52	0.119	0.044	0.075	0.37
1983	0.157	0.063	0.103	0.40	0.067	0.032	0.035	0.48	0.263	0.097	0.166	0.37
1984	0.095	0.040	0.064	0.37	0.043	0.022	0.021	0.51	0.166	0.056	0.110	0.33
1985	0.151	0.060	0.099	0.38	0.098	0.046	0.052	0.47	0.220	0.079	0.141	0.36

1986	0.127	0.052	0.084	0.39	0.042	0.022	0.020	0.52	0.230	0.083	0.147	0.36
1987	0.105	0.044	0.070	0.38	0.041	0.022	0.019	0.53	0.187	0.063	0.124	0.34
1988	0.105	0.044	0.065	0.41	0.055	0.027	0.027	0.50	0.166	0.059	0.108	0.35
1989	0.103	0.046	0.068	0.40	0.055	0.024	0.031	0.44	0.172	0.063	0.109	0.37
1990	0.159	0.057	0.107	0.34	0.050	0.027	0.023	0.54	0.278	0.087	0.191	0.31
1991	0.109	0.045	0.079	0.38	0.031	0.016	0.015	0.51	0.216	0.072	0.143	0.34
1992	0.139	0.060	0.085	0.39	0.055	0.026	0.030	0.46	0.235	0.089	0.145	0.38
1993	0.155	0.063	0.097	0.39	0.076	0.040	0.036	0.52	0.247	0.091	0.156	0.37
1994	0.091	0.034	0.068	0.34	0.029	0.015	0.014	0.51	0.174	0.054	0.120	0.31
1995	0.072	0.030	0.055	0.35	0.027	0.014	0.014	0.50	0.141	0.044	0.097	0.31
1996	0.112	0.040	0.079	0.33	0.054	0.026	0.027	0.49	0.186	0.056	0.129	0.30
1997	0.164	0.063	0.107	0.41	0.194	0.075	0.119	0.38	0.148	0.055	0.093	0.37
1998	0.099	0.041	0.065	0.39	0.062	0.031	0.031	0.50	0.151	0.054	0.097	0.36
1999	0.087	0.037	0.060	0.40	0.047	0.024	0.023	0.51	0.146	0.050	0.096	0.34
2000	0.077	0.033	0.051	0.38	0.044	0.022	0.022	0.50	0.124	0.040	0.084	0.32
2001	0.139	0.052	0.099	0.37	0.031	0.016	0.015	0.51	0.270	0.084	0.185	0.31
2002	0.120	0.054	0.074	0.40	0.085	0.040	0.045	0.47	0.172	0.064	0.108	0.37
2003	0.056	0.027	0.039	0.40	0.055	0.026	0.029	0.47	0.079	0.028	0.051	0.35
2004	0.072	0.032	0.048	0.39	0.045	0.024	0.021	0.53	0.115	0.041	0.075	0.35
2005	0.093	0.039	0.067	0.38	0.037	0.019	0.019	0.50	0.173	0.060	0.113	0.35
2006	0.123	0.035	0.097	0.26	0.031	0.015	0.015	0.50	0.231	0.051	0.180	0.22
2007	0.101	0.042	0.069	0.39	0.040	0.020	0.020	0.49	0.179	0.063	0.116	0.35
2012	0.090	0.039	0.067	0.39	0.034	0.019	0.015	0.55	0.176	0.060	0.116	0.34
2013	0.125	0.050	0.082	0.39	0.059	0.029	0.030	0.50	0.205	0.068	0.137	0.33
2014	0.107	0.049	0.064	0.40	0.074	0.036	0.037	0.49	0.153	0.057	0.096	0.38
2015	0.052	0.026	0.036	0.41	0.039	0.020	0.019	0.52	0.084	0.031	0.053	0.37
2016	0.058	0.027	0.042	0.39	0.025	0.012	0.013	0.49	0.111	0.040	0.071	0.36
2017	0.035	0.020	0.030	0.39	0.025	0.013	0.012	0.52	0.070	0.025	0.045	0.35
2018	0.067	0.029	0.051	0.38	0.029	0.014	0.014	0.50	0.129	0.043	0.086	0.33
2019	0.070	0.033	0.048	0.38	0.033	0.016	0.016	0.50	0.127	0.045	0.082	0.36
2020					0.043	0.021	0.022	0.48				
Mean	**0.110**	**0.045**	**0.074**	**0.38**	**0.055**	**0.027**	**0.028**	**0.50**	**0.183**	**0.062**	**0.121**	**0.34**
Min	0.035	0.020	0.030	0.26	0.025	0.012	0.012	0.37	0.070	0.025	0.045	0.22
Max	0.266	0.100	0.167	0.41	0.194	0.075	0.119	0.62	0.411	0.146	0.302	0.38
Std.dev	0.041	0.014	0.027	0.026	0.025	0.010	0.015	0.033	0.071	0.023	0.050	0.029
CV%	37.5	30.2	37.4	**7.02**	45.9	39	53.8	**6.71**	39.3	36.2	42.5	**8.4**

Appendix D

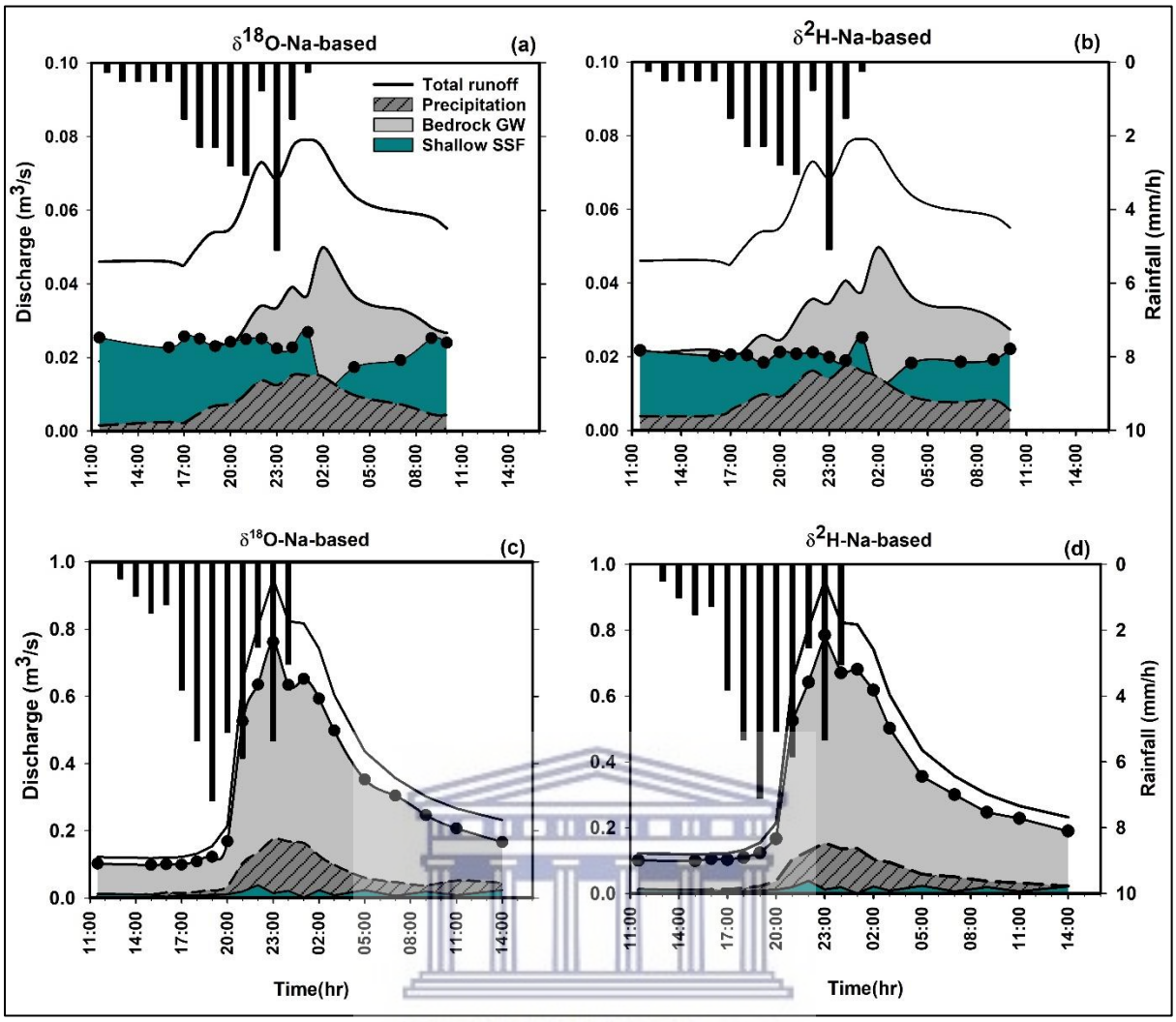

Figure.D. 1. Comparison of the three component separation using Na in (a-b) Bosboukloof and (c-d) Langrivier. The black dots indicate sampling times.

Table.D.1. Summary of event samples from the stream, piezometer, rainfall, boreholes and seepage water for Bosboukloof. Please note BH1 is located in the sub-catchment while BH3 is located within the main catchment.

Timestamp	EC (uS/cm)	pH	Na (mg/l)	Cl (mg/l)	δ2H (‰)	δ18O (‰)	Sample type
Stream							
2019/07/05 11:30	78.8	7.71	8.58	20.8	-18.8	-4.37	Pre-event
2019/07/05 15:30	78	7.62	11		-18.8	-4.45	Pre-event
2019/07/06 11:30	63.5	7.59	13	32.9	-19.9	-4.60	Event
2019/07/06 15:30	63.1	7.17	13.3	31.9	-19.8	-4.55	Event
2019/07/06 17:00	62.9	7.14	12.5	43.3	-19.3	-4.56	Event
2019/07/06 18:00	62.8	7.16	12.5	38.6	-18.8	-4.44	Event
2019/07/06 19:00	62.3	7.22	12.7	31.8	-18.4	-4.35	Event
2019/07/06 20:00	61.3	6.95	12.4	35.4	-18.6	-4.34	Event
2019/07/06 21:00	61	6.73	12.5	27.5	-18.1	-4.27	Event
2019/07/06 22:00	58.8	6.39	12.5	29.2	-17.7	-4.20	Event
2019/07/06 23:00	60.9	6.51	12.8	31.7	-18.0	-4.21	Event
2019/07/07 00:00	59	6.48	12.9	41.2	-17.6	-4.17	Event
2019/07/07 01:00	60.8	6.32	12.5	48.3	-18.0	-4.19	Event
2019/07/07 02:00	61.6	6.62	14.6	38.7	-18.2	-4.18	Event
2019/07/07 04:00	62.9	6.7	14	36.6	-18.9	-4.29	Event
2019/07/07 06:30	64.2	6.65	14	39.7	-19.2	-4.37	Event
2019/07/07 08:30	65	6.76	13.5	36.5	-18.9	-4.48	Event
2019/07/07 10:30	64.4	6.42	13.5	43.2	-19.6	-4.48	Event
2019/07/09 11:53	75.2	6.79	12.1	32.4	-19.9	-4.45	Post-event
Piezometer							
2019/07/05 12:15	64	6.77	12	20.3	-20.4	-4.64	Pre-event
2019/07/06 12:00	68.1	7.61	12.6	34.4	-19.8	-4.61	Pre-event
2019/07/07 11:58	72.6	4.36	15	33.4	-19.9	-4.62	Post-event
2019/07/09 15:30	67.3	5.31	14.8	33	-19.7	-4.37	Post-event
Rainfall							
Bulk			1.65	0.5	-3.9	-2.46	Event
sample 1			2.12	3.4	1.3	-1.95	Event
sample 2			0.77	0.12	-3.8	-2.39	Event
Sample 3			0.77	0.4	-7.5	-1.78	Event
Sample 4				0.3	-9.1	-2.20	Event
Sub-surface water							
BH1 (2019/07/05)	161.4	5.02	20	27	-21.1	-4.68	Pre-event
BH1(2019/07/09)	165.2	6.76	22.3	36.7	-22.7	-4.81	Post-event
BH3 (2019/07/05)	122.9	6.22	13.3	17.2	-18.7	-4.28	Pre-event
BH3(2019/07/09)	124.0	5.61	12.7	34.7	-19.4	-4.51	Post-event
Seep (2019/07/05)	39.1	4.28	8.14	8.5	-21.2	-4.70	Pre-event
Seep(2019/07/09)	42.8	5.96	8.86	9.4	-21.4	-4.81	Post-event

Table.D.2. Summary of samples collected during/before and after from the stream, piezometer, spring, and rainfall for Langrivier. Please note the borehole is located within the main catchment.

Time stamp	EC (uS/cm)	pH	Na (mg/l)	Cl (mg/l)	δ^2H (‰)	$\delta^{18}O$ (‰)	Sample type
Stream							
2019/07/05 12:02	28	5.42	**5.47**	**7.2**	-23.1	-5.09	Pre-event
2019/07/05 17:23	29	6.16	**5.47**	**7.0**	-23.1	-5.14	Pre-event
2019/07/06 11:30	27.6	6.08	6.8	9.2	-23.2	-5.06	Pre-event
2019/07/06 15:00	27.8	5.92	6.1	9.2	-23.3	-4.99	Event
2019/07/06 16:00	30.7	5.89	4.24	9.1	-23.1	-4.98	Event
2019/07/06 17:00	32.7	5.59	5.59	8.5	-22.6	-4.97	Event
2019/07/06 18:00	33.4	6.33	4.94	8.1	-22.1	-4.91	Event
2019/07/06 19:00	33.2	6.69	5.16	8.3	-21.4	-4.87	Event
2019/07/06 20:00	38.5	6.56	4.85	7.1	-21.9	-4.91	Event
2019/07/06 21:00	26.8	5.31	4.23	5.5	-21.8	-4.86	Event
2019/07/06 22:00	24	5.54	4.79	4.3	-22.0	-4.85	Event
2019/07/06 23:00	31.4	6.45	3.71	4.2	-21.9	-4.77	Event
2019/07/07 00:00	18.9	6.2	4.01	4.6	-22.0	-4.82	Event
2019/07/07 01:00	18.5	5.56	3.27	4.5	-22.4	-4.87	Event
2019/07/07 02:00	21.1	7.23	4.25	4.5	-22.1	-4.92	Event
2019/07/07 03:00	21.3	6.23	3.71	4.4	-22.3	-4.95	Event
2019/07/07 05:00	23.7	6.39	5.06	4.4	-22.4	-5.02	Event
2019/07/07 07:00	23	5.74	3.89	4.8	-22.5	-4.99	Event
2019/07/07 09:00	25.2	5.57	5.37	6.3	-22.9	-4.81	Event
2019/07/07 11:00	23.2	6.14	4.15	6.3	-22.9	-4.73	Event
2019/07/07 14:00	27.6	4.52	6.32	9.1	-22.9	-4.73	Post-event
2019/07/09 11:53	28	6.61	5.59	11.2	-21.4	-4.84	Post-event
Piezometer							
2019/07/05 12:00	57.8	4.25	6.57	13.1	-17.4	-4.04	Pre-event
2019/07/05 15:00	58.1	4.56	7.2	15.1	-17.2	-4.13	Pre-event
2019/07/06 11:30	64.2	5.71	10.4	37.4	-18.1	-4.14	Pre-event
2019/07/06 15:00	69.1	5.96	10.3	37.5	-18.6	-4.09	Event
2019/07/06 16:00	70.5	4.22	10.4	30.3	-18.2	-4.02	Event
2019/07/06 17:00	64.5	5.42	10.5	34.9	-18.4	-4.11	Event
2019/07/06 18:00	70.3	5.54	10.9	32.1	-18.2	-4.04	Event
2019/07/07 09:00	61	5.03	10.4	30.2	-18.1	-4.09	Event
2019/07/07 11:00	62	4.36	11.2	38	-18.3	-4.16	Event
2019/07/07 14:00	64	4.81	10.6	30.3	-18.1	-4.14	Post-event
2019/07/09 11:46	79.4	4.18	9.44	35.5	-17.5	-4.04	Post-event
Rain							
Sample 1			2.3	2.9	2.4	-1.62	Event
Sample 2			0.85	0.2	-2.7	-1.76	Event
Sample 3			1.01	0.5	-0.6	-2.11	Event
Sample 4			0.819	0.4	-3.5	-2.60	Event
Sample 5			0.378	0.1	-5.2	-2.73	Event
Sample 6			0.993	0.2	-5.4	-2.69	Event

Bulk sample			0.9	0.3	-3.5	-2.38	Event
Sub-surface water							
BH1 (2019/07/05)	161.4	5.02	20	27.0	-21.1	-4.68	Pre-event
BH1(2019/07/09)	165.2	6.76	22.3	37.6	-22.7	-4.81	Post-event
BH3(2019/07/05)	122.9	6.22	13.3	17.2	-18.7	-4.28	Pre-event
BH3(2019/07/09)	124	5.61	12.7	34.7	-19.4	-4.51	Post-event
Spring(2019/07/05)	22.5	4.08	2.16	4.6	-25.8	-5.45	Pre-event
Spring(2019/07/09)	25.6	5.16	4	8.2	-21.9	-4.77	Post-event